

# Optimal Sum-Rate of Multi-Band MIMO Interference Channel

Harpreet Singh Dhillon

Thesis submitted to the Faculty of the  
Virginia Polytechnic Institute and State University  
in partial fulfillment of the requirements for the degree of

Master of Science  
in  
Electrical Engineering

R. Michael Buehrer, Chair  
Jeffrey H. Reed  
Claudio da Silva

July 23, 2010  
Blacksburg, Virginia

Keywords: Interference channel, MIMO, capacity, sum-rate maximization, non-linear  
non-convex optimization, global optimal solution, power control

Copyright 2010, Harpreet Singh Dhillon

# Optimal Sum-Rate of Multi-Band MIMO Interference Channel

Harpreet S. Dhillon

## ABSTRACT

While the channel capacity of an isolated noise-limited wireless link is well-understood, the same is not true for the interference-limited wireless links that coexist in the same area and occupy the same frequency band(s). The performance of these wireless systems is coupled to each other due to the mutual interference. One such wireless scenario is modeled as a network of simultaneously communicating node pairs and is generally referred to as an *interference channel* (IC). The problem of characterizing the capacity of an IC is one of the most interesting and long-standing open problems in information theory.

A popular way of characterizing the capacity of an IC is to maximize the achievable sum-rate by treating interference as Gaussian noise, which is considered optimal in low-interference scenarios. While the sum-rate of the single-band SISO IC is relatively well understood, it is not so when the users have multiple-bands and multiple-antennas for transmission. Therefore, the study of the optimal sum-rate of the multi-band MIMO IC is the main goal of this thesis. The sum-rate maximization problem for these ICs is formulated and is shown to be quite similar to the one already known for single-band MIMO ICs. This problem is reduced to the problem of finding the optimal fraction of power to be transmitted over each spatial channel in each frequency band. The underlying optimization problem, being non-linear and non-convex, is difficult to solve analytically or by employing local optimization techniques. Therefore, we develop a global optimization algorithm by extending the Reformulation and Linearization Technique (RLT) based Branch and Bound (BB) strategy to find the provably optimal solution to this problem.

We further show that the spatial and spectral channels are surprisingly similar in a multi-band multi-antenna IC from a sum-rate maximization perspective. This result is especially interesting because of the dissimilarity in the way the spatial and frequency channels affect

the perceived interference. As a part of this study, we also develop some rules-of-thumb regarding the optimal power allocation strategies in multi-band MIMO ICs in various interference regimes.

Due to the recent popularity of *Interference Alignment* (IA) as a means of approaching capacity in an IC (in high-interference regime), we also compare the sum-rates achievable by our technique to the ones achievable by IA. The results indicate that the proposed power control technique performs better than IA in the low and intermediate interference regimes. Interestingly, the performance of the power control technique improves further relative to IA with an increase in the number of orthogonal spatial or frequency channels.

*This thesis is dedicated to my parents.*



# Acknowledgments

To my advisor Dr. R. Michael Buehrer: it has been a true privilege to study under your guidance at Virginia Tech. Your boundless knowledge and a clear perspective on research and academia has always been a source of inspiration for me. I feel honored to have worked with an advisor of such tremendous and well-deserved reputation. Above all, your compassion for your students is something I have cherished the most during the past two years. Your invaluable support and sincere guidance has helped in shaping my research and academic careers. I hope our collaboration continues for the years to come.

To Dr. Claudio da Silva: thank you for always taking out time for me to talk about research and academics. Your honest suggestions, especially the ones from international student perspective, have been of immense help during my stay at VT. I feel fortunate to have known you for the past two years. I sincerely hope to get a chance of collaborating with you in future.

To Dr. Jeffrey H. Reed and Dr. Claudio da Silva: thank you for being on my committee. Your suggestions were extremely helpful in improving the quality of this thesis.

To my parents, brother and grandparents: thank you for your unconditional love. I would not have simply reached this stage without your encouragement and support. In particular, thanks to mom and dad for all the sacrifices you have made to ensure a quality education for us.

To my fiancée: thanks for always being just a phone call away. Your encouragement to work

hard everyday has helped me remain focused towards my goals. Thank you for maintaining faith in my abilities and cheering me up during the discouraging times. I am truly fortunate to have you in my life.

To my colleagues: I am fortunate to have met some wonderful people in MPRG. To Haris, I am thankful for your help in my research and for all the discussions we were able to have during the lunches. To Chris Phelps, thanks for always being there for the discussions on MIMO topics. Your explanations have always helped me understand this topic better. To Justin, thanks for your help during the initial phase of my research. To Nitin and Gautham, thanks for always being there to help whenever I needed. To Jeong, thanks for your suggestions during the group meetings to improve the quality of this work. To Tao, thanks for the discussions on optimization algorithms. To Chris Headley, thanks for all the conversations we shared on various topics. To Manik, thanks for the discussions we were able to have during the lunches. To Dinesh, Sahana and Kshitija, thanks for being so helpful when I was new to MPRG. Thank you Dinesh for the research collaboration we were able to have outside my MS research. To Umair, thanks for the discussions we were able to have on various research topics. Special thanks to Dr. Timothy Newman for his help in the hardware project.

To my friends at Blacksburg: it has been a real pleasure to make some great friends during the past two years. Thanks to Nitin, Prashant and Maninder for not letting me miss Punjab. To Yashodhan, Barathram and Umesh: thanks for being always cooperative and cheerful at home. To Rishi, Swati and Avinash: thanks for all those fun moments we shared at San Diego.

To Nancy Goad, Hilda Reynolds, Cindy Hopkins, Natasha Smith, and Cyndy Graham: thank you for your help and advice in many administrative tasks that saved a lot of my time during the past two years.

I am thankful to Qualcomm Inc. for supporting this research.

# Contents

<b>Abstract</b>	<b>ii</b>
<b>Acknowledgments</b>	<b>v</b>
<b>List of Figures</b>	<b>xiii</b>
<b>List of Tables</b>	<b>xxiv</b>
<b>1 Introduction</b>	<b>1</b>
1.1 Capacity Characterization of Interference Channel . . . . .	2
1.1.1 State of the Art . . . . .	3
1.2 Generalized Degrees of Freedom and Interference Alignment . . . . .	4
1.3 Maximum Sum-Rate Treating Interference as Noise . . . . .	6
1.3.1 Single-Band Single-Antenna IC . . . . .	7
1.3.2 Single-Band Multi-Antenna IC . . . . .	8
1.3.3 Multi-Band Multi-Antenna IC . . . . .	10
1.4 Application of this Work to Cognitive Radios . . . . .	11

1.5	Contributions and Main Findings . . . . .	13
<b>2</b>	<b>System Model</b>	<b>17</b>
2.1	Mathematical Notations . . . . .	18
2.2	General Assumptions . . . . .	18
2.3	Simulation Model . . . . .	20
2.3.1	Placement of Nodes on a Plane . . . . .	21
2.3.2	Channel Model . . . . .	22
2.3.3	SIR, SNR and SINR Distributions . . . . .	25
2.4	MIMO Link Capacity . . . . .	33
2.4.1	Decomposition of MIMO Channel into Parallel SISO Channels . . . . .	33
2.4.2	Ergodic and Outage Capacities in Fading Channels . . . . .	34
2.4.3	Numerical Results of MIMO Capacity . . . . .	35
2.4.4	Distribution of the Eigen-modes of the MIMO Channel . . . . .	43
2.5	System Variables . . . . .	50
2.6	Summary of the Chapter . . . . .	51
<b>3</b>	<b>Single Antenna Interference Channels</b>	<b>52</b>
3.1	Introduction . . . . .	52
3.2	Maximum Sum-Rate of Single Antenna IC . . . . .	55
3.3	Two-User Single-Band SISO IC . . . . .	57
3.3.1	Effect of $SNR_{min}$ . . . . .	58

3.3.2	Effect of $MUI$ . . . . .	64
3.3.3	Effect of Random Topology on the Optimal Sum-Rate . . . . .	69
3.3.4	Effect of Rayleigh Fading on the Optimal Sum-Rate . . . . .	69
3.4	Three-User Single-Band SISO IC . . . . .	72
3.4.1	Effect of $SNR_{min}$ . . . . .	72
3.4.2	Effect of $MUI$ . . . . .	77
3.5	Four-User Single-Band SISO IC . . . . .	85
3.5.1	Effect of $SNR_{min}$ . . . . .	86
3.5.2	Effect of $MUI$ . . . . .	86
3.6	Conclusions . . . . .	87
<b>4</b>	<b>Multi-Antenna Interference Channels</b>	<b>90</b>
4.1	Introduction . . . . .	90
4.2	Sum-Rate of MIMO Interference Channel . . . . .	91
4.2.1	Defining the Variables . . . . .	92
4.2.2	Maximum Capacity of a single Link in a MIMO IC . . . . .	92
4.2.3	Maximum Ergodic Sum-Rate of a MIMO IC . . . . .	94
4.3	The Proposed BB/RLT Global Optimization Algorithm . . . . .	96
4.3.1	Brief Overview of BB/RLT . . . . .	96
4.3.2	LPR Construction for MIMO IC Sum-Rate Maximization Problem . . . . .	99
4.4	Two-User 2x2 MIMO IC (Case of $N = n_t$ ) . . . . .	102
4.4.1	Numerical Results for Scenario 1 ( $\rho = 0$ ) . . . . .	105

4.4.2	Numerical Results for Scenario 2 ( $\rho = 1$ ) . . . . .	111
4.5	Three-User $2 \times 2$ MIMO IC (Case of $N > n_t$ ) . . . . .	114
4.5.1	Numerical Results . . . . .	116
4.5.2	Summary of the Main Results . . . . .	121
4.6	Two-User $4 \times 4$ Symmetric MIMO IC (Case of $N < n_t$ ) . . . . .	122
4.6.1	Numerical Results . . . . .	123
4.6.2	Summary of the Main Results . . . . .	128
4.7	Four-User $4 \times 4$ MIMO IC (Second Case of $N > n_t$ ) . . . . .	129
4.7.1	Numerical Results . . . . .	130
4.7.2	Summary of the Main Results . . . . .	136
4.8	Conclusions . . . . .	136
<b>5</b>	<b>Multi-Band Interference Channels</b>	<b>139</b>
5.1	Introduction . . . . .	139
5.2	Sum-Rate of Multi-Band MIMO IC . . . . .	141
5.2.1	Defining the Variables . . . . .	141
5.2.2	Capacity of a Single MIMO link in a Multi-Band IC . . . . .	142
5.2.3	Maximum Sum-rate of a Multi-Band MIMO IC . . . . .	144
5.3	The BB/RLT Global Optimization Algorithm . . . . .	147
5.3.1	Constructing an LPR for the multi-band MIMO IC Problem . . . . .	147
5.4	Two-User Symmetric SISO IC with Two Frequency Bands (Case of $N = N_b$ )	150
5.4.1	Numerical Results . . . . .	152

5.4.2	Summary of Main Results . . . . .	156
5.5	Two-User Symmetric SISO IC with Four Frequency Bands (Case of $N < N_b$ )	157
5.5.1	Numerical Results . . . . .	159
5.5.2	Summary of the main Results . . . . .	164
5.6	Four-User SISO IC with Four Frequency Bands . . . . .	165
5.6.1	Numerical Results . . . . .	167
5.6.2	Summary of the Main Results . . . . .	173
5.7	Two-User $2 \times 2$ MIMO IC with Two Frequency Channels . . . . .	174
5.7.1	Numerical Results . . . . .	176
5.7.2	Summary of Main Results . . . . .	180
5.8	Four-User $2 \times 2$ MIMO IC with Two Frequency Bands . . . . .	181
5.8.1	Numerical Results . . . . .	183
5.8.2	Summary of the Main Results . . . . .	189
5.9	Conclusions . . . . .	190
<b>6</b>	<b>Optimal Sum-Rate vs. Beamforming and Interference Alignment</b>	<b>193</b>
6.1	Optimal Beamforming . . . . .	194
6.1.1	Two-User Single-Band $2 \times 2$ MIMO IC . . . . .	196
6.1.2	Three-User Single-Band $2 \times 2$ MIMO IC . . . . .	198
6.2	Comparison with Interference Alignment . . . . .	200
6.2.1	Effect of the Number of Bands and Antennas . . . . .	202
6.2.2	Effect of $SNR_{min}$ . . . . .	204

6.3 Conclusion . . . . .	205
<b>7 Conclusions</b>	<b>207</b>
<b>Bibliography</b>	<b>211</b>



# List of Figures

1.1	Two-user Gaussian Interference Channel. . . . .	3
2.1	System model depicting various Tx-Rx pairs. . . . .	22
2.2	Distribution of SIR for various $MUI$ values ( $SNR_{min} = 1$ dB, $\sigma = 1$ dB, $N_b = 1$ , $N = 2$ , $n_t = n_r = 1$ , $P_{Tx} = P_{max}$ ). . . . .	26
2.3	Distribution of SIR for various $SNR_{min}$ values ( $MUI = 2$ , $\sigma = 1$ dB, $N_b = 1$ , $N = 2$ , $n_t = n_r = 1$ , $P_{Tx} = P_{max}$ ). . . . .	27
2.4	Distribution of SIR for various $\sigma$ values ( $MUI = 2$ , $SNR_{min} = 1$ dB, $N_b = 1$ , $N = 2$ , $n_t = n_r = 1$ , $P_{Tx} = P_{max}$ ). . . . .	28
2.5	Distribution of SNR for various $MUI$ values ( $SNR_{min} = 1$ dB, $\sigma = 1$ dB, $N_b = 1$ , $N = 2$ , $n_t = n_r = 1$ , $P_{Tx} = P_{max}$ ). . . . .	29
2.6	Distribution of SNR for various $SNR_{min}$ values ( $MUI = 2$ , $\sigma = 1$ dB, $N_b = 1$ , $N = 2$ , $n_t = n_r = 1$ , $P_{Tx} = P_{max}$ ). . . . .	30
2.7	Distribution of SNR for various $\sigma$ values ( $MUI = 2$ , $SNR_{min} = 1$ dB, $N_b = 1$ , $N = 2$ , $n_t = n_r = 1$ , $P_{Tx} = P_{max}$ ). . . . .	30
2.8	Distribution of SINR for various $MUI$ values ( $SNR_{min} = 1$ dB, $\sigma = 1$ dB, $N_b = 1$ , $N = 2$ , $n_t = n_r = 1$ , $P_{Tx} = P_{max}$ ). . . . .	31

2.9	Distribution of SINR for various $SNR_{min}$ values ( $MUI = 2, \sigma = 1$ dB, $N_b = 1, N = 2, n_t = n_r = 1, P_{Tx} = P_{max}$ ).	31
2.10	Distribution of SINR for various $\sigma$ values ( $MUI = 2, SNR_{min} = 1$ dB, $N_b = 1, N = 2, n_t = n_r = 1, P_{Tx} = P_{max}$ ).	32
2.11	Comparison of the ergodic capacities of a single antenna link in no-fading and Rayleigh fading environments.	37
2.12	Comparison of the optimal ergodic capacity with the ones achievable with beamforming and equal power distribution in a perfectly uncorrelated channel (Normalized-channel, $\rho = 0$ ).	38
2.13	Comparison of the optimal ergodic capacity with the ones achievable with beamforming and equal power distribution in a perfectly uncorrelated channel (Normalized-channel, $\rho = 0$ , Log Scale).	39
2.14	Comparison of the optimal ergodic capacity with the ones achievable with beamforming and equal power distribution in a perfectly uncorrelated channel (Rayleigh fading, $\rho = 0$ ).	40
2.15	Comparison of the optimal ergodic capacity with the ones achievable with beamforming and equal power distribution (Normalized channel, $\rho = 0.5$ ).	41
2.16	Comparison of the optimal ergodic capacity with the ones achievable with beamforming and equal power distribution (Rayleigh fading, $\rho = 0.5$ ).	41
2.17	Comparison of the optimal ergodic capacity with the ones achievable with beamforming and equal power distribution (Normalized channel, $\rho = 0.95$ ).	42
2.18	Comparison of the optimal ergodic capacity with the ones achievable with beamforming and equal power distribution (Rayleigh fading, $\rho = 0.95$ ).	42
2.19	Distribution of the maximum Eigen value of $\mathbf{H}\mathbf{H}^\dagger$ in a $2 \times 2$ MIMO link for several values of antenna correlation (Normalized-channel case).	44

2.20	Distribution of the minimum Eigen value of $\mathbf{H}\mathbf{H}^\dagger$ in a $2 \times 2$ MIMO link for several values of antenna correlation (Normalized-channel case). . . . .	45
2.21	Distribution of the maximum Eigen value of $\mathbf{H}\mathbf{H}^\dagger$ in a $2 \times 2$ MIMO link for several values of antenna correlation (Rayleigh-fading case). . . . .	46
2.22	Distribution of the minimum Eigen value of $\mathbf{H}\mathbf{H}^\dagger$ in a $2 \times 2$ MIMO link for several values of antenna correlation (Rayleigh-fading case). . . . .	47
2.23	Distribution of the maximum Eigen value of $\mathbf{H}\mathbf{H}^\dagger$ in a $4 \times 4$ MIMO link for several values of antenna correlation (Normalized-channel case). . . . .	48
2.24	Distribution of the minimum Eigen value of $\mathbf{H}\mathbf{H}^\dagger$ in a $4 \times 4$ MIMO link for several values of antenna correlation (Normalized-channel case). . . . .	48
2.25	Distribution of the maximum Eigen value of $\mathbf{H}\mathbf{H}^\dagger$ in a $4 \times 4$ MIMO link for several values of antenna correlation (Rayleigh-fading case). . . . .	49
2.26	Distribution of the minimum Eigen value of $\mathbf{H}\mathbf{H}^\dagger$ in a $4 \times 4$ MIMO link for several values of antenna correlation (Rayleigh-fading case). . . . .	49
3.1	Two-User Symmetric SISO IC. . . . .	58
3.2	Numerical results of the sum-rate for various values of $SNR_{min}$ in the two-user symmetric IC ( $N = 2$ , $N_b = 1$ , $MUI = 1$ , No fading). . . . .	59
3.3	Sum-Rate region for the two-user symmetric SISO IC in the low $SNR$ regime ( $SNR_{min} = 1dB$ , $N_b = 1$ , $MUI = 1$ , No fading). . . . .	60
3.4	Sum-Rate region for the two-user symmetric SISO IC in the moderate $SNR$ regime ( $SNR_{min} = 10dB$ , $N_b = 1$ , $MUI = 1$ , No fading). . . . .	61
3.5	Sum-Rate region for the two-user symmetric SISO IC in the high $SNR$ regime ( $SNR_{min} = 20dB$ , $N_b = 1$ , $MUI = 1$ , No fading). . . . .	62

3.6	Sum-Rate region for the two-user symmetric SISO IC in very high $SNR$ regime ( $SNR_{min} = 30dB$ , $N_b = 1$ , $MUI = 1$ , No fading). . . . .	63
3.7	Numerical results on the sum-rate for various values of $MUI$ factor in the two-user symmetric IC ( $N = 2$ , $N_b = 1$ , $SNR_{min} = 1$ dB, No fading). . . . .	64
3.8	Sum-Rate region for the two-user symmetric SISO IC for $MUI$ factor of 5 ( $SNR_{min} = 1$ dB, $N_b = 1$ , No fading). . . . .	65
3.9	Sum-Rate region for the two-user symmetric SISO IC for $MUI$ factor of 6 ( $SNR_{min} = 1$ dB, $N_b = 1$ , No fading). . . . .	66
3.10	Sum-Rate region for the two-user symmetric SISO IC in high interference regime ( $SNR_{min} = 1$ dB, $MUI = 10$ , $N_b = 1$ , No fading). . . . .	67
3.11	Sum-Rate region for the two-user symmetric SISO IC in very high interference regime ( $SNR_{min} = 1$ dB, $MUI = 20$ , $N_b = 1$ , No fading). . . . .	68
3.12	Ergodic sum-rate for various values of $SNR_{min}$ in the two-user IC where the nodes are placed randomly for each instantiation ( $N = 2$ , $N_b = 1$ , $MUI = 1$ , No fading). . . . .	70
3.13	Ergodic sum-rate for various values of $MUI$ in the two-user IC where the nodes are placed randomly for each instantiation ( $N = 2$ , $N_b = 1$ , $MUI = 1$ , No fading). . . . .	71
3.14	Numerical Results of the sum-rate for various values of $MUI$ in the two-user symmetric IC ( $N = 2$ , $N_b = 1$ , $MUI = 1$ , No fading). . . . .	71
3.15	Three-User SISO IC. . . . .	73
3.16	Numerical results of the sum-rate for various values of $SNR_{min}$ in the three- user SISO IC ( $N = 3$ , $N_b = 1$ , $MUI = 1$ , No fading). . . . .	73
3.17	Sum-Rate region for the three-user SISO IC in the low $SNR$ regime ( $P_1 = 0$ , $SNR_{min} = 1$ dB, $N_b = 1$ , $MUI = 1$ , No fading). . . . .	74

3.18	Sum-Rate region for the three-user SISO IC in the low $SNR$ regime ( $P_1 = 0.5$ , $SNR_{min} = 1$ dB, $N_b = 1$ , $MUI = 1$ , No fading). . . . .	75
3.19	Sum-Rate region for the three-user SISO IC in the low $SNR$ regime ( $P_1 = 1$ , $SNR_{min} = 1$ dB, $N_b = 1$ , $MUI = 1$ , No fading). . . . .	76
3.20	Sum-Rate region for the three-user SISO IC of Example 2 in the very high $SNR$ regime ( $P_2 = 0$ , $SNR_{min} = 30$ dB, $N_b = 1$ , $MUI = 1$ , No fading). . . . .	77
3.21	Sum-Rate region for the three-user SISO IC in the very high $SNR$ regime ( $P_2 = 0.5$ , $SNR_{min} = 30$ dB, $N_b = 1$ , $MUI = 1$ , No fading). . . . .	78
3.22	Sum-Rate region for the three-user SISO IC in the very high $SNR$ regime ( $P_2 = 1$ , $SNR_{min} = 30$ dB, $N_b = 1$ , $MUI = 1$ , No fading). . . . .	79
3.23	Numerical results of the sum-rate for various values of $MUI$ factor in the three-user symmetric IC ( $N = 3$ , $N_b = 1$ , $SNR_{min} = 1$ dB, No fading). . . . .	80
3.24	Sum-Rate region for the three-user SISO IC in low interference regime ( $P_1 = 0$ , $MUI = 5$ , $SNR_{min} = 1dB$ , $N_b = 1$ , No fading). . . . .	81
3.25	Sum-Rate region for the three-user SISO IC in low interference regime ( $P_1 = 0.5$ , $MUI = 5$ , $SNR_{min} = 1dB$ , $N_b = 1$ , No fading). . . . .	82
3.26	Sum-Rate region for the three-user SISO IC in low interference regime ( $P_1 = 1$ , $MUI = 5$ , $SNR_{min} = 1dB$ , $N_b = 1$ , No fading). . . . .	83
3.27	Sum-Rate region for the three-user SISO IC in high interference regime ( $P_2 = 0$ , $MUI = 20$ , $SNR_{min} = 1dB$ , $N_b = 1$ , No fading). . . . .	83
3.28	Sum-Rate region for the three-user SISO IC in high interference regime ( $P_2 = 0.5$ , $MUI = 20$ , $SNR_{min} = 1dB$ , $N_b = 1$ , No fading). . . . .	84
3.29	Sum-Rate region for the three-user SISO IC in high interference regime ( $P_2 = 1$ , $MUI = 20$ , $SNR_{min} = 1dB$ , $N_b = 1$ , No fading). . . . .	84

3.30	Four-User SISO IC. . . . .	86
3.31	Simulation Results ( $N = 4, N_b = 1, MUI = 1$ , No fading). . . . .	87
3.32	Simulation Results for various values of $MUI$ factor ( $N = 4, N_b = 1, SNR_{min} = 1$ dB, No fading). . . . .	88
4.1	Convergence of BB/RLT algorithm for a single instantiation of the interference channel ( $\epsilon = 10^{-4}, N = 2$ and $MUI = 1$ ). . . . .	97
4.2	Polyhedral approximation of $w = \ln z$ . . . . .	99
4.3	Numerical results of the ergodic sum-rate achievable in the two-user $2 \times 2$ symmetric MIMO IC, Scenario 1 ( $n_t = n_r = 2, N = 2, N_b = 1, \rho = 0, MUI = 1, \sigma = 0$ , Rayleigh fading assumed). . . . .	105
4.4	Numerical results of the ergodic sum-rate achievable in the two-user $2 \times 2$ symmetric MIMO IC plotted on the log-scale, Scenario 1 ( $n_t = n_r = 2, N = 2, N_b = 1, \rho = 0, MUI = 1, \sigma = 0$ , Rayleigh fading assumed). . . . .	106
4.5	Distribution of the total power transmitted by each user in the two-user $2 \times 2$ symmetric MIMO IC, Scenario 1 ( $n_t = n_r = 2, N = 2, N_b = 1, \rho = 0, MUI = 1, \sigma = 0$ , Rayleigh fading assumed). . . . .	107
4.6	Distribution of the power transmitted by each user over stronger Eigen-mode in the two-user $2 \times 2$ symmetric MIMO IC, Scenario 1 ( $n_t = n_r = 2, N = 2, N_b = 1, \rho = 0, MUI = 1, \sigma = 0$ , Rayleigh fading assumed). . . . .	108
4.7	Distribution of the power transmitted by each user over weaker Eigen-mode in the two-user $2 \times 2$ symmetric MIMO IC, Scenario 1 ( $n_t = n_r = 2, N = 2, N_b = 1, \rho = 0, MUI = 1, \sigma = 0$ , Rayleigh fading assumed). . . . .	109

4.8	Numerical results of the ergodic sum-rate achievable in the two-user $2 \times 2$ symmetric MIMO IC, Scenario 2 ( $n_t = n_r = 2, N = 2, N_b = 1, \rho = 1, MUI = 1, \sigma = 0$ , Rayleigh fading assumed). . . . .	111
4.9	Distribution of the total power transmitted by each user in the two-user $2 \times 2$ symmetric MIMO IC, Scenario 2 ( $n_t = n_r = 2, N = 2, N_b = 1, \rho = 1, MUI = 1, \sigma = 0$ , Rayleigh fading assumed). . . . .	112
4.10	Numerical results of the ergodic sum-rate achievable in the three-user $2 \times 2$ MIMO IC ( $n_t = n_r = 2, N = 3, N_b = 1, \rho = 0, MUI = 1, \sigma = 0$ , Rayleigh fading assumed). . . . .	116
4.11	Distribution of the total power transmitted by each user in the three-user $2 \times 2$ MIMO IC ( $n_t = n_r = 2, N = 3, N_b = 1, \rho = 0, MUI = 1, \sigma = 0$ , Rayleigh fading assumed). . . . .	117
4.12	Distribution of the power transmitted by each user over stronger Eigen-mode in the three-user $2 \times 2$ MIMO IC ( $n_t = n_r = 2, N = 3, N_b = 1, \rho = 0, MUI = 1, \sigma = 0$ , Rayleigh fading assumed). . . . .	118
4.13	Distribution of the power transmitted by each user over weaker Eigen-mode in the three-user $2 \times 2$ MIMO IC ( $n_t = n_r = 2, N = 3, N_b = 1, \rho = 0, MUI = 1, \sigma = 0$ , Rayleigh fading assumed). . . . .	119
4.14	Distribution of the total power transmitted by each user in the three-user $2 \times 2$ MIMO IC assuming perfectly correlated antennas ( $n_t = n_r = 2, N = 3, N_b = 1, \rho = 1, MUI = 1, \sigma = 0$ , Rayleigh fading assumed). . . . .	120
4.15	Numerical results of the ergodic sum-rate achievable in the two-user $4 \times 4$ MIMO IC ( $n_t = n_r = 4, N = 2, N_b = 1, \rho = 0, MUI = 1, \sigma = 0$ , Rayleigh fading assumed). . . . .	124

4.16	Distribution of the total power transmitted by each user in the two-user $4 \times 4$ MIMO IC ( $n_t = n_r = 4, N = 2, N_b = 1, \rho = 0, MUI = 1, \sigma = 0$ , Rayleigh fading assumed). . . . .	125
4.17	Distribution of the power transmitted by each user over stronger Eigen-mode in the two-user $4 \times 4$ MIMO IC ( $n_t = n_r = 4, N = 2, N_b = 1, \rho = 0, MUI = 1, \sigma = 0$ , Rayleigh fading assumed). . . . .	126
4.18	Distribution of the power transmitted by each user over weaker Eigen-mode in the two-user $4 \times 4$ MIMO IC ( $n_t = n_r = 4, N = 2, N_b = 1, \rho = 0, MUI = 1, \sigma = 0$ , Rayleigh fading assumed). . . . .	127
4.19	Numerical results of the sum-rate achievable in the four-user $4 \times 4$ MIMO IC ( $n_t = n_r = 4, N = 4, N_b = 1, \rho = 0, MUI = 1, \sigma = 0$ , Rayleigh fading assumed). . . . .	131
4.20	Distribution of the total power transmitted by each user in the four-user $4 \times 4$ MIMO IC ( $n_t = n_r = 4, N = 4, N_b = 1, \rho = 0, MUI = 1, \sigma = 0$ , Rayleigh fading assumed). . . . .	132
4.21	Distribution of the power transmitted by each user over stronger Eigen-mode in the four-user $4 \times 4$ MIMO IC ( $n_t = n_r = 4, N = 4, N_b = 1, \rho = 0, MUI = 1, \sigma = 0$ , Rayleigh fading assumed). . . . .	133
4.22	Distribution of the power transmitted by each user over weaker Eigen-mode in the four-user $4 \times 4$ MIMO IC ( $n_t = n_r = 4, N = 4, N_b = 1, \rho = 0, MUI = 1, \sigma = 0$ , Rayleigh fading assumed). . . . .	134
5.1	Numerical results of the sum-rate achievable in the two-user symmetric SISO IC with two frequency channels ( $n_t = n_r = 1, N = 2, N_b = 2, \rho = 0, MUI = 1, \sigma = 0$ , Rayleigh fading assumed). . . . .	152



5.2	Distribution of the total power transmitted by each user in the two-user symmetric SISO IC with two frequency channels ( $n_t = n_r = 1, N = 2, N_b = 2, \rho = 0, MUI = 1, \sigma = 0$ , Rayleigh fading assumed). . . . .	153
5.3	Distribution of the power transmitted by each user over the stronger frequency channel in the two-user symmetric SISO IC with two frequency channels ( $n_t = n_r = 1, N = 2, N_b = 2, \rho = 0, MUI = 1, \sigma = 0$ , Rayleigh fading assumed). . . . .	154
5.4	Distribution of the power transmitted by each user over the weaker frequency channel in the two-user symmetric SISO IC with two frequency channels ( $n_t = n_r = 1, N = 2, N_b = 2, \rho = 0, MUI = 1, \sigma = 0$ , Rayleigh fading assumed). . . . .	155
5.5	Numerical results of the sum-rate achievable in the two-user symmetric SISO IC with four frequency channels ( $n_t = n_r = 1, N = 2, N_b = 4, \rho = 0, MUI = 1, \sigma = 0$ , Rayleigh fading assumed). . . . .	160
5.6	Distribution of the total power transmitted by each user in the two-user symmetric SISO IC with four frequency channels ( $n_t = n_r = 1, N = 2, N_b = 4, \rho = 0, MUI = 1, \sigma = 0$ , Rayleigh fading assumed). . . . .	161
5.7	Distribution of the power transmitted by each user over stronger frequency channel in the two-user symmetric SISO IC with four frequency channels ( $n_t = n_r = 1, N = 2, N_b = 4, \rho = 0, MUI = 1, \sigma = 0$ , Rayleigh fading assumed). . . . .	162
5.8	Distribution of the power transmitted by each user over weaker frequency channel in the two-user symmetric SISO IC with four frequency channels ( $n_t = n_r = 1, N = 2, N_b = 4, \rho = 0, MUI = 1, \sigma = 0$ , Rayleigh fading assumed). . . . .	163
5.9	Numerical results of the sum-rate achievable in the four-user SISO IC with four frequency channels ( $n_t = n_r = 1, N = 4, N_b = 4, \rho = 0, MUI = 1, \sigma = 0$ , Rayleigh fading assumed). . . . .	168

5.10	Distribution of the total power transmitted by each user in the four-user SISO IC with four frequency channels ( $n_t = n_r = 1, N = 4, N_b = 4, \rho = 0, MUI = 1, \sigma = 0$ , Rayleigh fading assumed). . . . .	169
5.11	Distribution of the power transmitted by each user over stronger frequency channel in the four-user SISO IC with four frequency channels ( $n_t = n_r = 1, N = 4, N_b = 4, \rho = 0, MUI = 1, \sigma = 0$ , Rayleigh fading assumed). . . . .	170
5.12	Distribution of the power transmitted by each user over weaker frequency channel in the four-user SISO IC with four frequency channels ( $n_t = n_r = 1, N = 4, N_b = 4, \rho = 0, MUI = 1, \sigma = 0$ , Rayleigh fading assumed). . . . .	171
5.13	Numerical results of the sum-rate achievable in all the cases in the two-user two-band $2 \times 2$ MIMO IC ( $n_t = n_r = 2, N = 2, N_b = 2, \rho = 0, MUI = 1, \sigma = 0$ , Rayleigh fading assumed). . . . .	176
5.14	Distribution of the total power transmitted by each user in the two-user two-band $2 \times 2$ MIMO IC ( $n_t = n_r = 1, N = 2, N_b = 2, \rho = 0, MUI = 1, \sigma = 0$ , Rayleigh fading assumed). . . . .	177
5.15	Distribution of the power transmitted by each user over stronger Eigen-mode in the two-user two-band $2 \times 2$ MIMO IC ( $n_t = n_r = 1, N = 2, N_b = 2, \rho = 0, MUI = 1, \sigma = 0$ , Rayleigh fading assumed). . . . .	178
5.16	Distribution of the power transmitted by each user over weaker Eigen-mode in the two-user two-band $2 \times 2$ MIMO IC ( $n_t = n_r = 1, N = 2, N_b = 2, \rho = 0, MUI = 1, \sigma = 0$ , Rayleigh fading assumed). . . . .	179
5.17	Numerical results of the sum-rate achievable in the four-user $2 \times 2$ MIMO IC with two frequency channels ( $n_t = n_r = 2, N = 4, N_b = 2, \rho = 0, MUI = 1, \sigma = 0$ , Rayleigh fading assumed). . . . .	184

5.18	Distribution of the total power transmitted by each user in the four-user $2 \times 2$ MIMO IC with two frequency channels ( $n_t = n_r = 2, N = 4, N_b = 2, \rho = 0, MUI = 1, \sigma = 0$ , Rayleigh fading assumed). . . . .	185
5.19	Distribution of the power transmitted by each user over stronger frequency channel in the four-user $2 \times 2$ MIMO IC with two frequency channels ( $n_t = n_r = 2, N = 4, N_b = 2, \rho = 0, MUI = 1, \sigma = 0$ , Rayleigh fading assumed). . . . .	186
5.20	Distribution of the power transmitted by each user over weaker frequency channel in the four-user $2 \times 2$ MIMO IC with two frequency channels ( $n_t = n_r = 2, N = 4, N_b = 2, \rho = 0, MUI = 1, \sigma = 0$ , Rayleigh fading assumed). . . . .	187
6.1	Comparison of the sum-rates achievable by beamforming with the optimal case in the two-user $2 \times 2$ MIMO IC. ( $n_t = n_r = 2, N = 2, MUI = 1, \sigma = 0, \rho = 0$ ). . . . .	197
6.2	Comparison of the sum-rates achievable by beamforming with the optimal case in the three-user $2 \times 2$ MIMO IC. ( $n_t = n_r = 2, N = 3, MUI = 1, \sigma = 0, \rho = 0$ ). . . . .	199
6.3	Comparison of sum-rates of the single band and multiple band systems in low ( $MUI = 1$ ) and high ( $MUI = 5$ ) interference scenarios ( $n_t = n_r = 2$ ). . . . .	201
6.4	Comparison of the sum-rates of single and multiple band systems for the case when $MUI = N$ ( $n_t = n_r = 1$ ). . . . .	202
6.5	Comparison of the sum-rates of single and multiple band systems for the case when $MUI = N$ ( $n_t = n_r = 2$ ). . . . .	203
6.6	Comparison of the sum-rates of single and multiple band systems at various values of $SNR_{min}$ ( $MUI = N = 4, n_t = n_r = 1$ ). . . . .	204
6.7	Comparison of the sum-rates of single and multiple band systems at various values of $SNR_{min}$ ( $MUI = N = 4, n_t = n_r = 2$ ). . . . .	205

# List of Tables

4.1	BB/RLT Algorithm . . . . .	98
-----	----------------------------	----

# Chapter 1

## Introduction

Radio signal attenuation is one of the main characteristics of wireless communication systems. Contrary to the intuition, the attenuation is a blessing from the coexistence perspective. The cellular concept is based on this phenomenon, where the same portion of spectrum can be used simultaneously by multiple users operating independently at different geographical locations. In the same cell, if the attenuation is large and the systems are not very close to each other, the performance of one system is not affected by others. Thus the interference power is less than the noise power and the performance is said to be *noise-limited*. However, if the interference between the co-existing users is large, the performance of one user is coupled to the others through mutual interference. This is generally referred to as the *interference-limited* case. While the noise-limited wireless communication systems are reasonably well understood, the same is not true for interference-limited systems. One of the most interesting and long-standing open problems in interference-limited systems is the capacity characterization of *interference-channels*. We discuss the interference channel and its capacity characterization problem in detail in the next section.

## 1.1 Capacity Characterization of Interference Channel

In 1948, in the introduction of his classic paper, ‘A mathematical theory of communication’, Shannon wrote: “The fundamental problem of communication is that of reproducing at one point exactly or approximately a message selected at another point”. To model this problem, he developed a new branch of applied mathematics, which is known today as Information Theory [1]. One of the fundamental questions answered by information theory is about the ultimate transmission rate at which information can be reliably transmitted through an information channel. This rate is generally referred to as the channel capacity [2]-[4].

Channel capacity of the isolated link is well understood since it is fundamentally noise-limited. However, the same is not true for wireless links that coexist in the same area and transmit over the same frequency band(s). The performance of these wireless systems is coupled to each other due to the mutual interference. One such scenario is modeled as a network of simultaneously communicating node pairs and is generally referred to as an *interference channel* (IC). Each transmitter node in an IC has an intended receiver and acts as an interferer for the rest of the receiver nodes. The simplest IC is a two-user Gaussian IC where two transmitter-receiver pairs coexist as shown in Fig. 1.1. In this IC,  $x_i \in \mathcal{C}$ , for  $i = 1$  and  $2$ , is subject to a maximum power constraint  $P_{max}$ , i.e.,  $E[|x_i|] \leq P_{max}$ , and the noise processes are modeled as zero-mean complex Gaussian with variance  $\sigma_N^2$ .

The fundamental problem in the two-user Gaussian IC is to determine the *capacity region*, which is defined as the set of all simultaneously achievable rates for the two users. The characterization of the capacity region is challenging due to the mutual interference amongst the users. This can be easily understood by arguing that the increase in power of one user, along with increasing its link capacity, increases the interference perceived by the rest of the user(s). The study of the two-user Gaussian IC from an information theoretical perspective was initiated by Shannon [5] in 1961 and its exact capacity region characterization has been an open problem ever since. The only case in which we have a good insight is the high interference case, in which the interference signal is higher than the intended signal [6]. In

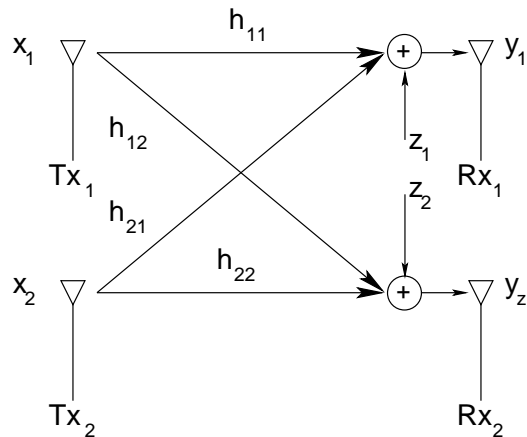


Figure 1.1: Two-user Gaussian Interference Channel.

this case, the interference is so high that it can be successfully decoded by the receiver and then canceled from the received signal. Fundamental lower and upper bounds to the capacity region of this two-user IC were proposed in [7]-[8]. The best known strategy to achieve the capacity region in the cases where interference is not very strong is due to Han and Kobayashi [10]. This strategy is a natural one and involves splitting of the transmit information into two parts: private information and common information. The private information is meant to be decoded at the intended receiver and the common information can be decoded at any receiver. The common information can be used to cancel off a part of the interference, while the private information from other users can be treated as noise.

### 1.1.1 State of the Art

In a recent development [11]-[13], a simple Han-Kobayashi technique is shown to achieve rates within 1 bit/sec/Hz of the two-user Gaussian IC capacity for all channel parameters (all interference regimes). The key feature of the proposed scheme is that the power of the private information of each user should be set such that it is received at the level of the Gaussian noise at the other receiver. In this way, the interference caused by the private information has a small effect on the other link beyond the impairment that is already caused

by noise. The rates achievable by this simple strategy are then compared to the known upper bounds and the difference between the two is shown to be always less than 1 bit/sec/Hz. The upper bounds to the capacity are typically determined by considering a *genie*-aided IC, where a *genie* provides some side information to the receiver and thus simplifies the capacity characterization. Eg., in one such IC a *genie* provides complete information of the interference signal to one of the receivers so that it can be completely canceled. Thus one of the links essentially becomes interference free and the resulting IC is referred to as the one-sided Gaussian IC. Due to the side information, the capacity achievable in this IC is at least equal to that of the original IC [14]. Thus, the capacity of the *genie* aided channel acts as an upper bound to the capacity of the corresponding Gaussian IC. In addition to this work, there has been some progress in characterizing the capacity of a two-user Gaussian IC in the weak interference regime. In particular, it has been shown that it is optimal to perform single user detection by treating interference as noise in the low interference regime [15]-[17].

Although the above mentioned works take a big stride towards the understanding of the capacity region of a two-user Gaussian IC, the exact solution is still open. More importantly, the capacity characterization of a general  $N$ -user IC ( $N > 2$ ) is little understood [18]-[19]. To work around this problem, some researchers have taken an alternate approach and mapped this capacity characterization problem to the problem of characterizing the degrees of freedom of an IC. This idea is discussed next.

## 1.2 Generalized Degrees of Freedom and Interference Alignment

It is well known that the capacity of a point-to-point AWGN link (in bits/s/Hz) at high Signal-to-Noise-Ratio (SNR) is approximately [20]:

$$C_{AWGN}(SNR) \approx \log(SNR). \quad (1.1)$$



It is further known that if  $n_t$  transmit and  $n_r$  receive antennas are available at the transmitter and receiver, respectively, and if the antennas are uncorrelated, the capacity of the point-to-point MIMO link (in bits/s/Hz) can be approximated as [21]-[22]:

$$C_{MIMO}(SNR) \approx \min\{n_t, n_r\} \log(SNR). \quad (1.2)$$

In this equation,  $\min\{n_t, n_r\}$  is the scaling factor with which  $C_{AWGN}$  scales up. This corresponds to the dimension of the signal space over which communication takes place and is termed as the *degrees of freedom* of the channel. Similarly, it is known that a multiple access channel formed by two transmitters with  $n_{t_1}$  and  $n_{t_2}$  antennas, respectively, and a receiver with  $n_r$  antennas, has  $\min\{n_{t_1} + n_{t_2}, n_r\}$  degrees of freedom [23]. Likewise, it is also known that a broadcast channel formed by a transmitter with  $n_t$  antennas and two receivers with  $n_{r_1}$  and  $n_{r_2}$  receivers, respectively, has  $\min\{n_t, n_{r_1} + n_{r_2}\}$  degrees of freedom [24]-[26].

Knowledge of the degrees of freedom is important to characterize the capacity of the channel and gives a fundamental measure of the available resources for communication. As shown in [12] for a two-user case, this classical notion of degrees of freedom for point-to-point noise-limited communication systems can be easily extended to an IC. In a general sense, an IC is said to have  $D$  degrees of freedom, if the sum of the capacities of all the links (generally referred to as the sum-rate ( $SR$ )) can be expressed as:

$$SR = D \log(SNR) + o(\log(SNR)), \quad (1.3)$$

where  $\log(SNR)$  represents the capacity of an isolated user and  $o(\log(SNR))$  is the residual capacity term [27]-[28]. It should be noted that the  $o(\log(SNR))$  term becomes negligible when the  $SNR$  is very high and thus  $D \log(SNR)$  provides a tight upper bound to the achievable sum-rate. The most significant finding of these studies is that an  $N$ -user IC has  $N/2$  degrees of freedom per orthogonal spectral, spatial or temporal slot and can thus achieve at least half the sum-rate of its no-interference counterpart for any number of interferers [28]. This is a remarkable result since it indicates that the capacity of an IC (or multi-user network) is not fundamentally limited by interference, as was initially believed. It further indicates that the capacity of an IC should increase linearly with an increase in the number of users.

It is further shown that it is possible to achieve these  $N/2$  degrees of freedom by *Interference Alignment* (IA) [28]. The basic idea of IA is to pre-code the transmit signal such that it aligns with the interference signals at all receivers where it acts as interference and is orthogonal to interference at the desired receiver. Several pre-coding methods are shown to achieve IA for single antenna interference channels with time or frequency selectivity [29]-[30].  $N$ -user MIMO interference channels are also shown to achieve  $N/2$  degrees of freedom when the channels have infinite selectivity [31]. However, it is difficult to find analytical solutions to the interference alignment problems in general and even the feasibility of interference alignment over a limited number of signalling dimensions is an open problem [32]-[33]. Since this work deals with a finite number of signalling dimensions, IA will not be the focus of our work. Instead, we will concentrate on another popular way of characterizing the capacity of an IC which is to maximize the sum-rate by treating interference as Gaussian noise, which is discussed in the next section. We will compare our results with the ones achievable by IA (assuming achievability of  $N/2$  degrees of freedom even in the finite signalling dimensions) in Chapter 6.

### 1.3 Maximum Sum-Rate Treating Interference as Noise

The main goal of our work is to study the maximum *ergodic sum-rate* achievable in a general (multi-band multi-antenna) IC by treating interference as noise. As noted in the previous section, this strategy is known to achieve the IC capacity in the low-interference regime at least in the single-band single-antenna IC. Moreover, since the feasibility of IA in finite number of signalling dimensions is yet to be established, the study of this strategy is strongly justified from an implementation perspective. In this section, we present the background study on the research in this topic and clearly delineate our contributions to the field at large. Please note that we refer to the *ergodic sum-rate* as just the *sum-rate* in the rest of this work for the ease of presentation.

### 1.3.1 Single-Band Single-Antenna IC

The problem of maximizing the sum-rate of a single-antenna and single frequency-band IC assuming interference as noise is relatively well studied. By single frequency-band we mean that all the users forming an IC share a single frequency-channel for transmission. This problem essentially reduces to a power control optimization problem where the goal is to find the optimal value of power to be transmitted by each user forming an IC [34]. The problem of power control has been traditionally studied with the aim of achieving a desired signal to noise plus interference level at all the users [35]-[37]. However, due to the advancement in coding and modulation with power control [38], [39], throughput maximization became a more important goal. The problem of finding the optimal power allocation to maximize the uplink information capacity in a single-cell was studied in [40]. It was shown that the main characteristic of the optimal scheme is that the users with the better channels are allowed to transmit at a higher power and the ones with worse channels are allowed to transmit at a lower power. The work was extended to a two-cell scenario in [41], where binary power control was reported to be optimal in a two-user scenario. Binary power control in a two-user scenario leads to only two optimal strategies: 1) both the users transmit at the maximum power, and 2) one user transmits at the maximum power and the other at the minimum power. It should be noted that a two-cell scenario is essentially a two-user IC if we assume that there is only one transmitter and one receiver in each cell. Binary power control is also reported to be optimal in a two-user IC in [42] and [43]. In [42] an asymptotic analysis for a general  $N$ -user IC is also carried out to show that the average sum-rate scales at least as  $\log(N)$  in a Rayleigh fading channel. In some recent works, binary power control is shown to be optimal in the symmetric  $N$ -user ICs and some specific scenarios of general  $N$ -user ICs [44], [45]. However, the exact solution of a general  $N$ -user power control problem is difficult to find analytically because of its non-linear non-convex nature [46]. Numerical optimization algorithms with guaranteed convergence to the global solution were recently reported in [34], [47]. The latter is based on the generalized linear fractional programming and the former on the coupling of the branch and bound strategy and the reformulation and

linearization technique.

We will look more into this problem in Chapter 3. We now discuss the sum-rate maximization problem of multi-antenna single-band IC next.

### 1.3.2 Single-Band Multi-Antenna IC

Most of the recent information theoretic works studying single-band multi-antenna ICs are focused on the two-user case [48]-[51]. In [48], some insight is provided into the two-user problem by showing that the optimal parameters that maximize the sum-rate assuming interference as noise also maximize the *genie*-aided upper bound. Some new upper bounds to the capacity of the two-user MIMO IC are presented in [49]. In [50], the recent results of the two-user SISO IC presented in [11]-[13] are extended to the two-user MIMO IC case. In particular, it presents a rate region that characterizes the whole capacity region up to a fixed number of bits in the fast fading scenario. In [51], a two-user MIMO Z-IC (single-sided IC) is studied from the information theoretic perspective with the assumption that one of the transmitters has knowledge of the signal transmitted by the other transmitter. In addition to these two-user works, there are only a few recent works that study the general  $N$ -user MIMO IC case [52]-[53]. Specifically, [52] deals with the design of the optimal linear transmitters and receivers for an  $N$ -user Gaussian IC with the aim of maximizing the weighted sum-rate. The optimization problem is solved by developing an iterative algorithm. In a recent interesting work [53], a rate duality is established between the forward and reverse links of a MIMO IC, where the reverse links are obtained by exchanging the roles of transmitters and receivers in the forward links. The corresponding channel matrices are the conjugate transpose of those of the forward link. By treating interference as noise, it is shown that the rate region of the forward and reverse link is same. A duality based iterative algorithm is further proposed to maximize the sum-rate of the MIMO IC under some power constraint.

While the above-mentioned information theoretic works have provided some insight into MIMO ICs, the general capacity region is little understood. To overcome this obstacle,

some researchers have focused on finding the maximum achievable sum-rate for the general MIMO ICs through numerical methods by assuming interference as noise. This sum-rate maximization problem was first formulated in [54]. The problem reduces to finding the optimal set of transmit symbol covariance matrices for each user forming the MIMO IC. This is hard to solve by numerical methods because we have to check all the sets of covariance matrices to arrive at the optimal solution. To overcome this problem, the formulation can be further simplified to arrive at an alternate formulation where it is sufficient to find the optimal power to be transmitted over each Eigen-channel [54]. Thus the problem essentially reduces to a power control problem over Eigen-channels. Even this problem is hard to solve numerically due to its non-linear and non-convex nature. Due to this, the solution to this problem has, to date, only been approximated by local optimization techniques [55]-[56]. Though these approaches can quickly find a locally optimal solution, they cannot guarantee the global optimum for non-convex problems. A global optimization algorithm was recently developed in [57] by coupling the branch and bound method with the reformulation and linearization technique (BB/RLT) to find the maximum sum-rate of a MIMO interference channel under the assumption that each user's transmit power is equally distributed over all the spatial channels [58]-[59]. This assumption eases the mathematical formulation of the problem significantly, but unfortunately, the simplified results do not provide the maximum achievable sum-rate for the interference channel under consideration.

In this work, we extend the BB/RLT algorithm to solve the general MIMO interference channel sum-rate maximization problem by treating interference as Gaussian noise [60]. Using this algorithm, we evaluate the maximum achievable sum-rate of some fixed multi-antenna ICs to gain insight into the optimal power allocation strategies. The optimal results are compared to some sub-optimal power allocation strategies, such as beamforming and equal power allocation over all spatial channels. From these comparisons, we note that it is optimal for the users to distribute power over the spatial channels in the low SNR (low interference) scenario and confine power over a small number of spatial channels in the very low SNR (noise-limited) and high SNR (interference-limited) scenarios. We will look into

these results in detail in Chapter 4.

### 1.3.3 Multi-Band Multi-Antenna IC

We initiated the study of maximum achievable sum-rate in a multi-antenna multi-band IC by treating interference as noise in [61]. The problem is formulated by extending the corresponding sum-rate maximization problem for single-band MIMO IC to multiple bands. We show that the two problems are mathematically quite similar and hence the solution techniques developed for the single-band MIMO ICs can be easily extended to solve the current problem. The problem being non-linear non-convex, is difficult to solve analytically. Even the local optimization techniques, such as gradient based search, are not guaranteed to converge to the global optimal solution in such non-convex problems. Therefore, we extend the BB/RLT global optimization algorithm developed for the single-band MIMO IC case in Chapter 4 to solve this sum-rate maximization problem.

We will further establish a similarity between the presence of spatial and frequency channels in an IC. In particular, we will show that the optimal power allocation strategies for a single-band  $n_t \times n_r$  MIMO IC (with  $n_t = n_r$ ) are nearly same as those of  $N_b$ -band SISO IC whenever  $n_t = N_b$ . In other words, the results indicate that the fundamental factor affecting the sum-rate in an IC is the number of orthogonal channels and not their nature (such as frequency channels, Eigen-channels, etc.). We will further generalize this result by showing that the the optimal power allocation strategies for an  $N_b$ -band  $n_t \times n_t$  MIMO IC are similar to those of single-band  $n \times n$  MIMO IC and  $n$ -band SISO IC whenever  $n_t N_b = n$ . This is an interesting result since it implies that spatial and frequency channels are surprisingly similar from the sum-rate maximization perspective. This result is especially important because of the dissimilarity in the way the spatial and frequency channels affect the perceived interference. On one hand, the frequency channels are common to all the users and are perfectly isolated from each other at each user. In other words, the signal transmitted by one user over a particular frequency channel acts as interference for all the users accessing

this band and does not affect the ones transmitting over other bands. On the other hand, this demarkation is not so clear in the case of spatial channels because they are defined for a particular user and are not same for the whole IC. Thus, the net interference perceived by each user depends upon the alignment of its Eigen-channels with the Eigen-channels of the transmitting users. Due to this fundamental difference, there are some small differences in the optimal power allocation strategies for the multi-band and the MIMO ICs. We will study these results in detail in Chapter 5.

This work on the sum-rate maximization of multi-band multi-antenna ICs has a direct application in the field of Cognitive Radios. We discuss this application in detail in the next section.

## 1.4 Application of this Work to Cognitive Radios

The most important goals in spectrum assignment are avoiding interference and maximizing utilization. The traditional solution to this problem is to divide the spectrum into several non-overlapping frequency bands and assign each band to a wireless user/technology. Though this static assignment avoids interference between systems, it does not maximize spectrum utilization. Federal Communications Commission (FCC) measurements have clearly indicated that a significant number of licensed bands remain unused or under-utilized for more than 90% of the time [63]. The high variability in the spectrum usage over frequency, time and space has attracted the interest of wireless communications community to develop efficient spectrum management methods. This has led to a flurry of research activity around the concept of dynamically utilizing the available spectrum [64]-[66]. The general idea is to equip a wireless device with “cognitive” capabilities so that it can adapt to the changing electromagnetic environment in order to maximize the utilization of the available resources [67]. Many terms are coined for variants of this basic idea which are well explained in [64]. The one most relevant to our work is the overlay or the opportunistic dynamic spectrum

access approach [67].

The opportunistic dynamic spectrum access approach (referred henceforth as DSA) is a hierarchical approach where the spectrum is available to a secondary user (SU) only when the primary user (licensee) is not transmitting in that frequency band. The main concern in DSA is to first identify the available frequency bands (white-spaces) by sensing the spectrum and then to allocate them to the SUs. For our work, we assume that we have perfect knowledge of the available white-space and will focus on spectrum sharing between SUs. Interested readers can refer to [68] for a discussion of various spectrum sensing techniques and to [69] for the benefit of cooperative spectrum sensing in cognitive radios. After identifying the available frequency bands, these are then allocated to various SUs with two primary goals: maximum spectrum utilization and fairness. These two goals lead to a number of utility (cost) functions that can be optimized for specific network applications. Some cost functions concentrate more on maximizing the utilization and others give more emphasis on fairness. Some examples of these cost functions for single-antenna systems can be found in [70], [71].

The problem of dynamic spectrum allocation to achieve the globally optimal system capacity in a single antenna system is known to be NP-hard [72]. In this case, a centralized server obtains information about the topology along with the user demand and assigns frequency bands to various SUs in order to maximize the spectral utilization. If the topology and user demand is fixed, these calculations can be performed only once to obtain conflict-free spectrum assignments that closely approximate the global optimum. If however, they are variable, a centralized system will have to find the optimal frequency allocation after each change, which adds significant computational and communication overhead. To overcome this problem, several central and distributed suboptimal spectrum allocation techniques are discussed in the literature [73]-[75]. In some distributed techniques, each user tries to optimize its own utility function and requires no collaboration from other users. In other distributed techniques, users group themselves into small groups based on geography or similarities in the technologies being used and optimize the spectrum allocation within the group to approximate the global optimum.



As is evident from the above discussion, the problem of optimal frequency allocation for SUs employing a single antenna is well-defined and solved from different perspectives in the literature [64]-[75]. The extension of this problem from single-antenna systems to multiple-antenna systems is not straight-forward because of the presence of an additional degree of freedom. The global optimum of system capacity in this case can be achieved only when both the spectral and spatial (due to the presence of multiple-antennas) domains are optimized simultaneously. It should be noted that in the most general system model, time is also considered as a transmit degree of freedom in addition to space and frequency. It is not taken into consideration in the present discussion because we are assuming that all the SUs are concurrently transmitting. Assuming cost function to be the sum-rate maximization, this problem can be easily mapped to the problem of sum-rate maximization of the multi-band multi-antenna IC studied in the previous section. Consequently, all the results and ideas developed in this thesis can be very well applied to cognitive radios. Due to this reason, we will use the words *SU* and *users* interchangeably in this work.

## 1.5 Contributions and Main Findings

In this section, we briefly discuss the contributions made in this thesis to the study of multi-band multi-antenna IC. It should be noted that the single-band SISO, single-band MIMO and multi-band SISO ICs are the special cases of our work and hence won't be explicitly mentioned in this section. All the results found for the general case of multi-band multi-antenna IC extend to these special cases too.

- **Sum-Rate Maximization Problem Formulation:** We provide a mathematical framework to determine the maximum ergodic sum-rate of a multi-band multi-antenna IC treating interference as Gaussian noise. The problem is reduced to finding the optimal fraction of power to be transmitted over each Eigen-channel in each frequency band. The underlying optimization problem is shown to be quite similar to the one

already known for the single-band MIMO IC. This enables us to extend the solution methods studied for the single band MIMO ICs easily to the current problem [61].

- **BB/RLT Global Optimization Algorithm:** The sum-rate maximization problem of multi-band multi-antenna IC is very difficult to solve both analytically and numerically due to its non-linear and non-convex nature. We extend the BB/RLT global optimization algorithm to solve this problem, which was first proposed to find the maximum sum-rate of a MIMO IC under the assumption that each user's transmit power is equally distributed over all the spatial channels. This assumption eases the mathematical formulation of the problem significantly, but unfortunately, the simplified results do not provide the maximum achievable sum-rate, in general. Thus our contributions include the global optimal solution to the sum-rate maximization problems of single-band MIMO [60] and multi-band MIMO [62] ICs.
- **Similarity Between the Spatial and Frequency channels:** We show that the spatial and frequency channels are surprisingly similar from the sum-rate perspective in an IC. The optimal power allocation strategies for a single-band  $n_t \times n_r$  MIMO IC (with  $n_t = n_r$ ) are nearly the same as those of  $N_b$ -band SISO IC whenever  $n_t = N_b$ . In other words, the fundamental factor affecting the sum-rate in an IC is the number of orthogonal channels and not their type (such as frequency channels, Eigen-channels, etc.). We generalize this result further by showing that the optimal power allocation strategies for an  $N_b$ -band  $n_t \times n_t$  MIMO IC are similar to those of single-band  $n \times n$  MIMO IC and  $n$ -band SISO IC whenever  $n_t N_b = n$ . This generalization is based on the fact that an  $N_b$ -band  $n_t \times n_r$  MIMO IC has  $\min\{n_t, n_r\}N_b$  degrees of freedom. This result is especially important because of the dissimilarity in the way the spatial and frequency channels affect the perceived interference. On one hand, the frequency channels are common to all the users and are perfectly isolated from each other at each user. On the other hand, this demarkation is not so neat in the case of spatial channels because they are defined for a particular user and are not same for the whole IC. Thus

the spatial channel of different users are not orthogonal to each other.

- **Rules-of-Thumb for Optimal Power Allocation Strategies:** From our study of some special cases of the multi-band multi-antenna ICs, we put forth some rules-of-thumb for understanding the optimal power allocation strategies. These rules are discussed below in terms of the number of orthogonal channels  $n = \min\{n_t, n_r\}N_b$  (assuming uncorrelated antennas). Please note that these channels can be spatial, spectral or mix of both due to the above mentioned equivalence.

  - *Very Low SNR Regime:* In this regime, the system is essentially noise limited and it is optimal for all the users to transmit at the full power  $P_{max}$  over a single orthogonal channel.
  - *Low SNR Regime:* It is optimal to distribute power over all orthogonal channels for all users in the low SNR regime. Equal power distribution, however, is not optimal in general. This is due to the fact that in most of the optimal power allocation strategies, the weaker channels are turned off for interference avoidance.
  - *Intermediate SNR Regime:* It is optimal to transmit most of the power in the strongest channels in the intermediate SNR regime. In some cases, it is even optimal to confine all the power in the strongest channel. This is due to the increasing importance of interference avoidance as we move from low to high SNR regimes.
  - *High SNR Regime:* In the high SNR regime, it is optimal in most of the cases to let  $n$  users transmit at the maximum power  $P_{max}$  by confining it in their respective strongest channels. Thus, it is optimal to avoid interference completely in this regime. However, in some cases the spatial channels are so aligned that complete interference avoidance is not possible. In such cases, ‘bad’ users are turned off and the rest of the users ( $< n$ ) are allowed to distribute power over the orthogonal channels appropriately.

- **Lower Bound on the Optimal Sum-Rate:** A lower bound on the sum-rate achievable by power control can be found by letting  $n$  users transmit simultaneously at the maximum power  $P_{max}$  by confining it in their respective strongest channels. This bound will be reasonably tight in the interference-limited high SNR regime due to above mentioned rule-of-thumb.
- **Comparison of Power Control with Interference Alignment:** We show that the sum-rate achievable by optimal power control while treating interference as noise in a multi-band multi-antenna IC is much higher than the one achievable by IA in low and intermediate SNR regimes. The performance of the power control technique improves further relative to IA when we increase the number of frequency-channels and/or antennas. This result is especially promising from a cognitive radio perspective, where SUs typically operate in a relatively low SNR regime and are generally expected to have multiple frequency bands available for transmission. In the high SNR (high interference) regime, however, IA performs better than the power control technique.
- **Value of Power Control in Beamforming:** We also study the value of power control in beamforming by comparing the optimal power control results with the ones achievable by letting each user perform ‘optimal’ beamforming. We show that it is important to perform power control in beamforming when the number of orthogonal channels is less than the number of users. Moreover, the value of power control in this case increases as we move from low to high interference scenarios.

# Chapter 2

## System Model

In this chapter, we introduce the system model used in this research. We begin by discussing the major underlying assumptions of our work. We then discuss the two main parts of the simulation model: the procedure for placing the nodes and the MIMO channel model. To gain insight into the system model, we study the effect of various system parameters on the distributions of the signal to interference ratio, signal to noise ratio and signal to noise plus interference ratio. Using our channel model, we study the ergodic capacity of an isolated MIMO link for various levels of antenna correlation in *normalized* and *Rayleigh-faded* channels. Normalized MIMO channel is not a standard channel type and is considered to highlight certain points about the relative strengths of the Eigen-channels and the ergodic capacity of the MIMO channel. Please note that the words *ergodic capacity* and *capacity* will be used interchangeably in this chapter. As expected, there is a significant increase in capacity as we increase the number of antennas. On the other hand, an increase in the antenna correlation is shown to decrease the MIMO capacity. It is further shown that the Rayleigh fading does not degrade the MIMO capacity significantly as compared to the normalized channel case. With this understanding, we then study the distribution of the strengths of the Eigen-modes of the MIMO channel. We show that the distribution is quite uneven and one of the Eigen-modes dominates over the others. The difference between the

strongest and the weakest Eigen-modes increases with an increase in the number of antennas. This observation will be quite helpful in understanding the ergodic capacity results of the multi-band MIMO IC presented in the subsequent chapters.

## 2.1 Mathematical Notations

Boldface is used to denote matrices and vectors. For a matrix  $\mathbf{A}$ ,  $\mathbf{A}^\dagger$  denotes the conjugate transpose and  $\mathbf{A}^T$  denotes the transpose.  $Tr\{\mathbf{A}\}$  denotes the trace of the matrix  $\mathbf{A}$ .  $\mathbf{I}$  denotes the identity matrix, whose dimensions can be determined from the context.  $\mathbf{A} \succ \mathbf{0}$  represents that  $\mathbf{A}$  is Hermitian and positive semi-definite. The scalar  $a_{m,n}$  represents the entry in the  $m^{th}$ -row and  $n^{th}$ -column of  $\mathbf{A}$ . For a complex scalar  $a$ ,  $\Re(a)$  and  $\Im(a)$  represent the real and imaginary parts of  $a$ , respectively, and  $a'$  represents the conjugate of  $a$ .  $\text{diag}\{\mathbf{A}\}$  denotes a vector of the diagonal elements of  $\mathbf{A}$  and  $\text{diag}\{\mathbf{A}\} \succeq \mathbf{0}$  means that all the diagonal elements of  $\mathbf{A}$  are non-negative.

## 2.2 General Assumptions

In this section, we discuss the main assumptions that are made to facilitate the system layout. It should be noted that some of the assumptions will be explained from the DSA perspective due to a potential application of our work in cognitive radio field.

The following assumptions are made to facilitate the system layout:

- **Perfect Spectrum Sensing:** Since the main focus of this work is to find efficient spectrum *allocation* strategies, we assume perfect spectrum sensing so that we have a complete knowledge of the available spectrum (or the white spaces). With this assumption, we can say that there is no primary user (PU) present in the white space and the spectrum is available for the exclusive use of the secondary users (SUs).

- **Interference Channel Model:** Secondly, we assume that each SU consists of a transmitter (Tx) comprised of  $n_t$  transmit antennas and a receiver (Rx) comprised of  $n_r$  receive antennas. In this peer-to-peer network model each Tx has only one intended Rx and acts as an interferer for the rest of the SUs. This type of model is termed the *interference channel* in the literature and will be discussed in detail in the next chapter [5].
- **Gaussian Interference:** We make the Gaussian interference channel assumption in which both interference and noise are modeled as Gaussian random variables. This assumption is particularly valid when the Rx nodes do not have information about the structure of interference signals. We also assume that all the transmit symbols are drawn from a Gaussian distributed code-book. This allows us to use the Shannon capacity formulation to approximate the capacity of each wireless link.
- **Orthogonal Frequency Bands:** We assume that the available spectrum is divided into a countable number of non-overlapping frequency bands. These frequency bands are termed *channels* or just *bands* in this work. The data-rate of a link is expressed in bits per second by assuming the bandwidth of each channel to be 1 Hz. In case the bandwidth of the link is not 1 Hz, the rate can be determined easily by multiplying the 1 Hz rate with the actual channel bandwidth.
- **Multi-channel Transmission:** SUs are not restricted to transmit over a single band and may split their transmit power over multiple frequency bands. This assumption holds throughout this work until specified otherwise. The purpose of this assumption is to keep the formulation general and study its effect on the link capacities in various SNR regimes. It should be noted that it is not trivial to split the transmit power unevenly over various frequency bands. Thus, it becomes even more important to study if power splitting really yields any advantage in the interference channel.
- **Finite Transmit Power:** We assume that each Tx node can transmit a finite maximum transmit power of  $P_{max}$  over all frequency bands and all  $n_t$  transmit antennas.

The maximum transmit power is the same for all the users unless specified.

- **Greedy Scheduling and Infinite Queue Length:** We assume that the schedulers of all the users are greedy and the queue lengths for all the users are infinite. This simply means that a particular user keeps on transmitting the data as long as it is optimal for it to transmit. The decision about this optimality is taken by the central server, which is described next.
- **Central Server:** We also assume that all the users share complete information. This information sharing is achieved via central server that obtains information about the topology, channel gains, number of antennas at each node, etc. Based on this information, the central server determines whether it is optimal for a user to transmit or not. As would be explained later in detail, it actually finds the fraction of total power to be transmitted by each user over each spatio-spectral channel.
- **Network Topology:** In this work, we consider both random and fixed network topologies. In the random topology, we assume that all the Tx and Rx nodes are randomly placed for each instantiation. The exact procedure of placing these nodes will be discussed in the next section. In the fixed topology, we will fix the geometry of the nodes forming the interference channel. We will use the fixed topologies to understand the fundamental behavior of the cognitive IC and then extend the results to more general random topologies.

## 2.3 Simulation Model

There are two main steps involved in setting up the simulation model in this work. The first step is to place the Tx-Rx nodes on a plane and the second step is to model the MIMO wireless channel between the nodes. We now discuss these two steps in detail.



### 2.3.1 Placement of Nodes on a Plane

The main steps involved in placing the nodes on a plane are discussed next.

- **Select the number of users  $N$ .** For each simulation, we select the number of Tx-Rx pairs  $N$  that form an IC.
- **Define the maximum distance between a Tx node and its corresponding Rx node to be  $d_{max}$ .** We define the maximum allowable distance between a Tx node and its corresponding Rx node as  $d_{max}$ .  $d_{max}$  is considered to be a system constant and its value does not depend upon any other variable. Its value is set to 10000 for this work. As would be clear from the following discussion, the choice of the value of  $d_{max}$  is immaterial and it may well be set to any other value without affecting the basic system model. It should be further noted that the units of  $d_{max}$  do not matter and can represent the physical distance in meters or kilometers without affecting the final results.
- **Define the value of Multi-User Interference ( $MUI$ ) factor.** The density of the SUs is handled by defining a Multi-User Interference ( $MUI$ ) factor.  $MUI$  represents the expected number of Rx nodes within a circle of radius  $d_{max}$  centered at any Tx node assuming a constant density. Increasing the  $MUI$  factor increases the density of interferers and hence increases the mutual interference.  $MUI$  is thus a system constant and controls the Signal to Interference Ratio (SIR) in this model.
- **Define the area of interest to be a square with side length  $L$ .** We define the area of interest (over which the nodes are to be placed) to be a square of side length  $L$ .  $L$  is variable and depends upon two system constants defined above, viz.,  $d_{max}$  and  $MUI$ . We now describe the procedure to find the value of  $L$ .

For a fixed  $MUI$  and  $d_{max}$  value, the density ( $\mu$ ) in terms of users per unit area can be evaluated as:  $\mu = MUI/\pi d_{max}^2$ . To place  $N$  users within a square with density  $\mu$ , the square should have an area  $L^2 = \frac{N}{\mu}$ . The side length  $L$  should thus be set to  $\sqrt{\frac{N}{\mu}}$ .

- **Place the Tx-Rx pairs in the square of side length  $L$ .** In the random topology case, we place a number of Rx units uniformly distributed in the chosen square area of side length  $L$  (for each analysis). Each Tx is then placed in the circle of radius  $d_{max}$  centered at the corresponding Rx, as shown in Fig. 2.1. The fixed topologies also follow the same underlying node placement rules with the only difference that the topologies remain same for each analysis. In other words, we fix the topology (satisfying rules of  $d_{max}$  and  $MUI$ ) and keep it the same for each system instantiation.

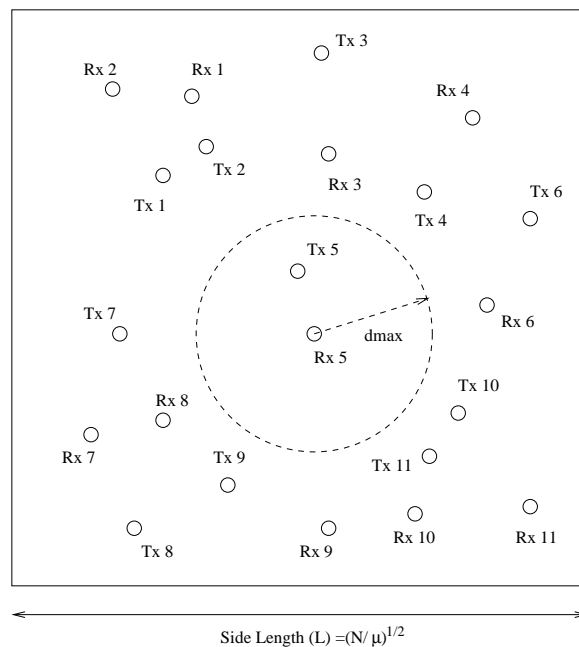


Figure 2.1: System model depicting various Tx-Rx pairs.

### 2.3.2 Channel Model

We discuss the main attributes of the channel model in this section.

- **Define the path loss  $PL(d)$  at a distance  $d$  from the Tx node assuming path loss exponent to be  $\eta$ .** The path loss exponent,  $\eta$ , is considered to be 3 in all the

simulations unless specified otherwise. The path loss at a distance  $d$  from the Tx node can be expressed as:

$$PL(d) = PL(d_0) \left[ \frac{d_0}{d} \right]^\eta; \quad (2.1)$$

where  $PL(d_0)$  is the path loss at the minimum (reference) distance and is generally modeled using a free space propagation model:  $PL(d_0) = \left( \frac{4\pi d_0}{\lambda} \right)^2$ , where  $\lambda$  is the wavelength.

- **Log-normal shadowing.** Assume that the channel suffers from log-normal shadowing with a standard deviation of  $\sigma$  dB. Log-normal shadowing can be incorporated in the channel model by defining a multiplicative gain term  $S$  that scales the path loss. As the name implies,  $S$ , is Normal distributed in the log domain. Hence,  $S$  can be expressed as:

$$S = 10^{-\frac{X_\sigma}{10}}, \quad (2.2)$$

where  $X_\sigma$  is a Gaussian random variable with zero mean and  $\sigma$  standard deviation. The negative sign in the exponent of  $S$  is not important because  $X_\sigma$  is a zero-mean Gaussian random variable. This sign is included just to highlight the fact that  $S$  is multiplied (and not divided) with  $PL(d)$ .

- **Define the MIMO channel model using the Kronecker assumption.** We assume that the antenna correlation at the Tx node is independent of the antenna correlation at the Rx node. Using the Kronecker assumption, the channel matrix  $\mathbf{H}$  between a Tx node and an Rx node can be expressed as [76]:

$$\mathbf{H} = \sqrt{\frac{P_{Tx} PL(d) S}{N_t}} \sqrt{\mathbf{R}_{Tx}} \mathbf{H}_w \sqrt{\mathbf{R}_{Rx}}, \quad (2.3)$$

where  $\mathbf{R}_{Tx}$  is the covariance matrix of the Tx antennas,  $\mathbf{R}_{Rx}$  is the covariance matrix of the Rx antennas, and  $\mathbf{H}_w$  is a matrix of independent unit power complex Gaussian random variables. We will discuss the antenna covariance matrices  $\mathbf{R}_{Tx}$  and  $\mathbf{R}_{Rx}$  later in this section.

- **Define the minimum received Signal to Noise Ratio (SNR) per Rx antenna to be  $SNR_{min}$  dB.** The distribution of SNR is controlled by defining the minimum received SNR per antenna as  $SNR_{min}$  dB assuming that the Tx node is transmitting at the maximum power and there is no fading in the channel.
- **Set the noise power  $\sigma_n^2$ .** The noise power is assumed to be same for all the Rx nodes. It is set according to the  $SNR_{min}$  as:

$$\sigma_n^2 = P_{max} PL(d_{max}) 10^{-SNR_{min}/10}. \quad (2.4)$$

$10^{-SNR_{min}/10}$  term ensures that the minimum received SNR per antenna is always greater than  $SNR_{min}$  dB (assuming Tx is transmitting at maximum power  $P_{max}$ ).

### Antenna Correlation

The spatial correlation at the Tx and Rx antennas is an important aspect in the current work. The existence of orthogonal spatial channels depends upon the antenna correlation. If the antennas are perfectly uncorrelated, the number of orthogonal spatial channels is  $\min\{n_t, n_r\}$ . On the other hand, if the antennas are perfectly correlated, there is only one spatial channel available in the MIMO link. As shown mathematically later in this section, this has a direct effect on the achievable capacity of the MIMO link.

The spatial correlation can be controlled in the current model by appropriately choosing the antenna correlation matrices ( $\mathbf{R}_{Tx}$  and  $\mathbf{R}_{Rx}$ ). In this work, we assume that the magnitude of the correlation among any two consecutive Tx (and Rx) antennas of each user is  $\rho$ . Please note that the phase of antenna correlation does not have any effect in the current study.  $\mathbf{R}_{Tx}$  (and  $\mathbf{R}_{Rx}$ ) can thus be written as:

$$\mathbf{R}_{Tx} = \begin{bmatrix} 1 & \rho^2 & \dots & \rho^{n_t-1} \\ \rho & 1 & \dots & \rho^{n_t-2} \\ \vdots & \vdots & \ddots & \vdots \\ \rho^{n_t-1} & \rho^{n_t-2} & & 1 \end{bmatrix} \quad (2.5)$$

To simulate a perfectly uncorrelated channel (high scattering scenario), both  $\mathbf{R}_{Tx}$  and  $\mathbf{R}_{Rx}$  should be considered as identity matrices by setting  $\rho = 0$ . On the other hand, perfectly correlated MIMO channel should be simulated by setting  $\rho = 1$ .

### 2.3.3 SIR, SNR and SINR Distributions

In this section, we study the effect of various system parameters, such as  $SNR_{min}$ ,  $MUI$  and  $\sigma$ , on the distributions of Signal to Interference Ratio (SIR), Signal to Noise Ratio (SNR) and Signal to Interference plus Noise Ratio (SINR). In all the cases considered in this section, we assume that there are two users forming an interference channel and transmitting simultaneously at the maximum power,  $P_{max}$ , in a single frequency band.

#### SIR Distribution

The distribution of SIR is plotted for various values of  $MUI$  in Fig. 2.2. As expected, the SIR values tend to be higher when the  $MUI$  is small (and vice-versa). This is due to the fact that increasing  $MUI$  increases interference power, thereby reducing the SIR. We also observe that the basic shape of the CDF plot does not change with the change in the  $MUI$  value. The CDF plot just shifts towards a higher SIR regime if we reduce  $MUI$  and towards a lower SIR regime if we increase  $MUI$ .

The distribution of SIR for various values of  $SNR_{min}$  is plotted in Fig. 2.3.  $MUI$  and  $SNR_{min}$  are fixed at 2 and 1 dB, respectively, for this simulation. As expected, the SIR distribution does not change with the change in  $SNR_{min}$  value. This is due to the fact

that  $SNR_{min}$  only influences the scaling of noise, which does not have any effect on SIR distribution. Thus the value of  $SNR_{min}$  can be changed without affecting the interference power in the current model.

We now study the effect of log-normal shadowing on the SIR distribution in Fig. 2.4. We observe that the increase in the standard deviation,  $\sigma$ , of the log-normal shadowing smears out the distribution of SIR. This means that the probability of getting very high and very low values of SIR increases with the increase in log-normal shadowing.

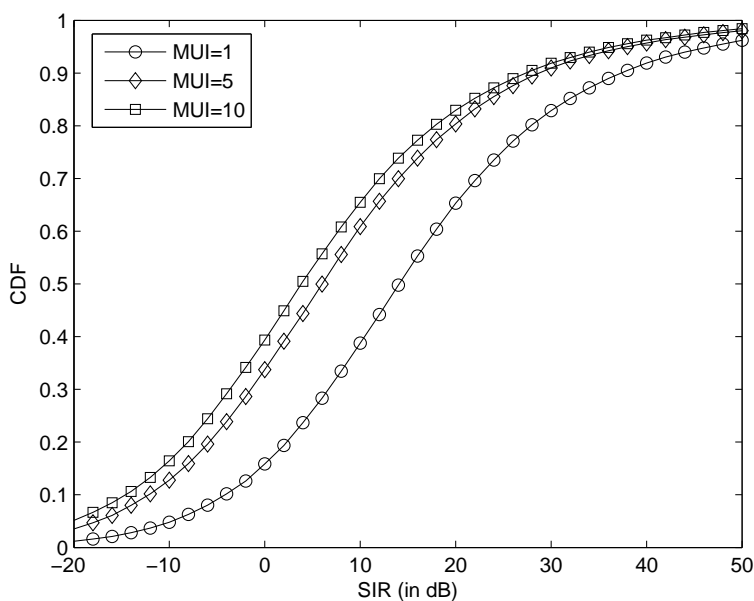


Figure 2.2: Distribution of SIR for various  $MUI$  values ( $SNR_{min} = 1$  dB,  $\sigma = 1$  dB,  $N_b = 1$ ,  $N = 2$ ,  $n_t = n_r = 1$ ,  $P_{Tx} = P_{max}$ ).

## SNR Distribution

We now study the effect of various system parameters on the distribution of SNR. In Fig. 2.5, we plot the SNR distribution for various values of  $MUI$  factor. As expected, the SNR distribution does not depend upon the  $MUI$  factor. This is due to the fact that  $MUI$  determines the interference power, which does not have any effect on the SNR distribution.

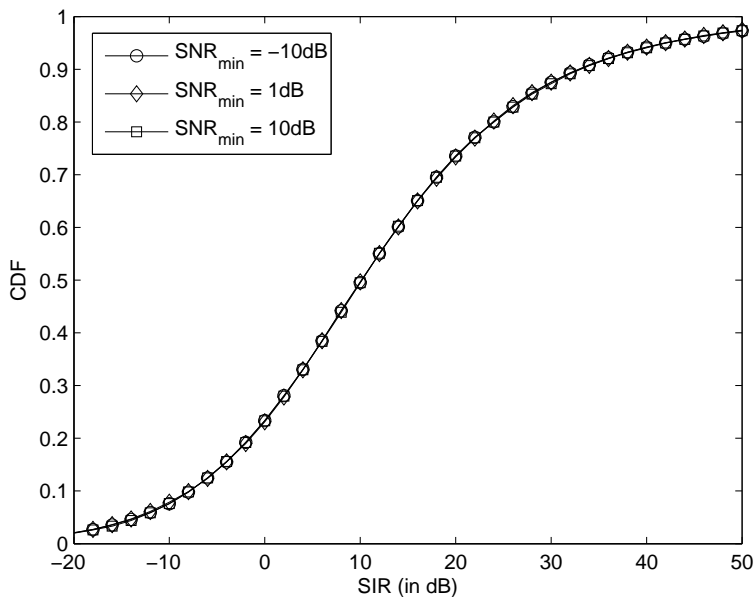


Figure 2.3: Distribution of SIR for various  $SNR_{min}$  values ( $MUI = 2$ ,  $\sigma = 1$  dB,  $N_b = 1$ ,  $N = 2$ ,  $n_t = n_r = 1$ ,  $P_{Tx} = P_{max}$ ).

Thus,  $MUI$  values can be varied in the current model without having any effect on the SNR distribution.

The effect of changing the value of  $SNR_{min}$  on the SNR distribution is studied in Fig. 2.6. As expected, higher SNR values are achieved for higher  $SNR_{min}$  values and vice-versa. It is interesting to note that the basic nature of SNR distribution plot is independent of the value of  $SNR_{min}$ . It just shifts towards the higher SNR regime for higher values of  $SNR_{min}$  and towards lower SNR regime for lower values of  $SNR_{min}$ .

We now study the effect of log-normal shadowing on the SNR distribution in Fig. 2.7. As noted earlier in the case of SIR distribution, the SNR distribution smears out more with an increase in the standard deviation of log-normal shadowing. This means that the occurrence of very high and very low SNR values is more likely when the channel suffers from a high log-normal shadowing.

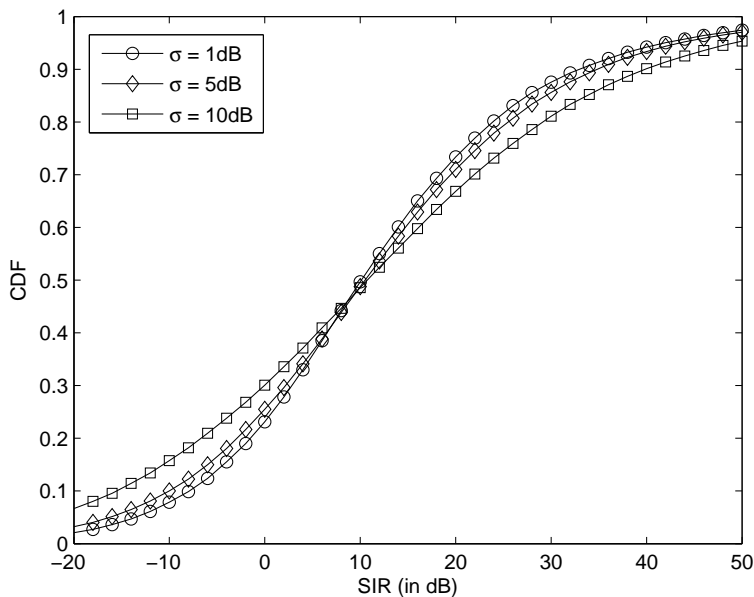


Figure 2.4: Distribution of SIR for various  $\sigma$  values ( $MUI = 2$ ,  $SNR_{min} = 1$  dB,  $N_b = 1$ ,  $N = 2$ ,  $n_t = n_r = 1$ ,  $P_{Tx} = P_{max}$ ).

### SINR Distribution

We now study the effect of changing the system parameters on the SINR distribution. The SINR distribution for various values of  $MUI$  factor is presented in Fig. 2.8. As expected, the SINR is higher for lower values of  $MUI$  factor (and vice-versa). The effect of varying  $MUI$  on SINR distribution is not as high as it is on SIR distribution (presented in Fig. 2.2). This is due to the fact that there is a constant noise term in SINR that ‘shrinks’ its distribution as compared to SIR distribution.

We study the effect of changing  $SNR_{min}$  on the SINR distribution in Fig. 2.9. As expected, the increase in the  $SNR_{min}$  value moves the SINR distribution towards the high SNR regime (and vice-versa). However, as observed in the previous case, the effect of changing the  $SNR_{min}$  values on SINR distribution is not as high as it is on SNR distribution (presented in Fig. 2.6). This is due to the constant interference term in the denominator of SINR, that



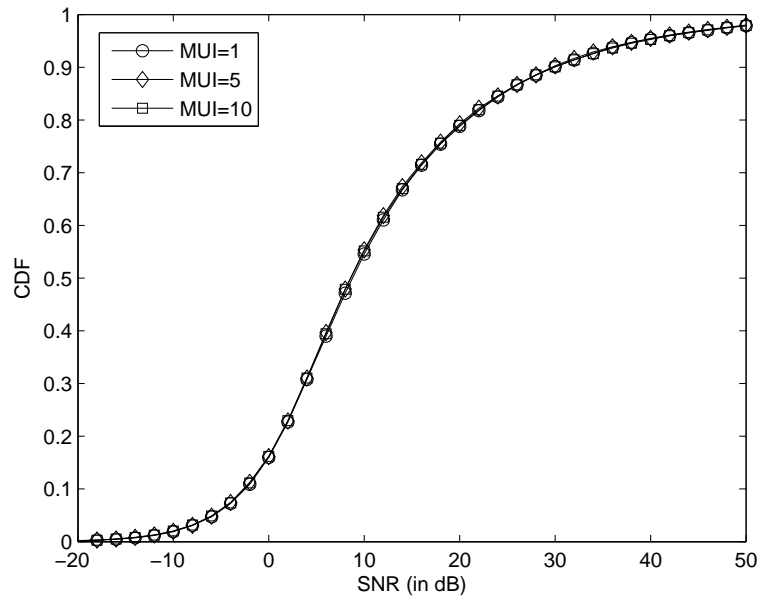


Figure 2.5: Distribution of SNR for various  $MUI$  values ( $SNR_{min} = 1$  dB,  $\sigma = 1$  dB,  $N_b = 1$ ,  $N = 2$ ,  $n_t = n_r = 1$ ,  $P_{Tx} = P_{max}$ ).

shrinks its distribution as compared to SNR distribution.

The SINR distribution for various levels of log-normal shadowing is studied in Fig. 2.10. As noted in the case of SNR and SIR distributions, stronger log-normal shadowing leads to the smearing of SINR distribution. Thus, it is more likely to get very high or very low values of SINR when the channel suffers from high log-normal shadowing.

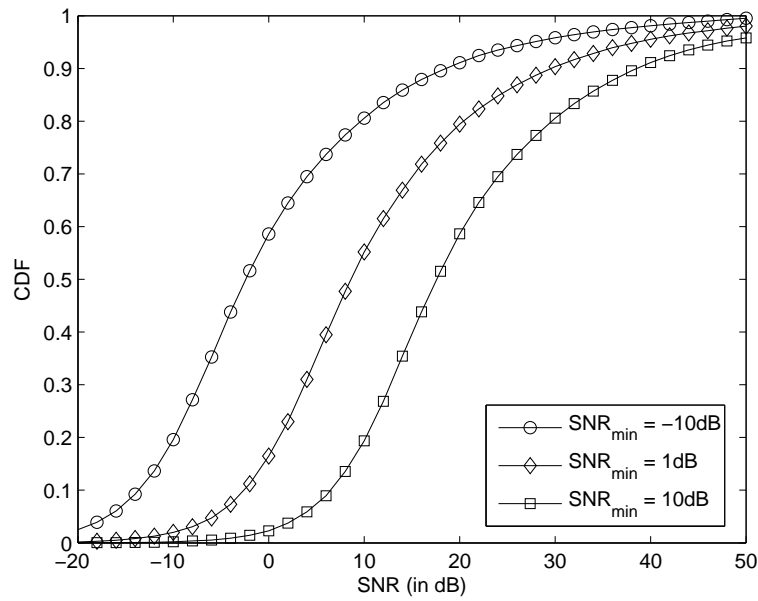


Figure 2.6: Distribution of SNR for various  $SNR_{min}$  values ( $MUI = 2$ ,  $\sigma = 1\text{ dB}$ ,  $N_b = 1$ ,  $N = 2$ ,  $n_t = n_r = 1$ ,  $P_{Tx} = P_{max}$ ).

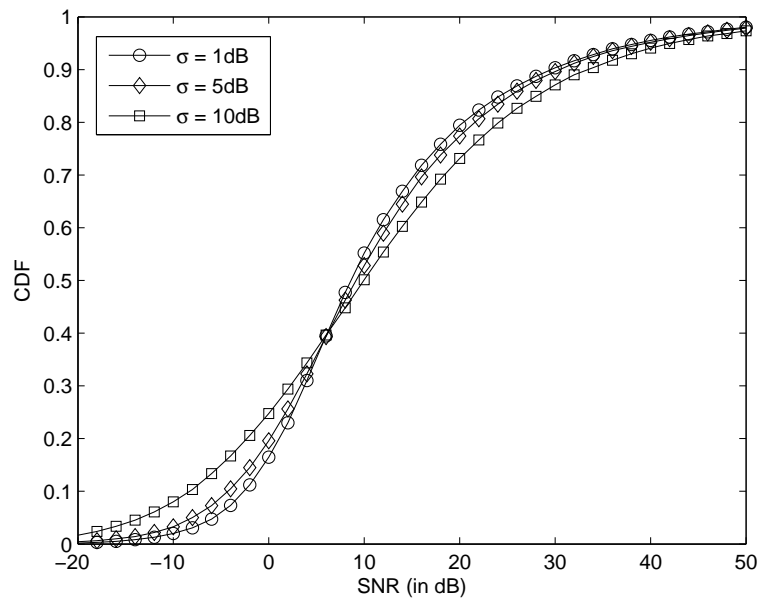


Figure 2.7: Distribution of SNR for various  $\sigma$  values ( $MUI = 2$ ,  $SNR_{min} = 1\text{ dB}$ ,  $N_b = 1$ ,  $N = 2$ ,  $n_t = n_r = 1$ ,  $P_{Tx} = P_{max}$ ).

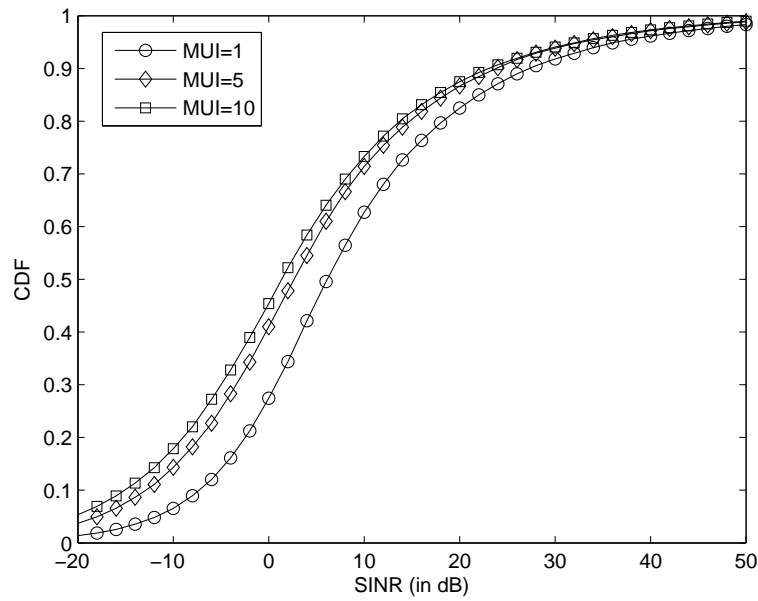


Figure 2.8: Distribution of SINR for various  $MUI$  values ( $SNR_{min} = 1$  dB,  $\sigma = 1$  dB,  $N_b = 1$ ,  $N = 2$ ,  $n_t = n_r = 1$ ,  $P_{Tx} = P_{max}$ ).

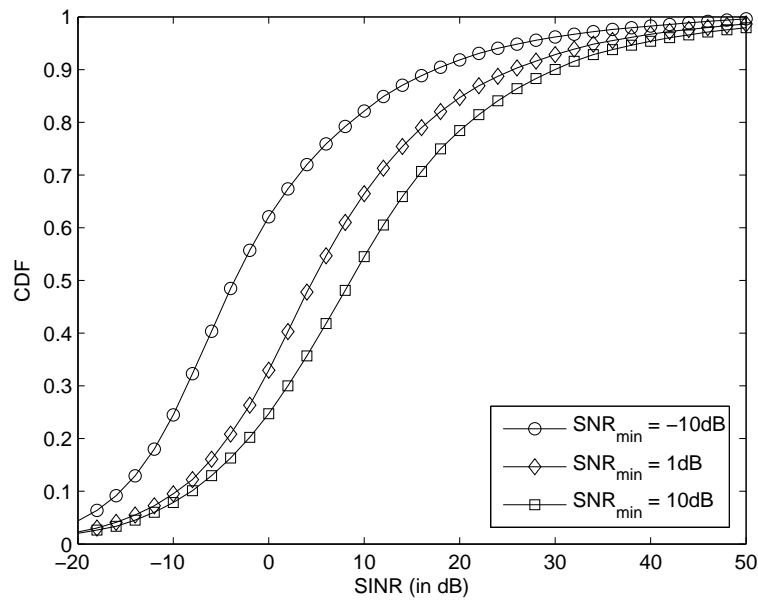


Figure 2.9: Distribution of SINR for various  $SNR_{min}$  values ( $MUI = 2$ ,  $\sigma = 1$  dB,  $N_b = 1$ ,  $N = 2$ ,  $n_t = n_r = 1$ ,  $P_{Tx} = P_{max}$ ).

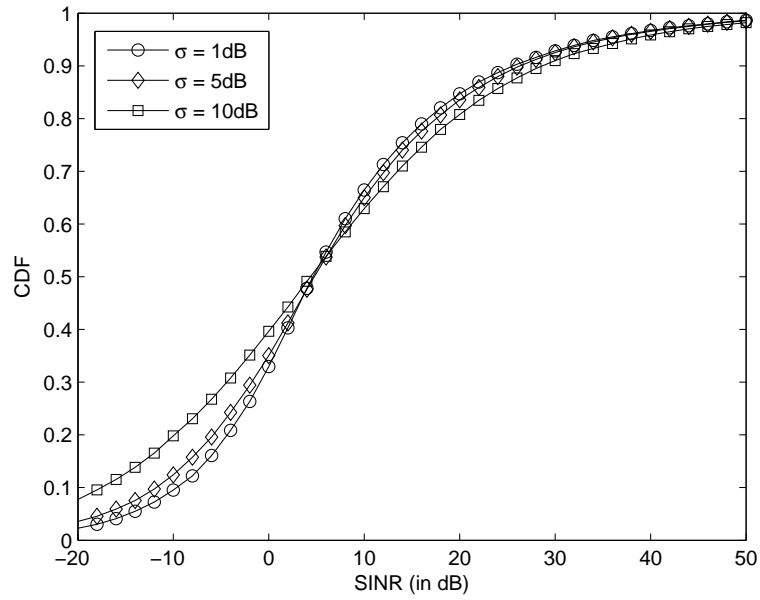


Figure 2.10: Distribution of SINR for various  $\sigma$  values ( $MUI = 2$ ,  $SNR_{min} = 1$  dB,  $N_b = 1$ ,  $N = 2$ ,  $n_t = n_r = 1$ ,  $P_{Tx} = P_{max}$ ).

## 2.4 MIMO Link Capacity

In this section, we consider an isolated  $n_t \times n_r$  MIMO link described by:

$$\mathbf{y} = \mathbf{H}\mathbf{x} + \mathbf{w}, \quad (2.6)$$

where  $\mathbf{x} \in \mathbb{C}^{n_t}$  is the transmit signal,  $\mathbf{y} \in \mathbb{C}^{n_r}$  is the received signal,  $\mathbf{H} \in \mathbb{C}^{n_r \times n_t}$  is the channel matrix and  $\mathbf{w} \sim \mathcal{CN}(0, \sigma_N^2 \mathbf{I}_{n_r})$  is the white Gaussian noise. The goal is to study the capacity of this MIMO link for various levels of antenna correlation in various SNR regimes. Assuming perfect channel knowledge at the transmitter and receiver, the link capacity (maximum mutual information) can be expressed as [77]:

$$C = \max_{\mathbf{Q}: \text{tr}(\mathbf{Q})=P_{max}} \log_2 \det \left( \mathbf{I} + \frac{1}{\sigma_N^2} \mathbf{H}\mathbf{Q}\mathbf{H}^\dagger \right), \quad (2.7)$$

where the optimization is performed over input symbol covariance matrix  $\mathbf{Q}$ .  $\sigma_N^2$  is the power of the Gaussian noise at each receive antenna. Using the singular value decomposition (SVD), it is possible to decompose the MIMO channel in  $\min\{n_t, n_r\}$  SISO channels, which is discussed next.

### 2.4.1 Decomposition of MIMO Channel into Parallel SISO Channels

By applying SVD,  $\mathbf{H}$  can be expressed as  $\mathbf{H} = \mathbf{U}\mathbf{D}\mathbf{V}^\dagger$ , where  $\mathbf{U}$  and  $\mathbf{V}$  are unitary matrices and  $\mathbf{D}$  is a diagonal matrix. Substituting this in (2.7), we get:

$$C = \max_{\mathbf{Q}: \text{tr}(\mathbf{Q})=P_{max}} \log_2 \det \left( \mathbf{I} + \frac{1}{\sigma_N^2} \mathbf{U}\mathbf{D}\mathbf{V}^\dagger \mathbf{Q}\mathbf{V}\mathbf{D}^\dagger \mathbf{U}^\dagger \right) \quad (2.8)$$

Using the identities  $\det(\mathbf{I} + \mathbf{A}\mathbf{B}) = \det(\mathbf{I} + \mathbf{B}\mathbf{A})$  and  $\mathbf{U}\mathbf{U}^\dagger = \mathbf{I}$ , (2.8) can be expressed as:

$$C = \max_{\mathbf{Q}: \text{tr}(\mathbf{Q})=P_{max}} \log_2 \det \left( \mathbf{I} + \frac{1}{\sigma_N^2} \mathbf{D}\mathbf{V}^\dagger \mathbf{Q}\mathbf{V}\mathbf{D}^\dagger \right) \quad (2.9)$$

Using the identity  $\det(\mathbf{I} + \mathbf{A}\mathbf{B}) = \det(\mathbf{I} + \mathbf{B}\mathbf{A})$  again and defining  $\Sigma = \mathbf{D}\mathbf{D}^\dagger$ , (2.9) can be expressed as:

$$C = \max_{\mathbf{Q}: \text{tr}(\mathbf{Q})=P_{max}} \log_2 \det \left( \mathbf{I} + \frac{1}{\sigma_N^2} \Sigma \mathbf{V}^\dagger \mathbf{Q}\mathbf{V} \right) \quad (2.10)$$

It should be noted that  $\Sigma = \mathbf{D}\mathbf{D}^\dagger$  is a diagonal matrix with the diagonal elements as the Eigen-values of  $\mathbf{H}\mathbf{H}^\dagger$ . To decompose the MIMO channel into  $\min\{n_t, n_r\}$  parallel non-interfering SISO channels,  $\mathbf{V}^\dagger\mathbf{Q}\mathbf{V}$  should result in a diagonal matrix. This can be achieved by choosing  $\mathbf{Q}$  of the form  $\mathbf{Q} = \mathbf{V}\Lambda\mathbf{V}^\dagger$ . We get  $\mathbf{Q}$  of this form when  $\mathbf{V}$  is chosen as the pre-coding matrix. In this case, the capacity of the isolated link can be expressed as:

$$C = \max_{\Lambda: \text{tr}(\Lambda) = P_{max}} \log_2 \det \left( \mathbf{I} + \frac{\Sigma\Lambda}{\sigma_N^2} \right) \quad (2.11)$$

Hence, we note that the MIMO channel is decomposed into parallel non-interfering SISO channels, which are generally referred to as Eigen-modes or Eigen-channels. Each diagonal value of  $\Lambda$  denotes the amount of power transmitted over the corresponding Eigen-channel. The diagonal values of  $\Sigma$  denote the strength of Eigen-channels, with a condition that  $E[\text{tr}(\Sigma)] = n_r$ . It should be noted that this expectation would have been equal to  $n_t n_r$ , if we would not have not included  $\sqrt{1/n_t}$  term in the channel matrix. The optimal power allocation (optimal  $\Lambda$ ) that maximizes the mutual information can be found by employing the ‘water-filling strategy’ [20], [77]. As noted earlier, we use the Kronecker assumption to model the MIMO channel by assuming that the antenna correlations at the Tx and Rx are independent of each other.

## 2.4.2 Ergodic and Outage Capacities in Fading Channels

The ‘instantaneous’ capacity studied so far is defined for a particular channel realization. It is the only capacity metric when the channel gain is fixed and there is no fading, e.g., AWGN channel. However, the instantaneous capacity keeps on changing with the change in the channel gains when the channel suffers from fading. In such a scenario, there are two main metrics to characterize channel capacity: *outage capacity* and *ergodic capacity*. Outage capacity  $C_0$ , as the name signifies, is defined such that the probability of the instantaneous capacity  $C$  being lower than  $C_0$  is equal to the predefined outage probability  $P_0$ , i.e.,  $P(C < C_0) = P_0$ . In the physical sense, it means that even with the use of the ideal code, the transmit symbol will be in error with a probability  $P_0$  if the spectral efficiency is

$C_0$  bits/sec/Hz. This metric of capacity is most relevant in the slow-fading or quasi-static environment when the codeword length or the delay constraint is short as compared to the channel coherence time. Second important metric to study the capacity in fading channels is the ergodic capacity. As the name suggests, it is the ensemble average of the ‘instantaneous’ capacity over all possible channel realizations. It should be noted that it is not always possible to achieve ergodic capacity. It can be achieved only when the codeword is spanned over all the possible channel realizations. Thus, it is a suitable metric to study the channel capacity in fast fading environments, where the codeword length or the delay constraint is longer than the channel coherence time. Interested readers can refer to [20] for a detailed discussion on this subject.

In this work, we will assume fast fading and will concentrate only on the ergodic capacity. It should be noted that the words *ergodic capacity* and *capacity* will be used interchangeably in this thesis.

### 2.4.3 Numerical Results of MIMO Capacity

To gain insight into the ergodic capacity of the MIMO channel, we consider the following power allocation strategies:

- **Optimal MIMO:** In this case, we assume that the optimal power allocation solution is found by employing ‘water-filling strategy’. Since the optimization problem is convex, this solution can also be found by a simple gradient-based search.
- **Beamforming:** In this case, we assume that the Tx is forced to transmit at the maximum power over the strongest Eigen-mode.
- **Equal Power Allocation:** In this case, we assume that the Tx node distributes equal power over all the available Eigen-modes, irrespective of their strengths.

In addition to these MIMO cases, we also consider a SISO case as a bench-mark to compare the capacities. These cases are simulated in two channel scenarios: normalized-channel and Rayleigh-faded channel. It should be noted that the MIMO channel model described earlier in this chapter inherently assumes Rayleigh fading because of the Kronecker assumption. This can be inferred from the fact that the  $tr(\Sigma) \neq n_r$  in general for any particular instantiation of the channel; it is the expected value that tends to  $n_r$ . In addition to this standard channel model, we consider a normalized-channel model where the net gain of all the Eigen-channels is fixed to  $n_r$ , i.e.,  $tr(\Sigma) = n_r$ , for each channel realization. This can be achieved by multiplying  $\sqrt{\frac{n_r}{tr(\Sigma)}}$  to the channel matrix  $\mathbf{H}$ . This model will be helpful in understanding the relative strengths of the Eigen-channels later in this chapter. This model is considered just to gain insight and won't be considered in the rest of our work. This normalized MIMO channel model is analogous to the SISO AWGN channel in the sense that the net channel strength remains constant over all channel realizations.

At this point, it is important to note that Rayleigh fading does not degrade the ergodic channel capacity significantly [78]. We highlight this point by comparing the capacity of a SISO channel in Rayleigh-fading and no-fading scenarios in Fig. 2.11. Thus we expect the ergodic capacity of the MIMO channel to be almost similar in the Rayleigh-faded and normalized-channel scenarios. Interested readers can go through [21], [78] for further discussion on the subject.

### Perfectly Uncorrelated Case ( $\rho = 0$ )

In this case, we assume that the antennas at both the Tx and Rx nodes are perfectly uncorrelated ( $\rho = 0$ ). We consider  $2 \times 2$  and  $4 \times 4$  MIMO systems along with a SISO system to understand the effect of the number of antennas on the MIMO link capacity. The numerical results for the normalized-channel and Rayleigh-fading cases are presented in Fig. 2.12 and Fig. 2.14, respectively. As expected, we observe a significant increase in the link capacity with the increase in the number of antennas. The asymptotic slopes of



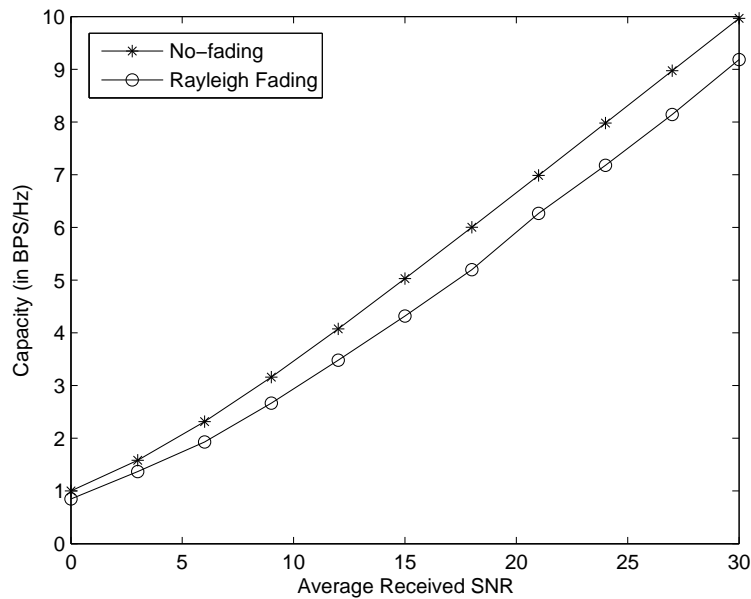


Figure 2.11: Comparison of the ergodic capacities of a single antenna link in no-fading and Rayleigh fading environments.

the capacity plots signify the diversity gains in various MIMO systems. As expected, the  $4 \times 4$  MIMO system achieves maximum diversity gain amongst the systems considered in this study.

Comparing the optimal results with beamforming and equal power allocation results, we note that it is optimal to transmit all the power in the strongest mode (beamforming) in the low SNR regime and distribute power equally over all the Eigen-modes in the high SNR regime. Optimality of beamforming in the low SNR regime is not evident from the results presented in Fig. 2.12. Therefore, we plot the ergodic capacity results on a log-scale in Fig. 2.13 to highlight the low SNR regime, where beamforming is clearly observed to be optimal. We further note that the capacity achievable by performing beamforming is marginally greater than the capacity of the SISO link. The asymptotic slopes of the MIMO beamforming and SISO plots are nearly same, thereby suggesting that both the systems have same number of parallel channels. The slight difference in capacity is due to the SNR gain in the MIMO

system due to the presence of multiple antennas. All these trends are observed in both the normalized-channel and Rayleigh-faded cases, with the only difference that the achievable capacity in Rayleigh-fading case is slightly less than the capacity in the normalized-channel case. This reiterates the fact that Rayleigh fading does not degrade the ergodic capacity of a channel significantly.

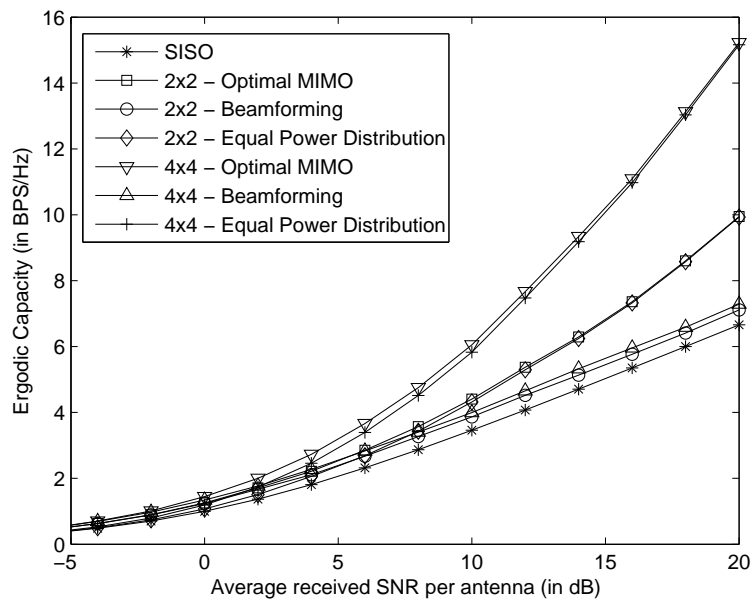


Figure 2.12: Comparison of the optimal ergodic capacity with the ones achievable with beamforming and equal power distribution in a perfectly uncorrelated channel (Normalized-channel,  $\rho = 0$ ).

### Partially Correlated Case ( $\rho = 0.5$ )

Now we consider a case, where antennas at both the Tx and Rx nodes are partially correlated with  $\rho = 0.5$ . The maximum achievable capacities in the normalized-channel and Rayleigh-fading cases are presented in Fig. 2.15 and Fig. 2.16, respectively. As expected, the diversity gain reduces in this case as compared to the perfectly correlated case. However, there is still a significant improvement in the MIMO capacity as we increase the number of antennas.

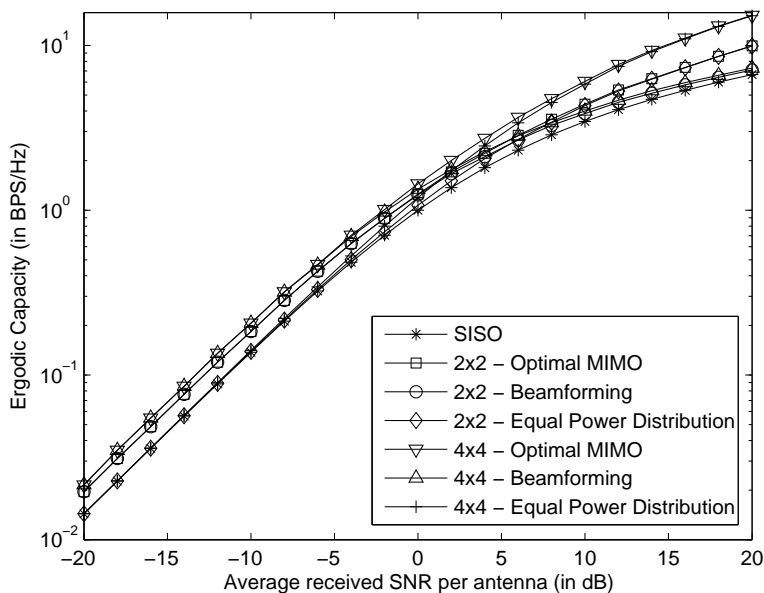


Figure 2.13: Comparison of the optimal ergodic capacity with the ones achievable with beamforming and equal power distribution in a perfectly uncorrelated channel (Normalized-channel,  $\rho = 0$ , Log Scale).

Beamforming is observed to be optimal in the low SNR regime and equal power allocation in the high SNR regime. As observed in the previous case, all the results are similar for the normalized-channel and Rayleigh-fading cases, with the only difference being the slight reduction in ergodic capacity in the Rayleigh-fading case.

### Nearly Perfect Correlation ( $\rho = 0.95$ )

We now consider a case where the antennas at both the Tx and Rx nodes are nearly perfectly correlated with  $\rho = 0.95$ . It should be noted that a perfectly correlated case reduces to a SISO case with a SNR gain due to the presence of multiple antennas. Due to this reason, there is only one spatial channel available most of the time. This idea is illustrated in the numerical results presented for the normalized-channel and Rayleigh-fading cases in Fig. 2.17 and Fig. 2.18, respectively. The optimal capacity in both the  $2 \times 2$  and the  $4 \times 4$  MIMO

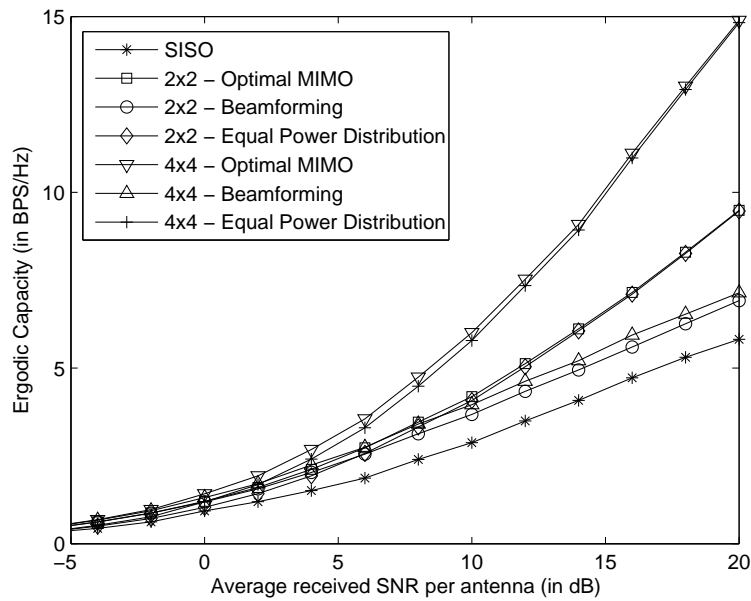


Figure 2.14: Comparison of the optimal ergodic capacity with the ones achievable with beamforming and equal power distribution in a perfectly uncorrelated channel (Rayleigh fading,  $\rho = 0$ ).

cases is observed to be slightly higher than the SISO capacity due to the SNR gain. As in the earlier cases, beamforming is observed to be optimal in the low SNR regime and equal power distribution capacity tends towards the optimal capacity in the high SNR regime. These trends are observed both in the normalized-channel and Rayleigh-fading cases.

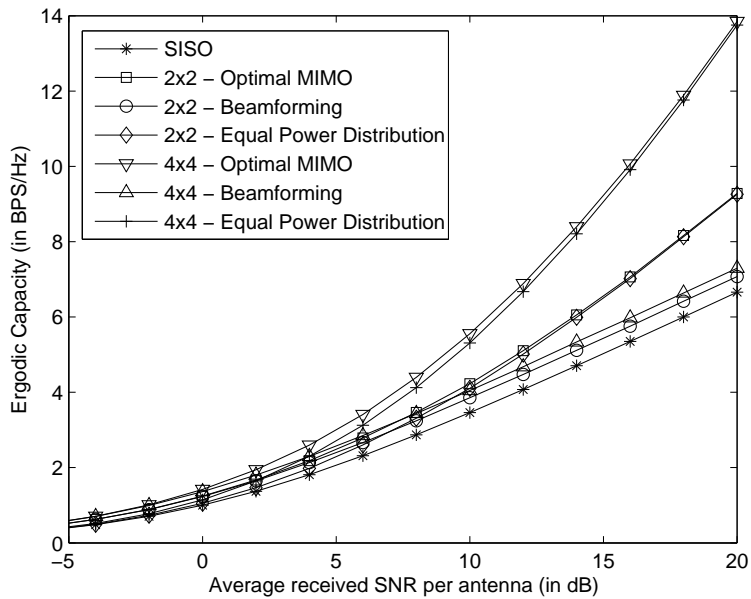


Figure 2.15: Comparison of the optimal ergodic capacity with the ones achievable with beamforming and equal power distribution (Normalized channel,  $\rho = 0.5$ ).

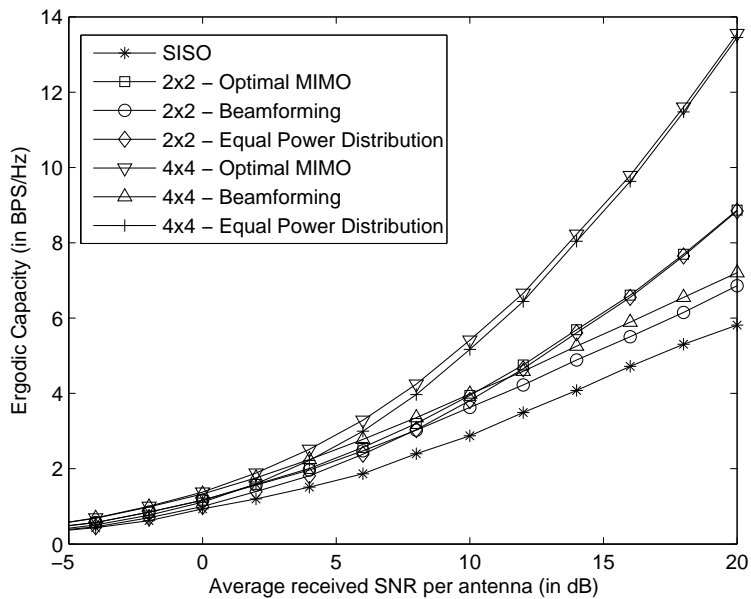


Figure 2.16: Comparison of the optimal ergodic capacity with the ones achievable with beamforming and equal power distribution (Rayleigh fading,  $\rho = 0.5$ ).

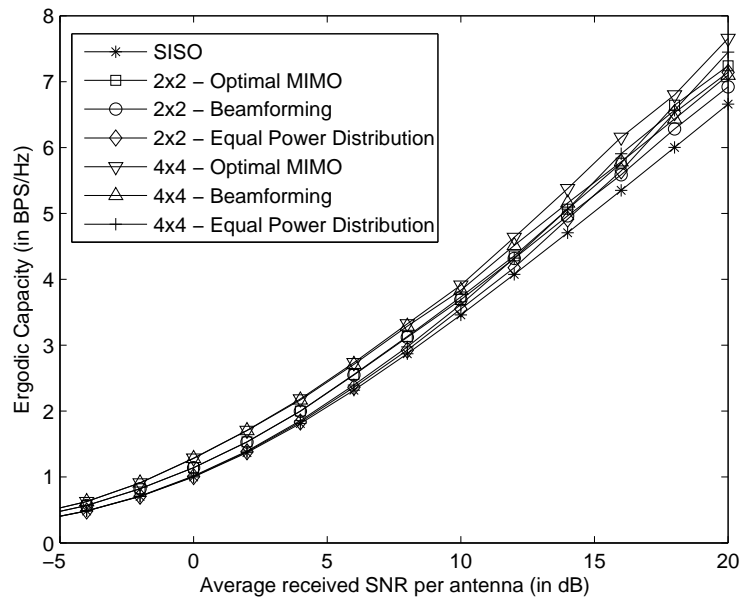


Figure 2.17: Comparison of the optimal ergodic capacity with the ones achievable with beamforming and equal power distribution (Normalized channel,  $\rho = 0.95$ ).

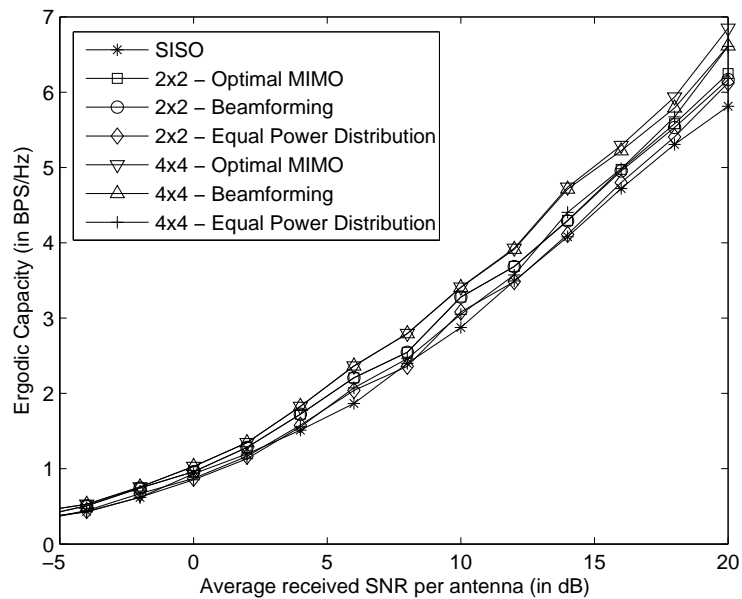


Figure 2.18: Comparison of the optimal ergodic capacity with the ones achievable with beamforming and equal power distribution (Rayleigh fading,  $\rho = 0.95$ ).

### 2.4.4 Distribution of the Eigen-modes of the MIMO Channel

In this section, we study the distribution of the Eigen-modes for an isolated MIMO link. Understanding of the relative strengths of Eigen-modes will be helpful in analyzing the capacity results of the ICs studied in the subsequent chapters. For this study, we consider a fixed MIMO link where the distance between the Tx and Rx nodes is fixed at  $d_{max}/2$ . As in the previous section, we consider two main channel scenarios: normalized-channel and Rayleigh-fading. We study the distributions of the strongest and the weakest Eigen-modes in  $2 \times 2$  and  $4 \times 4$  MIMO systems to gain insight into the simulation model considered in this work. In particular, the normalized-channel model will help us understand the relative strengths of the two Eigen-modes. The strength of the Eigen-mode is given by the corresponding Eigen-value of  $\mathbf{H}\mathbf{H}^\dagger$ . Thus, we perform Eigen-Value Decomposition of  $\mathbf{H}\mathbf{H}^\dagger$  and denote the largest Eigen-value by  $\lambda_{max}$  and smallest by  $\lambda_{min}$ . Thus, the numerical study of the distributions of  $\lambda_{max}$  and  $\lambda_{min}$  is the main goal of this section.

#### $2 \times 2$ MIMO System

We begin our discussion by considering the distribution of  $\lambda_{max}$  and  $\lambda_{min}$  in a  $2 \times 2$  MIMO system for various levels of antenna correlation. Since, there are only two possible Eigen-channels, the stronger mode corresponds to  $\lambda_{max}$  and the weaker mode to  $\lambda_{min}$ . As noted earlier, the expected value of  $\lambda_{max} + \lambda_{min}$  should be equal to  $n_r = 2$ , in general. For the normalized-channel case, this sum is forced to be 2 for each channel instantiation. The distributions of  $\lambda_{max}$  and  $\lambda_{min}$  for the normalized-channel case are presented in Fig. 2.19 and Fig. 2.20, respectively. It is straightforward to note that the distributions of  $\lambda_{max}$  and  $\lambda_{min}$  are complementary, since their sum is forced to be equal to 2. As expected, the likelihood of  $\lambda_{max}$  achieving high values increases with the increase in antenna correlation. At  $\rho = 0.95$ , we note that it is highly likely for  $\lambda_{max}$  to achieve a value of 2. Likewise, the probability of  $\lambda_{min}$  achieving very low values increases with the increase in the antenna correlation.  $\lambda_{max}$  and  $\lambda_{min}$  achieve values of 2 and 0, respectively, for the perfectly correlated case. Physically,

this means that there would be a single Eigen-channel with a SNR gain of 2.

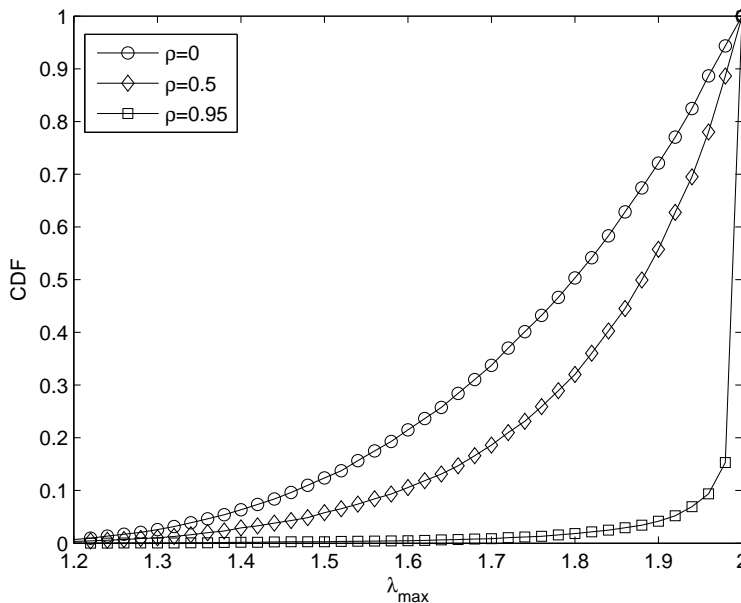


Figure 2.19: Distribution of the maximum Eigen value of  $\mathbf{H}\mathbf{H}^\dagger$  in a  $2 \times 2$  MIMO link for several values of antenna correlation (Normalized-channel case).

The distributions of  $\lambda_{max}$  and  $\lambda_{min}$  for the Rayleigh fading case are presented in Fig. 2.21 and Fig. 2.22, respectively. In this case too, the probability of  $\lambda_{max}$  achieving very high values increases with the increase in antenna correlation. Contrary to the previous case,  $\lambda_{max}$  can also achieve values greater than 2 due to the presence of fading. The distribution of  $\lambda_{min}$  in the Rayleigh fading case is quite similar to the normalized-channel case, with the only difference that the CDF plots are steeper towards the lower values of  $\lambda_{min}$ , thereby suggesting that the probability of achieving lower values is higher in this case than in the normalized-channel case. Thus the presence of Rayleigh fading forces  $\lambda_{max}$  towards relatively higher values and  $\lambda_{min}$  towards relatively lower values (as compared to the normalized-channel case).



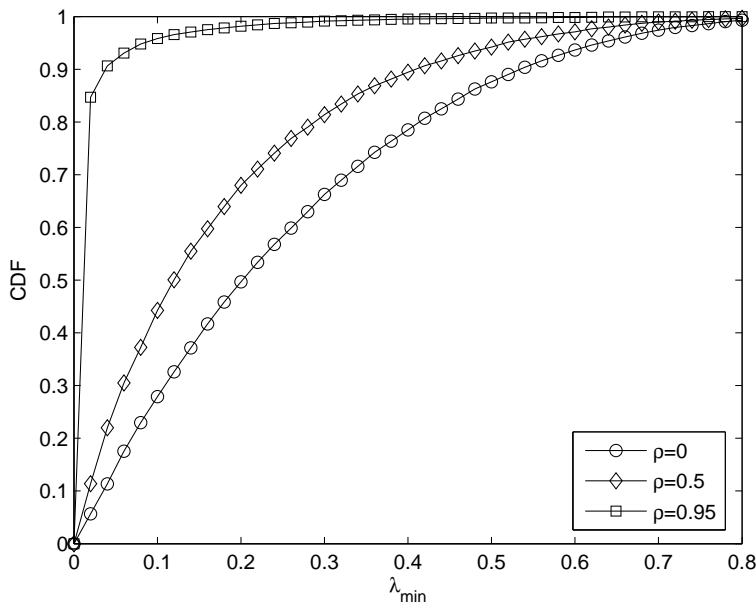


Figure 2.20: Distribution of the minimum Eigen value of  $\mathbf{H}\mathbf{H}^\dagger$  in a  $2 \times 2$  MIMO link for several values of antenna correlation (Normalized-channel case).

#### $4 \times 4$ MIMO System

We now study the distributions of the strongest and weakest Eigen-modes in a  $4 \times 4$  MIMO system. As discussed earlier,  $4 \times 4$  MIMO system has 4 Eigen-channels. The largest Eigen-value of  $\mathbf{H}\mathbf{H}^\dagger$  corresponds to the strongest Eigen-mode and is denoted by  $\lambda_{max}$ . Similarly, the smallest Eigen-value corresponds to the weakest Eigen-mode and is termed as  $\lambda_{min}$ . The other two intermediate Eigen-values are not considered for the simplicity of presentation.

The distributions of  $\lambda_{max}$  and  $\lambda_{min}$  in the normalized-channel case are presented in Fig. 2.23 and Fig. 2.24, respectively. In this case, the sum of the Eigen-values of  $\mathbf{H}\mathbf{H}^\dagger$  is forced to  $n_r = 4$ . The probability of  $\lambda_{max}$  achieving high values increases with antenna correlation. At  $\rho = 0.95$ ,  $\lambda_{max}$  achieves value of 4 with a very high probability, thereby suggesting that there is only a single spatial channel present in this MIMO setup. On the other hand, the probability of  $\lambda_{min}$  achieving very small values increases with the increase in antenna

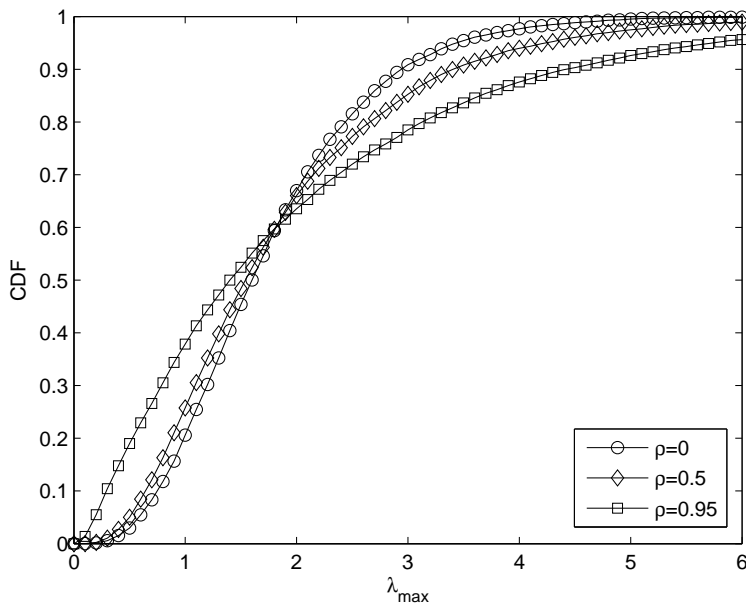


Figure 2.21: Distribution of the maximum Eigen value of  $\mathbf{H}\mathbf{H}^\dagger$  in a  $2 \times 2$  MIMO link for several values of antenna correlation (Rayleigh-fading case).

correlation. At  $\rho = 0.95$ ,  $\lambda_{min}$  achieves value of 0 with a very high probability.

The distributions of  $\lambda_{max}$  and  $\lambda_{min}$  in the Rayleigh-fading case are presented in Fig. 2.25 and Fig. 2.26, respectively. Due to fading, the sum of all the Eigen-values of  $\mathbf{H}\mathbf{H}^\dagger$  is not necessarily equal to  $n_r = 4$  for each channel instantiation. Thus, the value of  $\lambda_{max}$  is not upper bounded by 4. We observe this in the distribution where  $\lambda_{max}$  achieves much higher values than 4, especially when the antenna correlation is high. In fact, the probability of  $\lambda_{max}$  achieving higher values increases with the antenna correlation. On the other hand, the distribution of  $\lambda_{min}$  becomes steeper towards the lower values as compared to the normalized-channel case. This means that  $\lambda_{min}$  achieves lower values for all the cases as compared its counterpart in the normalized-channel case. Likewise, the probability of  $\lambda_{min}$  achieving lower values increases with the increase in antenna correlation.

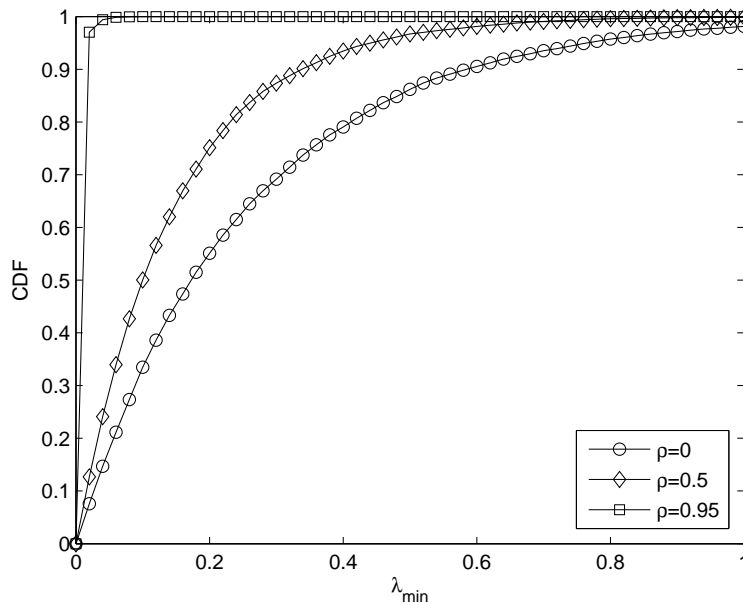


Figure 2.22: Distribution of the minimum Eigen value of  $\mathbf{H}\mathbf{H}^\dagger$  in a  $2 \times 2$  MIMO link for several values of antenna correlation (Rayleigh-fading case).

### Summary

The distributions of  $\lambda_{max}$  and  $\lambda_{min}$  discussed for various cases in this section clearly indicate that the strengths of Eigen-modes is quite uneven in the MIMO channels. In almost all the cases, one of the Eigen-modes clearly dominates over the others. The results further indicate that the difference between the strengths of the strongest and the weakest Eigen-modes increases with the increase in the number of antennas. This observation is important from the MIMO IC perspective where the optimal power allocation will depend upon the interactions of the Eigen-modes of each user. We will discuss about this in detail in the subsequent chapters.

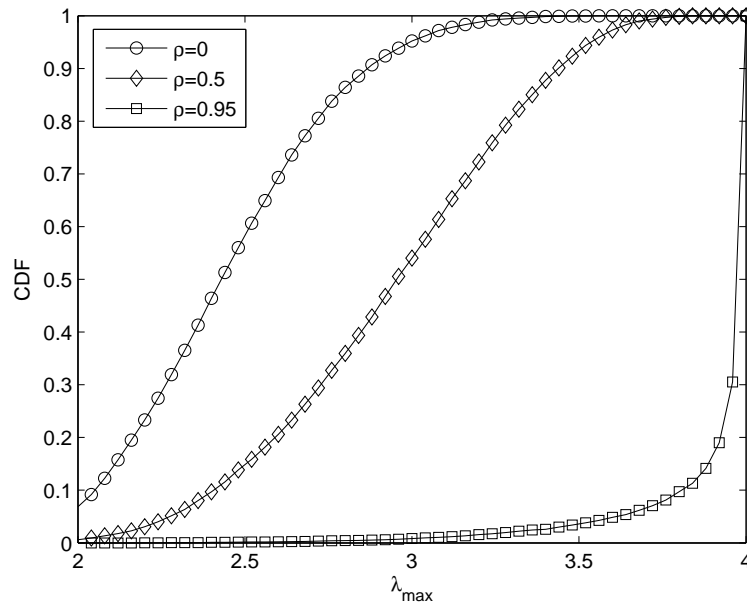


Figure 2.23: Distribution of the maximum Eigen value of  $\mathbf{H}\mathbf{H}^\dagger$  in a  $4 \times 4$  MIMO link for several values of antenna correlation (Normalized-channel case).

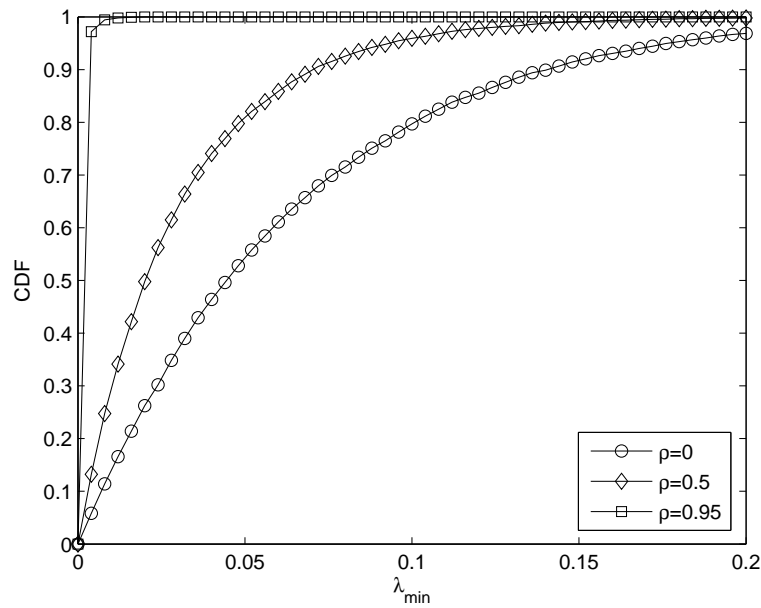


Figure 2.24: Distribution of the minimum Eigen value of  $\mathbf{H}\mathbf{H}^\dagger$  in a  $4 \times 4$  MIMO link for several values of antenna correlation (Normalized-channel case).

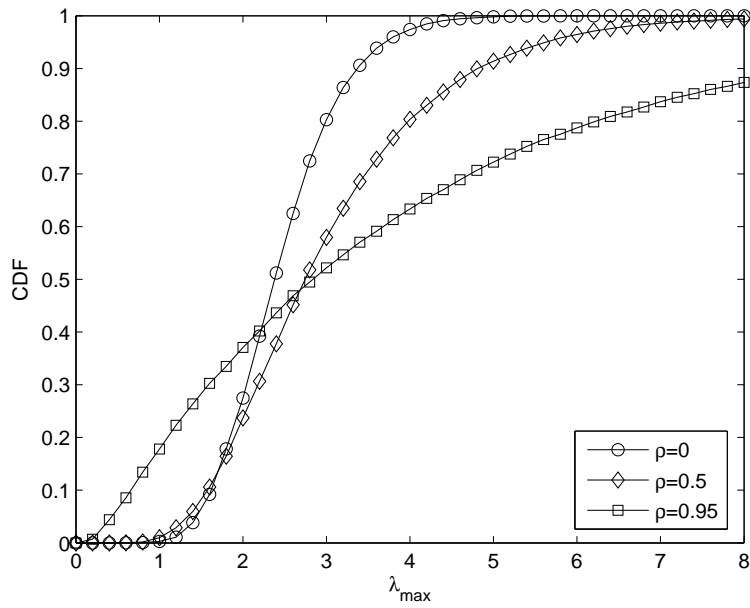


Figure 2.25: Distribution of the maximum Eigen value of  $\mathbf{H}\mathbf{H}^\dagger$  in a  $4 \times 4$  MIMO link for several values of antenna correlation (Rayleigh-fading case).

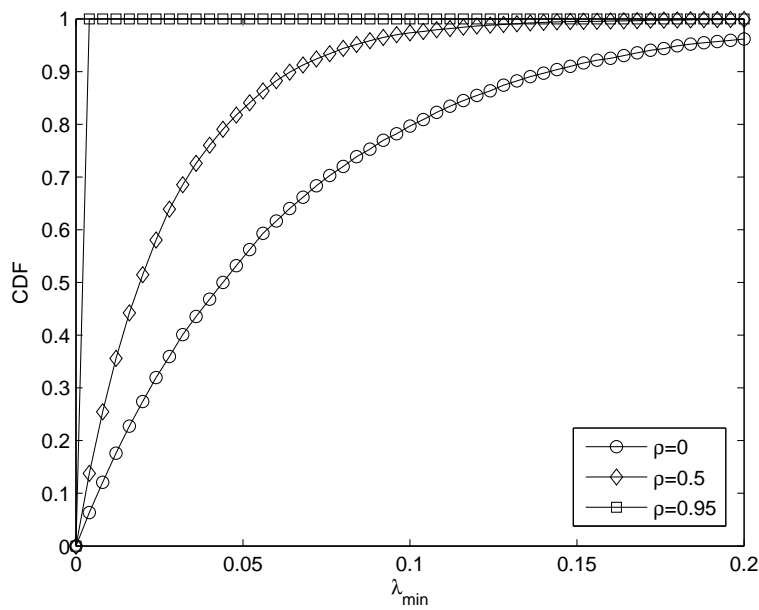


Figure 2.26: Distribution of the minimum Eigen value of  $\mathbf{H}\mathbf{H}^\dagger$  in a  $4 \times 4$  MIMO link for several values of antenna correlation (Rayleigh-fading case).

## 2.5 System Variables

For the easy reference, we list all the system variables in this separate section.

- $N$ : Number of SUs forming the interference channel.
- $N_b$ : Number of orthogonal frequency channels (bands) available for allocation to SUs.
- $n_t$ : Number of transmit antennas at each Tx node. For simplicity, we assume that all the Tx nodes have same number of antennas. However, this doesn't limit the scope of our analysis and the developed techniques can be extended easily to the general case where each Tx node has a different number of transmit antennas.
- $n_r$ : Number of receive antennas at each Rx node. In this case too, we assume that that all the Rx nodes have same number of receive antennas.
- $P_{max}$ : Maximum total power allowed to be transmitted by each Tx node over all frequency bands and over all transmit antennas.
- $\eta$ : Path loss factor.  $\eta$  is assumed to be 3 unless explicitly mentioned in the specific simulation case.
- $d_{max}$ : Maximum allowable distance between the Tx and Rx node of each SU. This is chosen such that the minimum received signal to noise ratio (SNR) per receive antenna in the absence of shadowing and fading is  $SNR_{min}$ .
- $SNR_{min}$ : As explained above, this is the minimum received SNR per antenna in the absence of shadowing and fading.
- $MUI$ : Multiuser Interference factor.  $MUI$  represents the expected number of Rx nodes within a circle of radius  $d_{max}$  centered at any Tx node assuming a constant density.

- $L$ : Length of the side of the square (area of interest). It can be calculated as  $L = \sqrt{N\pi d_{max}^2/MUI}$ .
- $\sigma$ : Standard deviation of the log-normal shadowing in dB.
- $\sigma_N^2$ : Noise power per receive antenna.
- $\rho$ : Magnitude of the correlation between any two adjacent antennas at the Tx node or the Rx node.

## 2.6 Summary of the Chapter

In this chapter, we have introduced the system model used in this research. After discussing the key underlying assumptions of our work, we discussed the two main parts of our simulation model: the procedure for placing the nodes and the channel model. While explaining the node placement procedure, we introduced two important variables,  $MUI$  and  $SNR_{min}$ , to control the level of interference and noise powers, respectively.  $MUI$  controls the density of the nodes and represents the expected number of Rx nodes in a circle of radius  $d_{max}$  centered at any Tx node.  $SNR_{min}$  represents minimum received SNR per receive antenna. We then studied the effect of changing these key parameters on the distributions of SIR, SNR and SINR. After introducing the simulation model, we studied the capacity of an isolated MIMO link for various levels of antenna correlation in normalized-channel and Rayleigh-fading environments. We have further shown that the presence of Rayleigh fading does not degrade the capacity significantly. After studying the capacity of a MIMO link, we studied the strengths of the Eigen-modes of the MIMO channel. We have shown that the distribution of Eigen-modes is quite uneven and the strongest mode dominates over the rest of them in almost all the cases. The difference in the strengths of the strongest and weakest modes increases further with an increase in the number of antennas. This result is quite important from a MIMO IC perspective, where the optimal power allocation depends upon the interaction between the Eigen-modes of various users.

# Chapter 3

## Single Antenna Interference Channels

### 3.1 Introduction

The idea of spectrum sharing is central to wireless communication systems. In a general sense, the need of spectrum sharing arises when multiple wireless systems co-exist in the same area and transmit over the same frequency band(s). The performance of these wireless systems is coupled to each other due to the mutual interference. Increasing the transmit power of one user, in addition to increasing its link capacity, also increases the interference perceived by the other users. This coupling effect makes the analysis of interference channels quite challenging. The problem of characterizing the capacity of interference channels is open for more than 40 years.

The study of interference channels from an information theoretical perspective was initiated by Shannon [5]. Fundamental lower and upper bounds to the capacity region of a two user interference channel were proposed in [7] - [8]. The exact characterization of this region is still an open problem. The only case in which we have a good insight is the high interference case, in which the interference signal is higher than the intended signal [6]. In this case, the interference is so high that it can be successfully decoded by the receiver and then canceled



from the received signal. The best known strategy for the other cases, where interference is not very strong, is due to Han and Kobayashi [10]. This strategy involves the splitting of the transmit information into two parts: private information and common information. The private information is meant to be decoded at the intended receiver and the common information can be decoded at any receiver. The common information can be used to cancel off the part of the interference, while the private information from other users can be treated as noise. In some recent developments [11]-[13], a simple Han-Kobayashi technique is shown to achieve rates within 1 bit/sec/Hz of the two-user interference channel capacity for all channel parameters. The key feature of their proposed scheme is that the power of the private information of each user should be set such that it is received at the level of the Gaussian noise at the other receiver. In this way, the interference caused by the private information has a small effect on the other link beyond the impairment that is already caused by the noise.

To work around this problem, some researchers have taken an alternate approach and mapped this capacity characterization problem to the problem of characterizing the degrees of freedom of the IC [27], [28]. An IC is said to have  $D$  degrees of freedom, if the sum-rate ( $SR$ ) can be expressed as:

$$SR = D \log(SNR) + o(\log(SNR)), \quad (3.1)$$

where  $\log(SNR)$  represents the capacity of an isolated user,  $o(\log(SNR))$  is the residual capacity term and  $SNR$  is the signal-to-noise ratio. It should be noted that the  $o(\log(SNR))$  term becomes negligible when the  $SNR$  is very high and thus  $D \log(SNR)$  provides a tight upper bound to the achievable sum-rate. The most remarkable result of these studies is that an  $N$ -user IC has  $N/2$  degrees of freedom per orthogonal spectral, spatial or temporal slot and can thus achieve at least half the sum-rate of its no-interference counterpart for any number of interferers [28]. It has been further shown that these  $N/2$  degrees of freedom are achievable by Interference Alignment (IA). The basic idea of IA is to pre-code the transmit signal such that it aligns with the interference signals at all receivers where it acts as interference and is orthogonal to interference at the desired receiver. Several pre-coding methods

are shown to achieve IA for single antenna interference channels with time or frequency selectivity [29], [30].  $N$ -user MIMO interference channels are also shown to achieve  $N/2$  degrees of freedom when the channels have infinite selectivity [31]. However, it is difficult to find the analytical solutions to the interference alignment problems in general and even the feasibility of interference alignment over a limited number of signalling dimensions is an open problem [32]-[33]

IA is not the main focus of this chapter. We will return to this idea in a later chapter. The main goal of this chapter is to study the maximum achievable sum-rate of a single antenna IC in the light of the current system model by treating interference as Gaussian noise. This problem essentially reduces to a power control optimization problem [34]. The goal thus is to find the optimal value of power to be transmitted by each user forming the IC. The problem of power control has been traditionally studied with the aim of achieving a desired signal to noise plus interference level at all the users [35]-[37]. However, due to the advancement in coding and modulation with power control [38], [39], throughput maximization became a more important goal. The problem of finding the optimal power allocation to maximize the uplink information capacity in a single-cell was studied in [40]. It was shown that the main characteristic of the optimal scheme is that the users with the better channels are allowed to transmit at a higher power and the ones with worse channels are allowed to transmit at a lower power. The work was extended to a two-cell scenario in [41], where binary power control was reported to be optimal in a two-user scenario. Binary power control in a two-user scenario leads to only two optimal strategies: 1) both the users transmit at the maximum power, and 2) one user transmits at the maximum power and the other at the minimum power. It should be noted that a two-cell scenario is essentially a two-user interference channel if we assume that there is only one transmitter and one receiver in each cell. Binary power control is also reported to be optimal in a two-user IC in [42], where an asymptotic analysis for a general  $N$ -user IC is also carried out to show that the average sum-rate scales at least as  $\log(N)$  in a Rayleigh fading channel. In some recent works, binary power control is shown to be optimal in the symmetric  $N$ -user ICs and some specific scenarios of general

$N$ -user ICs [44], [45]. However, the exact solution of a general  $N$ -user power control problem is difficult to find analytically because of its non-linear non-convex nature [46]. Numerical optimization algorithms with guaranteed convergence to the global solution are recently reported in [34], [47]. The latter is based on the generalized linear fractional programming and the former on the coupling of the branch and bound strategy and the reformulation and linearization technique.

In this chapter, we will revisit some of the above mentioned results in the light of the present system model. The main goal of this chapter is to understand the effect of various system parameters on the sum-rate and to develop bench-mark principles that will help in analyzing the sum-rates of more complicated single-band and multi-band MIMO ICs in the subsequent chapters.

We begin our study by formulating the problem of maximizing the sum-rate of a single antenna IC in the next section.

## 3.2 Maximum Sum-Rate of Single Antenna IC

We consider the same general system model that we developed for MIMO ICs in the previous chapter by setting  $n_t = n_r = 1$ . We assume that there are  $N$  users trying to access single frequency band ( $N_b = 1$ ). Each Rx node is capable of just single user detection and treats signals from the other users as Gaussian noise. We denote the channel gain from the Tx node of  $i^{th}$  user to the Rx node of  $j^{th}$  user by  $h_{ij}$ . It should be recalled that the channel gain term accounts for path-loss, log-normal shadowing and Rayleigh fading. Let the transmit power of  $i^{th}$  Tx node be  $P_i$ , where  $P_i \leq P_{max}$ . Received Signal to Noise Ratio (SINR) for  $i^{th}$  user can be expressed as:

$$SINR_i = \frac{P_i |h_{ii}|^2}{\sigma_N^2 + \sum_{\substack{j=1 \\ j \neq i}}^N P_j |h_{ji}|^2}, \quad (3.2)$$

where  $\sigma_N^2$  is the noise power. Assuming that the Tx node is using a Gaussian codebook, the link capacity of the  $i^{th}$  user can be expressed as:

$$C_i = \log_2(1 + SINR_i). \quad (3.3)$$

The goal now is to find the maximum value of  $\sum_{i=1}^N C_i$  subject to the power constraints of each user. The optimization problem can be formulated as:

$$\begin{aligned} \max \quad & \sum_{i=1}^N C_i, \\ \text{s.t.} \quad & C_i = \log_2(1 + SINR_i); \\ & SINR_i = \frac{P_i |h_{ii}|^2}{\sigma_N^2 + \sum_{\substack{j=1 \\ j \neq i}}^N P_j |h_{ji}|^2}; \\ & P_i \leq P_{max}, \forall i; \\ & 1 \leq i \leq N. \end{aligned} \quad (3.4)$$

This optimization problem is known to be non-linear, non-convex and hence difficult to solve analytically for general ICs [34]. Branch and Bound (BB) was coupled with Reformulation and Linearization Technique (RLT) in [34] to develop BB/RLT global optimization algorithm to find the provably optimal solution to this problem. Interested readers can refer to [34] and [59] for further details about the algorithm. We will discuss BB/RLT in detail when we linearize and reformulate sum-rate maximization problem of single-band and multi-band MIMO ICs in the coming chapters. It should be noted that the linearization of the sum-rate maximization problem of MIMO ICs is significantly more involved than that of SISO ICs. Moreover, they encompass SISO ICs as a special case when  $n_t$  and  $n_r$  are both fixed at 1. For the time being, it is enough to note that the numerical results presented in this chapter are provably optimal (found through the BB/RLT algorithm). It should also be noted that the near-optimal results can be found using gradient-based search by solving the sum-rate maximization problem multiple times with random starting point and combining the results. In this chapter, we will provide some insight into the number of random starting points required to approach the optimal results.

The main goal of this chapter is to understand the effect of various system parameters, especially  $SNR_{min}$  and  $MUI$  factor, on the optimal power allocation strategies that max-

imize the sum-rate of a SISO IC. In particular, we will show that the relative strengths of interference and noise determine the optimal transmission strategy in SISO ICs. Since it is the relative strength that fundamentally affects the optimal transmission strategy, it can be argued that the problem can be studied by varying one of the two parameters ( $SNR_{min}$  and  $MUI$  factor) while keeping the other fixed. In other words, increasing  $SNR_{min}$  while keeping  $MUI$  factor fixed, and increasing  $MUI$  factor while keeping  $SNR_{min}$  fixed, both lead to higher interference power relative to noise power. To validate this point, we will study the effect of changing both the  $SNR_{min}$  and  $MUI$  on the sum-rate in the following sections.

### 3.3 Two-User Single-Band SISO IC

In this section, we study the optimal power allocation strategy in a two-user single band SISO IC. We first consider a symmetric SISO IC, as shown in Fig. 3.1. The effect of the random geometry on the sum-rate will be studied in a later section of this chapter. The distance between the Tx-Rx pairs is fixed at  $d_{max}/2$  for this case. The distance between the Rx nodes (or Tx nodes) of the two users is fixed at  $L/2$ , where  $L$  is the side of the square area of interest in which we place the Tx-Rx nodes. For the purpose of fixing the ideas, we keep the model simple and do not consider fading or shadowing. We will study the effect of fading on the optimal sum-rate in a later section of this chapter. To gain insight into the optimal power allocation, we consider the following five transmission strategies in this study:

- **Optimal Sum-Rate:** In this case, we find the optimal power allocation by solving the sum-rate maximization problem. This will act as a benchmark case to determine which of the specific transmission strategies considered in this case are optimal in different operating scenarios.
- **Max Power Sum-Rate:** In this case, both the users transmit at their maximum power and there is no optimization involved.

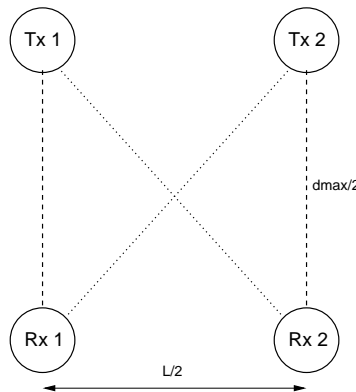


Figure 3.1: Two-User Symmetric SISO IC.

- **One Transmitting User:** In this case, one of the two users transmits at the maximum power and the other user is just turned off. Please note that in the absence of fading either of the two users can transmit without affecting the net sum-rate. However, the selection of the user is critical when fading is considered.
- **Special Case 1:** In this special case, one of the two users transmit at the maximum power and the other user transmits at 50% of the maximum power. Again, the choice of user for either role is immaterial in the case when fading is not considered.
- **Special Case 2:** In this special case, one of the two users transmit at the maximum power and the other user transmits at 10% of the maximum power.

### 3.3.1 Effect of $SNR_{min}$

We first study the effect of  $SNR_{min}$  on the sum-rate of the two-user SISO IC. Interference power is kept constant by fixing the MUI factor at 1.

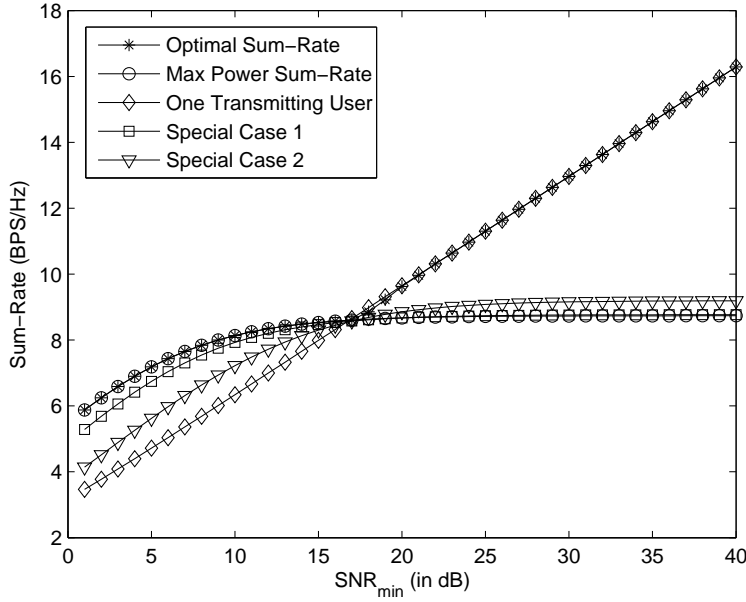


Figure 3.2: Numerical results of the sum-rate for various values of  $SNR_{min}$  in the two-user symmetric IC ( $N = 2$ ,  $N_b = 1$ ,  $MUI = 1$ , No fading).

**Note:**

It should be noted that  $SNR_{min}$  is the received SNR when Tx and Rx nodes are distance  $d_{max}$  apart (assuming no shadowing or fading). It should not be confused with the actual received SNR when the Tx and Rx nodes are distance  $d$  apart, where  $d \leq d_{max}$ . By definition, the actual received SNR (say  $SNR_d$ ) is always higher than  $SNR_{min}$ . In particular, the relationship between  $SNR_d$  (in dB) and  $SNR_{min}$  (in dB) can be established as:

$$SNR_d = SNR_{min} + 10 \log_{10} \left( \frac{d_{max}}{d} \right)^\eta. \quad (3.5)$$

Since both  $SNR_d$  and  $SNR_{min}$  affect only the noise power, the sum-rate results plotted against  $SNR_{min}$  can be easily plotted against average received SNR by using the above expression. This is most useful in fixed geometries where the distance between the Tx and Rx nodes of each user is same (such as the current case). In such cases, the average received SNR (assuming maximum transmit power) is well defined and can be used to study the effect

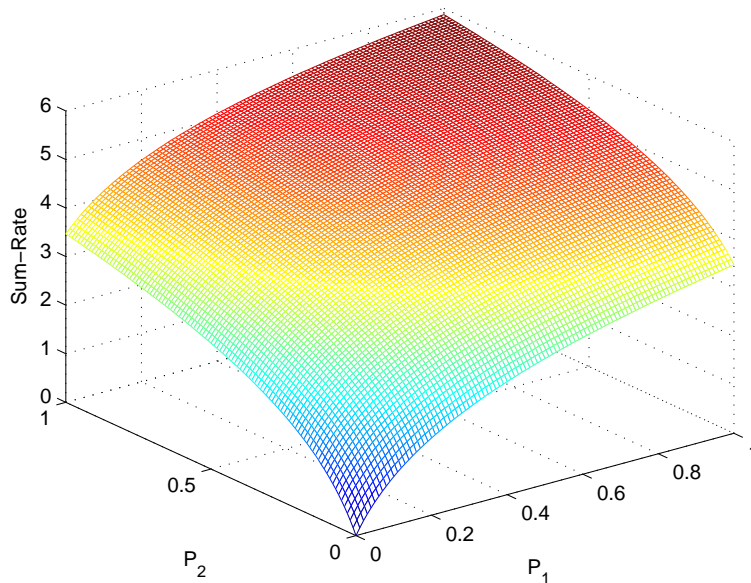


Figure 3.3: Sum-Rate region for the two-user symmetric SISO IC in the low  $SNR$  regime ( $SNR_{min} = 1dB$ ,  $N_b = 1$ ,  $MUI = 1$ , No fading).

of noise power on the sum-rate. However, we maintain consistency with the general system model defined in the previous chapter and adopt  $SNR_{min}$  as the parameter to study the effect of varying the noise power relative to the interference power on the sum-rate of the ICs.

### Optimal Sum-Rate

As noted in Fig. 3.2, it is optimal for both the users to transmit at their maximum power in the low  $SNR$  regime. However, it is optimal to turn one user off in the high  $SNR$  regime and allow only one user to access the channel. This is consistent with the analysis presented in [44]. It should be noted that this is one of the well-studied cases, where binary power control is known to be optimal. It is known that the selection of the transmission strategy depends upon the strength of the cross (or interference) channel.



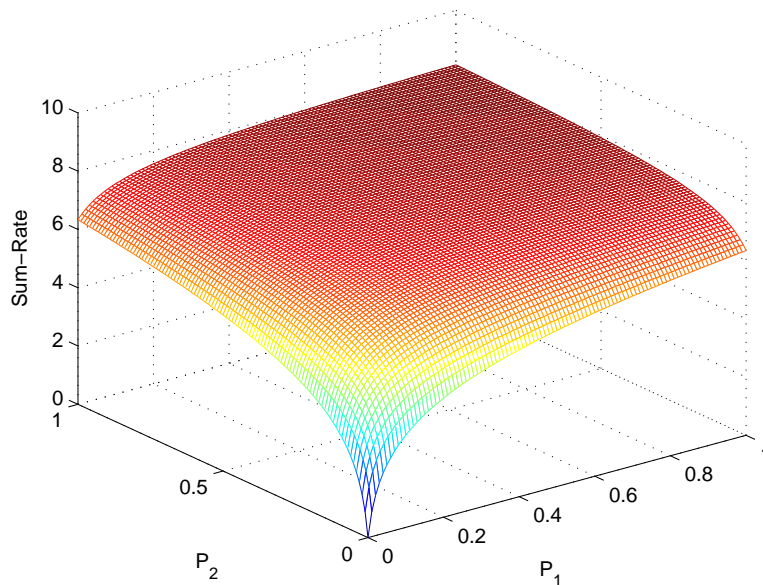


Figure 3.4: Sum-Rate region for the two-user symmetric SISO IC in the moderate  $SNR$  regime ( $SNR_{min} = 10dB$ ,  $N_b = 1$ ,  $MUI = 1$ , No fading).

In addition to the three main cases, we also consider two special cases. In the first special case, we do not simply turn off one user but allow it to transmit at half of its maximum power while allowing the other to transmit at the maximum power. We observe that the interference is dominant in this case in the high  $SNR$  regime and the achievable sum-rate is quite close to the one achieved in the interference limited max power case. To convince ourselves that it is indeed optimal to turn off the second user in the high  $SNR$  regime, we consider a second special case in which we allow one user to transmit at 10% of the maximum power while allowing the other to transmit at the maximum power. We note that the interference in this case is also too high and the sum-rate is not much better than the interference limited max power case.

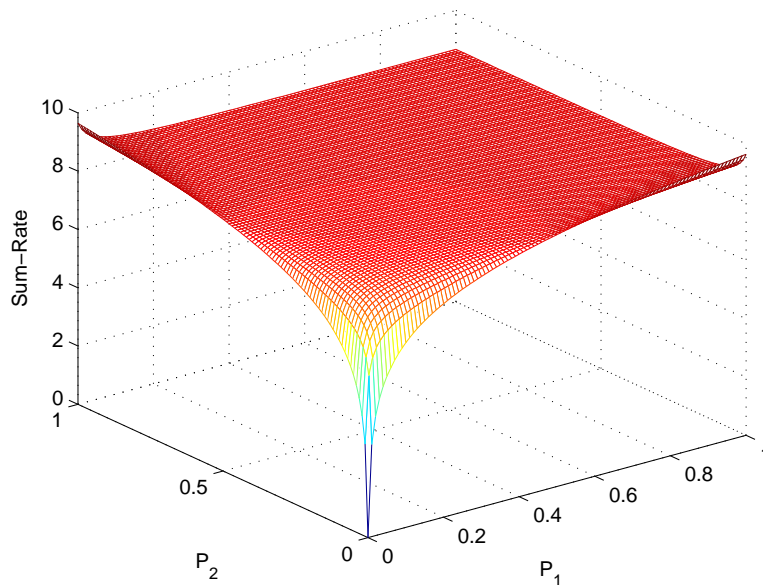


Figure 3.5: Sum-Rate region for the two-user symmetric SISO IC in the high  $SNR$  regime ( $SNR_{min} = 20dB$ ,  $N_b = 1$ ,  $MUI = 1$ , No fading).

### Rate-Region

We now characterize the rate region of this simple two-user symmetric IC. One of the aims of this characterization is to understand the underlying geometric structure (non-convex) of the rate region. We first plot the sum-rate region for the case when  $SNR_{min} = 1$  dB in Fig. 3.3. This operating point corresponds to a low  $SNR$  regime. The results clearly suggest that it is optimal for both the users to transmit at the maximum powers. A significant decrease in sum-rate is observed if one of the users reduces its transmit power.

The sum-rate region for  $SNR_{min} = 10$  dB is presented in Fig. 3.4. This corresponds to the moderate SNR regime. We observe that it still optimal for both the users to transmit at maximum power. However, there is relatively less loss in the sum-rate if one of the users reduces its power slightly.

Sum-rate region for  $SNR_{min} = 20$  dB is presented in Fig. 3.5. This operating point cor-

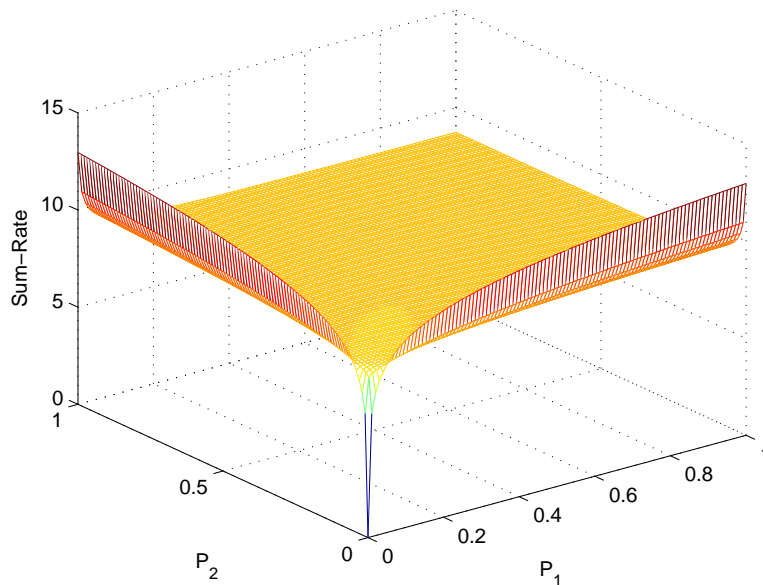


Figure 3.6: Sum-Rate region for the two-user symmetric SISO IC in very high  $SNR$  regime ( $SNR_{min} = 30dB$ ,  $N_b = 1$ ,  $MUI = 1$ , No fading).

responds to a high SNR regime. In this case, the global maximum shifts to the  $[0, P_{max}]$  and  $[P_{max}, 0]$  points. Thus, it is optimal for one of the users to transmit while keeping the other turned off. Letting both the users transmit, however, does not reduce the sum-rate significantly as compared to the optimal.

We also plot the sum-rate region for the two-user symmetric SISO IC for the very high  $SNR$  regime. For this case, we choose  $SNR_{min}$  to be 30 dB and the results are presented in Fig. 3.6. The results are quite similar to the  $SNR_{min} = 20$  dB case with the only difference that it becomes highly sub-optimal for one of the users to transmit even at a very low power while the other is transmitting at full power.

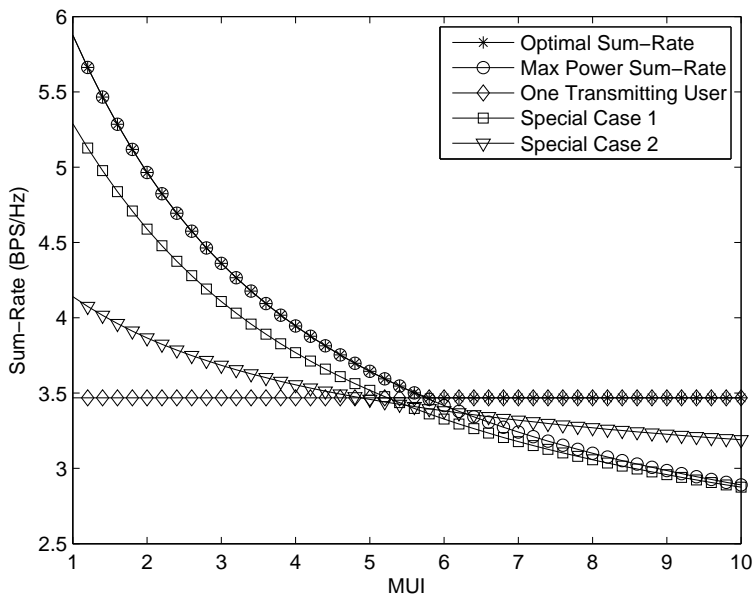


Figure 3.7: Numerical results on the sum-rate for various values of  $MUI$  factor in the two-user symmetric IC ( $N = 2$ ,  $N_b = 1$ ,  $SNR_{min} = 1$  dB, No fading).

### 3.3.2 Effect of $MUI$

We now study the effect of  $MUI$  factor on the optimal power allocation that maximizes the sum-rate of the two-user symmetric SISO IC. The noise power is kept constant in this case by fixing  $SNR_{min}$  at 1 dB. It should be recalled that  $MUI$  factor directly affects the value of  $L$  and hence determines the effective interference power. Readers should recall that  $L$  is the side of the square area of interest in which the nodes are placed. The main goal of this section is to draw analogies between the results obtained by varying  $MUI$  factor in this section and the ones obtained by varying  $SNR_{min}$  in the previous section.

#### Optimal Sum-Rate

The numerical results of the sum-rate achievable in the five transmission strategies for various values of  $MUI$  factor are presented in Fig. 3.7. Low  $MUI$  values correspond to the low

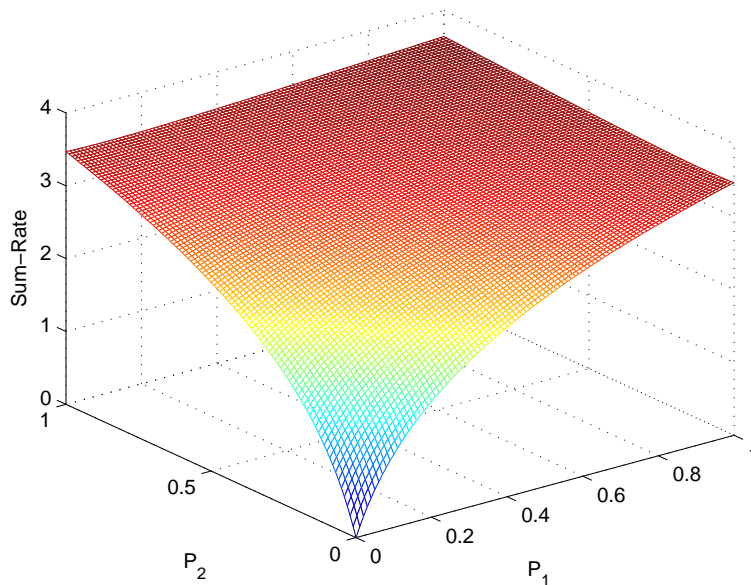


Figure 3.8: Sum-Rate region for the two-user symmetric SISO IC for  $MUI$  factor of 5 ( $SNR_{min} = 1$  dB,  $N_b = 1$ , No fading).

interference scenario because the users are relatively far apart. On the other hand, high values of  $MUI$  factor correspond to high interference scenario because the users are closely packed in the area of interest. From the simulation results, we note that the Max-power sum-rate is optimal in the low interference scenario. It is thus optimal for both the users to transmit at the maximum power for the lower values of  $MUI$  factor. We observed the same trend in the low SNR regime in the previous section. This is because the noise power is dominant over the interference power in both the low SNR and low  $MUI$  scenarios.

We further note that it is optimal to let only one user transmit in the high interference scenario. It is interesting to note that there is a brisk transition of the optimal transmission strategy from max-power to single user transmission, thus rendering binary power control optimal in this case. A similar trend was observed in the last section where it was optimal to let only one user transmit beyond a certain value of  $SNR_{min}$ . High SNR and high  $MUI$  scenarios are thus analogous because the interference power dominates the noise power in

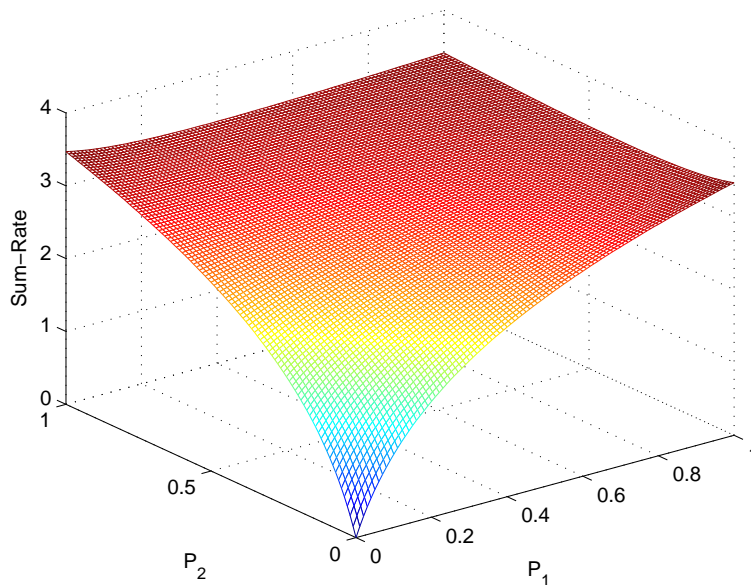


Figure 3.9: Sum-Rate region for the two-user symmetric SISO IC for  $MUI$  factor of 6 ( $SNR_{min} = 1$  dB,  $N_b = 1$ , No fading).

both of them. In addition to the three main cases, we also include results for two special cases, where we let one user transmit at the maximum power and the other at 50% and 10% of its maximum power, respectively. These cases are especially relevant in the high interference regime, where the optimal sum-rate degrades significantly when the second user is allowed to transmit even at a reduced power, while the first one is transmitting at the maximum power. We note that the sum-rate achievable in the first special case is nearly equal to the sum-rate achievable in the interference-limited Max-power transmission case. We will study this degradation in the sum-rate due to the transmission of the second user in detail by characterizing the rate-regions for various values of  $MUI$  factor.

### Rate-Region

Sum-rate region for  $MUI$  factor of 1 ( $SNR_{min} = 1$  dB) was studied in the previous section, where we noticed that it is optimal for both the users to transmit at maximum power. We

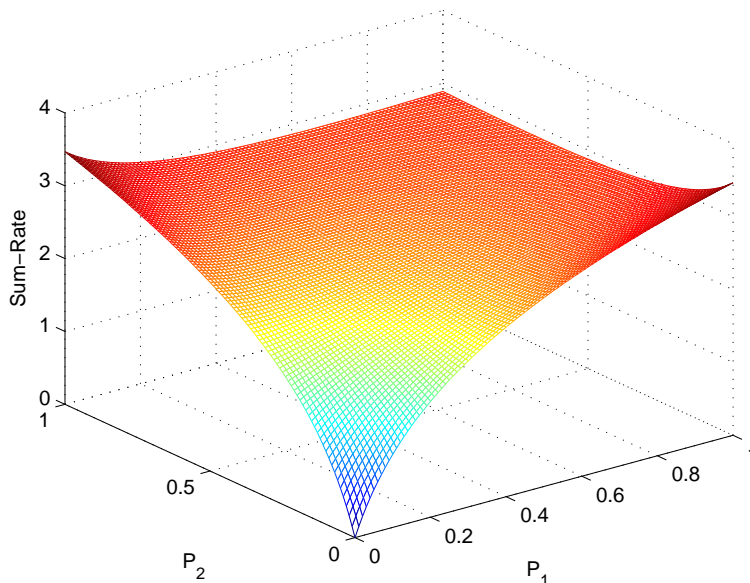


Figure 3.10: Sum-Rate region for the two-user symmetric SISO IC in high interference regime ( $SNR_{min} = 1$  dB,  $MUI = 10$ ,  $N_b = 1$ , No fading).

also noticed a significant degradation in sum-rate if one of the users reduces its transmission power. We now increase the value of  $MUI$  factor to 5 and present the resulting sum-rate region in Fig. 3.8. It is observed that there is negligible degradation in sum-rate if we reduce transmit power of one user. In other words, the max-power sum-rate (optimal) is just slightly better than the single user transmission. This result can be verified from the sum-rate plots presented in Fig. 3.7, where we notice that  $MUI = 5$  is quite close to the cross-over point after which single user transmission is optimal.

To gain further insight, we now consider the sum-rate region for  $MUI = 6$  in Fig. 3.9. It should be noted that  $MUI = 6$  is right next to the cross-over point and single user transmission is optimal in this regime. We note the same trend in the sum-rate region, where small peaks emerge at  $[0, P_{max}]$  and  $[P_{max}, 0]$ , thereby suggesting that it is optimal to turn off one user and let the other transmit at the maximum power. The sum-rate achievable at  $[P_{max}, P_{max}]$  is only slightly less than the optimal sum-rate, suggesting that



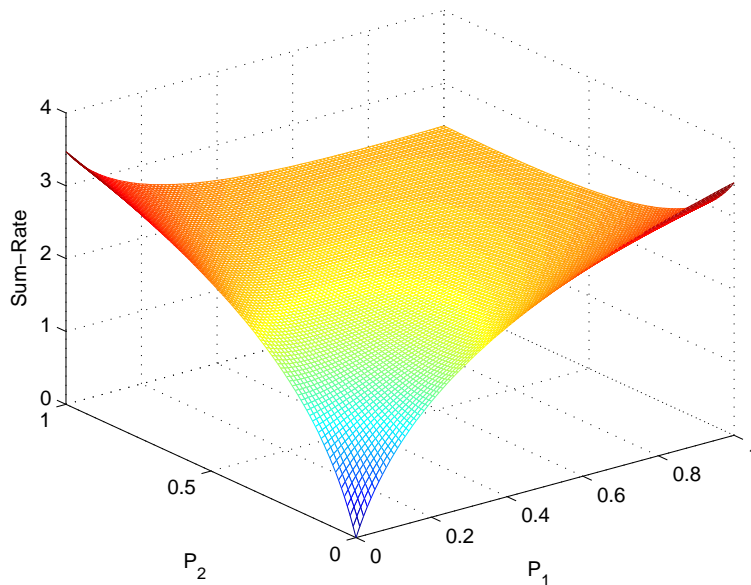


Figure 3.11: Sum-Rate region for the two-user symmetric SISO IC in very high interference regime ( $SNR_{min} = 1$  dB,  $MUI = 20$ ,  $N_b = 1$ , No fading).

the  $MUI$  factor under consideration is quite close to the cross-over point.

We now consider the sum-rate region of the two-user IC in the high interference regime ( $MUI = 10$ ). As expected, two prominent peaks are noticed at  $[P_{max}, 0]$  and  $[0, P_{max}]$ . This shows that it is optimal for only one user to transmit at the maximum power in the high interference regime. The sum-rate achievable at  $[P_{max}, P_{max}]$  is significantly less than the optimal sum-rate. Extending this result further, we present the sum-rate region of this IC in the very high interference regime ( $MUI = 20$ ) in Fig. 3.11. In this case, we observe even more prominent peaks at  $[P_{max}, 0]$  and  $[0, P_{max}]$ . This result signifies that the degradation in the sum-rate due to transmission of the second user, while the first user is transmitting at  $P_{max}$ , increases with the increase of the value of  $MUI$  factor.



### 3.3.3 Effect of Random Topology on the Optimal Sum-Rate

We now study the effect of random topology on the optimal sum-rate of a two-user IC. In this case, all the nodes are placed randomly for each instantiation by following the node placement procedure explained in the previous chapter. The ergodic sum-rate is then calculated by averaging the instantaneous sum-rates achievable in the large number of random topologies. It is already known that the binary power control is optimal in a general two-user IC [41]. Thus, there are only two possible optimal strategies: either both users transmit at the maximum power or one of the users transmit at the maximum power while keeping the other turned off. The choice of the optimal strategy depends upon the relative gains of the desired and the interference channels. In the random topology, nodes are placed according to the predefined node density (defined by  $MUI$  factor). For the low values of  $MUI$  factor, interference channels are generally weaker than the desired channels. However, this may be violated for some specific topologies, where interference channels may turn out to be stronger than the desired channels. Likewise, there may exist a small number of topologies for the high values of  $MUI$ , where the interference channels may be weaker than the desired channels. Due to this fact, max-power sum-rate and single-user sum-rate are not exactly optimal in the low SNR (and low interference) and high SNR (and high interference) scenarios, respectively. This can be verified from the ergodic sum-rates presented in Fig. 3.12 and Fig. 3.13, for various values of  $SNR_{min}$  and  $MUI$  factor, respectively. It should, however, be noted that the max-power and single-user sum-rates are still near-optimal in the extremes of their respective regimes, suggesting that the occurrence of odd-topologies decreases when we move towards the extreme of a regime (E.g., occurrence of the odd-topologies with relatively weaker interference channels decreases with the increase in the  $MUI$  factor).

### 3.3.4 Effect of Rayleigh Fading on the Optimal Sum-Rate

In this section, we again consider the symmetric two-user IC and study the effect of Rayleigh fading on the optimal sum-rate. Rayleigh fading introduces a similar uncertainty as the one

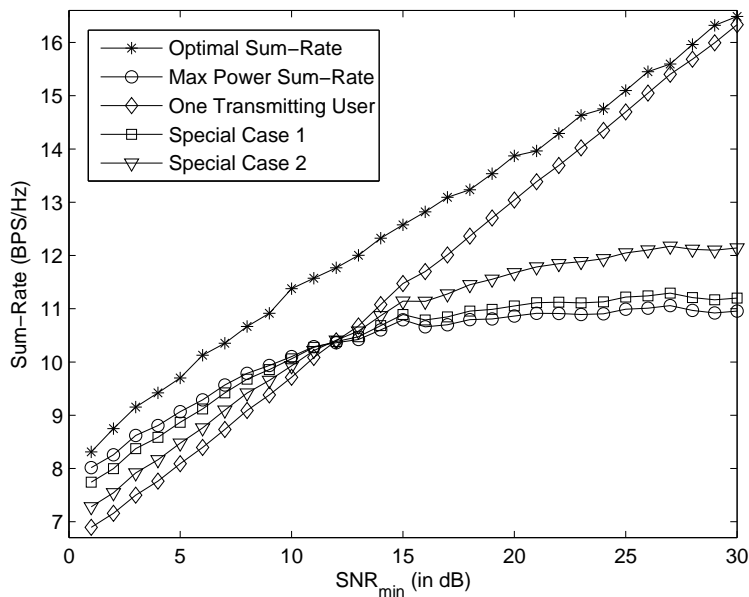


Figure 3.12: Ergodic sum-rate for various values of  $SNR_{min}$  in the two-user IC where the nodes are placed randomly for each instantiation ( $N = 2$ ,  $N_b = 1$ ,  $MUI = 1$ , No fading).

discussed in the previous section. Due to fading, we may get some cases in which the relative strengths of the interference and desired channels are contrary to the expected trend. E.g., we may get stronger interference channels than the desired channels in the low  $MUI$  case due to the presence of fading. Due to this fact, max-power and single user sum-rates are again not exactly optimal in their expected regimes. It should, however, be noted that these two specific transmission strategies converge towards the optimal sum-rate as we move to the extremes. This can be verified from the sum-rates results presented for various  $MUI$  values in Fig. 3.14. A comparison of these results with the corresponding results in the no-fading case suggests that the ergodic sum-rate in the fading case is higher. This interesting result is due to the presence of multiuser diversity in the fading case.

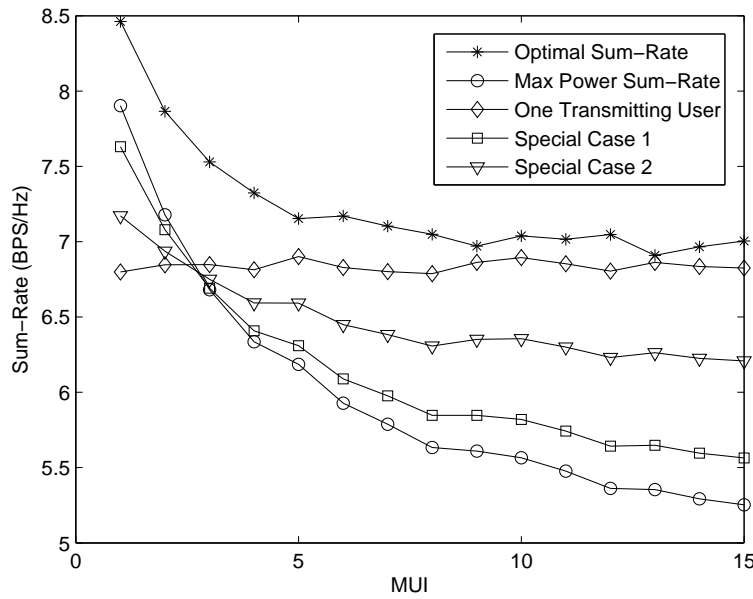


Figure 3.13: Ergodic sum-rate for various values of  $MUI$  in the two-user IC where the nodes are placed randomly for each instantiation ( $N = 2, N_b = 1, MUI = 1$ , No fading).

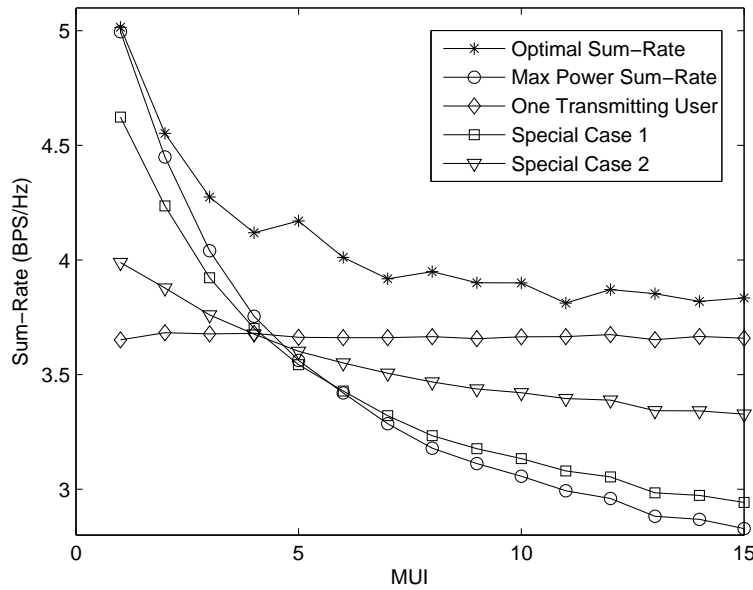


Figure 3.14: Numerical Results of the sum-rate for various values of  $MUI$  in the two-user symmetric IC ( $N = 2, N_b = 1, MUI = 1$ , No fading).

### 3.4 Three-User Single-Band SISO IC

In this section, we study the effect of adding an extra user to the two-user symmetric SISO IC considered in the previous section. Since we have already studied the effects of random geometry and fading, we will confine ourselves to the fixed three-user topology, shown in Fig. 3.15, and assume that the channel is not suffering from any fading or shadowing. It should be noted that this is not a symmetric IC. All the simulation parameters are the same as in the last section (symmetric two-user IC). In this section, we consider the following transmission strategies to gain insight into the optimal sum-rate:

- **Optimal Sum-Rate:** Optimal sum-rate is found by solving the sum-rate maximization problem. This again acts as a benchmark case for the identification of the optimal transmission strategies.
- **Max Power Sum-Rate:** There is no optimization involved and each user transmits at the maximum power.
- **One Transmitting User:** One of the three users transmits at a time. It should be noted that the choice of the user that should transmit is immaterial in this case. This is because the distance between all three Tx-Rx pairs is same and there is no fading.
- **Special Case 1:** In this case, SU1 and SU3 transmit at the maximum power and SU2 is denied transmission. Please note that there is no optimization involved in this case too.

#### 3.4.1 Effect of $SNR_{min}$

In this section, we study the effect of varying  $SNR_{min}$  on the optimal sum-rate of the three-user SISO IC. As was the case in the previous section, the interference power is kept constant by fixing  $MUI$  factor at 1.

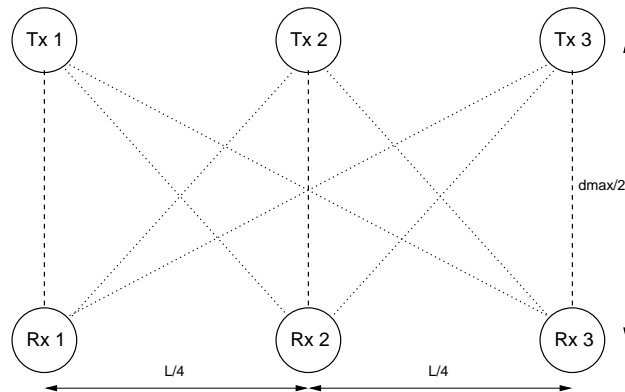


Figure 3.15: Three-User SISO IC.

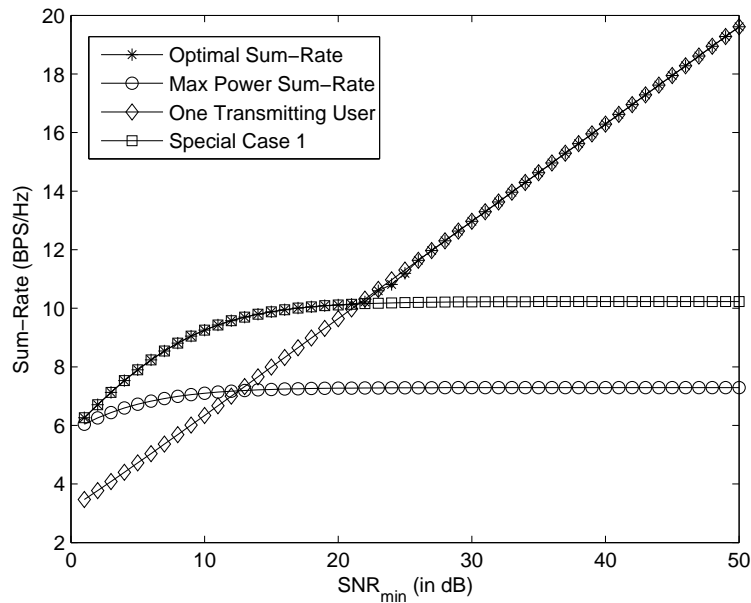


Figure 3.16: Numerical results of the sum-rate for various values of  $SNR_{min}$  in the three-user SISO IC ( $N = 3$ ,  $N_b = 1$ ,  $MUI = 1$ , No fading).

### Optimal Sum-Rate

We first identify the optimal transmission strategies for various SNR regimes. From the simulation results presented in Fig. 3.16, we observe that it is optimal for SU1 and SU3 to transmit at the maximum power while keeping SU2 turned off in the low  $SNR$  regime.

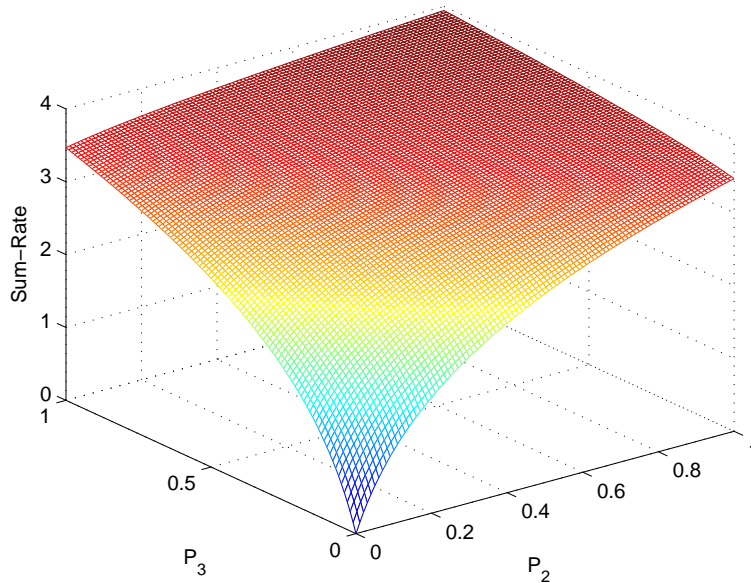


Figure 3.17: Sum-Rate region for the three-user SISO IC in the low  $SNR$  regime ( $P_1 = 0$ ,  $SNR_{min} = 1$  dB,  $N_b = 1$ ,  $MUI = 1$ , No fading).

However, as  $SNR_{min}$  is increased beyond a certain value, it is optimal for one of the three SUs to transmit at the maximum power while keeping the other two turned off. It should be noted that the local optimization routines face more convergence problems in the high  $SNR$  regime than in the low  $SNR$  regime. We had to provide as high as 50 initial starting points (feasible solutions) for this seemingly simple three-variable optimization problem to achieve near-optimal solutions. We will look at the reason for this in the next section where we characterize the sum-rate region for this example.

### Sum-Rate Region

Sum-rate region for this three-user SISO IC case is much more interesting than the case studied in the previous section. Since the rate region is characterized by three variables, it is not possible to depict it in a single plot. We will therefore show multiple 3-D plots for each SNR regime, where we fix the value of one of the variables in each plot.

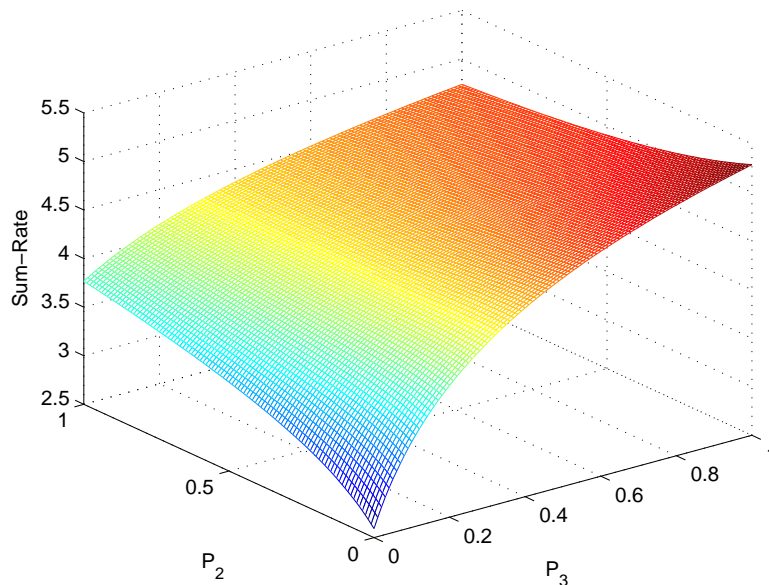


Figure 3.18: Sum-Rate region for the three-user SISO IC in the low  $SNR$  regime ( $P_1 = 0.5$ ,  $SNR_{min} = 1$  dB,  $N_b = 1$ ,  $MUI = 1$ , No fading).

We first consider a low  $SNR$  regime by setting  $SNR_{min} = 1$  dB. In Fig. 3.17, we fix the transmit power of SU1 to 0 and vary the transmit powers of SU2 and SU3. We observe that it is optimal for both SU2 and SU3 to transmit at the maximum power. We now fix the transmit power of SU1 to half of the maximum power and plot the rate region in Fig. 3.18. We note that it is now optimal to turn off SU2 while allowing SU3 to transmit at the maximum power. This depicts that it is optimal for SU1 and SU3 to simultaneously transmit in the low  $SNR$  regime. To validate our claim further, we consider one more case in which we allow SU1 to transmit at the maximum power. The rate region for this case is plotted in Fig. 3.19. The results are quite similar to the last case and reiterate the fact that it is optimal for SU1 and SU3 to transmit at the maximum power while turning SU2 off in the low  $SNR$  regime.

We now consider the more interesting case of the high  $SNR$  regime by setting  $SNR_{min} = 30$  dB. In this case, we fix the transmit power of SU2 at various values and plot the rate regions

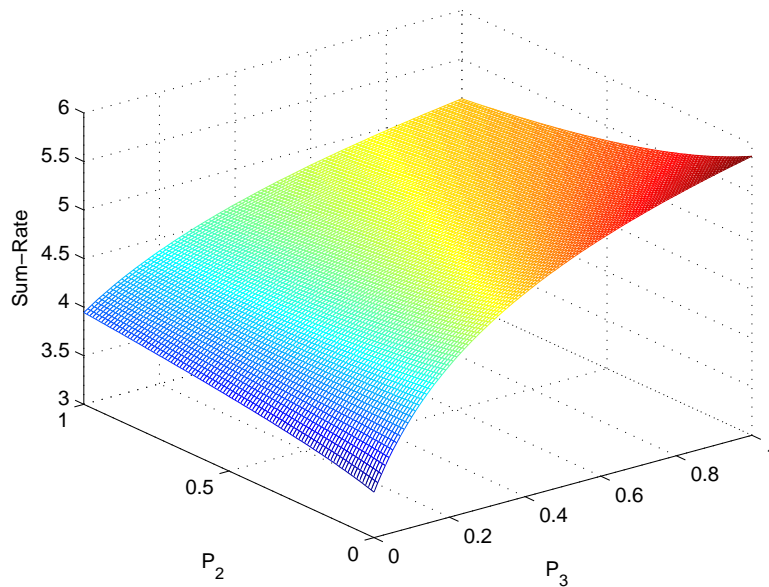


Figure 3.19: Sum-Rate region for the three-user SISO IC in the low  $SNR$  regime ( $P_1 = 1$ ,  $SNR_{min} = 1$  dB,  $N_b = 1$ ,  $MUI = 1$ , No fading).

by varying the transmit powers of the other two SUs. In Fig. 3.20, we turn SU2 off and let SU1 and SU3 transmit at the maximum power. The rate region clearly indicates that it is optimal for one of the SUs to transmit at the maximum power while turning the other two off. This result is consistent with our observations of the rate region in the two-user symmetric SISO IC in the last example. We now let SU2 transmit at half of its maximum power and plot the rate region in Fig. 3.21. First and foremost observation is that it is optimal to turn both SU1 and SU3 off even when SU2 is transmitting at half of its maximum power. We further note an interesting non-convexity in the rate region. The local optimization algorithms (such as gradient based search) will converge to the global optimal solution only if the starting feasible point is very close to  $[0, 0]$ . Even if the starting point is slightly away from  $[0, 0]$ , the local optimization algorithm will converge to  $[P_{max}, P_{max}]$  as the optimal solution. Due to this strong non-convexity, we had to run the local optimization routine for as high as 50 times with random starting points (feasible solutions) to achieve the global optimal solution.



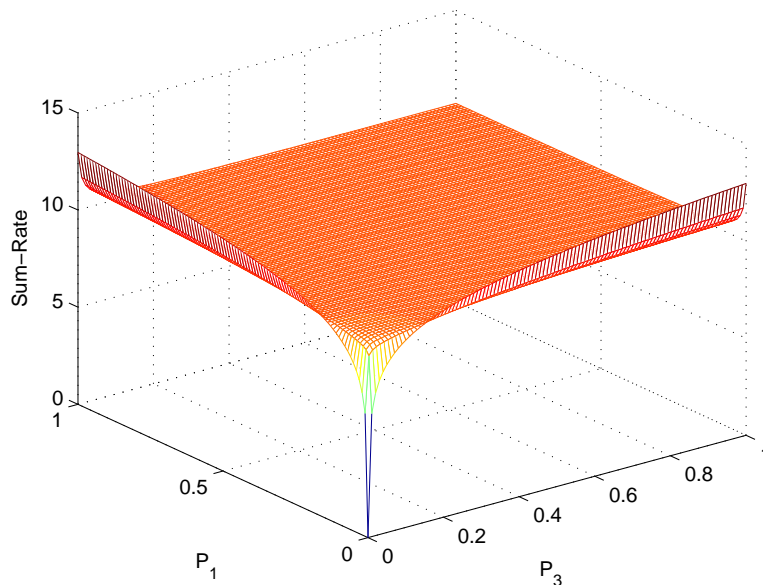


Figure 3.20: Sum-Rate region for the three-user SISO IC of Example 2 in the very high  $SNR$  regime ( $P_2 = 0$ ,  $SNR_{min} = 30$  dB,  $N_b = 1$ ,  $MUI = 1$ , No fading).

This highlights the need of a global optimal algorithm with a guaranteed convergence to solve the power control optimization problems. We now consider the last case for this  $SNR$  regime, where we let SU2 to transmit at the maximum possible power. We note that the rate region is quite similar to the previous case. From all these plots, we conclude that it is optimal for one of the SUs to transmit at the maximum power while keeping the other two turned off in the high  $SNR$  regime.

### 3.4.2 Effect of $MUI$

In this section, we study the effect of changing the  $MUI$  factor on the optimal sum-rate of a three-user SISO IC. As mentioned in the previous sections, the change in the value of  $MUI$  factor directly influences the interference power by changing the distance between the users. Noise power is kept constant by fixing  $SNR_{min}$  at 1 dB.

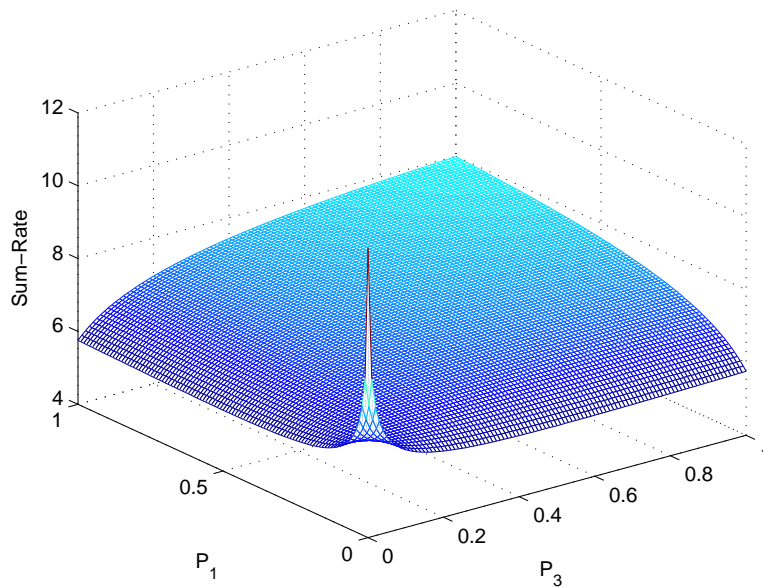


Figure 3.21: Sum-Rate region for the three-user SISO IC in the very high  $SNR$  regime ( $P_2 = 0.5$ ,  $SNR_{min} = 30$  dB,  $N_b = 1$ ,  $MUI = 1$ , No fading).

### Optimal Sum-Rate

We first study the effect of varying the  $MUI$  factor on the optimal transmission strategy that maximizes the sum-rate. The sum-rate achievable for various strategies is presented in Fig. 3.23. It is optimal to let SU1 and SU3 transmit at maximum power while keeping SU2 turned off in the low interference scenario (lower values of  $MUI$  factor). The same trend was observed in the low SNR scenario. It is interesting to note that max-power transmission yields almost the same sum-rate as the optimal case when the  $MUI$  factor is 1. This essentially means that it is optimal to let all the three users transmit at the maximum power in the very low interference scenario. This result can be verified by extrapolating the plots to  $MUI = 0$  that corresponds to a no-interference scenario (infinite distance between users). In this case, there is no reason to forbid any user from transmitting at the maximum power. For high values of  $MUI$  factor, we note that it is optimal to let only one of the three users

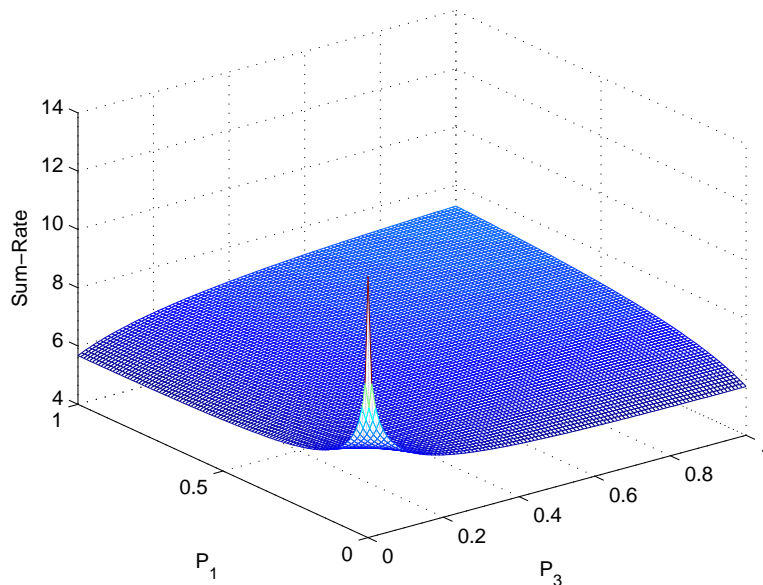


Figure 3.22: Sum-Rate region for the three-user SISO IC in the very high  $SNR$  regime ( $P_2 = 1$ ,  $SNR_{min} = 30$  dB,  $N_b = 1$ ,  $MUI = 1$ , No fading).

transmit at the maximum power. Any one of the three users can be chosen for transmission because there is no fading and the distance between the Tx and Rx nodes is the same for each user. It is interesting to note that the system is severely interference limited at high values of  $MUI$  factor and the sum-rate degrades significantly if we let more than one user transmit simultaneously. As was the case in the last section, we observe that the local optimization routines do not easily converge to the global solution. We have to provide as high as 50 initial feasible solutions to make the local optimization routines converge. We now study the reason for this behavior by characterizing the sum-rate region of the three-user IC.

### Sum-Rate Region

As we observed in the previous section, the sum-rate region of this IC is much more interesting than the two-user IC case. The rate-region in this case is characterized by three variables

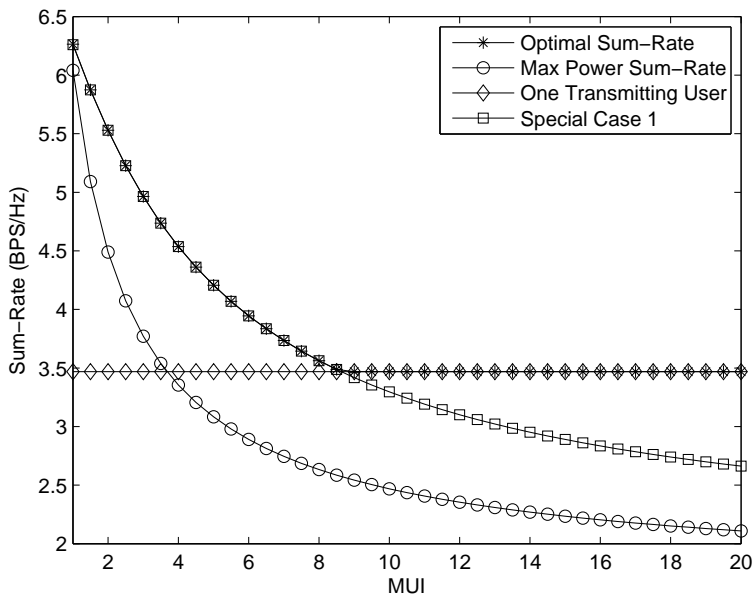


Figure 3.23: Numerical results of the sum-rate for various values of  $MUI$  factor in the three-user symmetric IC ( $N = 3$ ,  $N_b = 1$ ,  $SNR_{min} = 1$  dB, No fading).

and it is not possible to depict it on a single plot. We will therefore show multiple plots for each  $MUI$  factor under consideration. We will fix one of the variables in each plot and let the other two vary from 0 to  $P_{max}$ .

We first consider the sum-rate region in the low interference scenario by fixing  $MUI$  factor at 5. From our study of the optimal sum-rate, we know that it is optimal for SU1 and SU3 transmit at the maximum power while keeping SU2 turned off. Thus we fix the power transmitted by SU1 at  $0, P_{max}/2, P_{max}$  and plot the resulting sum-rate regions in Figures 3.24, 3.25 and 3.26, respectively. In the first plot we note that it is optimal for either SU2 or SU3 transmit at the maximum power while keeping SU1 turned off. We now let SU1 transmit at half of the maximum power and observe that it is optimal for SU3 to transmit at the maximum power while keeping SU2 turned off. The sum-rate degrades significantly if we let SU2 transmit even at a small power in this case. This result suggests that it is highly suboptimal to let SU2 transmit while both SU1 and SU3 are transmitting. To gain further

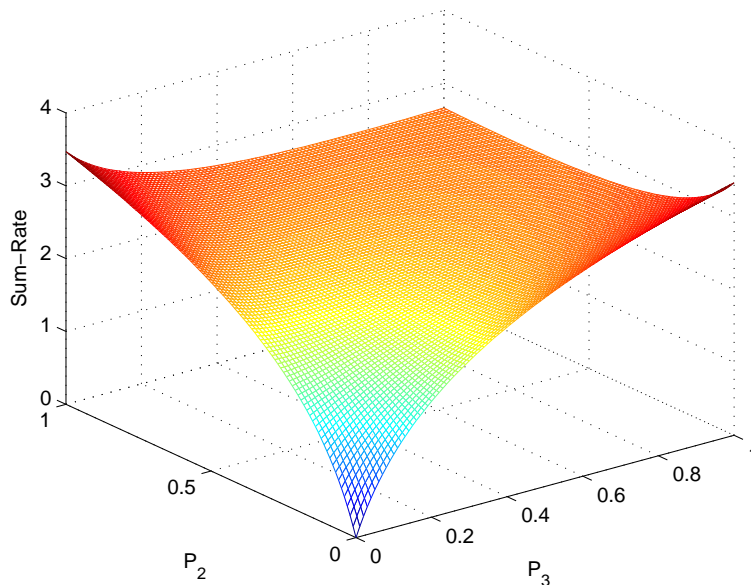


Figure 3.24: Sum-Rate region for the three-user SISO IC in low interference regime ( $P_1 = 0$ ,  $MUI = 5$ ,  $SNR_{min} = 1dB$ ,  $N_b = 1$ , No fading).

insight, we let SU1 transmit at the maximum power and note that it is optimal for SU3 to transmit at the maximum power and keep SU2 turned off. The degradation in sum-rate due to the transmission of SU2 is more in this case than the previous case.

We now consider the sum-rate region in the high interference scenario by fixing  $MUI$  factor at 20. In this case, we know that it is optimal for only one of the three users to transmit while keeping the other two turned off. Thus we can fix any one of the three variables and study the rate-region by varying the other two. For the purpose of illustration, we fix the power transmitted by SU2 at  $0, P_{max}/2, P_{max}$  and plot the resulting rate-regions in Figures 3.27, 3.28 and 3.29, respectively. When we fix  $P_2 = 0$ , we note that it is optimal for either SU1 or SU3 to transmit at maximum power. Since there is no fading, any one of the two users can transmit with equal probability. Now we look at the more interesting case, when SU2 is transmitting at half of the maximum power. We note that there are two peaks, one at  $[0, 0]$  and the other at  $[P_{max}, P_{max}]$ . The global optimal solution corresponds

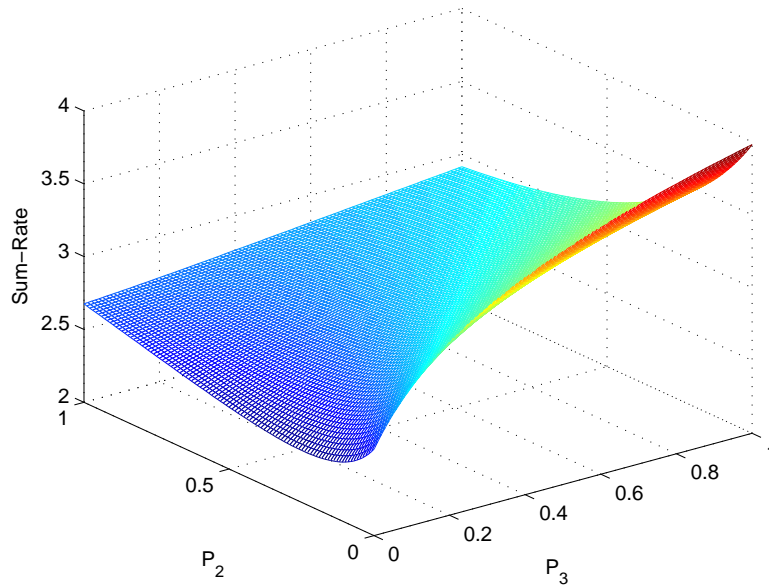


Figure 3.25: Sum-Rate region for the three-user SISO IC in low interference regime ( $P_1 = 0.5$ ,  $MUI = 5$ ,  $SNR_{min} = 1dB$ ,  $N_b = 1$ , No fading).

to the case when both SU1 and SU3 are turned off. However, it is easy to see that the local optimization techniques, especially the gradient based search, will converge to the local optimal unless the starting feasible solution is in the vicinity of  $[0, 0]$ . This is the reason for choosing a high number of initial solutions to ensure convergence to the global optimal solution. A similar trend is observed when we let SU2 transmit at the maximum power. In this case, the sum-rate degrades quite significantly if we let any one (or both) of the other two users transmit even at a reduced power.

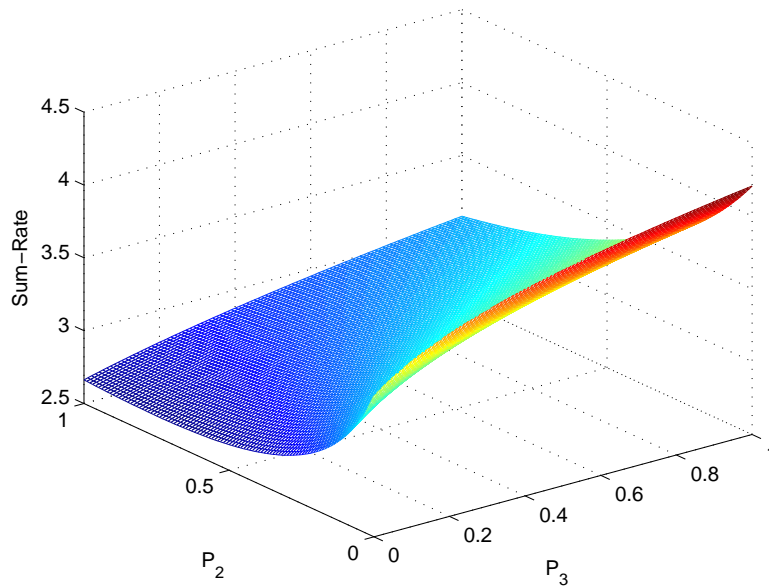


Figure 3.26: Sum-Rate region for the three-user SISO IC in low interference regime ( $P_1 = 1$ ,  $MUI = 5$ ,  $SNR_{min} = 1dB$ ,  $N_b = 1$ , No fading).

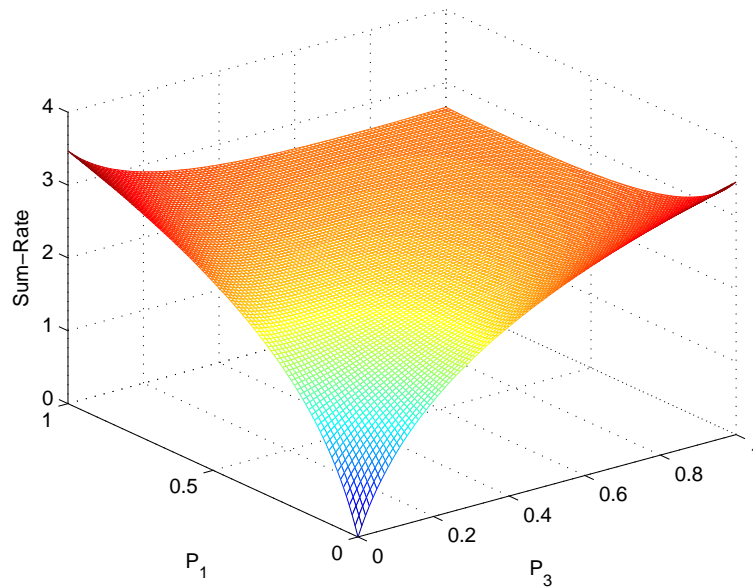


Figure 3.27: Sum-Rate region for the three-user SISO IC in high interference regime ( $P_2 = 0$ ,  $MUI = 20$ ,  $SNR_{min} = 1dB$ ,  $N_b = 1$ , No fading).



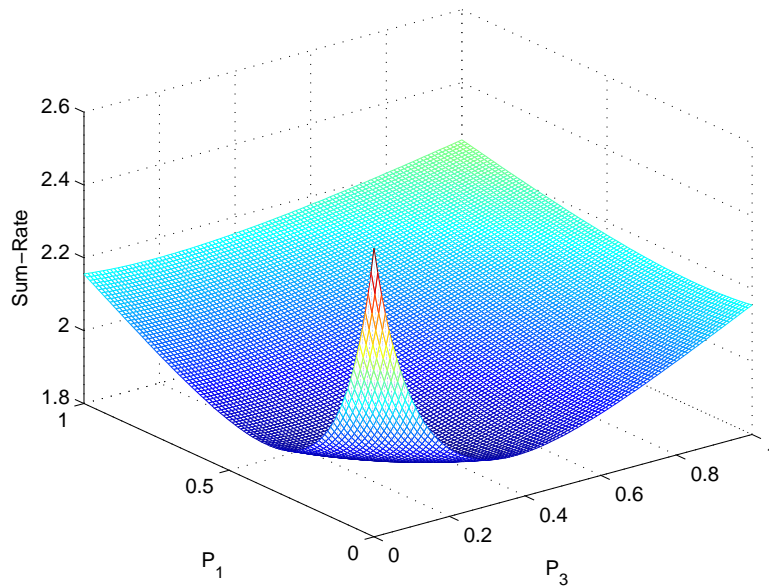


Figure 3.28: Sum-Rate region for the three-user SISO IC in high interference regime ( $P_2 = 0.5$ ,  $MUI = 20$ ,  $SNR_{min} = 1dB$ ,  $N_b = 1$ , No fading).

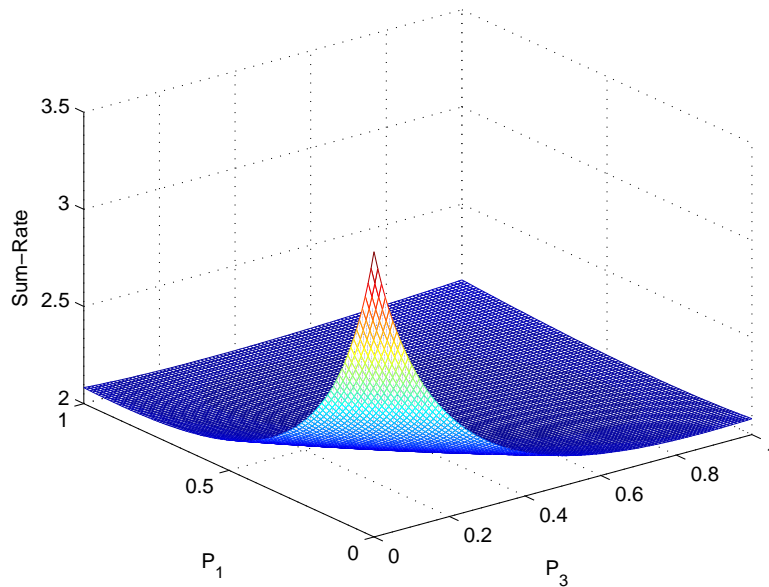


Figure 3.29: Sum-Rate region for the three-user SISO IC in high interference regime ( $P_2 = 1$ ,  $MUI = 20$ ,  $SNR_{min} = 1dB$ ,  $N_b = 1$ , No fading).



### 3.5 Four-User Single-Band SISO IC

We now add another user to the three-user IC studied in the last section and consider a four-user SISO IC shown in Fig. 3.30. All the simulation parameters, except the distances between the users (which are shown in Fig. 3.30), are same as those of the previous two cases. In this case too, we consider that there is no fading or shadowing. We consider following transmission strategies to gain insight into the optimal sum-rate:

- **Optimal Sum-Rate:** In this case, we find the maximum achievable sum-rate by performing optimal power control. As in the previous cases, we assume single user detection and hence no interference cancelation.
- **Max Power Sum-Rate:** In this case, we assume that each user is transmitting at the maximum power and there is no optimization involved.
- **One Transmitting User:** In this case, we assume that one of the four users is transmitting. As in the previous cases, the choice of the transmitting user is immaterial because all the users are alike due to the same distance between Tx-Rx nodes and the absence of any fading and shadowing.
- **Special Case 1:** In the first special case, we assume SU1 and SU4 are transmitting at the maximum power while SU2 and SU3 are turned off.
- **Special Case 2:** In the second special case, we assume that SU1 and SU3 (or SU2 and SU4) are transmitting at the maximum power while SU2 and SU4 (or SU1 and SU3) are turned off. This simply means that alternate SUs are turned on. Intuitively this case should yield lower sum-rate than the special case 1.

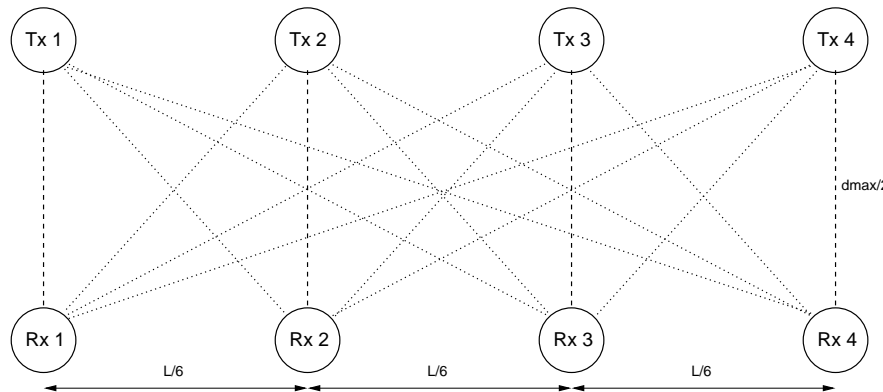


Figure 3.30: Four-User SISO IC.

### 3.5.1 Effect of $SNR_{min}$

The sum-rates achievable for various values of  $SNR_{min}$  are presented in Fig. 3.31 ( $MUI$  factor is fixed at 1). We observe that the special case 1 is optimal in the low  $SNR$  regime. This means that it is optimal to let the farthest SUs (SU1 and SU4) transmit while keeping SU2 and SU3 turned off. At the very low  $SNR_{min}$  (say 1 dB), this special case is much better than all the other cases. However, as we increase  $SNR_{min}$ , single transmitting user case starts performing better than the special case 1. This means that it is optimal for only one of the four users to transmit at the maximum power while all the other users are turned off. This is in consonance with the observations in the previous two ICs.

### 3.5.2 Effect of $MUI$

A comparison of the sum-rates achievable for various values of  $MUI$  factor is presented in Fig. 3.32 ( $SNR_{min}$  is fixed at 1 dB). As in the case of the low SNR regime, it is optimal for the farthest users (SU1 and SU4) transmit at the maximum power while the other two are turned off in the low-interference regime. Max-power sum-rate and the case where the alternate users transmit (special case 2) achieve significantly less sum-rate than the optimal case. As we increase the value of  $MUI$  factor, single user transmission case starts performing

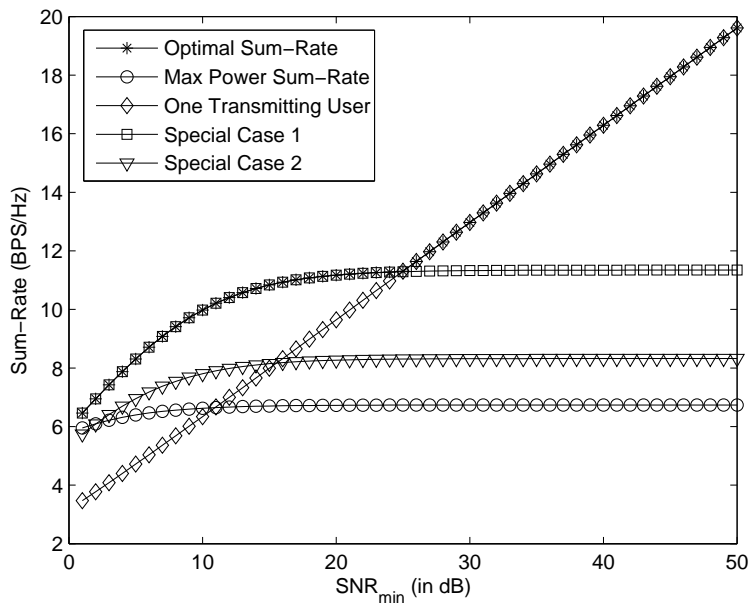


Figure 3.31: Simulation Results ( $N = 4$ ,  $N_b = 1$ ,  $MUI = 1$ , No fading).

better than the others. Beyond a certain value of  $MUI$  factor, it is optimal to let only one user transmit in the high interference regime (higher  $MUI$  values).

## 3.6 Conclusions

In this chapter, we have studied the optimal sum-rate of the single antenna ICs by treating interference as noise. We make following important conclusions regarding the optimal power allocation strategies in these ICs:

- The relative strength of the interference (cross) and the desired channels is the key factor governing the choice of the optimal power allocation strategies in the single antenna ICs. It is optimal to turn off more users as the strength of the interference channels increase relative to the desired channels. This happens in the present system model if we increase  $SNR_{min}$  or  $MUI$  factor.

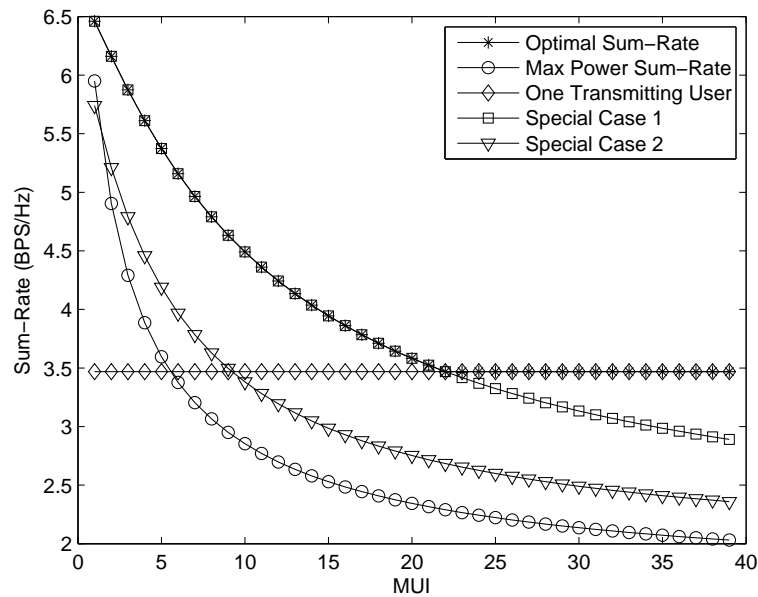


Figure 3.32: Simulation Results for various values of  $MUI$  factor ( $N = 4$ ,  $N_b = 1$ ,  $SNR_{min} = 1$  dB, No fading).

- It is optimal to let all the users transmit when the interference is not very high. On the other extreme, it is optimal to let only one user transmit when the interference channels become too strong. This is an important result and will help us immensely in the subsequent chapters.
- Binary power control is observed to be optimal in the fixed topologies considered in this chapter (in the absence of fading).
- It is also shown that the presence of fading in the ICs increases the ergodic sum-rate as compared to their no-fading counterparts due to the multiuser diversity.
- The results presented in this chapter have also highlighted the non-convex nature of the power control problems. In particular, we have shown that the problem is highly non-convex in the high SNR and high interference regimes. This implies that the sum-rates achievable by solving the problem by using local optimization methods may

be highly sub-optimal. Due to this reason, we had to solve the problem numerous times using random starting points (feasible solutions) to make the local optimization methods converge to the global optimal solution. This highlights the importance of devising provably global optimization algorithms (studied in the next two chapters).

# Chapter 4

## Multi-Antenna Interference Channels

### 4.1 Introduction

In this chapter, we study the maximum achievable sum-rate in the multi-antenna interference channels by treating interference as Gaussian noise. The multi-antenna IC, also referred to as the MIMO IC, is defined as an extension of the classical IC where each Tx and Rx node has multiple antennas. The sum-rate maximization problem in multi-antenna ICs (also termed as multiuser MIMO networks) was first formulated in [54]. The solution to this non-convex problem has, to date, only been approximated by local optimization techniques [55], [56]. Though these approaches can quickly find a locally optimal solution, they cannot guarantee the global optimum for non-convex problems. A global optimization algorithm was recently developed in [57] by coupling the branch and bound method with the reformulation and linearization technique (BB/RLT) to find the maximum sum-rate of a MIMO interference channel under the assumption that each user's transmit power is equally distributed over all the spatial channels [57]. This assumption eases the mathematical formulation of the problem significantly, but unfortunately, the simplified result does not provide the maximum achievable sum-rate for the interference channel under consideration.

In this chapter, we extend the BB/RLT algorithm to solve the general MIMO interference channel sum-rate maximization problem by treating interference as Gaussian noise. Using this algorithm, we evaluate the maximum achievable sum-rate of some specific multi-antenna ICs to gain insight into the optimal power allocation strategies. The optimal results are compared to some sub-optimal power allocation strategies, such as beamforming and equal power allocation over all spatial channels. From these comparisons, we note that it is optimal for the users to distribute power over the spatial channels in the low SNR (low interference) scenarios and confine power over a small number of spatial channels in the high SNR (high interference) scenarios. In other words, we note that more and more spatial degrees of freedom are used for interference avoidance as we move from low to high interference regimes. In the limiting case of high interference, it is optimal to suppress the interference completely by turning off bad users and/or transmitting over fewer Eigen-channels while using the rest of the channels for interference avoidance. The results are validated by doing a detailed study of the distribution of the powers transmitted over various Eigen-channels of each IC in different SNR regimes. We will look into these results in sufficient detail later in this chapter.

We begin our discussion by formulating the sum-rate maximization problem of MIMO IC by treating interference as noise in the next section.

## 4.2 Sum-Rate of MIMO Interference Channel

In this section, we formulate the sum-rate maximization problem for MIMO IC. We begin by defining the variables that would be used in the problem formulation.

### 4.2.1 Defining the Variables

Let us denote the MIMO link from the Tx of the  $j^{\text{th}}$  user to the Rx of the  $i^{\text{th}}$  user to be  $L_{ji}$ . Let  $\mathbf{H}_{ji} \in C^{n_r \times n_t}$  denote the channel matrix of link  $L_{ji}$ . Let  $\mathbf{Q}_i$  be the covariance matrix of the zero mean Gaussian input symbol vector  $\mathbf{x}_i$  of the  $i^{\text{th}}$  user, i.e.,  $\mathbf{Q}_i = E\{\mathbf{x}_i \mathbf{x}_i^\dagger\}$ . Further denote  $\rho_{ji}$  as the signal-to-noise ratio if  $j = i$ , or the interference-to-noise ratio if  $j \neq i$ . Let  $\mathbf{R}_i$  represent the covariance matrix of interference plus noise at the Rx node of the  $i^{\text{th}}$  user. Assuming interference plus noise to be Gaussian distributed,  $\mathbf{R}_i$  can be computed as:

$$\mathbf{R}_i = \sum_{\substack{j=1 \\ j \neq i}}^N \rho_{ji} \mathbf{H}_{ji} \mathbf{Q}_j \mathbf{H}_{ji}^\dagger + \mathbf{I}. \quad (4.1)$$

### 4.2.2 Maximum Capacity of a single Link in a MIMO IC

We begin our discussion by evaluating the maximum achievable capacity of a single MIMO link in an IC. To gain insight into the problem, we assume that the interference from other users is constant and is perfectly known at both the Tx and Rx nodes. Channel state information is also assumed to be perfectly known. In addition to finding the maximum link capacity, the analysis will also help us establish the notion of ‘Eigen-channels’ in a MIMO IC.

To begin the analysis, we express the capacity of the  $i^{\text{th}}$  MIMO link in terms of its channel matrix  $\mathbf{H}_{ii}$ , transmit symbol covariance matrix  $\mathbf{Q}_i$  and interference plus noise covariance matrix  $\mathbf{R}_i$  as [54]:

$$C_i = \max_{\mathbf{Q}: \text{tr}(\mathbf{Q})=P_{max}} \log_2 \det \left( \mathbf{I} + \rho_{ii} \mathbf{R}_i^{-1} \mathbf{H}_{ii} \mathbf{Q}_i \mathbf{H}_{ii}^\dagger \right), \quad (4.2)$$

where the optimization is performed over the input symbol covariance matrix  $\mathbf{Q}_i$ . Substituting  $\mathbf{R}_i = \mathbf{R}_i^{1/2} \mathbf{R}_i^{1/2 \dagger}$  in (4.2), we get:

$$\begin{aligned} C_i &= \log_2 \det \left( \mathbf{I} + \rho_{ii} (\mathbf{R}_i^{1/2} \mathbf{R}_i^{1/2 \dagger})^{-1} \mathbf{H}_{ii} \mathbf{Q}_i \mathbf{H}_{ii}^\dagger \right), \\ &= \log_2 \det \left( \mathbf{I} + \rho_{ii} \mathbf{R}_i^{-1/2 \dagger} \mathbf{R}_i^{-1/2} \mathbf{H}_{ii} \mathbf{Q}_i \mathbf{H}_{ii}^\dagger \right). \end{aligned} \quad (4.3)$$



Using the identity  $\det(\mathbf{I} + \mathbf{AB}) = \det(\mathbf{I} + \mathbf{BA})$ , (4.3) can be expressed as:

$$\begin{aligned} C_i &= \log_2 \det \left( \mathbf{I} + \rho_{ii} \mathbf{R}_i^{-1/2} \mathbf{H}_{ii} \mathbf{Q}_i \mathbf{H}_{ii}^\dagger \mathbf{R}_i^{-1/2} \right), \\ &= \log_2 \det \left( \mathbf{I} + \rho_{ii} (\mathbf{R}_i^{-1/2} \mathbf{H}_{ii}) \mathbf{Q}_i (\mathbf{R}_i^{-1/2} \mathbf{H}_{ii})^\dagger \right). \end{aligned} \quad (4.4)$$

Now let  $\tilde{\mathbf{H}}_{ii} = \mathbf{R}_i^{-1/2} \mathbf{H}_{ii}$ . Substituting this in the above equation, we get:

$$C_i = \log_2 \det \left( \mathbf{I} + \rho_{ii} \tilde{\mathbf{H}}_{ii} \mathbf{Q}_i \tilde{\mathbf{H}}_{ii}^\dagger \right). \quad (4.5)$$

Now we decompose the MIMO channel into  $\min\{n_t, n_r\}$  orthogonal Eigen-channels in the same way as we did for an isolated MIMO link in Chapter 2. The only difference is that the channel matrix  $\mathbf{H}_{ii}$  is replaced by the ‘whitened’ channel matrix  $\tilde{\mathbf{H}}_{ii}$  in this case. By applying SVD, the whitened channel matrix  $\tilde{\mathbf{H}}_{ii}$  can be expressed as:  $\tilde{\mathbf{H}}_{ii} = \mathbf{U} \mathbf{D} \mathbf{V}^\dagger$ , where  $\mathbf{U}$  and  $\mathbf{V}$  are unitary matrices and  $\mathbf{D}$  is a diagonal matrix. Substituting this in (4.5), we get:

$$C_i = \log_2 \det \left( \mathbf{I} + \rho_{ii} \mathbf{U} \mathbf{D} \mathbf{V}^\dagger \mathbf{Q}_i \mathbf{V} \mathbf{D}^\dagger \mathbf{U}^\dagger \right). \quad (4.6)$$

Using the identities  $\det(\mathbf{I} + \mathbf{AB}) = \det(\mathbf{I} + \mathbf{BA})$  and  $\mathbf{U} \mathbf{U}^\dagger = \mathbf{I}$ , (4.6) can be expressed as:

$$C_i = \log_2 \det \left( \mathbf{I} + \rho_{ii} \mathbf{D} \mathbf{V}^\dagger \mathbf{Q}_i \mathbf{V} \mathbf{D}^\dagger \right). \quad (4.7)$$

Using the identity  $\det(\mathbf{I} + \mathbf{AB}) = \det(\mathbf{I} + \mathbf{BA})$  again and defining  $\Sigma = \mathbf{D}^\dagger \mathbf{D}$ , (4.7) can be expressed as:

$$C_i = \log_2 \det \left( \mathbf{I} + \rho_{ii} \Sigma \mathbf{V}^\dagger \mathbf{Q}_i \mathbf{V} \right). \quad (4.8)$$

It should be noted that  $\Sigma = \mathbf{D}^\dagger \mathbf{D}$  is a diagonal matrix and the diagonal elements are the Eigen-values of  $\tilde{\mathbf{H}} \tilde{\mathbf{H}}^\dagger$ . To decompose the MIMO channel in  $\min\{n_t, n_r\}$  parallel non-interfering SISO channels,  $\mathbf{V}^\dagger \mathbf{Q}_i \mathbf{V}$  should result in a diagonal matrix. This can be achieved by choosing  $\mathbf{Q}_i$  of the form  $\mathbf{Q}_i = \mathbf{V} \Lambda \mathbf{V}^\dagger$ . We get  $\mathbf{Q}_i$  of this form when  $\mathbf{V}$  is chosen as the pre-coding matrix. It is worth noting that the pre-coding matrix in this case is dependent upon the structure of the interference signals through  $\tilde{\mathbf{H}}$ . In this case, the capacity of the isolated link can be expressed as:

$$C_i = \max_{\Lambda: \text{tr}(\Lambda) = P_{max}} \log_2 \det \left( \mathbf{I} + \rho_{ii} \Sigma \Lambda \right). \quad (4.9)$$

Thus, the problem of maximizing the capacity of a single link in a MIMO IC is reduced to finding the optimal fractions of the power to be transmitted in each Eigen-channel. Please recall that the Eigen-channels in this case are not same as the Eigen-channels of the interference-free channel. In-fact, they correspond to the singular values of the ‘whitened’ channel matrix. Since we have assumed perfect knowledge of the channel and interference,  $\Sigma$  is perfectly known and the optimal  $\Lambda$  can be found by employing a ‘water-filling’ strategy.

### Note on the Calculation of $\mathbf{R}^{1/2}$

In the above derivation, we factorize the interference and noise correlation matrix as  $\mathbf{R}_i = \mathbf{R}_i^{1/2} \mathbf{R}_i^{1/2\dagger}$ . It should be noted that this factorization is possible because  $\mathbf{R}_i$  is positive semi-definite. Furthermore, this factorization can be achieved by doing Eigen-Value Decomposition of  $\mathbf{R}_i$ , i.e.,  $\mathbf{R}_i = \mathbf{U}_R \Sigma_R \mathbf{U}_R^\dagger$  and noting that  $\mathbf{R}_i^{1/2} = \mathbf{U}_R \Sigma_R^{1/2} \mathbf{U}_R^\dagger$ . The left and right Eigen matrices of  $\mathbf{R}_i$  are same because  $\mathbf{R}_i$  is positive semi-definite. It is easy to verify that the derived expression of  $\mathbf{R}_i^{1/2}$  satisfies  $\mathbf{R}_i = \mathbf{R}_i^{1/2} \mathbf{R}_i^{1/2\dagger}$ .

We now extend this discussion to the multiuser case in the next section, where the goal is to maximize the sum of capacities of all the links (sum-rate) forming the interference channel.

### 4.2.3 Maximum Ergodic Sum-Rate of a MIMO IC

In this section, we develop a mathematical framework to maximize the sum-rate of a MIMO IC. This formulation is challenging because the capacities of all the links forming an IC are coupled to each other due to the mutual interference. In other words, the interference plus noise covariance matrices are not known *a priori* and hence we do not have the luxury of maximizing the capacity of each link independently. Due to the lack of knowledge of  $\mathbf{R}_i$ , it is quite difficult to find the exact pre-coding matrices for each system instantiation. To overcome this problem, we try to simplify the formulation by mapping each IC to an alternate IC where the pre-coding matrices are unity matrices and hence the input symbol

covariance matrices reduce to diagonal matrices (with real and non-negative elements). It will be further shown that the ergodic sum-rate of the new IC is same as that of the original IC. We now discuss this idea in detail in the rest of this section.

As noted in the previous section, the information theoretic capacity of a single link in a MIMO interference channel can be expressed as  $C_i = \log_2 \det(\mathbf{I} + \rho_{ii} \mathbf{R}_i^{-1} \mathbf{H}_{ii} \mathbf{Q}_i \mathbf{H}_{ii}^\dagger)$ . Since  $\mathbf{Q}_i \succ \mathbf{0}$ , it can be expressed as  $\mathbf{Q}_i = \mathbf{V}_i \Lambda_i \mathbf{V}_i^\dagger$ , where  $\Lambda_i$  is a diagonal matrix of the eigenvalues of  $\mathbf{Q}_i$  and  $\mathbf{V}_i$  is a unitary matrix with columns consisting of the eigenvectors of  $\mathbf{Q}_i$ . Please note that further insights into  $\mathbf{V}_i$  are not required for the current formulation. Defining  $\hat{\mathbf{H}}_{ii} = \mathbf{H}_{ii} \mathbf{V}_i$ , the capacity expression can be written as  $C_i = \log_2 \det(\mathbf{I} + \rho_{ii} \mathbf{R}_i^{-1} \hat{\mathbf{H}}_{ii} \Lambda_i \hat{\mathbf{H}}_{ii}^\dagger)$ . Since  $\mathbf{Q}_i \succ \mathbf{0}$ , it leads to the following two very important properties:

1. The distributions of  $\hat{\mathbf{H}}_{ii}$  and  $\mathbf{H}_{ii}$  are same [54].
2. All the eigenvalues of  $\mathbf{Q}_i$ , i.e., all the diagonal elements of  $\Lambda_i$ , are real and positive.

Due to these properties, it is sufficient to consider  $\Lambda_i$  instead of  $\mathbf{Q}_i$  in the problem formulation. From the simulation perspective it is important to note that even though the problem is transformed to a different IC, the ergodic sum-rate remains the same. This is because the distributions of  $\hat{\mathbf{H}}_{ii}$  and  $\mathbf{H}_{ii}$  are same and it does not really matter which one of them we consider for our simulation. We might very well consider  $\mathbf{H}_{ii}$  and  $\mathbf{Q}_i$  for the optimization but it is hard to formulate the problem and then solve it ensuring  $\mathbf{Q}_i$  is positive-semi-definite and satisfies the power constraint. Due to this reason, we consider an alternate IC and formulate the problem in terms of  $\Lambda_i$  and  $\hat{\mathbf{H}}_{ii}$ . The resulting problem formulation can be expressed as:

$$\begin{aligned}
 & \max \quad \sum_{i=1}^N C_i \\
 & s.t. \quad C_i = \log_2 \det(\mathbf{R}_i + \rho_{ii} \hat{\mathbf{H}}_{ii} \Lambda_i \hat{\mathbf{H}}_{ii}^\dagger) - \log_2 \det(\mathbf{R}_i), \\
 & \quad \mathbf{R}_i = \sum_{\substack{j=1 \\ j \neq i}}^N \rho_{ji} \hat{\mathbf{H}}_{ji} \Lambda_j \hat{\mathbf{H}}_{ji}^\dagger + \mathbf{I}, \\
 & \quad Tr\{\Lambda_i\} \leq P_{max}, \text{diag}\{\Lambda_i\} \succeq \mathbf{0}, 1 \leq i \leq N.
 \end{aligned} \tag{4.10}$$

This sum-rate maximization problem was first formulated by Blum in [54]. However, the exact solution to this problem is still open due to its non-linear and non-convex nature.

Some popular local optimization techniques, such as gradient based search, have been used to approximate the solution but are not guaranteed to converge to the global optimal due to the presence of multiple maxima. Exact solution was recently evaluated in [57] for a special case where each user distributes its transmit power equally over all the spatial channels. This algorithm, termed BB/RLT, was developed by coupling the Branch and Bound (BB) strategy with the Reformulation and Linearization Technique (RLT) [59], [58]. The RLT part was considerably simplified due to the equal power assumption and the optimization was essentially performed over the total power transmitted by each user.

We extend the BB/RLT algorithm to find the exact solution of the sum-rate maximization problem of a general IC in the next section.

### 4.3 The Proposed BB/RLT Global Optimization Algorithm

We begin our discussion on the global optimization algorithm by presenting a brief overview of its working principle.

#### 4.3.1 Brief Overview of BB/RLT

The basic idea of BB/RLT is to first find the upper bound (UB) and the lower bound (LB) to the optimal sum-rate by constructing a linear programming relaxation (LPR) of the original non-linear (NL) problem and then tightening the bounds by employing the BB algorithm [59]. While constructing the LPR, all of the NL terms in the objective function and the constraints are replaced by linear variables by introducing suitable linear constraints, thereby relaxing the feasible region. The optimal objective function value of this LP thus serves as an upper bound (UB) to the original NL problem (since it is a maximization problem). If the optimal solution of this relaxed LP is feasible to the original NL problem, it acts as a lower bound

(LB) to the globally optimal value (since it is sub-optimal to the original NL problem in general). Otherwise, it can be used as a starting point to find a feasible solution by local search. After finding the UB and LB, the BB strategy is employed to partition the search space so that both the largest UB and LB approach the global optimum. When the largest UB and the LB are within some threshold,  $\epsilon$ , the BB/RLT is complete and yields a LB to the global optimum that is within  $\epsilon$  of the true global optimum [59]. The working of the algorithm is shown in Fig. 4.1 for  $\epsilon = 10^{-4}$  and  $N = 3$ . The BB/RLT algorithm as summarized in [57] is presented in Table 4.1.

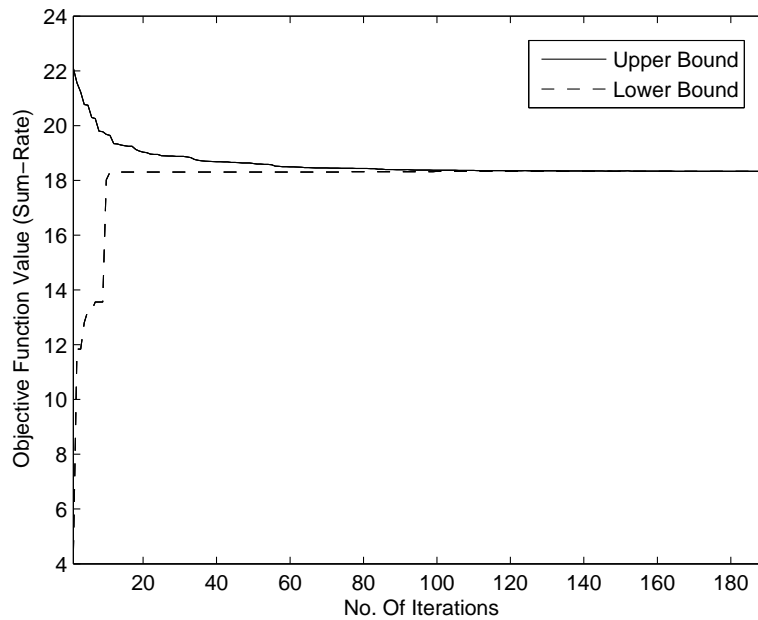


Figure 4.1: Convergence of BB/RLT algorithm for a single instantiation of the interference channel ( $\epsilon = 10^{-4}$ ,  $N = 2$  and  $MUI = 1$ ).

Table 4.1: BB/RLT Algorithm

Initialization:

1. Let optimal solution  $\alpha^* = \emptyset$ . The initial  $LB = -\infty$ .
2. Let the problem list contain only the original problem ( $P_1$ ).
3. Introduce one new variable for each nonlinear term. Add linear constraints for these variables to build a linear relaxation.
4. Denote the solution to linear relaxation as  $\hat{\alpha}$  and its objective value as upper bound  $UB_1$ .

Main Loop:

1. Select problem  $P_n$  with the largest  $UB$  from the problem list.
2. Find, if necessary, a feasible solution  $\alpha_n$  via a local search algorithm for problem  $P_n$ . Denote the objective value by  $LB_n$ .
3. If  $LB_n > LB$  then let  $\alpha^* = \alpha_n$  and  $LB = LB_n$ . If  $LB \geq (1 - \epsilon)UB$  then stop with the  $\epsilon$ -optimal solution  $\alpha^*$ ; else, remove all problems  $P_{n'}$  having  $(1 - \epsilon)UB_{n'} \leq LB$  from the problem list.
4. Select a partitioning variable and divide its bounding interval equally into two new intervals.
5. Remove the selected problem  $P_n$  from the problem list, construct two new problems  $P_{n1}$  and  $P_{n2}$  based on the two partitioned intervals.
6. Compute two new upper bounds  $UB_{n1}$  and  $UB_{n2}$  by solving the linear relaxations of  $P_{n1}$  and  $P_{n2}$ , respectively.
7. If  $(1 - \epsilon)UB_{n1} \geq LB$  then add problem  $P_{n1}$  to the problem list. Similarly, if  $(1 - \epsilon)UB_{n2} \geq LB$  then add problem  $P_{n2}$  to the problem list.
8. If the problem list is empty, stop with the  $\epsilon$ -optimal solution  $\alpha^*$ . Otherwise, go to the Main Loop again.

### 4.3.2 LPR Construction for MIMO IC Sum-Rate Maximization Problem

Our most important contribution towards evaluation of global optimal sum-rate is the LPR construction for the general MIMO IC sum-rate maximization problem. In this section, we explain this LPR construction in detail.

We begin by defining the following new variables to linearize the expression of  $C_i$ :

$$\begin{aligned} x_i &= \det(\mathbf{R}_i + \rho_{ii} \widehat{\mathbf{H}}_{ii} \Lambda_i \widehat{\mathbf{H}}_{ii}^\dagger); u_i = \ln(x_i); \\ y_i &= \det(\mathbf{R}_i); v_i = \ln(y_i). \end{aligned} \quad (4.11)$$

$C_i$  can be expressed in terms of the new variables as:  $C_i = \frac{1}{\ln 2}(u_i - v_i)$ . The constraints given

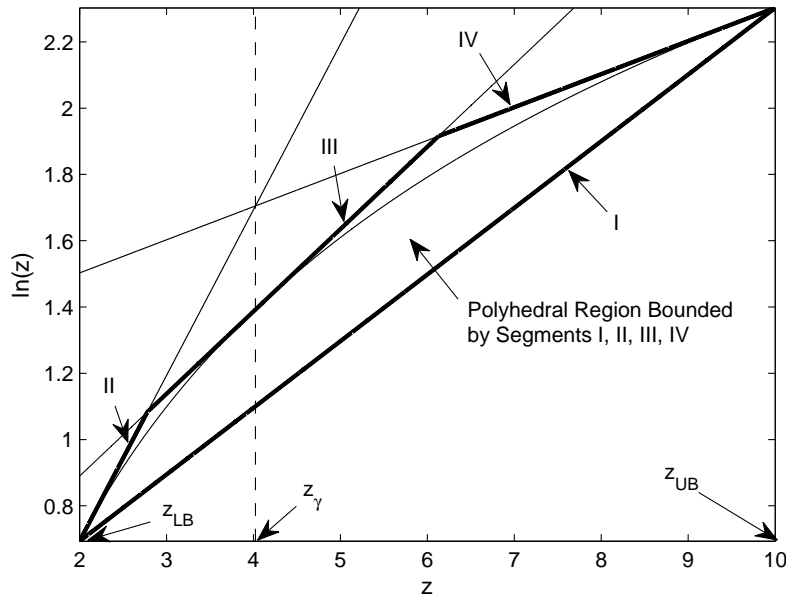


Figure 4.2: Polyhedral approximation of  $w = \ln z$ .

by (5.14) are added to the problem formulation given by (4.10).  $u_i$  and  $v_i$  are logarithmic functions of the form  $w = \ln z$ , where  $z \in [z_{LB} z_{UB}]$ . Since,  $x_i$  and  $y_i$  are dependent upon  $\Lambda_i$ , their LB and UB can be calculated by evaluating their expressions at the LB and UB of  $\Lambda_i$  respectively. A convex polygonal outer approximation is used to linearize the

logarithmic function [57]. As shown in Fig. 4.2, the convex region is defined by the tangents at  $(z_{LB}, \ln z_{LB})$ ,  $(z_\gamma, \ln z_\gamma)$  and  $(z_{UB}, \ln z_{UB})$ , and the chord joining  $(z_{LB}, \ln z_{LB})$  and  $(z_{UB}, \ln z_{UB})$ , where  $z_\gamma$  is the  $z$ -coordinate of the point of intersection of the tangents at  $(z_{LB}, \ln z_{LB})$  and  $(z_{UB}, \ln z_{UB})$ , which is given by:

$$z_\gamma = \frac{z_{LB}z_{UB}(\ln z_{UB} - \ln z_{LB})}{z_{UB} - z_{LB}}. \quad (4.12)$$

The convex region defined by these four segments can be expressed by the following linear constraints:

$$\begin{aligned} z_{LB}w - z &\leq z_{LB}(\ln z_{LB} - 1), \\ z_\gamma w - z &\leq z_\gamma(\ln z_\gamma - 1), \\ z_{UB}w - z &\leq z_{UB}(\ln z_{UB} - 1), \\ (z_{UB} - z_{LB})w + (\ln z_{LB} - \ln z_{UB})z &\geq \\ & z_{UB} \ln z_{LB} - z_{LB} \ln z_{UB}. \end{aligned} \quad (4.13)$$

After linearizing  $u_i$  and  $v_i$ , we linearize  $x_i$  and  $y_i$ . The expressions for  $x_i$  and  $y_i$  are quite similar and this similarity can be established by substituting  $\mathbf{R}_i$  in (5.14):

$$\begin{aligned} x_i &= \det \left( \sum_{j=1}^N \left( \rho_{ji} \widehat{\mathbf{H}}_{ji} \Lambda_j \widehat{\mathbf{H}}_{ji}^\dagger + \mathbf{I} \right) \right) \triangleq \det \mathbf{S}_i, \\ y_i &= \det \left( \sum_{\substack{j=1 \\ j \neq i}}^N \left( \rho_{ji} \widehat{\mathbf{H}}_{ji} \Lambda_j \widehat{\mathbf{H}}_{ji}^\dagger + \mathbf{I} \right) \right) \triangleq \det \mathbf{R}_i. \end{aligned} \quad (4.14)$$

Keeping in mind this similarity, we illustrate the linearization process for only  $x_i$ , and the results for  $y_i$  can be inferred directly. For the purpose of illustration, we assume that Tx and Rx nodes of each user have two antennas each. Since  $\Lambda_j$  ( $\forall j$ ) is an  $n_t \times n_t$  ( $= 2 \times 2$ ) matrix, it can be expressed as:

$$\Lambda_j = \begin{bmatrix} \lambda_{j1} & 0 \\ 0 & \lambda_{j2} \end{bmatrix}, \quad (4.15)$$

where  $\lambda_{j1}$  and  $\lambda_{j2}$  are the fractions of power transmitted by the  $j^{\text{th}}$  user over the two Eigenmodes of the channel. To simplify the expressions for  $x_i$  and  $y_i$  (given by (5.17)), let us define  $\widetilde{\mathbf{H}}_{ji} = \sqrt{\rho_{ji}} \widehat{\mathbf{H}}_{ji}$ .  $\mathbf{S}_i$  can now be expressed as:

$$\begin{bmatrix} 1 + \sum_{j=1}^N \lambda_{j1} (\tilde{h}_{ji})_{11} (\tilde{h}_{ji})'_{11} + \lambda_{j2} (\tilde{h}_{ji})_{12} (\tilde{h}_{ji})'_{12} & \sum_{j=1}^N \lambda_{j1} (\tilde{h}_{ji})_{11} (\tilde{h}_{ji})'_{21} + \lambda_{j2} (\tilde{h}_{ji})_{12} (\tilde{h}_{ji})'_{22} \\ \sum_{j=1}^N \lambda_{j1} (\tilde{h}_{ji})_{21} (\tilde{h}_{ji})'_{11} + \lambda_{j2} (\tilde{h}_{ji})_{22} (\tilde{h}_{ji})'_{12} & 1 + \sum_{j=1}^N \lambda_{j1} (\tilde{h}_{ji})_{21} (\tilde{h}_{ji})'_{21} + \lambda_{j2} (\tilde{h}_{ji})_{22} (\tilde{h}_{ji})'_{22} \end{bmatrix}. \quad (4.16)$$



Taking the determinant of  $\mathbf{S}_i$ ,  $x_i$  can be expressed as:

$$\begin{aligned}
x_i = 1 + \sum_{j=1}^N \left( (\tilde{h}_{ji})_{11}(\tilde{h}_{ji})'_{11} + (\tilde{h}_{ji})_{21}(\tilde{h}_{ji})'_{21} \right) \lambda_{j1} + \sum_{j=1}^N \left( (\tilde{h}_{ji})_{12}(\tilde{h}_{ji})'_{12} + (\tilde{h}_{ji})_{22}(\tilde{h}_{ji})'_{22} \right) \lambda_{j2} + \\
\sum_{j=1}^N \sum_{k=1}^N \left( (\tilde{h}_{ji})_{11}(\tilde{h}_{ji})'_{11}(\tilde{h}_{ki})_{21}(\tilde{h}_{ki})'_{21} - (\tilde{h}_{ji})_{11}(\tilde{h}_{ji})'_{21}(\tilde{h}_{ki})'_{11}(\tilde{h}_{ki})_{21} \right) \lambda_{j1}\lambda_{k1} + \\
\sum_{j=1}^N \sum_{k=1}^N \left( (\tilde{h}_{ji})_{12}(\tilde{h}_{ji})'_{12}(\tilde{h}_{ki})_{22}(\tilde{h}_{ki})'_{22} - (\tilde{h}_{ji})_{22}(\tilde{h}_{ji})'_{12}(\tilde{h}_{ki})'_{22}(\tilde{h}_{ki})_{12} \right) \lambda_{j2}\lambda_{k2} + \\
\sum_{j=1}^N \sum_{k=1}^N \left( (\tilde{h}_{ji})_{11}(\tilde{h}_{ji})'_{11}(\tilde{h}_{ki})_{22}(\tilde{h}_{ki})'_{22} + (\tilde{h}_{ji})_{21}(\tilde{h}_{ji})'_{21}(\tilde{h}_{ki})_{12}(\tilde{h}_{ki})'_{12} - \right. \\
\left. 2\Re((\tilde{h}_{ji})_{11}(\tilde{h}_{ji})'_{21})\Re((\tilde{h}_{ji})_{12}(\tilde{h}_{ji})'_{22}) - 2\Im((\tilde{h}_{ji})_{11}(\tilde{h}_{ji})'_{21})\Im((\tilde{h}_{ji})_{12}(\tilde{h}_{ji})'_{22}) \right) \lambda_{j1}\lambda_{k2}
\end{aligned} \tag{4.17}$$

The expression for  $y_i$  is similar to that for  $x_i$  with the only difference being that the terms corresponding to  $i^{\text{th}}$  users are not included in the summations. From (6.1) we observe that  $x_i$  is a quadratic polynomial with three types of quadratic terms, viz.,  $\lambda_{j1}\lambda_{k1}$ ,  $\lambda_{j2}\lambda_{k2}$  and  $\lambda_{j1}\lambda_{k2}$ . It is important to note that  $\lambda_{j1}\lambda_{k1}$  is the same as  $\lambda_{k1}\lambda_{j1}$  and hence the number of unique quadratic terms for this category is  $\sum_{j=1}^N j = \frac{N}{2}(N+1)$ . The same argument holds for  $\lambda_{j2}\lambda_{k2}$ . The number of unique terms for  $\lambda_{j1}\lambda_{k2}$  ( $\forall j, k$ ) is  $N^2$ , which makes the total number of quadratic terms in (6.1) equal to  $N(2N+1)$ . Each of these quadratic terms is replaced by a new variable:  $\Gamma_{j1k1} = \lambda_{j1}\lambda_{k1}$ ,  $\Gamma_{j1k2} = \lambda_{j1}\lambda_{k2}$  and  $\Gamma_{j2k2} = \lambda_{j2}\lambda_{k2}$ . These equalities are relaxed by including the following linear inequalities called bounding factor constraints (illustrated for  $\Gamma_{j1k2}$ ), for each non-linear term:

$$\begin{aligned}
\Gamma_{j1k2} - \lambda_{j1LB}\lambda_{k2} - \lambda_{j1}\lambda_{k2LB} &\geq -\lambda_{j1LB}\lambda_{k2LB} \\
\Gamma_{j1k2} - \lambda_{j1UB}\lambda_{k2} - \lambda_{j1}\lambda_{k2LB} &\leq -\lambda_{j1UB}\lambda_{k2LB} \\
\Gamma_{j1k2} - \lambda_{j1LB}\lambda_{k2} - \lambda_{j1}\lambda_{k2UB} &\leq -\lambda_{j1LB}\lambda_{k2UB} \\
\Gamma_{j1k2} - \lambda_{j1UB}\lambda_{k2} - \lambda_{j1}\lambda_{k2UB} &\geq -\lambda_{j1UB}\lambda_{k2UB}
\end{aligned} \tag{4.18}$$

This completes LPR construction of the original problem (4.10) and the corresponding LP

can be expressed as:

$$\begin{aligned}
\max \quad & \sum_{i=1}^N C_i \\
s.t. \quad & C_i = \frac{1}{\ln 2}(u_i - v_i), \\
& \text{Polynomial approximation of } u_i \text{ and } v_i \text{ given by (5.16),} \\
& \text{Linear expressions for } x_i \text{ and } y_i \text{ (using (6.1)),} \\
& \text{Bounding constraints for } \Gamma_{j1k1}, \Gamma_{j1k2} \text{ and } \Gamma_{j2k2} \text{ (5.21),} \\
& Tr\{\Lambda_i\} \leq P_{max}, \text{diag}\{\Lambda_i\} \succeq \mathbf{0}, 1 \leq i \leq N.
\end{aligned} \tag{4.19}$$

The LPR essentially relaxes the feasible region of the original NL problem (4.10) and hence the optimal objective function value of the LP (5.22) serves as an UB to the optimal sum-rate. Since the LP is subject to the same power constraint as the original NL problem (4.10), the optimal solution to the LP is also a feasible solution to (4.10). In general, this feasible solution is not optimal to the original problem (4.10) and the corresponding objective function value of (4.10) yields a LB to the optimal sum-rate. After finding these bounds, BB strategy is employed to partition the search space so that both the largest UB and LB approach towards the global maximum as explained in Table 4.1. Please note that the implementation of BB strategy is not unique. In this work, we select the partitioning variable as the one which has the highest bounding interval (highest difference between the LB and UB). The bounding interval of this variable is then partitioned equally into two intervals to construct two new problems. BB strategy is carried out in the similar way until global optimum is achieved.

After developing the global optimization algorithm with a guaranteed convergence to the globally optimal solution, we now look into the optimal power allocation strategies of various ICs in the following sections.

#### 4.4 Two-User 2x2 MIMO IC (Case of $N = n_t$ )

We start our discussion by considering the simplest possible case of the MIMO IC, i.e., the two-user  $2 \times 2$  symmetric MIMO IC. This case is a simple extension of the classical two-user

symmetric IC discussed in the previous chapter. In this case, we assume that each user has 2 transmit and 2 receive antennas. Thus, an additional spatial dimension is available for interference avoidance as compared to the classical single antenna IC. We assume that a single frequency band is available for transmission. Small scale fading effects are modeled as being Rayleigh distributed. We also assume that the MIMO links do not suffer from shadowing. The *MUI* factor is fixed at 1 and the effect of varying  $SNR_{min}$  on the optimal sum-rate is studied. It should be recalled that it is enough to study the sum-rate by varying one of the two parameters (*MUI* or  $SNR_{min}$ ) while keeping the other constant, to capture all the important characteristics of the optimal power allocation. We further assume that the simulation is set-up in the same way as explained for the classic two-user symmetric IC in the previous chapter.

To gain some insight into the optimal power allocation strategy, we consider following power allocation strategies:

- **Optimal MIMO:** This case provides maximum achievable sum-rate by employing optimal power control over spatial channels of each user. This acts as a benchmark for the special cases considered in this study. The comparison of this benchmark with the special cases will help us understand the optimal power allocation strategy in various interference scenarios.
- **Max Power Beamforming:** In this case, each user transmits at maximum power  $P_{max}$  in only one spatial channel (Eigen-mode of  $\mathbf{R}_i^{-1}\mathbf{H}_{ii}\mathbf{H}_{ii}^\dagger$ ). It should be noted that the selection of optimal Eigen-mode is not trivial in this case. In other words, it is not optimal in general for a user to choose the strongest Eigen-mode of its interference-free channel (as is the case in isolated MIMO links). As explained before, this is due to the presence of mutual interference in the MIMO IC. We will discuss this problem of optimal Eigen-mode selection in detail in a later chapter. For this study, we perform an exhaustive search over all the available choices of Eigen-modes to find the optimal set. It is worth noting here that exhaustive search is quite feasible because there are

only  $\binom{2}{1}\binom{2}{1}(= 4)$  choices to check.

- **Equal Power Distribution:** In this case, both the users transmit at maximum power  $P_{max}$  and distribute the power equally over the spatial channels. It should be noted that there is no optimization involved in this case.
- **One User - Equal Power Distribution:** In this case, the user with the stronger MIMO channel is allowed to transmit. The allowed user transmits at the maximum power by distributing it equally over the spatial channels. For the sake of this example, we calculate the capacity of each user by turning off the other and select the one with the higher capacity.
- **One User - Beamforming:** In this case too, only one of the two users is allowed to transmit. The allowed user transmits maximum power  $P_{max}$  in the stronger Eigenmode of its ‘interference-free’ channel. This problem also involves the selection of the ‘optimal’ user. As in the previous case, we calculate the beamforming capacities of each user by turning off the other user and selects the one with the higher capacity.

To study the effect of antenna correlation, we simulate all the above cases in the following two scenarios:

- **Scenario 1: Perfectly Uncorrelated Antennas ( $\rho = 0$ ):** In this scenario, we assume that the Tx and Rx antennas of each user are perfectly uncorrelated. Due to the presence of two orthogonal spatial channels, we expect to get interesting insights into the power allocation strategy in this case.
- **Scenario 2: Perfectly Correlated Antennas ( $\rho = 1$ ):** In this scenario, we assume that the Tx and Rx antennas of each user are perfectly correlated. In this case, each MIMO link has only one spatial channel on which to transmit. It would be interesting to compare the optimal power allocation strategy in this case to that of the single antenna IC (studied in the previous chapter).

#### 4.4.1 Numerical Results for Scenario 1 ( $\rho = 0$ )

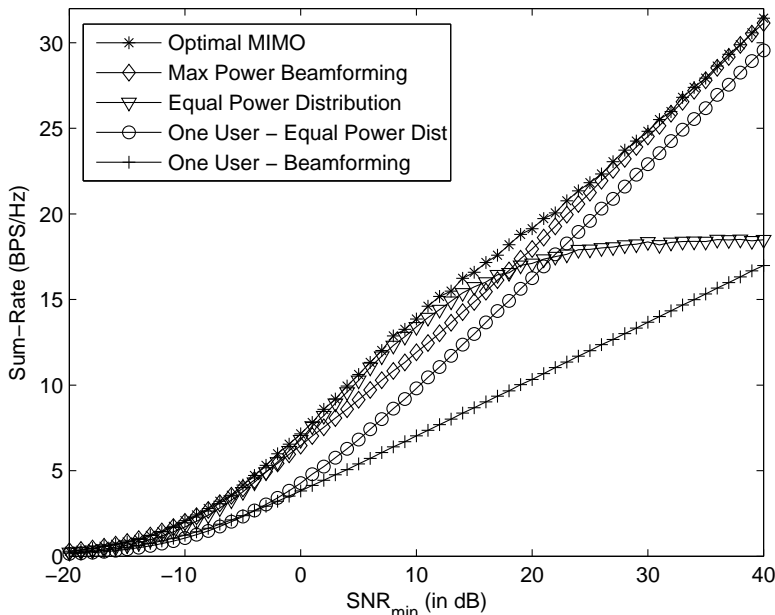


Figure 4.3: Numerical results of the ergodic sum-rate achievable in the two-user  $2 \times 2$  symmetric MIMO IC, Scenario 1 ( $n_t = n_r = 2$ ,  $N = 2$ ,  $N_b = 1$ ,  $\rho = 0$ ,  $MUI = 1$ ,  $\sigma = 0$ , Rayleigh fading assumed).

The sum-rates achievable in this scenario are presented in Fig. 4.3. The most important observation is that it is usually optimal for both the users to simultaneously transmit at the maximum power  $P_{max}$  in all the SNR regimes. This means that the presence of two spatial channels helps in avoiding interference at least to a level where the sum-rate of the two users is higher than the interference-free capacity of any of the two individual links. As will be discussed later in detail, beamforming is observed to be optimal in the (interference-limited) high SNR regime. The comparison of the optimal sum-rate with the interference-free beamforming capacity of a single link in the high SNR regime suggests that the effect of interference is negligible from the beamforming sense (optimal sum-rate is  $\approx 2$  times the interference-free beamforming capacity of a single link). Thus, it is optimal for each user to use one of the degrees of freedom for beamforming and other to avoid interference from the

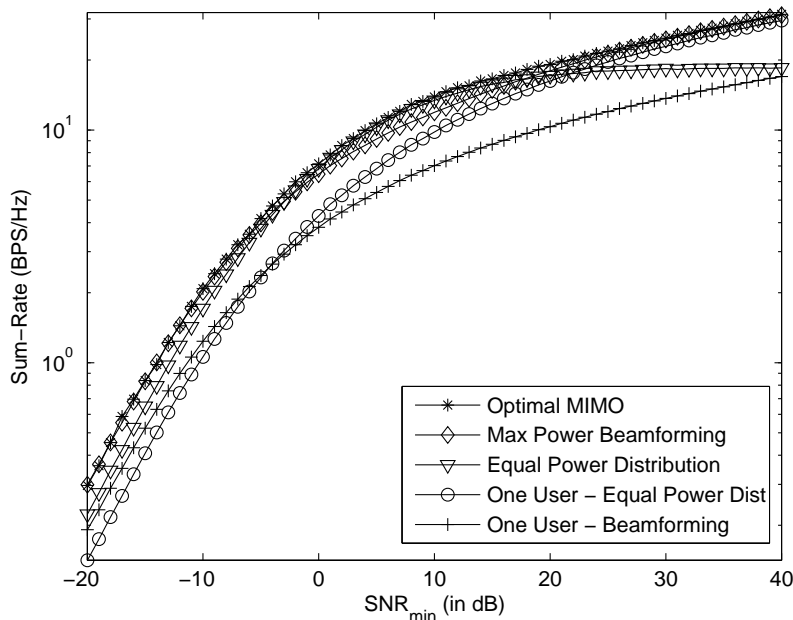


Figure 4.4: Numerical results of the ergodic sum-rate achievable in the two-user  $2 \times 2$  symmetric MIMO IC plotted on the log-scale, Scenario 1 ( $n_t = n_r = 2$ ,  $N = 2$ ,  $N_b = 1$ ,  $\rho = 0$ ,  $MUI = 1$ ,  $\sigma = 0$ , Rayleigh fading assumed).

other user. It would be interesting to see how the IC behaves if we add an extra user keeping the number of spatial channels to be 2. We will study this case in the next section. As a side note, it is worth recalling here that high  $SNR_{min}$  also implies a stronger interference channel (high interference power relative to the noise power).

Beamforming is also observed to be optimal in the very low SNR (noise-limited) regime. This may not be prominent from the results presented in Fig. 4.3 but the same results plotted on the log-scale in Fig. 4.4 clearly reveal the trend. This scenario is not very interesting since it corresponds to a very weak interference regime due to which the links are fundamentally noise-limited. From the knowledge of the noise-limited MIMO links, we already know that beamforming is optimal strategy to adopt when the received SNR per antenna is low. Since, this regime is already well-understood, we won't consider it in the rest of the thesis.

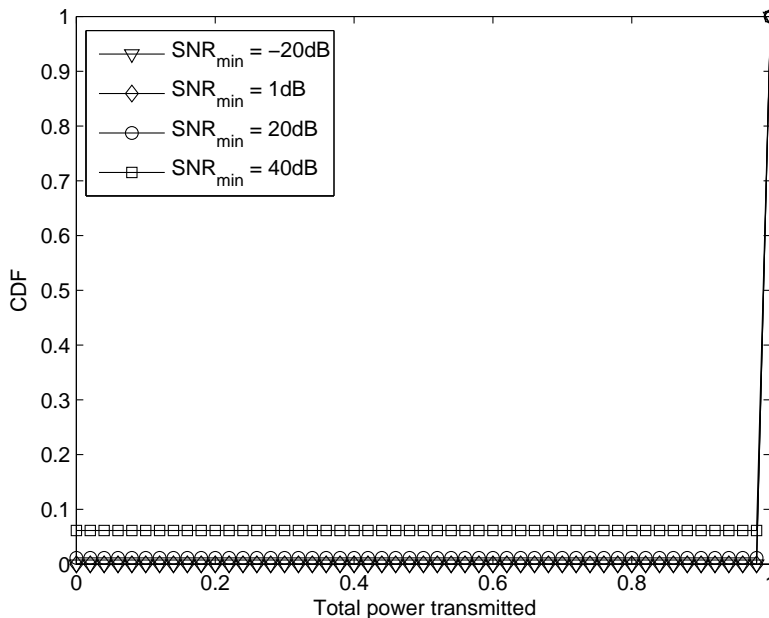


Figure 4.5: Distribution of the total power transmitted by each user in the two-user  $2 \times 2$  symmetric MIMO IC, Scenario 1 ( $n_t = n_r = 2$ ,  $N = 2$ ,  $N_b = 1$ ,  $\rho = 0$ ,  $MUI = 1$ ,  $\sigma = 0$ , Rayleigh fading assumed).

In the low SNR regime (around  $SNR_{min} \approx 0$  dB), it is optimal to distribute the transmit power ( $P_{max}$ ) over the two spatial channels. The exact nature of the distribution will be studied later in this section. On the other hand, it is optimal to transmit at maximum power in one of the spatial channels in the high SNR regime. In other words, Eigen-vector beamforming is optimal. This is an interesting observation since it is in contrast to the isolated MIMO link, where beamforming is optimal in the low SNR regime and equal power distribution is optimal in the high SNR regime. This highlights the fact that the importance of interference avoidance (e.g., by beamforming or turning off bad users) increases as we move from the low SNR (low interference) regime to the high SNR (high interference) regime.

With this newly found insight, we now look at the optimal power allocation strategy more closely. In Fig. 4.5, we plot the CDF of the total power transmitted by each user mainly in four SNR regimes: very-low ( $SNR_{min} = -20$  dB), low ( $SNR_{min} = 1$  dB), intermediate

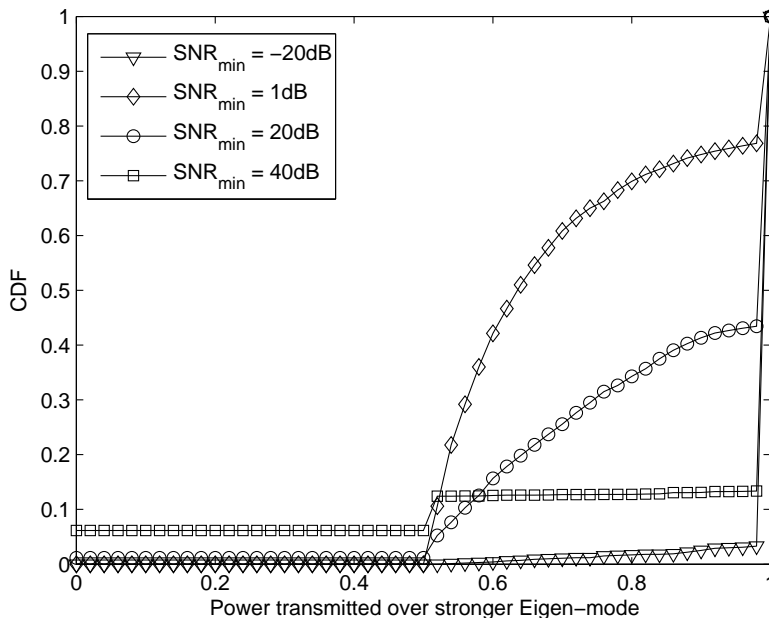


Figure 4.6: Distribution of the power transmitted by each user over stronger Eigen-mode in the two-user  $2 \times 2$  symmetric MIMO IC, Scenario 1 ( $n_t = n_r = 2$ ,  $N = 2$ ,  $N_b = 1$ ,  $\rho = 0$ ,  $MUI = 1$ ,  $\sigma = 0$ , Rayleigh fading assumed).

( $SNR_{min} = 20$  dB) and high ( $SNR_{min} = 40$  dB). Since the very-low SNR regime corresponds to a noise-limited case and beamforming is already known to be optimal, we won't discuss it in detail in this thesis. Instead, we will concentrate only on the rest of the three SNR scenarios: low, intermediate and high.

The most important observation in this study is that the binary power control is optimal for all the three scenarios. This may not be completely obvious in low and intermediate SNR regimes because it is mostly optimal for both the users to transmit at the maximum power. However, it is evident from the results in the high SNR regime. In particular, it is optimal to keep one of the users completely off for around 10% of the time while letting the other user transmit at the maximum power. For the rest of the time, it is optimal for both the users to transmit at maximum power (no intermediate states are optimal). This is one of the reasons for the slight difference in the optimal sum-rate and the max power beamforming sum-rate.



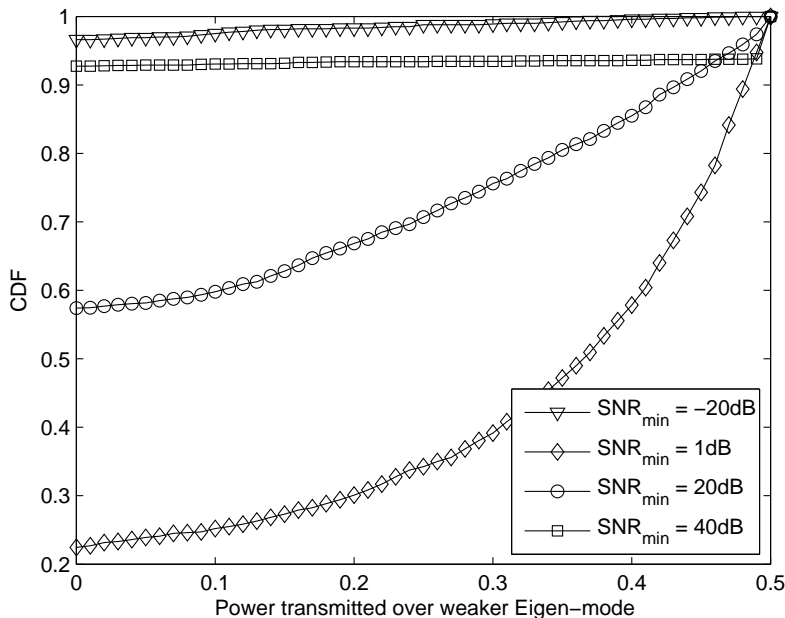


Figure 4.7: Distribution of the power transmitted by each user over weaker Eigen-mode in the two-user  $2 \times 2$  symmetric MIMO IC, Scenario 1 ( $n_t = n_r = 2$ ,  $N = 2$ ,  $N_b = 1$ ,  $\rho = 0$ ,  $MUI = 1$ ,  $\sigma = 0$ , Rayleigh fading assumed).

We now study the distribution of the power over spatial channels by plotting the CDF of the power transmitted over stronger and weaker Eigen-modes in Fig. 4.6 and Fig. 4.7, respectively. It is important to note that the stronger Eigen-mode is defined in this study as the one over which higher power is transmitted in the optimal power allocation. It does not necessarily correspond to the strongest Eigen-mode of the whitened channel matrix. We look at the same three SNR regimes: low, intermediate and high. As observed earlier, it is usually optimal for both users to simultaneously beamform in the high SNR regime. In a small fraction of cases, it is optimal for only one of the users to transmit while keeping the other turned off. In these cases, the allowed user distributes equal power over the two spatial channels. This can be inferred from a small step at 0.5 (corresponding to  $P_{max}/2$ ) in the CDF of the power transmitted over both the stronger and the weaker Eigen-modes. Except these two cases, there is no other optimal case in the high SNR regime. In the low

SNR regime, we observe that distributing power over both of the spatial channels is optimal in most of the cases and beamforming is optimal in a small number of cases. In most of the cases, it is optimal for the user to transmit  $\approx 50\% - 70\%$  of the power in the stronger Eigen-mode and rest in the weaker Eigen-mode. In the intermediate SNR regime, the probability of beamforming increases as compared to the low SNR case. In particular, it is optimal for each user to perform beamforming in  $\approx 58\%$  of the cases in the intermediate SNR regime as opposed to  $\approx 25\%$  of the cases in the low SNR regime. In the rest of the cases, it is optimal to transmit a higher power in the stronger Eigen-mode (as expected).

### Summary of the Main Results from Scenario 1:

- Presence of two orthogonal spatial channels enables the simultaneous transmission of both the users in the two-user symmetric  $2 \times 2$  MIMO IC. It is observed that interference can be avoided to a large extent by performing beamforming. In particular, each user employs one of the degrees of freedom for beamforming and other for avoiding interference from the other user (in interference-limited high SNR regime).
- It is optimal to distribute power over the two spatial channels in the low SNR regime. However, equal power distribution is not necessarily optimal. In most of the cases,  $\approx 50\% - 70\%$  of the power is transmitted in the stronger Eigen-mode and rest in the weaker Eigen-mode.
- Binary power control is optimal in all the SNR scenarios considered in this case: low, intermediate and high.
- There are only two optimal states in the high SNR regime: 1) Both users perform beamforming, and 2) One user distributes power equally over the two spatial channels and the other user turned off.
- Beamforming is optimal in the very-low SNR regime. This regime corresponds to a very weak interference regime due to which the links are fundamentally noise-limited. From

the knowledge of the noise-limited MIMO links, we already know that beamforming is optimal strategy to adopt when the received SNR per antenna is low.

#### 4.4.2 Numerical Results for Scenario 2 ( $\rho = 1$ )

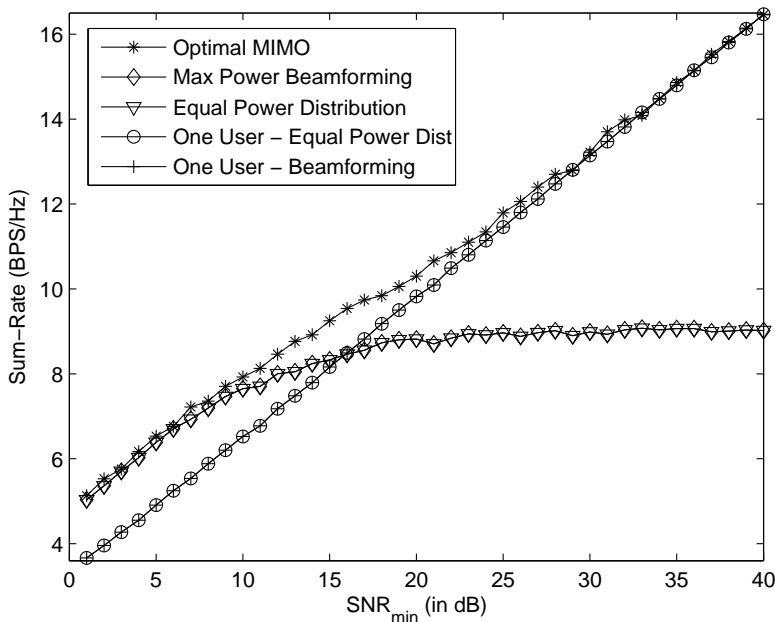


Figure 4.8: Numerical results of the ergodic sum-rate achievable in the two-user  $2 \times 2$  symmetric MIMO IC, Scenario 2 ( $n_t = n_r = 2$ ,  $N = 2$ ,  $N_b = 1$ ,  $\rho = 1$ ,  $MUI = 1$ ,  $\sigma = 0$ , Rayleigh fading assumed).

We now consider the scenario where the antennas at all the Tx and Rx nodes are perfectly correlated ( $\rho = 1$ ). In this case, each MIMO link effectively has a single spatial channel to transmit. Due to this reason, we do not expect a good interference avoidance capability in this scenario.

The sum-rates achievable in all the five cases in this scenario are presented in Fig. 4.8. First observation in this case is that the distribution of power does not really make any difference. This is because there is only one spatial Eigen-mode and hence the distribution of power

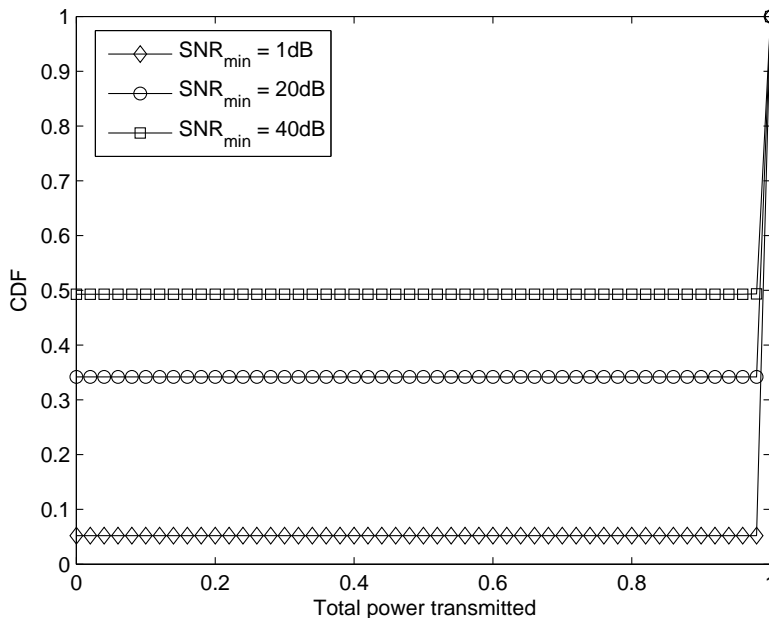


Figure 4.9: Distribution of the total power transmitted by each user in the two-user  $2 \times 2$  symmetric MIMO IC, Scenario 2 ( $n_t = n_r = 2$ ,  $N = 2$ ,  $N_b = 1$ ,  $\rho = 1$ ,  $MUI = 1$ ,  $\sigma = 0$ , Rayleigh fading assumed).

does not matter. We will explain this in detail later in this section.

From the simulation results, we note that it is optimal for both the users to simultaneously transmit in the low SNR regime and for only one of them to transmit at the high SNR regime. This result is in perfect coherence with our observations in the classical 2-user SISO IC. This is due to the fact that there is only one spatial channel available in the present case and it is essentially a SISO system with an SNR gain. To gain some further insight, we plot the CDF of the total power transmitted by each user in Fig. 4.9. We study the CDF of the total transmit power in three SNR regimes: low ( $SNR_{min} = 1$  dB), intermediate ( $SNR_{min} = 20$  dB) and high ( $SNR_{min} = 40$  dB). One prominent observation in all the three scenarios is the optimality of the binary power control. This is again consistent with the classical SISO IC. We observe that each user is turned off in around 50% of the cases in high SNR regime. Since 50% corresponds to half the users, this actually means that one of the users is always

turned off in this regime.

In the intermediate SNR regime, each user is turned off in around 35% of the cases. Thus, at least one of the two users is turned off in around 70% of the cases. On the other hand, in the low SNR regime it is optimal for both the users to transmit in most of the cases (one user is turned off in only around 10% of the cases).

We now explain the reason for the same sum-rate being achieved irrespective of the fractions of the power transmitted over the ‘mathematical’ Eigen-modes. We will consider an isolated  $2 \times 2$  MIMO link for this explanation. As mentioned earlier, the capacity of a single MIMO link can be expressed as:

$$C_i = \log_2 \det(\mathbf{I} + \rho_{ii} \mathbf{H}_{ii} \Lambda_i \mathbf{H}_{ii}^\dagger), \quad (4.20)$$

where all the variables are defined earlier. The capacity essentially depends upon the strength of the Eigen-modes and the fraction of power distributed over them, i.e., it depends upon the  $\mathbf{H}_{ii} \Lambda_i \mathbf{H}_{ii}^\dagger$  term. Ignoring the scaling factors, the channel matrix  $\mathbf{H}_{ii}$  can be generated as:

$$\mathbf{H}_{ii} = \sqrt{\mathbf{R}_{Tx}} \mathbf{H}_w \sqrt{\mathbf{R}_{Rx}}. \quad (4.21)$$

For the perfectly correlated case, we assume  $\rho = 1$ , so  $\mathbf{R}_{Tx}$  and  $\mathbf{R}_{Rx}$  can be written as:

$$\mathbf{R}_{Tx} = \mathbf{R}_{Rx} = \begin{bmatrix} 1 & 1 \\ 1 & 1 \end{bmatrix}. \quad (4.22)$$

The expression of  $\mathbf{H}_{ii}$  can now be expanded as:

$$\mathbf{H}_{ii} = \sqrt{\begin{bmatrix} 1 & 1 \\ 1 & 1 \end{bmatrix}} \begin{bmatrix} h_{11} & h_{12} \\ h_{21} & h_{22} \end{bmatrix} \sqrt{\begin{bmatrix} 1 & 1 \\ 1 & 1 \end{bmatrix}}. \quad (4.23)$$

This expression can be simplified to:

$$\mathbf{H}_{ii} = \frac{1}{2} \begin{bmatrix} h_{11} + h_{12} + h_{21} + h_{22} & h_{11} + h_{12} + h_{21} + h_{22} \\ h_{11} + h_{12} + h_{21} + h_{22} & h_{11} + h_{12} + h_{21} + h_{22} \end{bmatrix}. \quad (4.24)$$

We observe that all the terms of  $\mathbf{H}_{ii}$  are same. One of the physical interpretations of this is that both the antennas are located at same point in space (both at the Tx node and Rx

node). Now we substitute  $h_{11} + h_{12} + h_{21} + h_{22} = h$  and try to simplify  $\mathbf{H}_{ii}\Lambda_i\mathbf{H}_{ii}^\dagger$  assuming  $\lambda_1$  and  $\lambda_2$  is transmitted on the two ‘mathematical’ Eigen-modes. We neglect the scaling factors of  $\mathbf{H}_{ii}$  for the simplicity of presentation.

$$\mathbf{H}_{ii}\Lambda_i\mathbf{H}_{ii}^\dagger = \begin{bmatrix} h & h \\ h & h \end{bmatrix} \begin{bmatrix} \lambda_1 & 0 \\ 0 & \lambda_2 \end{bmatrix} \begin{bmatrix} h & h \\ h & h \end{bmatrix} = (\lambda_1 + \lambda_2)h^2 \begin{bmatrix} 1 & 1 \\ 1 & 1 \end{bmatrix}. \quad (4.25)$$

The above expression clearly shows that the link capacity is dependent upon the total power transmitted, i.e.,  $\lambda_1 + \lambda_2$ , and not on the fraction of the power transmitted on each ‘mathematical’ mode.

## 4.5 Three-User $2 \times 2$ MIMO IC (Case of $N > n_t$ )

We now extend the previous case to the three-user case by adding an extra user while keeping all the other simulation parameters same. The resulting three-user IC is the same as the one studied in the previous chapter, with the only difference that each node now has 2 antennas. The motivation to study this case is to understand the effect of having more users than the available spatial channels (per user) on the optimal power allocation strategy. It would be particularly interesting to see how the interference is avoided in the high SNR (essentially high interference) scenario. For this study, we consider following simulation scenarios to get insight into the optimal power allocation:

- **Optimal MIMO:** This case represents the maximum sum-rate achievable in the three-user  $2 \times 2$  MIMO IC considered in this study. As explained in the previous case, this sum-rate acts as a benchmark to decide which power allocation strategies perform close to optimal in various interference scenarios.
- **Max Power Beamforming:** In this case, each user transmits at the maximum allowable power in an optimal spatial channel. The problem of choosing optimal spatial channel will be discussed in detail in a later chapter. For this case, we perform an

exhaustive search over all the possible choices. Exhaustive search is feasible because the number of choices is just  $\binom{2}{1}\binom{2}{1}\binom{2}{1}(= 8)$

- **Equal Power Distribution:** Each user transmits at the maximum power  $P_{max}$  and distributes the transmit power equally over all the spatial channels. As mentioned earlier, there is no optimization involved in this case.
- **One User - Equal Power Distribution:** In this case, only one of the three users is allowed to transmit. The allowed user is the one that achieves highest capacity amongst the three by distributing power equally over all the Eigen-modes. The optimal user is selected by an exhaustive search in this case (since there are just 3 choices to check).
- **Two User - Max Power Beamforming:** This special case is included to understand to optimality of turning one of the users off (especially in the high interference scenarios). In this case, two of the three users are selected to transmit simultaneously. Each selected user then selects an optimal spatial channel for transmission. The selection of the users and spatial channel is done to maximize the sum-rate under the said constraints. This problem of user and Eigen-channel selection can be formulated as a non-linear mixed-integer optimization problem. We will briefly look such formulations in a later chapter. For this example, we perform an exhaustive search through all the feasible options. The exhaustive search in this case is quite feasible since there are only  $\binom{3}{2}\binom{2}{1}\binom{2}{1}(= 12)$  cases to check.

Since we are more interested in understanding the effect of the availability of spatial channels on the optimal power allocation strategies, we will mainly focus on the case when the antennas at both the Tx and Rx nodes of all the users are perfectly uncorrelated. For the sake of completeness, we will briefly look at the perfectly correlated case.

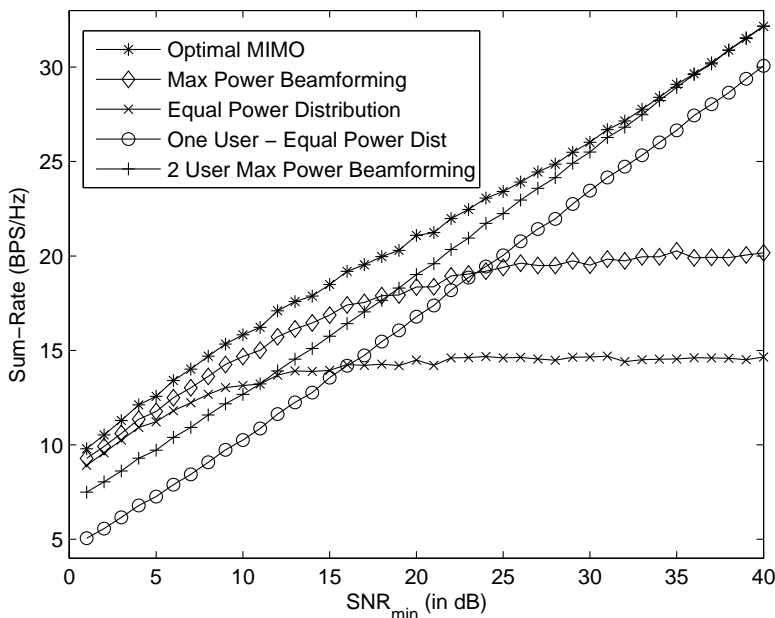


Figure 4.10: Numerical results of the ergodic sum-rate achievable in the three-user  $2 \times 2$  MIMO IC ( $n_t = n_r = 2$ ,  $N = 3$ ,  $N_b = 1$ ,  $\rho = 0$ ,  $MUI = 1$ ,  $\sigma = 0$ , Rayleigh fading assumed).

### 4.5.1 Numerical Results

The achievable sum-rate in all the above mentioned cases is presented in Fig. 4.10. We observe that the optimal sum-rate is better than all the special cases in the low and intermediate SNR regimes. This essentially means that none of the special cases studied in this example is optimal in these SNR regimes. As will be discussed later in detail, we note that all the three users are allowed to transmit in almost all of the cases in the low SNR regime. The exact power distribution, however, depends upon the channel conditions and the interaction of the Eigen-modes of the interfering users with the intended link. We will look more into the exact power distributions when we look at the CDFs of the power distributed over spatial channels later in this section.

We observe that it is better to turn off one user and let the other two perform beamforming than to let all of them simultaneously transmit in the intermediate SNR regime. We further



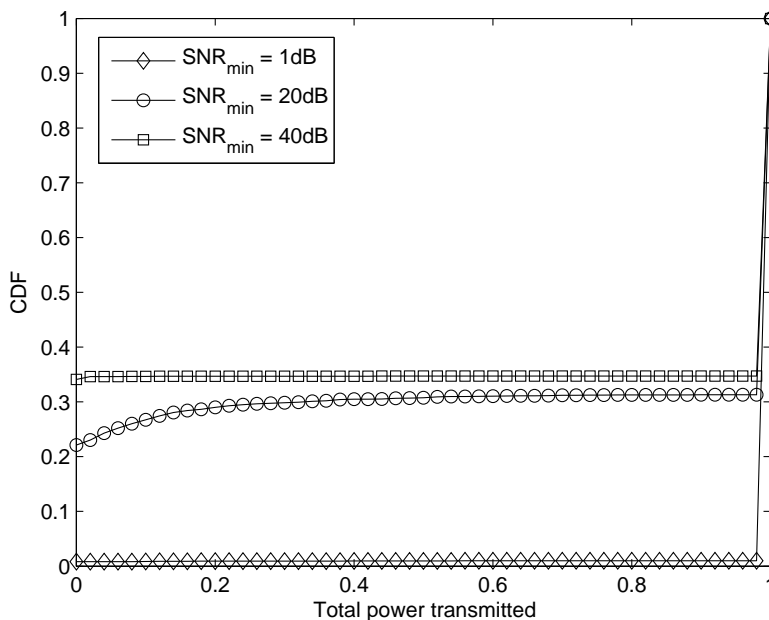


Figure 4.11: Distribution of the total power transmitted by each user in the three-user  $2 \times 2$  MIMO IC ( $n_t = n_r = 2$ ,  $N = 3$ ,  $N_b = 1$ ,  $\rho = 0$ ,  $MUI = 1$ ,  $\sigma = 0$ , Rayleigh fading assumed).

note that the optimal sum-rate is even better than the 2-user beamforming case. This suggests that it is optimal to selectively turn off a user in some cases and let all of them transmit in the rest of the cases. We will validate this point when we study the CDFs of the power distributed across spatial channels.

The sum-rate results show that the system is most well-behaved in the high SNR regime. It is optimal in this regime to turn off one user and let the other two perform beamforming while transmitting at the maximum power  $P_{max}$ . This result establishes a nice relationship between the number of spatial channels and number of users allowed to transmit in the high SNR regime. It is important to note here that the presence of 2 antennas at both the Tx and Rx nodes provides two degrees of freedom to each user. One degree of freedom can be used to perform beamforming and the other can be used to avoid interference from one user. It is, however, not possible in general to avoid interference from both the users simultaneously due to the lack of a sufficient number of degrees of freedom. This result highlights the importance

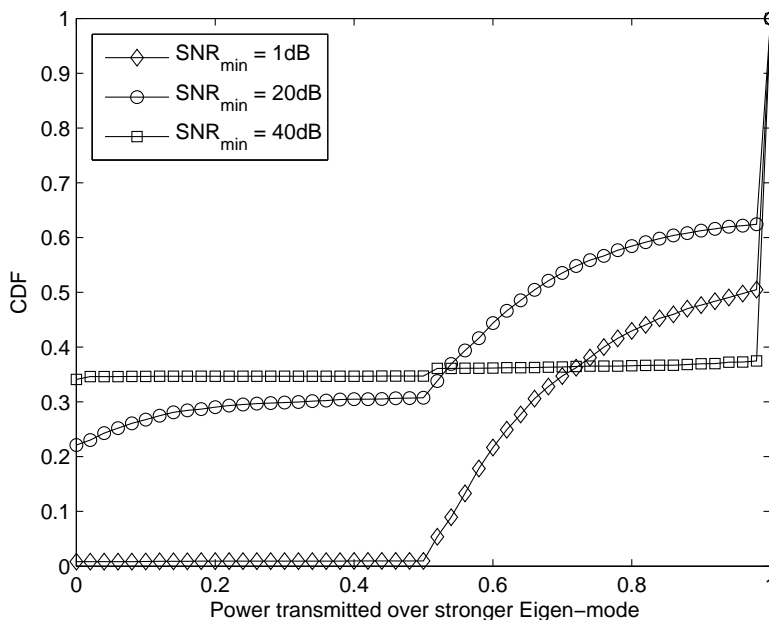


Figure 4.12: Distribution of the power transmitted by each user over stronger Eigen-mode in the three-user  $2 \times 2$  MIMO IC ( $n_t = n_r = 2$ ,  $N = 3$ ,  $N_b = 1$ ,  $\rho = 0$ ,  $MUI = 1$ ,  $\sigma = 0$ , Rayleigh fading assumed).

of interference avoidance in the high SNR regime. This is consistent with our observations in single band SISO ICs, where it is optimal for only one of the users to transmit in the high SNR regime (only a single degree of freedom was available).

With this understanding about the optimal power allocation strategy, we now look at the CDFs of the power transmitted by each user and their distributions over the spatial channels. We first study the CDF of the total power transmitted at three different SNR regimes: low ( $SNR_{min} = 1$  dB), intermediate ( $SNR_{min} = 20$  dB) and high ( $SNR_{min} = 40$  dB) in Fig. 4.11. First observation is that it is optimal for all the users to transmit in the low SNR regime. This is in consonance with our previous results because it is a noise-limited case and interference power does not have a huge effect on the sum-rate. We further note that as we move from the low to high SNR regime, it is optimal to turn off more users due to the increasing effect of interference power (because of the scaling down of noise relative to

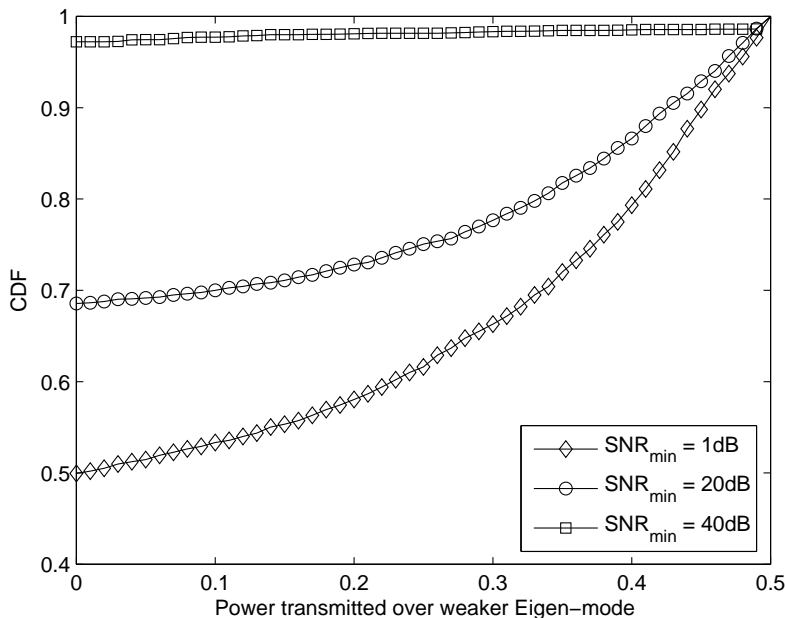


Figure 4.13: Distribution of the power transmitted by each user over weaker Eigen-mode in the three-user  $2 \times 2$  MIMO IC ( $n_t = n_r = 2$ ,  $N = 3$ ,  $N_b = 1$ ,  $\rho = 0$ ,  $MUI = 1$ ,  $\sigma = 0$ , Rayleigh fading assumed).

interference power). In particular, it is optimal to turn off one of the three users in almost 70% of the cases in intermediate SNR regime and almost 100% of the cases in high SNR regime. Distribution of the transmit power in the intermediate SNR regime also suggests that it is sometimes optimal to let the third user transmit at a reduced power while the other two are transmitting at maximum power  $P_{max}$ . This implies that binary power control is not optimal in the intermediate SNR regime. Interestingly, we note that binary power control is still optimal in the high SNR regime. In other words, it is either optimal for a user to transmit at the maximum power or remain silent. This is an interesting result and reiterates the fact that purely interference-limited system is more well-behaved than noise+interference limited system (intermediate SNR regime).

We now look at the distribution of the power transmitted by each user in the stronger Eigen-mode in all the three SNR regimes in Fig. 4.12. We first note that it is optimal for each

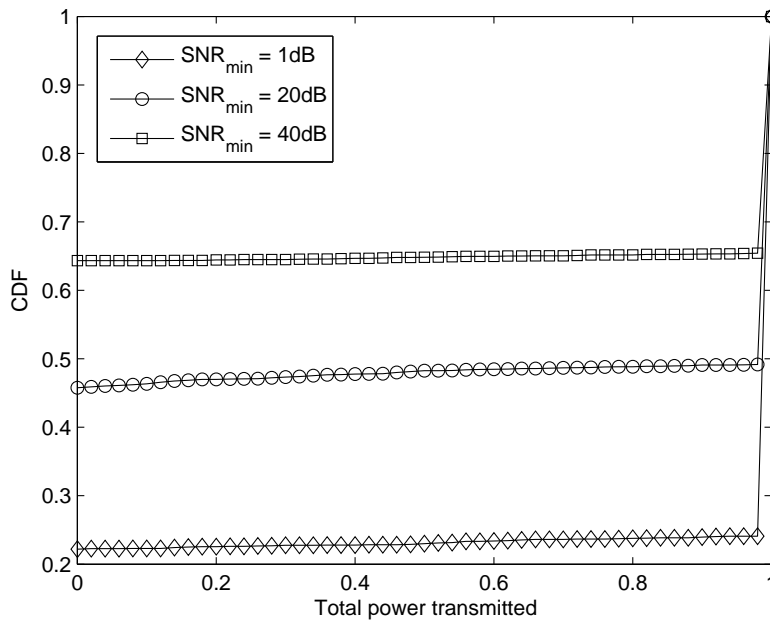


Figure 4.14: Distribution of the total power transmitted by each user in the three-user  $2 \times 2$  MIMO IC assuming perfectly correlated antennas ( $n_t = n_r = 2$ ,  $N = 3$ ,  $N_b = 1$ ,  $\rho = 1$ ,  $MUI = 1$ ,  $\sigma = 0$ , Rayleigh fading assumed).

user to remain silent around one-third of the time in the high SNR regime. Since the events of the users remaining silent are mutually exclusive, this actually means that it is optimal to always keep one user off in the high SNR regime (as noted earlier too). We also note an extremely small fraction of cases where it is optimal for a user to distribute equal power over the two spatial channels. The occurrence of these cases is extremely rare and represents the cases when the avoidance of interference is not possible and it is optimal for only one of the three users to transmit. Since the probability of occurrence of these cases is small, they do not affect the statistics much. The distribution of the power transmitted in the stronger spatial channel in the intermediate SNR regime suggests that it is optimal to keep each user turned off for around 20% of the cases and let it perform beamforming in around 60% of the cases. It is optimal to distribute power over spatial channels in the rest of the cases. Results in the low SNR regime suggest that it is highly unlikely for any user to be turned off in the

optimal power allocation strategy. It is optimal for each user to perform beamforming in around 50% of the cases and distribute power over the spatial channels in the rest of the cases.

The distributions of the power transmitted in the weaker mode are presented in Fig. 4.13. When the results indicate that it is optimal not to transmit any power in the weaker mode, it essentially means that beamforming is optimal. Results in the high SNR regime indicate that it is optimal not to transmit any power in the weaker mode. This means that either the user is turned off or it performs beamforming. The results in the other two cases just reiterate the facts discussed earlier. A detailed discussion of these results is hence omitted to avoid repetition.

For the sake of completeness, we present the distributions of the total power transmitted in various SNR regimes in perfectly correlated antenna case in Fig. 4.14. In a nut-shell, the results reiterate the importance of turning off more users in the high SNR regime as compared to the low SNR regime. As is the case in the SISO IC, it is optimal for only one of the users to transmit when the interference power is sufficiently higher than noise power (high  $SNR_{min}$  case).

## 4.5.2 Summary of the Main Results

- It is optimal to completely ‘avoid’ interference in the high SNR regime (high interference scenario). In the present system, it is achieved by turning off one of the three users and letting the other two perform beamforming by transmitting at the maximum power  $P_{max}$  over a single mode.
- All users are allowed to transmit in the low SNR regime. This is because the system is inherently noise limited and the interference power does not have a huge effect on the capacity.
- Binary power control is optimal in the high SNR regime. It is however not optimal

in the intermediate SNR regime, where it is sometimes optimal to let the third user transmit at a reduced power while the other two are transmitting at the maximum power.

- There are two optimal states in the interference-limited high SNR case: 1) Two users perform beamforming and the third one is turned off, and 2) One user transmits by distributing equal power over the spatial channels and the other two are turned off. This result was also observed in the previous example.

## 4.6 Two-User $4 \times 4$ Symmetric MIMO IC (Case of $N < n_t$ )

The goal of including this case is to understand the effect of having more spatial channels (per user) than the number of users on the optimal power allocation strategy. Due to the presence of extra spatial channels, the simultaneous transmission of both the users is expected to be optimal in all the cases. In other words, perfect interference avoidance is possible while allowing both the users transmit simultaneously. As we will see later in detail, one such interference avoidance strategy is to let each user transmit over two ‘optimal’ spatial channels leaving the other two for interference avoidance.

As was the case in the previous IC, we consider a few special simulation cases to gain insight into the optimal power allocation strategy. These simulation cases are briefly explained below:

- **Optimal MIMO:** In this case, we find the optimal sum-rate achievable in this IC by solving the sum-rate maximization problem. This comparison of the optimal sum-rate with the specific power allocation strategies will help us understand the exact nature of optimal power allocation strategy in this example.
- **Max Power Beamforming:** In this case, we assume that each user selects an optimal

spatial channel and transmits at maximum power  $P_{max}$  in that channel (such that the sum-rate is maximized). As mentioned earlier, the selection of the spatial channel is not trivial. It can be achieved by setting up a mixed-integer optimization problem. However, we will employ exhaustive search for this case. The exhaustive search is feasible since there are only  $\binom{4}{1}\binom{4}{1} = 16$  cases to check.

- **Equal Power Distribution:** This is the simplest case to simulate. In this case, each user transmits at maximum power and distributes it equally over all the spatial channels.
- **One User - Equal Power Distribution:** In this case, only the user with the better link capacity is allowed to transmit. The allowed user then transmits at the maximum power by distributing it equally over all the spatial channels.
- **Equal Power Distribution over two Modes:** This is a special case introduced in this example to understand the exact effect of having a higher number of degrees of freedom than the number of interferers. In this case, we assume that each user selects two optimal Eigen-modes (out of 4) and distributes its transmit power equally over these modes such that the sum-rate is maximized. The selection of these Eigen-modes is again not trivial due to the coupling of the capacity of the users in IC. Since there are only two users, we will employ exhaustive search to find the optimal set of Eigen-modes for each user. There are  $\binom{4}{2}\binom{4}{2} = 36$  options to check in this case.

### 4.6.1 Numerical Results

The ergodic sum-rates achievable in all the above mentioned cases are presented in Fig. 4.15. As we will see later in detail, it is optimal for both the users to transmit simultaneously in all cases. This is due to the fact that perfect interference avoidance is possible in the present case while allowing both the users transmit simultaneously. We further observe that it is optimal to distribute the power over the spatial channels in all the SNR regimes. However,

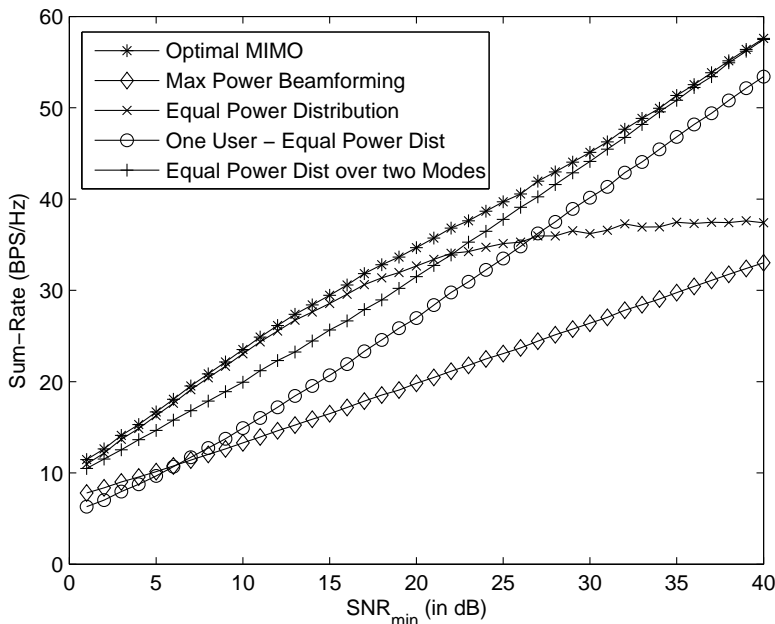


Figure 4.15: Numerical results of the ergodic sum-rate achievable in the two-user  $4 \times 4$  MIMO IC ( $n_t = n_r = 4$ ,  $N = 2$ ,  $N_b = 1$ ,  $\rho = 0$ ,  $MUI = 1$ ,  $\sigma = 0$ , Rayleigh fading assumed).

the exact nature of distribution is different in different SNR regimes. In the low SNR regime, the optimal sum-rate is very close to the sum-rate achieved by distributing equal power over all the spatial channels. We will study the reason for the small difference in the achievable sum-rates in the two cases in detail when we look at the distribution of the power transmitted by each user over various Eigen-modes. In the high SNR regime, it is optimal to transmit over just a few Eigen-modes and leave the rest for interference avoidance. This is inferred from the fact that the optimal sum-rate is quite close to the sum-rate achievable in the case when each user transmits over just two spatial channels. There is however a slight difference in the sum-rate achieved in these two cases too. We will try to understand the reason for this difference later in this section.

With this background, we now look at the distribution of the total power transmitted by each user in Fig. 4.16. The results indicate that it is optimal for all the users to simultaneously transmit in all the SNR regimes. As noted earlier, this is expected since each user has enough



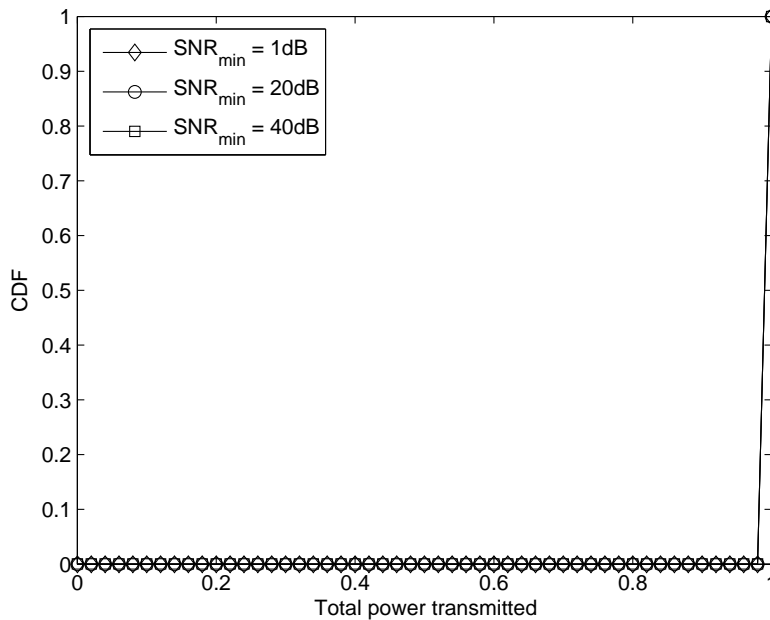


Figure 4.16: Distribution of the total power transmitted by each user in the two-user  $4 \times 4$  MIMO IC ( $n_t = n_r = 4$ ,  $N = 2$ ,  $N_b = 1$ ,  $\rho = 0$ ,  $MUI = 1$ ,  $\sigma = 0$ , Rayleigh fading assumed).

degrees of freedom to avoid interference from the other user as a part of the optimal strategy. We will look into these optimal strategies later in this section.

We now look at the distribution of the transmit power over the strongest and the weakest Eigen-mode of each user in Fig. 4.17 and Fig. 4.18, respectively. The strongest Eigen-mode is defined as the one over which the highest fraction of the total power is transmitted. Likewise, the weakest mode is defined as the one over which least amount of power is transmitted. It should be noted that the strongest and weakest Eigen-mode of a user may not necessarily be the same as the corresponding strongest and weakest Eigen-modes of the interference-free MIMO link. This is due to the interdependence of the capacity of one user over the transmission strategy of the other.

We specifically look at the three SNR regimes: low ( $\text{SNR}_{\min} = 1$  dB), intermediate ( $\text{SNR}_{\min} = 20$  dB) and high ( $\text{SNR}_{\min} = 40$  dB). In the low SNR regime, we observe that it is optimal

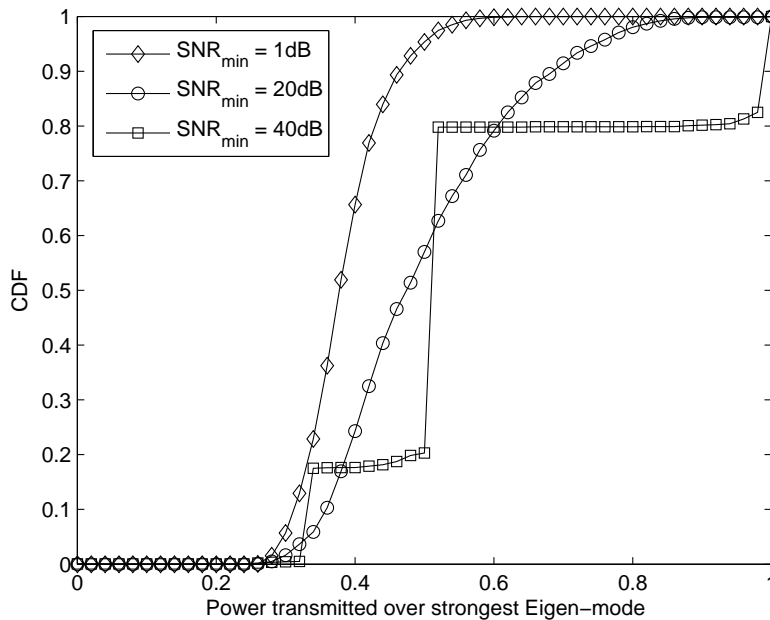


Figure 4.17: Distribution of the power transmitted by each user over stronger Eigen-mode in the two-user  $4 \times 4$  MIMO IC ( $n_t = n_r = 4$ ,  $N = 2$ ,  $N_b = 1$ ,  $\rho = 0$ ,  $MUI = 1$ ,  $\sigma = 0$ , Rayleigh fading assumed).

to distribute the transmit power almost equally over three of the four channel modes. It is optimal to keep the weakest mode silent in around 50% of the cases. In other cases, it is optimal to transmit very low power over this mode. This is essentially the reason for a small difference in the optimal sum-rate and the sum-rate achievable by distributing equal power over all the spatial channels in the low SNR regime.

In the intermediate SNR regime, it is optimal not to transmit over the weakest Eigen-mode in around 80% of the cases. It is optimal to transmit more power over the stronger Eigen-modes as indicated by the distribution of the power transmitted over the strongest Eigen-mode. In most of the cases, it is optimal to transmit around 40% to 60% of the maximum power over the strongest mode.

The results in the high SNR regime are the most well-behaved of all and also the most

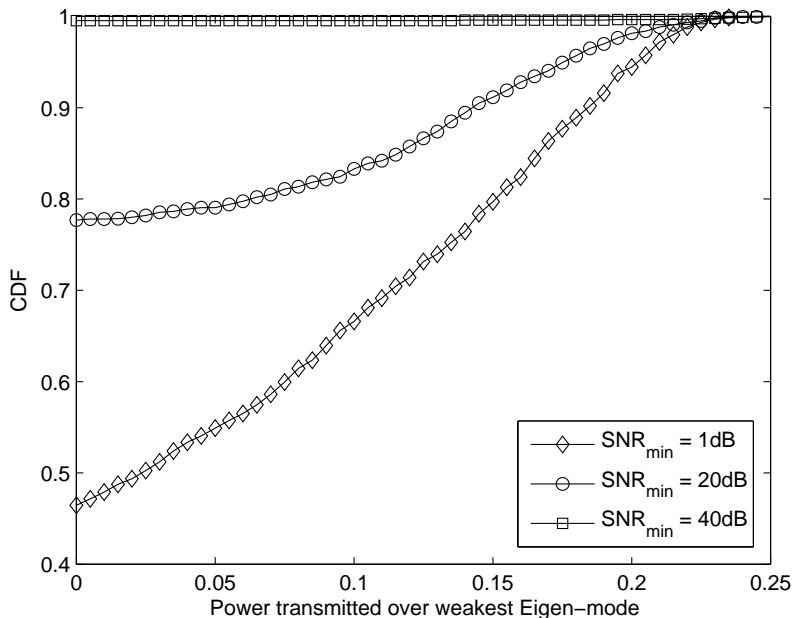


Figure 4.18: Distribution of the power transmitted by each user over weaker Eigen-mode in the two-user  $4 \times 4$  MIMO IC ( $n_t = n_r = 4$ ,  $N = 2$ ,  $N_b = 1$ ,  $\rho = 0$ ,  $MUI = 1$ ,  $\sigma = 0$ , Rayleigh fading assumed).

interesting. Our first observation is that no power is ever transmitted over the weakest mode. This is expected because at least one of the modes is required to avoid interference (since interference avoidance is optimal in the high SNR regime). We further observe that there are two optimal states that are most prevalent. First is the one in which one of the users perform beamforming and the other distributes its power equally over three modes (using one for interference avoidance). This case corresponds to two spikes (at  $1/3$  and  $1$ ) in the distribution of the transmit power over the strongest mode. The relationship between these two steps may not be obvious right away but the same probability of occurrence of the two confirms that they are actually parts of the same event. This was also verified during the simulations. The second, and the more probable, case is the one in which each user selects two Eigen-modes and distributes transmit power equally over them. This case corresponds to the step at  $1/2$  in the CDF of the power transmitted over the strongest mode. It should

be recalled that the sum-rate results had already indicated the optimality of this case. The slight difference in the optimal results and the special case (equal power distribution over two modes) is due to the fact that there is an additional power allocation strategy (one user beamforming and other transmitting over three modes) that is optimal in a small fraction of cases.

### 4.6.2 Summary of the Main Results

- It is optimal for both the users to transmit simultaneously in all the SNR regimes. This is expected because the presence of more degrees of freedom than the minimum required to avoid interference.
- It is further optimal for both the users to distribute the power over spatial channels in all SNR regimes. This is different from the previous examples where it was optimal for all the transmitting users to perform beamforming in the high SNR regime. This difference is due to the fact that more degrees of freedom are present in this case. The additional degrees of freedom let both the users simultaneously transmit over more than one mode while avoiding interference from each other.
- The sum-rate achievable by equal power allocation is quite close to the optimal sum-rate in the low SNR regime. However, this strategy is shown to be sub-optimal when we studied the distribution of power transmitted over strongest and weakest Eigen-modes.
- There are two optimal states in the high SNR regime. First is the one in which one of the users perform beamforming and the other distributes its power equally over three modes (using one for interference avoidance). The second, and the more probable, case is the one in which each user selects two Eigen-modes and distributes power equally over them. It should be noted that both these strategies involve using four total modes.

## 4.7 Four-User $4 \times 4$ MIMO IC (Second Case of $N > n_t$ )

In this section, we consider a four-user  $4 \times 4$  MIMO IC. The motivation of considering another case with  $N = n_t$  is to understand the effect of scaling up both the the number of antennas and the number of users on the optimal power allocation strategy. It should be remembered that our first case with  $N = n_t$  was a simple two-user  $2 \times 2$  MIMO IC, where we found that equal power distribution is nearly optimal in the low SNR regime and maximum power beamforming is optimal in the high SNR regime. The present four-user case is much more complicated than the two-user case simply because of the higher number of combinations of the transmit powers possible. Due to this reason, we expect to get some interesting insights into the optimal power allocation strategies for large ICs.

We consider following simulation scenarios to gain insight into the optimal power allocation strategy:

- **Optimal MIMO:** This case represents the optimal power allocation strategy that maximizes the sum-rate of the MIMO IC. The optimal sum-rate is found by solving the sum-rate maximization problem. As in the previous cases, this sum-rate acts as the benchmark for the other simulation scenarios considered in this section. The comparison of the sub-optimal sum-rates achievable in other scenarios with this benchmark provides some interesting insights into the optimal power allocation strategies in various SNR regimes.
- **Max Power Beamforming:** In this case, each user transmits at a maximum power  $P_{max}$  over an optimal Eigen-mode, chosen such that that sum-rate is maximized. The choice of the optimal Eigen-mode is not trivial due to the presence of interference and can be achieved by formulating a mixed integer optimization problem, which will be discussed in a later chapter. For the present case, we perform an exhaustive search to find the optimal combination of Eigen-modes that maximizes the sum-rate. Exhaustive search is feasible in this case since there are only  $\binom{4}{1}^4 = 256$  cases to check.

- **Equal Power Distribution:** In this case, we assume that each user transmits at the maximum power  $P_{max}$  by distributing the power equally over all the four spatial channels. Please recall that there is no need of optimization in this case.
- **Three User - Equal Power Distribution:** In this case, we turn one of the four users off and let the other three transmit at the maximum power by distributing it equally over all the four Eigen-channels (such that the sum-rate is maximized). The choice of the user that is turned off is not trivial. Even though the optimal solution can be found by setting up an optimization problem, we take a simpler approach. We turn off one user each time and note the sum-rate achieved by letting the other three transmit at the maximum power. We then choose the combination that provides the maximum sum-rate.
- **Two User - Equal Power Distribution:** This is similar to the previous case, with the only difference that we now turn off two users instead of one (such that the sum-rate of the resulting two is maximized). The other two are allowed to transmit at the maximum power by distributing the power equally over all the four Eigen-channels. The choice of the users to turn off is not trivial. As explained in the previous simulation scenario, we perform exhaustive search to find the optimal set of users to turn off.
- **One User - Equal Power Distribution:** In this case, only a single user (with the highest capacity) is allowed to transmit. The allowed user transmits at the maximum power  $P_{max}$  by distributing it equally over all the four Eigen-channels.

### 4.7.1 Numerical Results

The sum-rates achievable for all the scenarios considered in this section are presented in Fig. 4.19. In the low SNR regime, we note that the optimal sum-rate is closest to the one achievable by transmitting equal power over all the Eigen-channels. This observation is in consonance with our observations in the previous cases. However, we note that the

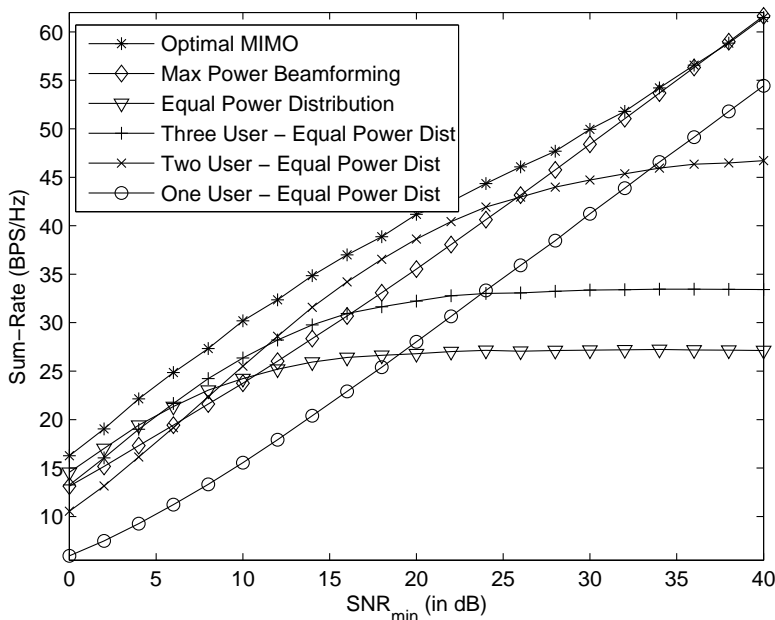


Figure 4.19: Numerical results of the sum-rate achievable in the four-user  $4 \times 4$  MIMO IC ( $n_t = n_r = 4$ ,  $N = 4$ ,  $N_b = 1$ ,  $\rho = 0$ ,  $MUI = 1$ ,  $\sigma = 0$ , Rayleigh fading assumed).

difference between the optimal and equal power allocation cases is much more than it was in the previous cases. This is the first major difference we observe in the two-user and the present four-user IC, where  $n_t$  is set equal to  $N$ . As will be discussed later in the section, the reason for this trend is that it is optimal in almost all the cases to turn off the weakest Eigen-mode. As shown in Chapter 2, the strength of the weakest mode is not significant as compared to the stronger modes. Hence, the transmission over the weakest mode do not contribute significantly towards the link capacity. Thus, it is optimal to avoid a part of the interference by turning off those modes, which do not contribute significantly towards the link capacity.

Even though it is implied from the above discussion, it is important to note that it is optimal for all the users to simultaneously transmit in the low SNR regime. This is not the case in the intermediate SNR regime, where it is optimal to turn some users off to maximize the sum-rate. This can be conjectured by noting the fact that ‘two-user-equal power distribution’

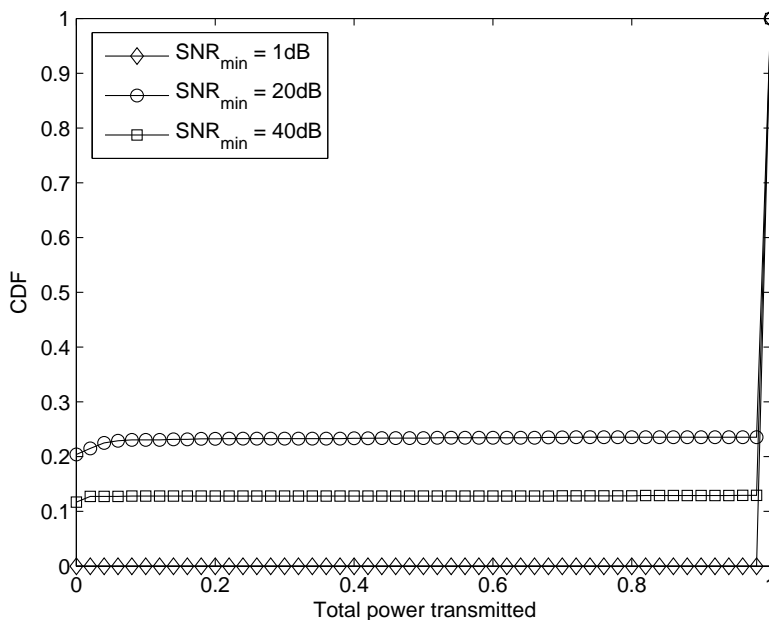


Figure 4.20: Distribution of the total power transmitted by each user in the four-user  $4 \times 4$  MIMO IC ( $n_t = n_r = 4$ ,  $N = 4$ ,  $N_b = 1$ ,  $\rho = 0$ ,  $MUI = 1$ ,  $\sigma = 0$ , Rayleigh fading assumed).

performs better than all the other sub-optimal strategies. This observation just supports our claim but does not validate it in any way. We will revisit it later in this section when we study the power distribution over the strongest and the weakest Eigen-modes of the each user. It is interesting to note that the strategies that ‘avoid’ interference, viz., two-user-equal power distribution and max power beamforming, perform better than the ones that ‘allow’ interference in the intermediate SNR regime. The two-user-equal power distribution strategy avoids interference by turning the users off and the max power beamforming approach avoids interference by turning off the weaker Eigen-modes. Furthermore, it is more profitable in the IC to turn off users in this regime than to give up the link capacity by concentrating power in single Eigen-mode.

As was the case in the previous sections, the high SNR regime is the most well-behaved in this IC. We note that max power beamforming is optimal in this regime. Thus it is optimal for all the users to transmit at the maximum power  $P_{max}$  over the optimal Eigen-mode in



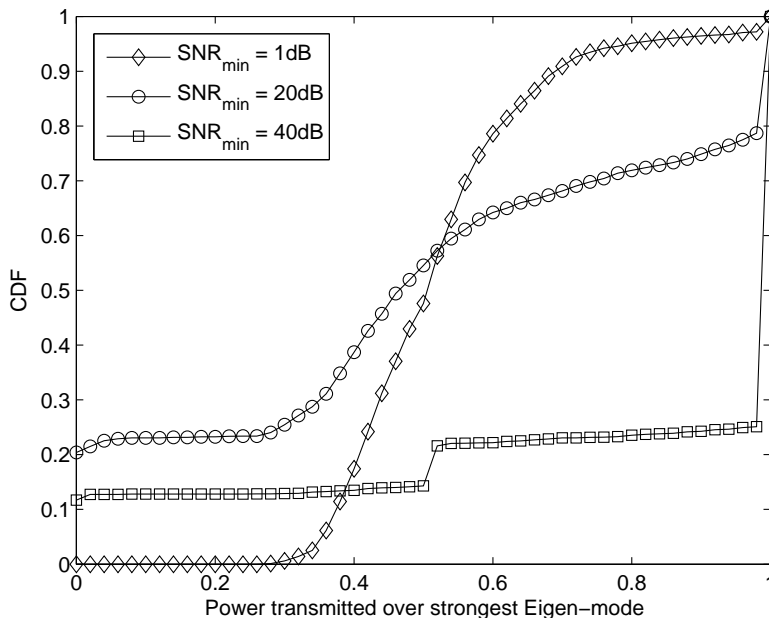


Figure 4.21: Distribution of the power transmitted by each user over stronger Eigen-mode in the four-user  $4 \times 4$  MIMO IC ( $n_t = n_r = 4$ ,  $N = 4$ ,  $N_b = 1$ ,  $\rho = 0$ ,  $MUI = 1$ ,  $\sigma = 0$ , Rayleigh fading assumed).

almost all the cases. The remainder of the three degrees of freedom are used for interference avoidance from the other users. Comparison of the sum-rates achievable in ‘max power beamforming’ and ‘two user - equal power distribution’ cases clearly suggests that it is more profitable to avoid interference by turning off the modes than to turn off the users in this regime.

With this insight into the optimal sum-rate, we now look at the optimal power allocation more closely. In Fig. 4.20, we plot the distribution of the total power transmitted by each user in three SNR regimes: low ( $SNR_{min} = 0$  dB), intermediate ( $SNR_{min} = 20$  dB) and high ( $SNR_{min} = 40$  dB). We first note that it is optimal for all the four users to transmit simultaneously in the low SNR regime. This is in consonance with the results obtained in the previous cases because the system is noise-limited and the interference power is not the deciding factor. We further note that it is optimal to turn off each user  $\approx 22\%$  of the time in

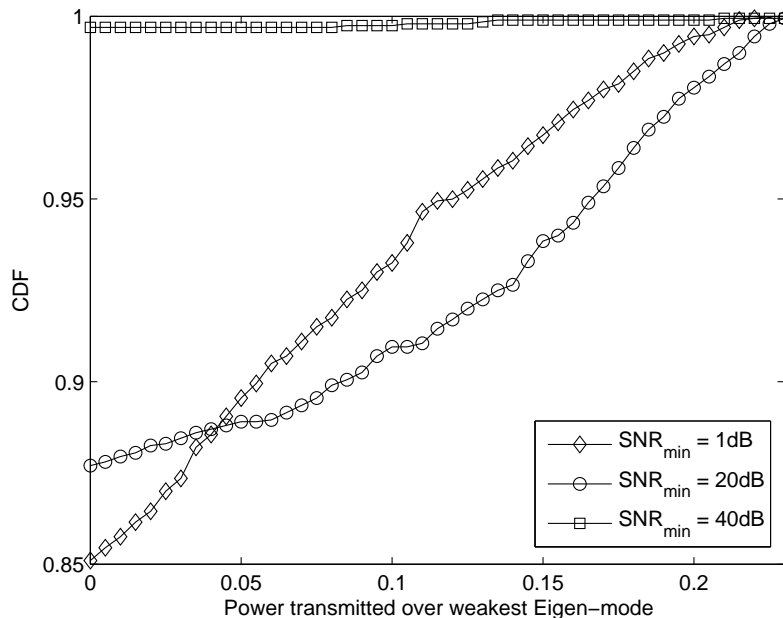


Figure 4.22: Distribution of the power transmitted by each user over weaker Eigen-mode in the four-user  $4 \times 4$  MIMO IC ( $n_t = n_r = 4$ ,  $N = 4$ ,  $N_b = 1$ ,  $\rho = 0$ ,  $MUI = 1$ ,  $\sigma = 0$ , Rayleigh fading assumed).

the intermediate SNR regime. Since there are 4-users, this also means that it is optimal on an average to turn off one user and let the other three transmit in nearly all the cases. We have already observed this trend in the sum-rate results, where we noted that it is optimal to avoid interference by turning off the users in this regime. We also note that there are a few cases in which it is optimal to let a user transmit at a reduced power, thus making binary power control sub-optimal in this regime. We noted a similar trend in the 3-user IC considered in the last section. Now moving on to the high SNR regime, we note that it is optimal to turn off each user for  $\approx 15\%$  of the time. This is an interesting observation because it states that it is optimal to let more users transmit in the high SNR regime than in the intermediate SNR regime. As we conjectured before and will validate later in this section, it is optimal to avoid interference by turning off the modes in the high SNR regime than by turning off the users. As a side note, we note that binary power control is optimal

in this regime.

We now present the distributions of the power transmitted by each user over the strongest Eigen-channel in three SNR regimes in Fig. 4.21. In the low SNR regime, we note that it is optimal for each user to transmit around 30% to 60% of the maximum power over the strongest mode in most of the cases. This suggests that the strategies involving distribution of the transmit powers over the modes are optimal in this regime. In the intermediate SNR regime, we note that it is optimal to turn off each user around 22% of the time. As noted earlier, this implies that one user is turned off on an average in this SNR regime. We further note that it is optimal for each user to perform beamforming for  $\approx 22\%$  of the time. In other words, this means that one of the four users performs beamforming in almost all the optimal strategies. The other users distribute power over the available spatial channels. Moving on to the high SNR regime, we note that it is highly optimal for all the users to simultaneously transmit by performing beamforming. This is in consonance with the results found in the previous sections. In addition to this strategy, there is another strategy which is optimal in small but notable number of cases. In this strategy, one user is turned off and one user is allowed to distribute its transmit power equally over two modes. The rest of the two users perform beamforming. This can be easily inferred from the spikes at 0 and 0.5. This strategy is optimal when it is not possible to avoid enough interference by beamforming of the each user.

The distributions of the power transmitted by each user over the weakest modes in the three SNR regimes are presented in Fig. 4.22. We note that it is optimal for each user to turn off the weakest mode for  $\approx 85\%$  of the time in the low SNR regime. This is precisely the reason why equal power allocation case is sub-optimal in this regime. The trend is quite similar in the intermediate SNR regime, where it is optimal to turn off the weakest mode for  $\approx 87\%$  of the time. In the high SNR regime, it is optimal to keep the weakest mode turned off in all the optimal strategies. This further supports the optimal strategies identified earlier in this section.

### 4.7.2 Summary of the Main Results

- It is optimal to let all the users transmit in the low SNR regime. However, equal power distribution is not optimal. It is highly optimal to turn off the weakest mode of each user in this regime.
- It is highly optimal to let all the users transmit in the high SNR regime too. The users avoid interference by beamforming. Whenever it is not feasible to avoid enough interference by beamforming, it is optimal to turn off one user, let one distribute power equally over two modes and let the rest perform beamforming.
- Binary power allocation is optimal in the low and high SNR regimes. However, it is optimal to let a user transmit at the reduced power in the intermediate SNR regime.
- We note that it is optimal to turn off more users in the intermediate SNR regime than in the high SNR regime. In the high SNR regime, interference is efficiently avoided by turning off the weaker modes, as opposed to turning off the users.

## 4.8 Conclusions

In this chapter, we have studied the problem of maximizing the sum-rate of the multi-antenna ICs by treating interference as Gaussian noise. Some of the main contributions and conclusions are as follows:

- We have extended the BB/RLT global optimization algorithm to solve the general sum-rate maximization problem of the MIMO ICs. The exact solution to this problem has been open for nearly a decade due to its non-linear and non-convex nature.
- Optimal power allocation strategy allows more users to transmit in the case of MIMO ICs as compared to the corresponding SISO ICs due to the presence of orthogonal spatial channels. The degrees of freedom provided by these spatial channels are used to

achieve better spectral efficiency in the low SNR scenarios and for interference avoidance in the high SNR (interference-limited) scenarios. In other words, we note that it is optimal to distribute power over the spatial channels in the low SNR regime and confine it to a limited number of spatial channels in the high SNR regime (while using the rest for interference avoidance). This also highlights the fact that the importance of interference avoidance increases as we move from low-interference to high-interference regimes.

- Beamforming is optimal in the very-low SNR regime, which corresponds to a very weak interference scenario due to which the links are fundamentally noise-limited. From the knowledge of the noise-limited MIMO links, we already know that beamforming is optimal strategy to adopt when the received SNR per antenna is low.
- In the case when  $N \geq n_t$  ( $\rho = 0$ ), at least  $n_t$  users are almost always guaranteed to get channel access in the optimal power allocation strategy. In the limiting case of high interference power, exactly  $n_t$  users are allowed to transmit where each user performs beamforming and uses the rest of the degrees of freedom to avoid interference from  $n_t - 1$  users. The use of beamforming strategy also avoids causing more interference to the other users. This also means that the sum-rate lower bound provided by maximizing the beamforming sum-rate of  $n_t$  ‘best’ users is tight in the high SNR (high interference) regime. In the low SNR regime, it is optimal to let more than  $n_t$  users transmit and hence the lower bound is not tight in general.
- In the case when  $N < n_t$  ( $\rho = 0$ ), the degrees of freedom of each user are more than the bare minimum required to avoid interference. In this case, each user uses a few degrees of freedom to avoid interference and the rest to improve its spectral efficiency. Since interference avoidance is optimal in the high SNR regime, more degrees of freedom are used for interference avoidance in this regime than in the low SNR regime.
- We note that the binary power control is optimal in the low SNR (noise-limited) and high SNR (interference-limited) regimes (in the cases considered in this chapter).

However, it is optimal in a noticeable number of cases to let some users transmit at a reduced power in the intermediate SNR regime.

- We note that the interference avoidance can be achieved either by turning off the ‘bad’ users or by turning off the weaker Eigen-modes of each user. The optimality of one strategy over the other depends upon the SNR regime and the IC topology. In the four-user  $4 \times 4$  MIMO IC studied in this chapter, we note that it is optimal to achieve interference avoidance by turning off users in the intermediate SNR regime and turning off weaker Eigen-modes in the high SNR regime.

# Chapter 5

## Multi-Band Interference Channels

### 5.1 Introduction

In this chapter, we address the problem of maximizing the sum-rate of an  $N$ -user multi-band interference channel by treating interference as Gaussian noise. We define a multi-band IC as an extension of the classical IC where each user has  $N_b$  frequency channels for transmission. We will first focus on the multi-band single-antenna IC, where the objective is to find the optimal fraction of power to be transmitted over each frequency band. We will further show that these optimal power allocation strategies are quite similar to the ones obtained for the MIMO ICs whenever the number of orthogonal<sup>1</sup> channels is same in both the cases. This corresponds to the scenario where the number of bands in a multi-band IC is equal to the number of uncorrelated antennas in a MIMO IC ( $N_b = n_t$ ). This is an interesting observation since it implies that the spatial and the frequency channels are surprisingly similar from the sum-rate maximization perspective. This result is especially

---

<sup>1</sup>It should be noted that the orthogonal spatial channels are locally defined for each user and are not globally orthogonal. On the other hand, the frequency channels are common to all the users and hence are globally orthogonal. For the ease of presentation, we will not make a distinction between the local and global orthogonality while addressing *orthogonal* channels.

important because of the dissimilarity in the way the spatial and frequency channels affect the perceived interference. On the one hand, the frequency channels are common to all the users and are perfectly isolated from each other at each user. In other words, the signal transmitted by one user over a particular frequency channel acts as interference for all the users accessing this band and does not affect the ones transmitting over other bands. On the other hand, this demarkation is not so neat in the case of spatial channels because they are defined for a particular user and are not the same for the whole IC. Thus, the net interference perceived by each user depends upon the alignment of its Eigen-channels with the Eigen-channels of the transmitting users. Due to this fundamental difference, there are some small differences in the optimal power allocation strategies for the multi-band and the MIMO ICs. We will study these differences in sufficient detail in this chapter.

With this insight, we will then study the effect of having multiple bands on the maximum sum-rate achievable in the MIMO ICs. The objective in this case is to find the optimal fraction of power to be transmitted by each user over each spatial channel in each frequency band. Interestingly, these power allocation strategies are similar to the ones obtained for the multi-band SISO and single-band MIMO ICs. In particular, the optimal power allocation strategies obtained for a single-band  $n \times n$  MIMO IC and an  $n$ -band SISO IC are similar to the  $N_b$ -band  $n_t \times n_t$  MIMO IC whenever  $n_t N_b = n$ . This is an interesting observation since it implies that the fundamental factor affecting the optimal power allocation is the total number of orthogonal channels and not the resource (antennas, frequency bands) which provides these channels. This also implies that the multi-band multi-antenna IC has  $\min\{n_t, n_r\} N_b$  degrees of freedom. To the best of our knowledge, we are the first ones to establish this similarity between the spatial and spectral channels in an interference channel.

To study these cases, we first need to formulate the sum-rate maximization problem. For the ease of presentation, we formulate the problem for the general multi-band MIMO IC and study the special case of multi-band SISO IC by substituting  $n_t = 1$  in the problem. We show that this problem is mathematically quite similar to that of a single band MIMO IC studied in the previous chapter. It can be easily shown that this problem is also non-



linear non-convex and hence difficult to solve analytically. As discussed in the previous chapter, local optimization techniques, such as a gradient based search, are not guaranteed to converge to the global optimal solution in such non-convex problems. Therefore, we extend the BB/RLT global optimization algorithm developed in the previous chapter to solve this sum-rate maximization problem. To the best of our knowledge, we are the first ones to formulate and solve this problem.

## 5.2 Sum-Rate of Multi-Band MIMO IC

In this section, we formulate the sum-rate maximization problem for a general multi-band MIMO IC. We begin our discussion by defining the variables required for the formulation. It should be noted that we are using the same notations and variables as the previous chapter with a superscript that denotes the frequency channel.

### 5.2.1 Defining the Variables

We consider an IC consisting of  $N$  mutually interfering users (SUs), which are indexed by  $1, 2, \dots, N$ . In this analysis, it is assumed that the transmitters have full channel state information. Let the available spectrum be divided into  $N_b$  frequency bands, indexed by  $1, 2, \dots, N_b$ . Let us denote the MIMO link from the Tx of the  $j^{th}$  SU to the Rx of the  $i^{th}$  SU to be  $L_{ji}$ . Let the matrix  $\mathbf{H}_{ji}^l \in C^{n_r \times n_t}$  denote the channel matrix of link  $L_{ji}$  in the  $l^{th}$  frequency band. Let the matrix  $\mathbf{Q}_i^l$  be the covariance matrix of the zero mean Gaussian transmit symbol vector  $\mathbf{x}_i^l$  of the  $i^{th}$  SU in  $l^{th}$  frequency band, i.e.,  $\mathbf{Q}_i^l = E\{\mathbf{x}_i^l \mathbf{x}_i^{l\dagger}\}$ . Further denote  $\rho_{ji}^l$  as the signal-to-noise ratio per unit transmit power in frequency band  $l$  if  $j = i$ , or the interference-to-noise ratio per unit transmit power if  $j \neq i$ . It is also assumed that each Tx in the network is subject to the maximum transmit power constraint, i.e., the total power transmitted over  $n_t$  transmit antennas and all  $N_b$  frequency bands should be less than or equal to  $P_{max}$ . Let  $\mathbf{R}_i^l$  represent the covariance matrix of the interference plus noise

observed at the  $i^{\text{th}}$  Rx node in the  $l^{\text{th}}$  frequency band. Assuming interference plus noise to be Gaussian distributed, it can be computed as:

$$\mathbf{R}_i^l = \sum_{\substack{j=1 \\ j \neq i}}^N \rho_{ji}^l \mathbf{H}_{ji}^l \mathbf{Q}_j^l \mathbf{H}_{ji}^{l\dagger} + \mathbf{I}. \quad (5.1)$$

### 5.2.2 Capacity of a Single MIMO link in a Multi-Band IC

As was the case in the previous chapter, we begin our discussion by evaluating the maximum achievable capacity of a single MIMO link in a multi-band IC. To gain insight into the problem, we assume that the interference from other users is constant and is perfectly known at both the Tx and Rx nodes. As we will see in the next section, this assumption will no longer hold when we try to maximize the sum-rate of the whole IC. We also assume that the channel state information is perfectly known. In addition to finding the maximum link capacity, the analysis will also help us establish similarity between the current problem and the one studied for single-band MIMO IC in the previous chapter.

To begin the analysis, we express the capacity of an  $i^{\text{th}}$  MIMO link in terms of its channel matrix  $\mathbf{H}_{ii}^l$ , transmit symbol covariance matrix  $\mathbf{Q}_i^l$  and interference plus noise covariance matrix  $\mathbf{R}_i^l$  as:

$$C_i = \max_{\{\mathbf{Q}_i^l\}: \sum_{l=1}^{N_b} \text{tr}(\mathbf{Q}_i^l) = P_{\max}} \sum_{l=1}^{N_b} \log_2 \det \left( \mathbf{I} + \rho_{ii}^l (\mathbf{R}_i^l)^{-1} \mathbf{H}_{ii}^l \mathbf{Q}_i^l \mathbf{H}_{ii}^{l\dagger} \right), \quad (5.2)$$

where the optimization is performed over the input symbol covariance matrices  $\mathbf{Q}_i^l$ . Using the definition  $\mathbf{R}_i^l = \mathbf{R}_i^{l/2} \mathbf{R}_i^{l/2\dagger}$  and the identity  $\det(\mathbf{I} + \mathbf{AB}) = \det(\mathbf{I} + \mathbf{BA})$ , this equation can be simplified to:

$$C_i = \sum_{l=1}^{N_b} \log_2 \det \left( \mathbf{I} + \rho_{ii}^l (\mathbf{R}_i^{l-1/2} \mathbf{H}_{ii}^l) \mathbf{Q}_i^l (\mathbf{R}_i^{l-1/2} \mathbf{H}_{ii}^l)^\dagger \right). \quad (5.3)$$

Defining the ‘whitened’ channel matrix in the  $l^{\text{th}}$  frequency band as  $\tilde{\mathbf{H}}_{ii}^l = \mathbf{R}_i^{l-1/2} \mathbf{H}_{ii}^l$ , the

capacity of the  $i^{\text{th}}$  user can be expressed as:

$$C_i = \sum_{l=1}^{N_b} \log_2 \det \left( \mathbf{I} + \rho_{ii}^l \tilde{\mathbf{H}}_{ii}^l \mathbf{Q}_i^l \tilde{\mathbf{H}}_{ii}^{l\dagger} \right). \quad (5.4)$$

The MIMO channel in each frequency band can now be decomposed into  $\min\{n_t, n_r\}$  SISO channels in the same way as we discussed for the MIMO link in a single-band IC in the previous chapter. Using singular value decomposition,  $\tilde{\mathbf{H}}_{ii}^l$  can be expressed as  $\tilde{\mathbf{H}}_{ii}^l = \mathbf{U}^l \mathbf{D}^l \mathbf{V}^{l\dagger}$ , where  $\mathbf{U}^l$  and  $\mathbf{V}^l$  are unitary matrices and  $\mathbf{D}^l$  is a diagonal matrix. Substituting this in the above equation, we get:

$$C_i = \sum_{l=1}^{N_b} \log_2 \det \left( \mathbf{I} + \rho_{ii}^l \mathbf{U}^l \mathbf{D}^l \mathbf{V}^{l\dagger} \mathbf{Q}_i^l \mathbf{V}^l \mathbf{D}^{l\dagger} \mathbf{U}^{l\dagger} \right). \quad (5.5)$$

Using the identities  $\det(\mathbf{I} + \mathbf{AB}) = \det(\mathbf{I} + \mathbf{BA})$  and  $\mathbf{U}^l \mathbf{U}^{l\dagger} = \mathbf{I}$ ,  $C_i$  can be expressed as:

$$C_i = \sum_{l=1}^{N_b} \log_2 \det \left( \mathbf{I} + \rho_{ii}^l \mathbf{D}^l \mathbf{V}^{l\dagger} \mathbf{Q}_i^l \mathbf{V}^l \mathbf{D}^{l\dagger} \right). \quad (5.6)$$

Using the identity  $\det(\mathbf{I} + \mathbf{AB}) = \det(\mathbf{I} + \mathbf{BA})$  again and defining  $\Sigma^l = \mathbf{D}^{l\dagger} \mathbf{D}^l$ ,  $C_i$  can be expressed as:

$$C_i = \sum_{l=1}^{N_b} \log_2 \det \left( \mathbf{I} + \rho_{ii}^l \Sigma^l \mathbf{V}^{l\dagger} \mathbf{Q}_i^l \mathbf{V}^l \right). \quad (5.7)$$

It should be noted that  $\Sigma_i^l = \mathbf{D}^{l\dagger} \mathbf{D}^l$  is a diagonal matrix with the diagonal elements as the Eigen-values of  $\tilde{\mathbf{H}}_{ii}^l \tilde{\mathbf{H}}_{ii}^{l\dagger}$ . To decompose the MIMO channel of the  $i^{\text{th}}$  user in the  $l^{\text{th}}$  band in  $\min\{n_t, n_r\}$  parallel non-interfering SISO channels,  $\mathbf{V}^{l\dagger} \mathbf{Q}_i^l \mathbf{V}^l$  should result in a diagonal matrix. This can be achieved by choosing  $\mathbf{Q}_i^l$  of the form  $\mathbf{Q}_i^l = \mathbf{V}^l \Lambda_i^l \mathbf{V}^{l\dagger}$ . We get  $\mathbf{Q}_i^l$  of this form when  $\mathbf{V}^l$  is chosen as the pre-coding matrix. It is worth noting that the pre-coding matrix in this case is dependent upon the structure of the interference signals through  $\tilde{\mathbf{H}}_{ii}^l$ . In this case,  $C_i$  can be expressed as:

$$C_i = \max_{\{\Lambda_i^l\}: \sum_{l=1}^{N_b} \text{tr}(\Lambda_i^l) = P_{\max}} \sum_{l=1}^{N_b} \log_2 \det \left( \mathbf{I} + \rho_{ii}^l \Sigma_i^l \Lambda_i^l \right). \quad (5.8)$$

Thus, the problem of maximizing the capacity of a single link in a multi-band MIMO IC is reduced to finding the optimal fractions of the power to be transmitted over each Eigen-channel in each frequency band. Please recall that the Eigen-channels in this case are not

same as the Eigen-channels of the interference-free channel. In-fact, they correspond to the singular values of the ‘whitened’ channel matrix in each frequency band. Since we have assumed perfect knowledge of the channel and interference,  $\Sigma_i^l$  is perfectly known and the optimal  $\Lambda_i^l$  can be found by employing ‘water-filling’ strategy.

We now extend this discussion to the multiuser case in the next section, where the goal is to maximize the sum of capacities of all the links (sum-rate) forming the interference channel.

### 5.2.3 Maximum Sum-rate of a Multi-Band MIMO IC

In this section, we develop a mathematical framework to maximize the sum-rate of a multi-band multi-antenna IC. As seen in the single-band MIMO IC case, such formulations are challenging because the capacities of all the links forming an IC are coupled to each other due to the mutual interference. In other words, the interference plus noise covariance matrices are not known *a priori* and hence we do not have the luxury of maximizing the capacity of each link independently. Due to the lack of knowledge of  $\mathbf{R}_i^l$ , it is quite difficult to find the exact pre-coding matrices for each system instantiation. To overcome this problem, we try to simplify the formulation by mapping each IC to an alternate IC where the pre-coding matrices for each user in each frequency channel are unitary matrices and hence the input symbol covariance matrices reduce to diagonal matrices (with real and non-negative elements). It will be further shown that the ergodic sum-rate of the new IC is same as that of the original IC. We now discuss this idea in detail in the rest of this section.

As noted in the previous section, the information theoretic capacity of a single link in a MIMO interference channel can be expressed as  $C_i = \sum_{l=1}^{N_b} \log_2 \det \left( \mathbf{I} + \rho_{ii}^l (\mathbf{R}_i^l)^{-1} \mathbf{H}_{ii}^l \mathbf{Q}_i^l \mathbf{H}_{ii}^{l\dagger} \right)$ . Since  $\mathbf{Q}_i^l \succ \mathbf{0}$ , it can be expressed as  $\mathbf{Q}_i^l = \mathbf{V}_i^l \Lambda_i^l \mathbf{V}_i^{l\dagger}$ , where  $\Lambda_i^l$  is a diagonal matrix of the eigenvalues of  $\mathbf{Q}_i^l$  and  $\mathbf{V}_i^l$  is a unitary matrix with columns consisting of the eigenvectors of  $\mathbf{Q}_i^l$ . Defining  $\widehat{\mathbf{H}}_{ii}^l = \mathbf{H}_{ii}^l \mathbf{V}_i^l$ , the capacity of the single MIMO link in this case can be written as  $C_i = \sum_{l=1}^{N_b} \log_2 \det \left( \mathbf{I} + \rho_{ii}^l (\mathbf{R}_i^l)^{-1} \widehat{\mathbf{H}}_{ii}^l \Lambda_i^l \widehat{\mathbf{H}}_{ii}^{l\dagger} \right)$ . As  $\mathbf{Q}_i^l \succ \mathbf{0}$ , it leads to the following two very important properties which are instrumental in the further simplification of the problem

formulation:

1. The distributions of  $\widehat{\mathbf{H}}_{ii}^l$  and  $\mathbf{H}_{ii}^l$  are same [54].
2. All the eigenvalues of  $\mathbf{Q}_i^l$ , i.e. all the diagonal elements of  $\Lambda_i^l$ , are real and positive.

Due to these properties, it is sufficient to consider  $\Lambda_i^l$  instead of  $\mathbf{Q}_i^l$  in the problem formulation. From the simulation perspective it is important to note that even though the problem is transformed to a different IC, the ergodic sum-rate remains the same. This is because the distributions of  $\widehat{\mathbf{H}}_{ii}^l$  and  $\mathbf{H}_{ii}^l$  are the same and it does not really matter which one of them we consider for our simulation. We might very well consider  $\mathbf{H}_{ii}^l$  and  $\mathbf{Q}_i^l$  for the optimization but it is hard to formulate the problem and then solve it ensuring  $\mathbf{Q}_i^l$  is positive-semi-definite and satisfies the power constraint. Due to this reason, we consider an alternate IC and formulate the problem in terms of  $\Lambda_i^l$  and  $\widehat{\mathbf{H}}_{ii}^l$ . The resulting problem formulation can be expressed as:

$$\begin{aligned}
\max \quad & \sum_{i=1}^N C_i \\
s.t. \quad & C_i = \sum_{l=1}^{N_b} \log_2 \det(\mathbf{I} + \rho_{ii}^l \mathbf{R}_i^{l-1/2} \widehat{\mathbf{H}}_{ii}^l \Lambda_i^l \widehat{\mathbf{H}}_{ii}^{l\dagger}) \\
& \mathbf{R}_i^l = \sum_{\substack{j=1 \\ j \neq i}}^N \rho_{ji} \widehat{\mathbf{H}}_{ji}^l \Lambda_j^l \widehat{\mathbf{H}}_{ji}^{l\dagger} + \mathbf{I} \\
& \sum_{l=1}^{N_b} Tr\{\Lambda_i^l\} \leq P_{max}, \text{diag}\{\Lambda_i^l\} \succeq \mathbf{0} \\
& 1 \leq i \leq N, 1 \leq l \leq N_b.
\end{aligned} \tag{5.9}$$

The above formulation basically finds the power transmitted by each user in each channel mode in each frequency band that maximizes the sum-rate. As was the case in the single-band MIMO IC, this problem is also non-linear non-convex and hence its global optimal solution can not be derived analytically. Even the popular local optimization algorithms, such as gradient based search do not guarantee global optimal solution. Thus, we extend the BB/RLT based global optimization algorithm that we developed in the previous chapter to find a guaranteed global optimal solution to this problem.

As a side note, it is intuitive that the link capacity expressions for the multi-band MIMO case studied in the section is quite similar to that of the single-band MIMO case studied in the

previous chapter. This fact will help us in constructing the linear programming relaxation for the current problem. We prove this similarity next.

### Similarity Between Single and Multi-Band MIMO Link Capacity Expressions

As seen in this section, the MIMO link capacity in the multi-band case can be expressed as:

$$C_i = \sum_{l=1}^{N_b} \log_2 \det \left( \mathbf{I} + \rho_{ii}^l \tilde{\mathbf{H}}_{ii}^l \mathbf{Q}_i^l \tilde{\mathbf{H}}_{ii}^{l\dagger} \right). \quad (5.10)$$

This expression can be further simplified by defining the following higher dimensional matrices:

$$\tilde{\Lambda}_i = \begin{bmatrix} \Lambda_i^1 & 0 & \dots & 0 \\ 0 & \Lambda_i^2 & \dots & 0 \\ \vdots & & \ddots & \vdots \\ 0 & 0 & \dots & \Lambda_i^m \end{bmatrix}, \quad (5.11)$$

$$\tilde{\mathbf{H}}_{ii} = \begin{bmatrix} \sqrt{\rho_{ii}^1} \tilde{\mathbf{H}}_{ii}^1 & 0 & \dots & 0 \\ 0 & \sqrt{\rho_{ii}^2} \tilde{\mathbf{H}}_{ii}^2 & \dots & 0 \\ \vdots & & \ddots & \vdots \\ 0 & 0 & \dots & \sqrt{\rho_{ii}^m} \tilde{\mathbf{H}}_{ii}^m \end{bmatrix}. \quad (5.12)$$

Substituting  $\tilde{\Lambda}_i$  and  $\tilde{\mathbf{H}}_{ii}$  in equation (5.10), we get:

$$C_i = \log_2 \det(\mathbf{I} + \tilde{\mathbf{H}}_{ii} \tilde{\Lambda}_i \tilde{\mathbf{H}}_{ii}^\dagger). \quad (5.13)$$

Thus the summation is absorbed in the expression by defining the power and channel matrices in the higher dimensions. The resulting expression is the same as the one we found for the single-band MIMO IC in the previous chapter. With this insight, we now study the BB/RLT algorithm to solve this problem in the next section.

### 5.3 The BB/RLT Global Optimization Algorithm

BB/RLT was developed for the single-band MIMO ICs in the previous chapter. Owing to the similarity in the sum-rate maximization problems of the single-band and multi-band MIMO ICs, it can be easily extended to find the optimal power allocation for a multi-band MIMO IC case too. To avoid repetition, we will not discuss the basics of BB/RLT in this chapter. We will only concentrate on constructing the linear programming relaxation (LPR), which is slightly different in this case as compared to the previous chapter.

#### 5.3.1 Constructing an LPR for the multi-band MIMO IC Problem

We begin by defining the following new variables to linearize the expression of  $C_i$ :

$$\begin{aligned} x_i^l &= \det(\mathbf{R}_i^l + \rho_{ii}^l \widehat{\mathbf{H}}_{ii}^l \Lambda_i^l \widehat{\mathbf{H}}_{ii}^{l\dagger}); u_i^l = \ln(x_i^l); \\ y_i^l &= \det(\mathbf{R}_i^l); v_i^l = \ln(y_i^l). \end{aligned} \quad (5.14)$$

$C_i$  can be expressed in terms of the new variables as:  $C_i = \sum_{l=1}^{N_b} \frac{1}{\ln 2} (u_i^l - v_i^l)$ . The constraints given by (5.14) are added to the problem formulation given by (5.9).  $u_i^l$  and  $v_i^l$  are logarithmic functions of the form  $w = \ln z$ , where  $z \in [z_{LB}, z_{UB}]$ . Since,  $x_i^l$  and  $y_i^l$  are dependent upon  $\Lambda_i^l$ , their LB and UB can be calculated by evaluating their expressions at the LB and UB of  $\Lambda_i^l$  respectively. A convex polygonal outer approximation is used to linearize the logarithmic function [57]. As shown in Fig. 4.2 in the previous chapter, the convex region is defined by the tangents at  $(z_{LB}, \ln z_{LB})$ ,  $(z_\gamma, \ln z_\gamma)$  and  $(z_{UB}, \ln z_{UB})$ , and the chord joining  $(z_{LB}, \ln z_{LB})$  and  $(z_{UB}, \ln z_{UB})$ , where  $z_\gamma$  is the z-coordinate of the point of intersection of the tangents at  $(z_{LB}, \ln z_{LB})$  and  $(z_{UB}, \ln z_{UB})$ , which is given by:

$$z_\gamma = \frac{z_{LB} z_{UB} (\ln z_{UB} - \ln z_{LB})}{z_{UB} - z_{LB}}. \quad (5.15)$$

The convex region defined by these four segments can be expressed by the following linear

constraints:

$$\begin{aligned}
z_{LB}w - z &\leq z_{LB}(\ln z_{LB} - 1), \\
z_{\gamma}w - z &\leq z_{\gamma}(\ln z_{\gamma} - 1), \\
z_{UB}w - z &\leq z_{UB}(\ln z_{UB} - 1), \\
(z_{UB} - z_{LB})w + (\ln z_{LB} - \ln z_{UB})z &\geq \\
z_{UB} \ln z_{LB} - z_{LB} \ln z_{UB}. &
\end{aligned} \tag{5.16}$$

After linearizing  $u_i^l$  and  $v_i^l$ , we linearize  $x_i^l$  and  $y_i^l$ . The expressions for  $x_i^l$  and  $y_i^l$  are quite similar and this similarity can be established by substituting  $\mathbf{R}_i^l$  in (5.14):

$$\begin{aligned}
x_i^l &= \det \left( \sum_{j=1}^N \left( \rho_{ji}^l \widehat{\mathbf{H}}_{ji}^l \Lambda_j^l \widehat{\mathbf{H}}_{ji}^{l\dagger} + \mathbf{I} \right) \right) \triangleq \det \mathbf{S}_i^l, \\
y_i^l &= \det \left( \sum_{\substack{j=1 \\ j \neq i}}^N \left( \rho_{ji}^l \widehat{\mathbf{H}}_{ji}^l \Lambda_j^l \widehat{\mathbf{H}}_{ji}^{l\dagger} + \mathbf{I} \right) \right) \triangleq \det \mathbf{R}_i^l.
\end{aligned} \tag{5.17}$$

Keeping in mind this similarity, we illustrate the linearization process for only  $x_i^l$ , and the results for  $y_i^l$  can be inferred directly. For the purpose of illustration, we assume that Tx and Rx nodes of each user have two antennas. Since  $\Lambda_j^l$  ( $\forall j, l$ ) is an  $n_t \times n_t$  ( $= 2 \times 2$ ) matrix, it can be expressed as:

$$\Lambda_j^l = \begin{bmatrix} \lambda_{j1}^l & 0 \\ 0 & \lambda_{j2}^l \end{bmatrix}, \tag{5.18}$$

where  $\lambda_{j1}^l$  and  $\lambda_{j2}^l$  are the fractions of power transmitted by the  $j^{\text{th}}$  user over the two Eigenmodes of the channel in the  $l^{\text{th}}$  frequency band. To simplify the expressions for  $x_i^l$  and  $y_i^l$  (given by (5.17)), let us define  $\widetilde{\mathbf{H}}_{ji}^l = \sqrt{\rho_{ji}^l} \widehat{\mathbf{H}}_{ji}^l$ .  $\mathbf{S}_i^l$  can now be expressed as:

$$\mathbf{S}_i^l = \begin{bmatrix} 1 + \sum_{j=1}^N \lambda_{j1}^l (\tilde{h}_{ji}^l)_{11} (\tilde{h}_{ji}^l)'_{11} + \lambda_{j2}^l (\tilde{h}_{ji}^l)_{12} (\tilde{h}_{ji}^l)'_{12} & \sum_{j=1}^N \lambda_{j1}^l (\tilde{h}_{ji}^l)_{11} (\tilde{h}_{ji}^l)'_{21} + \lambda_{j2}^l (\tilde{h}_{ji}^l)_{12} (\tilde{h}_{ji}^l)'_{22} \\ \sum_{j=1}^N \lambda_{j1}^l (\tilde{h}_{ji}^l)_{21} (\tilde{h}_{ji}^l)'_{11} + \lambda_{j2}^l (\tilde{h}_{ji}^l)_{22} (\tilde{h}_{ji}^l)'_{12} & 1 + \sum_{j=1}^N \lambda_{j1}^l (\tilde{h}_{ji}^l)_{21} (\tilde{h}_{ji}^l)'_{21} + \lambda_{j2}^l (\tilde{h}_{ji}^l)_{22} (\tilde{h}_{ji}^l)'_{22} \end{bmatrix} \tag{5.19}$$



Taking the determinant of  $\mathbf{S}_i^l$ ,  $x_i^l$  can be expressed as:

$$\begin{aligned}
x_i^l = & 1 + \sum_{j=1}^N \left( (\tilde{h}_{ji}^l)_{11} (\tilde{h}_{ji}^l)'_{11} + (\tilde{h}_{ji}^l)_{21} (\tilde{h}_{ji}^l)'_{21} \right) \lambda_{j1}^l + \sum_{j=1}^N \left( (\tilde{h}_{ji}^l)_{12} (\tilde{h}_{ji}^l)'_{12} + (\tilde{h}_{ji}^l)_{22} (\tilde{h}_{ji}^l)'_{22} \right) \lambda_{j2}^l + \\
& \sum_{j=1}^N \sum_{k=1}^N \left( (\tilde{h}_{ji}^l)_{11} (\tilde{h}_{ji}^l)'_{11} (\tilde{h}_{ki}^l)_{21} (\tilde{h}_{ki}^l)'_{21} - (\tilde{h}_{ji}^l)_{11} (\tilde{h}_{ji}^l)'_{21} (\tilde{h}_{ki}^l)_{11} (\tilde{h}_{ki}^l)'_{21} \right) \lambda_{j1}^l \lambda_{k1}^l + \\
& \sum_{j=1}^N \sum_{k=1}^N \left( (\tilde{h}_{ji}^l)_{12} (\tilde{h}_{ji}^l)'_{12} (\tilde{h}_{ki}^l)_{22} (\tilde{h}_{ki}^l)'_{22} - (\tilde{h}_{ji}^l)_{22} (\tilde{h}_{ji}^l)'_{12} (\tilde{h}_{ki}^l)_{22} (\tilde{h}_{ki}^l)'_{12} \right) \lambda_{j2}^l \lambda_{k2}^l + \\
& \sum_{j=1}^N \sum_{k=1}^N \left( (\tilde{h}_{ji}^l)_{11} (\tilde{h}_{ji}^l)'_{11} (\tilde{h}_{ki}^l)_{22} (\tilde{h}_{ki}^l)'_{22} + (\tilde{h}_{ji}^l)_{21} (\tilde{h}_{ji}^l)'_{21} (\tilde{h}_{ki}^l)_{12} (\tilde{h}_{ki}^l)'_{12} - \right. \\
& \left. 2\Re((\tilde{h}_{ji}^l)_{11} (\tilde{h}_{ji}^l)'_{21}) \Re((\tilde{h}_{ji}^l)_{12} (\tilde{h}_{ji}^l)'_{22}) - 2\Im((\tilde{h}_{ji}^l)_{11} (\tilde{h}_{ji}^l)'_{21}) \Im((\tilde{h}_{ji}^l)_{12} (\tilde{h}_{ji}^l)'_{22}) \right) \lambda_{j1}^l \lambda_{k2}^l
\end{aligned} \tag{5.20}$$

The expression for  $y_i^l$  is similar to that for  $x_i^l$  with the only difference being that the terms corresponding to  $i^{\text{th}}$  users are not included in the summations. From (6.1) we observe that  $x_i^l$  is a quadratic polynomial with three types of quadratic terms, viz.,  $\lambda_{j1}^l \lambda_{k1}^l$ ,  $\lambda_{j2}^l \lambda_{k2}^l$  and  $\lambda_{j1}^l \lambda_{k2}^l$ . It is important to note that  $\lambda_{j1}^l \lambda_{k1}^l$  is the same as  $\lambda_{k1}^l \lambda_{j1}^l$  and hence the number of unique quadratic terms for this category is  $\sum_{l=1}^{N_b} \sum_{j=1}^N j = \frac{N_b N}{2} (N+1)$ . The same argument holds for  $\lambda_{j2}^l \lambda_{k2}^l$ . The number of unique terms for  $\lambda_{j1}^l \lambda_{k2}^l$  ( $\forall j, k, l$ ) is  $N_b N^2$ , which makes the total number of quadratic terms in (6.1) equal to  $N_b N (2N+1)$ . Each of these quadratic terms is replaced by a new variable:  $\Gamma_{j1k1}^l = \lambda_{j1}^l \lambda_{k1}^l$ ,  $\Gamma_{j1k2}^l = \lambda_{j1}^l \lambda_{k2}^l$  and  $\Gamma_{j2k2}^l = \lambda_{j2}^l \lambda_{k2}^l$ . These equalities are relaxed by including the following linear inequalities called bounding factor constraints (illustrated for  $\Gamma_{j1k2}^l$ ), for each non-linear term:

$$\begin{aligned}
\Gamma_{j1k2}^l - \lambda_{j1LB}^l \lambda_{k2}^l - \lambda_{j1}^l \lambda_{k2LB}^l & \geq -\lambda_{j1LB}^l \lambda_{k2LB}^l \\
\Gamma_{j1k2}^l - \lambda_{j1UB}^l \lambda_{k2}^l - \lambda_{j1}^l \lambda_{k2LB}^l & \leq -\lambda_{j1UB}^l \lambda_{k2LB}^l \\
\Gamma_{j1k2}^l - \lambda_{j1LB}^l \lambda_{k2}^l - \lambda_{j1}^l \lambda_{k2UB}^l & \leq -\lambda_{j1LB}^l \lambda_{k2UB}^l \\
\Gamma_{j1k2}^l - \lambda_{j1UB}^l \lambda_{k2}^l - \lambda_{j1}^l \lambda_{k2UB}^l & \geq -\lambda_{j1UB}^l \lambda_{k2UB}^l
\end{aligned} \tag{5.21}$$

This completes LPR construction of the original problem (5.9) and the corresponding LP

can be expressed as:

$$\begin{aligned}
\max \quad & \sum_{i=1}^N C_i \\
s.t. \quad & C_i = \sum_{l=1}^{N_b} \frac{1}{\ln 2} (u_i^l - v_i^l), \\
& \text{Polynomial approximation of } u_i^l \text{ and } v_i^l \text{ given by (5.16),} \\
& \text{Linear expressions for } x_i^l \text{ and } y_i^l \text{ (using (6.1)),} \\
& \text{Bounding constraints for } \Gamma_{j1k1}^l, \Gamma_{j1k2}^l \text{ and } \Gamma_{j2k2}^l \text{ (5.21),} \\
& \sum_{l=1}^{N_b} Tr\{\Lambda_i^l\} \leq P_{max}, \text{diag}\{\Lambda_i^l\} \succeq \mathbf{0} \\
& 1 \leq i \leq N, 1 \leq l \leq N_b.
\end{aligned} \tag{5.22}$$

Except LPR construction, all the aspects of the BB/RLT algorithm are same as that of the one discussed for the single-band MIMO IC. Please refer to the previous chapter for details.

## 5.4 Two-User Symmetric SISO IC with Two Frequency Bands (Case of $N = N_b$ )

In this section, we study the optimal power allocation strategy in a simple two-user symmetric SISO IC, where each user has two frequency bands for transmission. The power can be distributed over multiple bands if it is the optimal strategy to adopt. The goal of this simple study is to understand the behavior of IC when the number of bands available is equal to the number of users. It should be noted that the results obtained in the two-user  $2 \times 2$  MIMO IC in the previous chapter are of particular interest while understanding this case. By comparing the two ICs we should be able to understand the similarities and differences of having orthogonal spatial channels and orthogonal spectral channels from sum-rate maximization perspective. To facilitate this comparison, we use the same simulation parameters as used in the two-user  $2 \times 2$  MIMO IC in the previous chapter. We additionally assume that the channel gains over the two frequency bands are independent from each other.

As has been the case in all the previous examples, we will consider a few special cases in addition to the optimal sum-rate case to gain some insight into the optimal power allocation strategy in this IC. The simulation cases considered in this example are briefly discussed below:

- **Optimal Sum-Rate:** In this case, we solve the sum-rate maximization problem and find the optimal fraction of power to be transmitted by each user over each frequency channel. The optimal sum-rate acts as a benchmark to evaluate the performance of the sub-optimal power allocation strategies considered in this section.
- **Two User - Single Band Transmission:** In this case, we assume that each user selects an optimal band and transmits at maximum power  $P_{max}$  in that frequency band. This case is analogous to the max power beamforming case studied in the MIMO ICs, where each user transmits in only one of the orthogonal spatial channels. The selection of the optimal frequency band for each user is not trivial. It can be achieved by formulating a mixed-integer optimization problem. We will discuss this type of formulation in detail later. For this study, we employ an exhaustive search to find the optimal set of bands to be allocated to each user. This exhaustive search is quite feasible since there are only  $\binom{2}{1}^2 = 4$  cases to check.
- **Equal Power Distribution:** In this case, each user transmits at the maximum power  $P_{max}$  and distributes its transmit power equally over the two frequency channels.
- **One User - Equal Power Distribution:** In this case, only one of the two users is allowed to transmit. The allowed user transmits at the maximum power and distributes the transmit power equally over the two spatial channels. The user with the higher individual capacity (better channel) is allowed to transmit.
- **One User - Single Band Transmission:** In this case, only one of the two users is allowed to transmit. The allowed user transmits at the maximum power  $P_{max}$  in only one of the two frequency bands. In this case too, we employ exhaustive search to

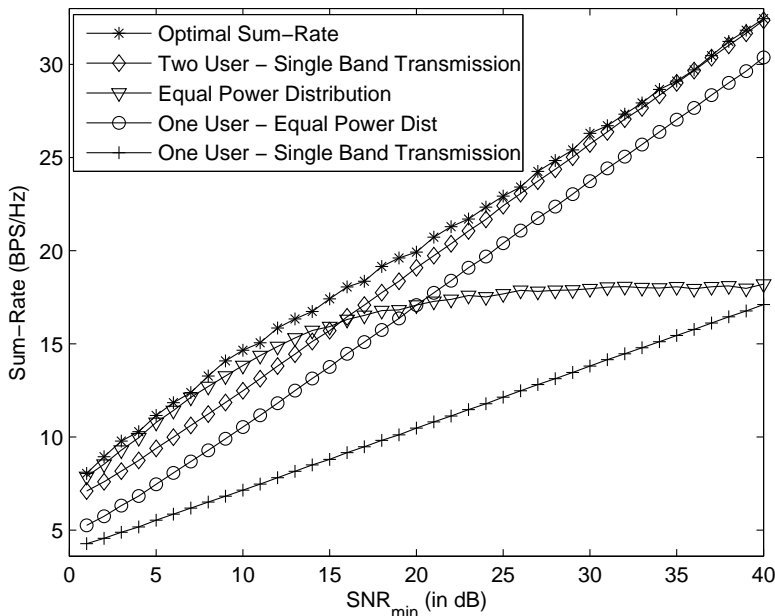


Figure 5.1: Numerical results of the sum-rate achievable in the two-user symmetric SISO IC with two frequency channels ( $n_t = n_r = 1$ ,  $N = 2$ ,  $N_b = 2$ ,  $\rho = 0$ ,  $MUI = 1$ ,  $\sigma = 0$ , Rayleigh fading assumed).

select the optimal user and optimal frequency band such that the resulting capacity is maximized. Exhaustive search is optimal since there are only 4 cases to check.

### 5.4.1 Numerical Results

The sum-rates achievable in all the above cases are presented in Fig. 5.1. The first and foremost observation is that the sum-rate results look nearly the same as the ones obtained for the two-user  $2 \times 2$  MIMO IC in the previous chapter ( $\rho = 0$  case), with just the spatial channels replaced by the frequency bands. This is an interesting observation and indicates that it is the number of degrees of freedom that eventually matters rather than their exact source (spatial or spectral). It is important to note that each user in the present system has two degrees of freedom due to the presence of two orthogonal frequency bands. Similarly,

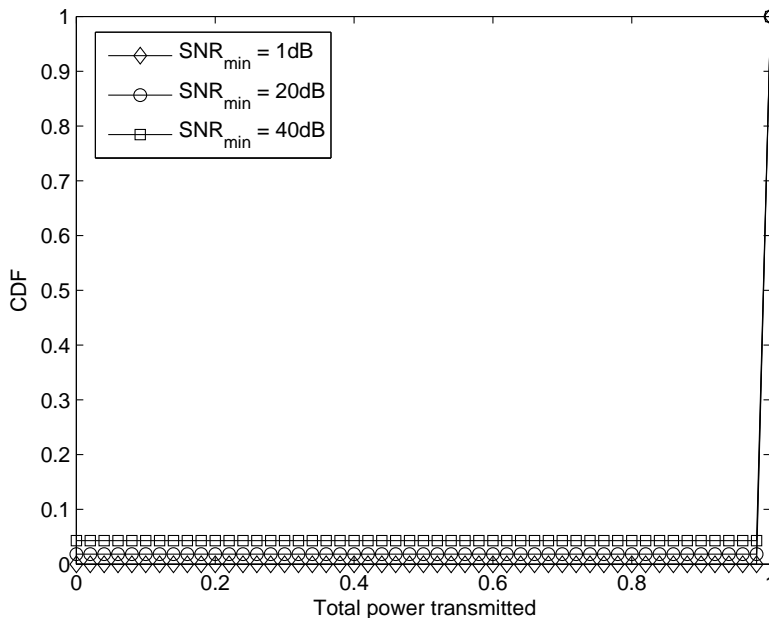


Figure 5.2: Distribution of the total power transmitted by each user in the two-user symmetric SISO IC with two frequency channels ( $n_t = n_r = 1$ ,  $N = 2$ ,  $N_b = 2$ ,  $\rho = 0$ ,  $MUI = 1$ ,  $\sigma = 0$ , Rayleigh fading assumed).

each user in the two-user  $2 \times 2$  MIMO IC also has two degrees of freedom but the source is the presence of two spatial channels (in  $\rho = 0$  case). We will look into this similarity between the two ICs in more detail as we go along.

The sum-rate results indicate that it is optimal in all the SNR regimes to let both the users transmit simultaneously. In the low SNR regime, it is optimal for each user to distribute the power over the two frequency bands. The comparison of the optimal sum-rate with the sum-rate achievable using equal power distribution suggests that equal power distribution is not exactly optimal in the low SNR regime. The exact nature of the distribution will be studied later when we look at the distributions of the powers transmitted over the stronger and the weaker frequency bands. In the high SNR regime, we observe that it is optimal for each user to just confine its transmit power in one of the two bands and avoid interference completely. The fact that interference is completely avoided can be verified by comparing

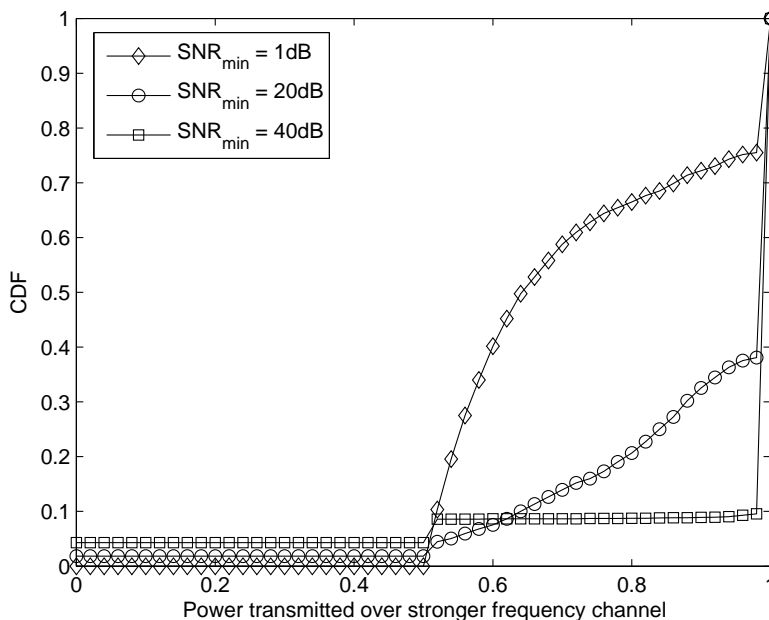


Figure 5.3: Distribution of the power transmitted by each user over the stronger frequency channel in the two-user symmetric SISO IC with two frequency channels ( $n_t = n_r = 1$ ,  $N = 2$ ,  $N_b = 2$ ,  $\rho = 0$ ,  $MUI = 1$ ,  $\sigma = 0$ , Rayleigh fading assumed).

the optimal sum-rate with the sum-rate of the single user when it just transmits over a single band. In particular, we observe that optimal sum-rate is nearly twice the sum-rate achieved in the said case. This is analogous to our observation in the two-user  $2 \times 2$  MIMO IC case, where we saw that it was optimal to avoid interference completely by performing beamforming. In other words, it is optimal for each user to use one of the degrees of freedom to transmit and the other for interference avoidance (allow other user to transmit without interference). This is an interesting result and we will generalize it as we go along in this chapter.

We now look at the distribution of the total power transmitted by each user in three main SNR regimes: low ( $SNR_{min} = 1$  dB), intermediate ( $SNR_{min} = 20$  dB) and high ( $SNR_{min} = 40$  dB), in Fig. 5.2. As mentioned earlier, it is highly likely that both the users will transmit at the maximum power in all the three SNR regimes. There are a very few cases, when it is

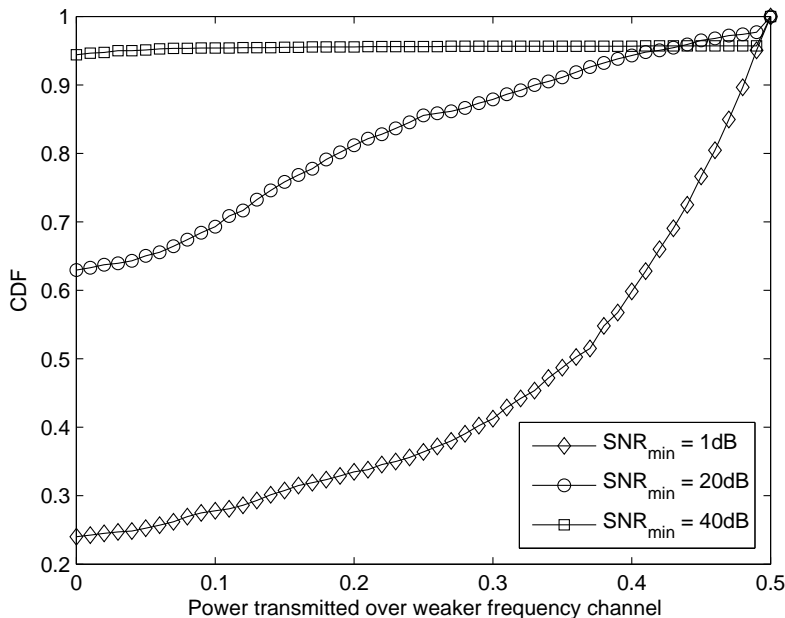


Figure 5.4: Distribution of the power transmitted by each user over the weaker frequency channel in the two-user symmetric SISO IC with two frequency channels ( $n_t = n_r = 1$ ,  $N = 2$ ,  $N_b = 2$ ,  $\rho = 0$ ,  $MUI = 1$ ,  $\sigma = 0$ , Rayleigh fading assumed).

optimal to turn off one user and let the other transmit by distributing its power over both the bands. The occurrence of these cases is observed to increase as we go from low to high SNR regime. Even though the trend was similar in the two-user  $2 \times 2$  MIMO IC, we note that the likelihood of turning off the user is comparatively less in the present case. We will study the reason for this difference in detail later in this section.

With this understanding, we now look at the distribution of the power transmitted over the stronger and the weaker frequency channels in Fig. 5.3 and Fig. 5.4, respectively. The stronger frequency band is defined as the one where it is optimal for the user to transmit more power. Likewise, the weaker band is the one where it is optimal to transmit less power. It should be noted that the stronger band may not always correspond to the band having a better channel gain. In Fig. 5.3, we observe that it is optimal for each user to perform beamforming for around 90% of the time in the high SNR regime. A small spike in the

CDF of power distribution at .5 suggests that it is optimal for one user to distribute the transmit power equally over the frequency bands when the other user is turned off. The distribution of power transmitted over the stronger channel in low SNR also presents an interesting case. It is optimal to transmit around 50% to 60% of the maximum power in the stronger mode in around half of the cases. It is optimal for a user to perform beamforming in around one-fourth of the cases. In the rest of the cases, the user distributes power over the frequency channels but transmits the major chunk of the power on one channel. This is precisely the reason for the sub-optimality of equal power distribution in the low SNR regime. The distribution of the transmit power in intermediate SNR regime is quite similar to that of low SNR regime. The only difference is that it is optimal in more cases to perform beamforming (similar observation was made in the two-user  $2 \times 2$  MIMO IC). Furthermore, it is optimal in rest of the cases to transmit major chunk of the power in the stronger mode and transmit less power in the weaker mode. All the above discussed results can also be inferred from the distribution of the transmit power over the weaker mode (Fig. 5.4). Additionally, we note that the likelihood of turning off the weaker mode as a part of the optimal power allocation strategy is higher in this case as compared to the corresponding two-user  $2 \times 2$  MIMO IC case. This result indicates that it is more profitable in this IC to avoid interference by turning off the weaker channel than by turning off the users as compared to the two-user  $2 \times 2$  MIMO IC case studied earlier. This also explains the slight difference observed in the distributions of the total power in the two cases.

### 5.4.2 Summary of Main Results

- Presence of two orthogonal frequency bands enables the simultaneous transmission of both the users in the 2-user symmetric SISO IC. It is observed that it is typically optimal for both the users to transmit simultaneously in all the SNR regimes.
- The sum-rate and transmit power distribution results in this case are observed to be similar to the ones obtained for the two-user  $2 \times 2$  MIMO IC (uncorrelated antenna



case), where each user has two spatial channels. This implies that sum-rate of the IC depends upon the number of degrees of freedom present with each user and not the source of the degrees of freedom. We will investigate this result in sufficient detail in this chapter.

- It is optimal to distribute power over the frequency bands in the low SNR regime. Equal power distribution, however, is not optimal.
- It is optimal for each user to confine its transmit power in a single band in the high SNR regime. It is optimal for the other user to occupy the other band and hence avoid interference. In a very few cases, it is optimal for only one user to transmit by distributing equal power over the two bands in the high SNR regime. These are the only two optimal states possible in high SNR regime.
- Binary power control is optimal in all the SNR regimes. It is therefore not optimal to let one of the users transmit at a reduced power.
- The number of cases in which one of the users is turned off is less in this case as compared to the corresponding MIMO IC case. Instead, the interference is avoided by turning off the weaker channels rather than by turning off the users. This is the reason for transmitting relatively more power in the stronger channel in this case as compared to the MIMO IC case.

## 5.5 Two-User Symmetric SISO IC with Four Frequency Bands (Case of $N < N_b$ )

In this section, we study the optimal sum-rate of the two-user symmetric SISO IC, where each user has four frequency bands for transmission. The goal of this study is to understand the effect of having more channels than users on the optimal power allocation strategy in various SNR regimes. It would be particularly interesting to compare the results obtained in

this section with the ones obtained for the two-user  $4 \times 4$  MIMO IC studied in the previous chapter. For a meaningful comparison, we keep all the simulation parameters in this section the same as the ones used in the two-user  $4 \times 4$  MIMO IC case. The comparison should further help us understand the similarities and differences of having spatial channels or spectral channels from the sum-rate maximization perspective when the resources present are more than required for interference avoidance. For a fair comparison with the uncorrelated antenna case, we assume that the channel gains over different frequency bands are independent of each other.

As was the case in the all the scenarios previously studied, we compare the optimal results with some known sub-optimal cases to gain insight into the optimal power allocation strategy in various SNR regimes. For this IC, we consider the following simulation scenarios:

- **Optimal Sum-Rate:** In this case, we find the optimal power allocation for each user with the goal of maximizing the sum-rate. Users are allowed to distribute power over multiple bands if that is the optimal strategy to adopt. We use this benchmark case to evaluate the performance of various sub-optimal strategies considered in this section.
- **Single Band Transmission:** In this case, each user selects an ‘optimal’ frequency band and transmits at the maximum power in that band. This is analogous to the max power beamforming case considered in the MIMO ICs of the previous chapter, where each user selected an optimal spatial channel. The selection of the optimal band is not trivial in general. We perform exhaustive search to find the optimal set. Since there are only  $\binom{4}{1}^2 = 16$  choices, exhaustive search is feasible in this case.
- **Equal Power Distribution:** In this case, we assume that each user transmits at the maximum power  $P_{max}$  by distributing it equally over all the frequency channels. It should be recalled that this case does not require any optimization.
- **One User - Equal Power Distribution:** In this case, only one of the two users is allowed to transmit. The chosen user transmits at the maximum power by distributing

it equally over the available frequency channels. The choice of optimal user is not trivial. However, since there are only two users in this case, we can easily find the capacity achievable by each one of them by turning off the other user. We then select the user which achieves higher capacity.

- **Equal Power Distribution over Two Bands:** We consider this additional case, where each user transmits at maximum power by distributing it over just two ‘optimal’ bands such that the sum-rate is maximized. This case is expected to be optimal where it is profitable to avoid interference by turning off weaker channels. In this particular case, each user transmits over just two frequency channels and uses the other two for interference avoidance.

### 5.5.1 Numerical Results

The sum-rates achievable in all the power allocation strategies considered in this section are presented in Fig. 5.5. We first note that it is optimal to let both the users transmit simultaneously in all the SNR regimes. This is expected since there are more number of orthogonal channels than the number of users in this case. Hence, it is always possible to find a strategy that completely avoids interference while letting both the users transmit simultaneously. We will again look at this result when we study the distribution of total power transmitted by each user later in this section.

We note that amongst all the cases considered in this section, equal power distribution achieves closest sum-rate to the optimal case in the low SNR regime. This is in consonance with the results of the two-user  $4 \times 4$  MIMO IC case. There is however a noticeable difference between the two cases suggesting that equal power distribution over all the channels is not exactly the optimal strategy to adopt. We will try to understand the reason for this difference in detail when we study the distributions of the power transmitted by each user over various frequency channels later in this section. We further note that as we increase  $SNR_{min}$ , the case where each user transmits equal power over two spatial channels performs better than equal

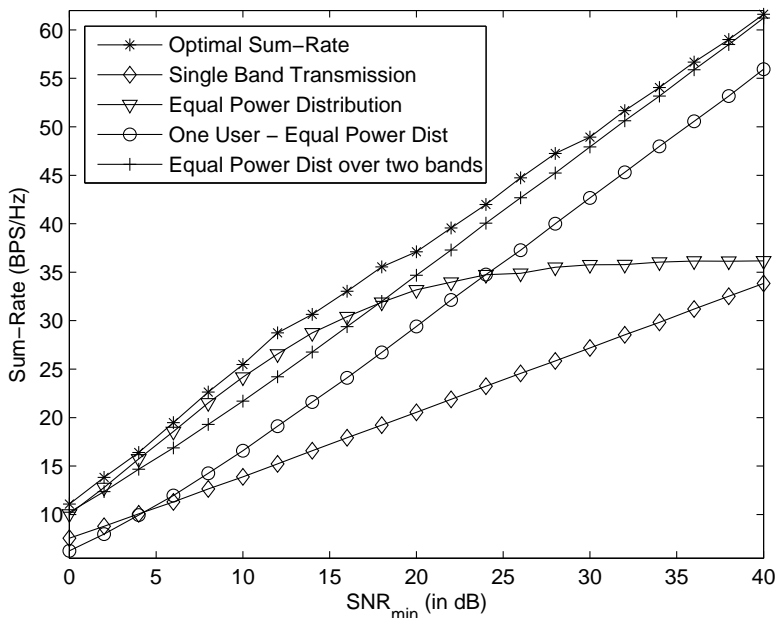


Figure 5.5: Numerical results of the sum-rate achievable in the two-user symmetric SISO IC with four frequency channels ( $n_t = n_r = 1$ ,  $N = 2$ ,  $N_b = 4$ ,  $\rho = 0$ ,  $MUI = 1$ ,  $\sigma = 0$ , Rayleigh fading assumed).

power distribution case. This highlights the increasing importance of interference avoidance as we move from the low SNR to the high SNR regime. A similar trend was noticed in the two-user  $4 \times 4$  MIMO IC case. Furthermore, we note that interference avoidance by turning off the weaker channels is relatively more important when the IC has frequency channels than when it has spatial channels. This is due to the fact that if two users transmit in the same frequency channel, they perfectly interfere with each other. However, the spatial channels of one user are not perfectly aligned with the spatial channels of the other user. Thus, if two users transmit on their respective spatial channels, their signals are not aligned in space (in general) and hence leads to only partial interference. Moving forward towards the high SNR regime, we note that it is nearly optimal for both the users to transmit at maximum power  $P_{max}$  by distributing it equally over only two frequency bands. Thus the optimal strategy in this scenario is to do interference-free transmission by giving up a part of the spectral

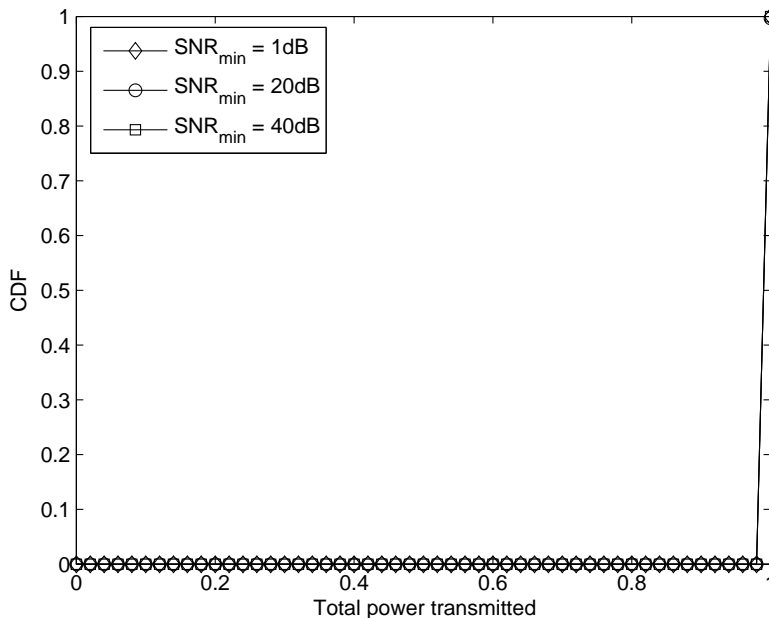


Figure 5.6: Distribution of the total power transmitted by each user in the two-user symmetric SISO IC with four frequency channels ( $n_t = n_r = 1$ ,  $N = 2$ ,  $N_b = 4$ ,  $\rho = 0$ ,  $MUI = 1$ ,  $\sigma = 0$ , Rayleigh fading assumed).

diversity. There is however a noticeable difference between the optimal sum-rate and the one achieved by transmitting over two bands. This was the case in the two-user  $4 \times 4$  MIMO IC too, where another interference-free strategy was optimal in a small number of cases. As we will study later in the section, this is the case in this IC too.

With this insight into the optimal power allocation strategy, we now study the distribution of the total power transmitted by each user over all the frequency channels in Fig. 5.6. For better understanding, we consider three SNR regimes: low SNR ( $\text{SNR}_{\min} = 1$  dB), intermediate SNR ( $\text{SNR}_{\min} = 20$  dB) and high SNR ( $\text{SNR}_{\min} = 40$  dB). As expected, it is optimal for both the users to transmit at maximum power in all the optimal transmission strategies in all SNR regimes. This is in consonance with the results found in the corresponding two-user  $4 \times 4$  MIMO IC.

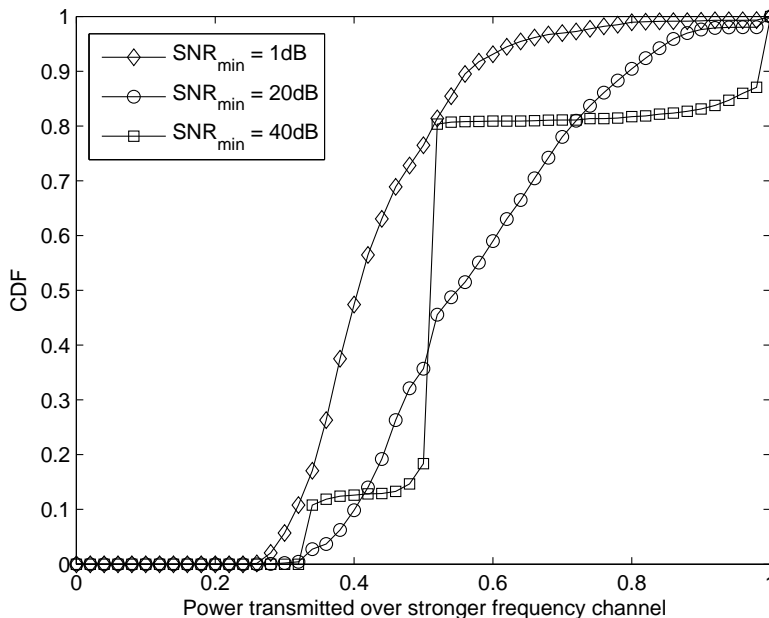


Figure 5.7: Distribution of the power transmitted by each user over stronger frequency channel in the two-user symmetric SISO IC with four frequency channels ( $n_t = n_r = 1$ ,  $N = 2$ ,  $N_b = 4$ ,  $\rho = 0$ ,  $MUI = 1$ ,  $\sigma = 0$ , Rayleigh fading assumed).

The distribution of the power transmitted over the stronger frequency channel in all the SNR regimes is presented in Fig. 5.7. Please note that the stronger frequency channel does not, in general, correspond to the one with the higher channel gain. In fact, we define this channel as the one where a user transmits the highest fraction of its power as a part of the optimal strategy. We first note that the CDF plots of the powers in the three SNR regimes are quite similar to the ones obtained for the two-user  $4 \times 4$  MIMO IC. This further establishes that the fundamental behavior of spatial and spectral channels in an IC is quite similar from sum-rate maximization perspective. In the low SNR regime, we note that it is optimal for each user to transmit  $\approx 30\% - 60\%$  of power in the stronger channel. This explains why the optimal sum-rate did not exactly match the equal power distribution sum-rate in the low SNR regime. Since there is no step at 1, we note that beamforming is not an optimal strategy in this regime. Moving forward towards the intermediate SNR regime, we note that

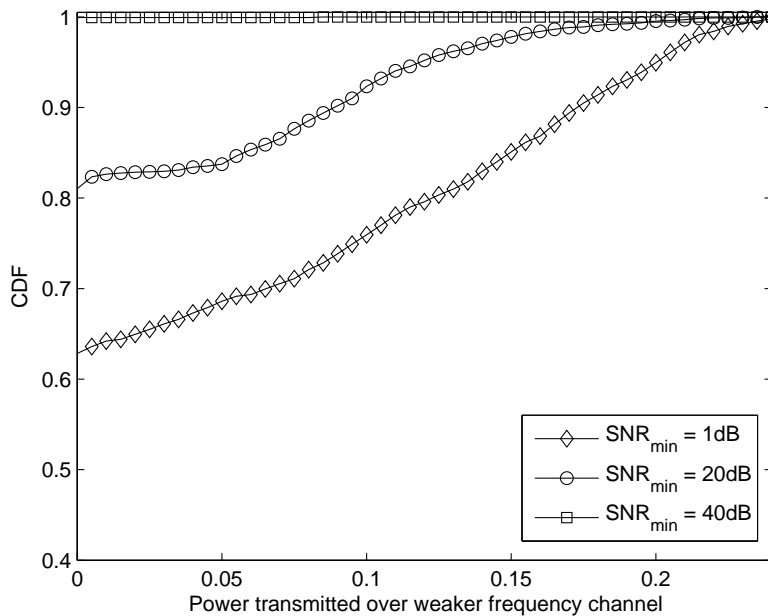


Figure 5.8: Distribution of the power transmitted by each user over weaker frequency channel in the two-user symmetric SISO IC with four frequency channels ( $n_t = n_r = 1$ ,  $N = 2$ ,  $N_b = 4$ ,  $\rho = 0$ ,  $MUI = 1$ ,  $\sigma = 0$ , Rayleigh fading assumed).

it is optimal to transmit  $\approx 40\% - 80\%$  power in the stronger frequency channel. This means that as we move from low SNR to intermediate SNR regime, it is profitable to transmit more power over the stronger channels and less on the weaker ones. This further highlights the increasing importance of interference avoidance as we move from low to intermediate (or high) SNR regimes. We also note a step at 0.5 which suggests that it is optimal in certain cases for each user to select two bands and distribute power equally over them. This result again highlights the relatively higher importance of interference avoidance in the case when IC has frequency channels than when it has spatial channels. Moving further towards the distribution of the power in the high SNR regime, we note that there are two main optimal power allocation strategies. In  $\approx 70\%$  of the cases (height of the step at .5), it is optimal for each user to select two optimal bands and transmit at the maximum power by distributing it equally over them. In the rest of the cases, it is optimal for one of the users to transmit

over one band and optimal for the other to distribute power equally over the remaining three bands. This case corresponds to the steps at  $1/3$  and  $1$  in the CDF plot. It should be recalled that the analogous strategies (replacing frequency channels with the spatial channels) were optimal in the high SNR regime of the two-user  $4 \times 4$  MIMO IC.

We now look at the power transmitted by each user over the weakest frequency band in all the three SNR regimes in Fig. 5.8. It is important to note that the weakest frequency band does not necessarily correspond to the band having the lowest channel gain. Instead, we define it as the one over which the lowest fraction of power is transmitted. We note that it is optimal to turn off this band in a relatively higher number of cases (in all the SNR regimes) as compared to the corresponding two-user  $4 \times 4$  MIMO IC. This reiterates the fact that interference avoidance yields more gains when the IC has frequency channels instead of equal number of spatial channels. As expected, it is optimal to turn off the weakest band in more cases as we move from low to intermediate SNR regime. Finally in the high SNR regime, it is optimal not to transmit any power in this band. This is because the two strategies that are identified as optimal in this regime, do not involve transmission over the weakest band.

### 5.5.2 Summary of the main Results

- We note that it is optimal for both the users to transmit simultaneously in all the SNR regimes.
- It is optimal for both the users to distribute power over multiple bands in the low SNR regime. However, equal power distribution is sub-optimal.
- The importance of interference avoidance, by turning off transmission over weaker bands, increases as we move from low to high SNR regime.
- There are two main optimal strategies in the high SNR regime. In the first strategy, each user selects two optimal bands and transmits at the maximum power by distributing it equally over the two bands. In the second strategy, one of the users transmits



over a single band and the other user transmits equal power over the rest of the three bands. Both these strategies avoid interference completely.

- Comparison of the results with the ones obtained for the corresponding two-user  $4 \times 4$  MIMO IC suggests that the frequency channels and spatial channels behave nearly the same way in an IC. There is however a slightly more importance of interference avoidance by turning off the transmission over weaker channels in the case of frequency channels than the spatial channels. This is because the frequency channels are same for all the users and hence the interference is very strong if more than one users transmit in the same band. However, this is not true in general for the spatial channels, which are locally defined for each user. The interference perceived by each user depends upon the relative alignment of the Eigen-channels of this user with the transmitting users.

## 5.6 Four-User SISO IC with Four Frequency Bands

In this section, we study the optimal power allocation strategies in the four-user SISO IC with four frequency channels. The motivation of studying this case is two-fold. Firstly, we wish to study the effect of scaling up both the number of users and the number of bands on the optimal sum-rate strategies in the two-user two band SISO IC studied earlier in this chapter. Even though both the cases have  $N = N_b$ , the four-user IC is considerably more complex simply because of the higher number of combinations of the transmit powers possible. Please recall that we performed a similar study in the previous chapter when we compared two-user  $2 \times 2$  MIMO IC with the four-user  $4 \times 4$  MIMO IC. The second objective of considering the present case is to find the similarities and differences between the optimal power allocation strategies in this case and the ones identified in the four-user  $4 \times 4$  MIMO IC studied in the previous chapter (both ICs have four orthogonal channels).

We consider following power allocation strategies to gain insight into the optimal sum-rate in the present case:

- **Optimal Sum-Rate:** In this case, we determine the optimal power allocation of each user over each frequency channel with the goal of maximizing the sum-rate. The optimal sum-rate is determined by solving sum-rate maximization problem. This case acts as a benchmark for evaluating the performance of the sub-optimal strategies in various interference regimes.
- **Single Band Transmission:** In this case, each user selects an optimal frequency band and transmits at the maximum power with the goal of maximizing the sum-rate. The selection of the optimal bands is not trivial though. It can be achieved by formulating a mixed-integer non-linear optimization problem (discussed briefly in the next chapter). As seen in the previous cases, exhaustive search is quite handy when the number of optimization parameters is not very high. In the present case, we have four optimization parameters, each with four possible choices. Thus there are  $\binom{4}{1}^4 = 256$  choices and exhaustive search can be effectively used to find the optimal choice. It should be further noted that this case is analogous to max-power beamforming case considered in the single-band MIMO ICs where the transmit power was confined only to a single Eigen-channel.
- **Equal Power Distribution:** In this case, each user transmits at the maximum power  $P_{max}$  by distributing it equally over the four frequency channels. There is no optimization involved in this case. It is analogous to equal power distribution case studied in the MIMO ICs, where transmit power was equally distributed over the Eigen-channels.
- **Three-User Equal Power Distribution:** In this case, only three of the four users are allowed to transmit. The allowed users transmit at the maximum power by distributing it equally over the four frequency channels. The selection of the ‘optimal’ users is done with the goal of maximizing the sum-rate. This selection is not straightforward and can be achieved by formulating a mixed-integer non-linear optimization problem. However, exhaustive search can be quite effective if the number of possible choices is not very high. In this case, there are  $\binom{4}{3} = \binom{4}{1} = 4$  choices and hence exhaustive search is used

to identify the optimal one.

- **Two-User Equal Power Distribution:** In this case, only two of the four users are allowed to transmit. The allowed users transmit at the maximum power  $P_{max}$  by distributing it equally over the four frequency channels. The selection of the optimal set of users is done by performing exhaustive search such that the sum-rate is maximized. Exhaustive search is feasible in this case since there are only  $\binom{4}{2} = 6$  choices to check.
- **One-User Equal Power Distribution:** In this case, only one of the four users is allowed to transmit. The allowed user transmits at the maximum power  $P_{max}$  by distributing it equally over the four frequency channels. The user that achieves highest capacity by transmitting in the interference-free environment is allowed to transmit.

### 5.6.1 Numerical Results

The sum-rates achievable for various power allocation strategies considered in this section are presented in Fig. 5.9. In the low SNR regime, we note that none of the power allocation strategies considered in this study achieve the optimal sum-rate. In fact, none of the schemes perform even close to the optimal. This observation is in contrast to the trend observed in the four-user  $4 \times 4$  MIMO IC studied in the previous chapter, where ‘equal power distribution’ at least performed better than the other sub-optimal strategies. We further note that the ‘single band transmission’ and ‘equal power distribution’ cases nearly achieve similar sum-rate in the low SNR regime. From this observation, it can be conjectured that it is optimal to distribute power over the frequency channels in some cases and confine it to a single frequency channel in the others. This also highlights the fact that unequal power distribution over the orthogonal channels is more favorable in this case than the four-user  $4 \times 4$  MIMO IC case. We will validate these claims when we study the distributions of the power transmitted over various frequency channels later in this section. It should be further noted that ‘three user - equal power distribution’ case performs slightly worse than the ‘single band transmission’

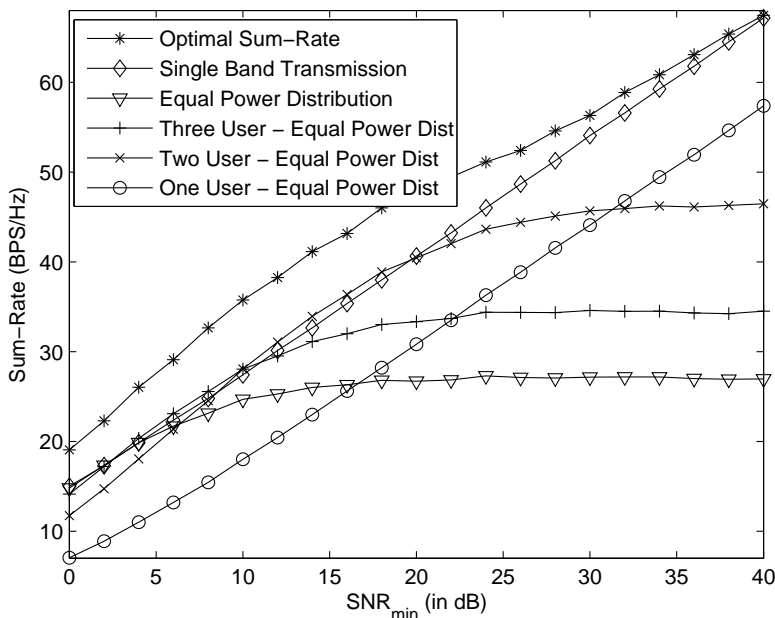


Figure 5.9: Numerical results of the sum-rate achievable in the four-user SISO IC with four frequency channels ( $n_t = n_r = 1$ ,  $N = 4$ ,  $N_b = 4$ ,  $\rho = 0$ ,  $MUI = 1$ ,  $\sigma = 0$ , Rayleigh fading assumed).

and ‘equal power distribution’ cases. This result indicates that it is optimal to let all the users transmit simultaneously in this regime. This claim will also be validated when we study the distribution of total power transmitted by each user later in this section.

In the intermediate SNR regime, we again note that none of the power allocation strategies achieve optimal sum-rate. ‘Two user - equal power distribution’ and ‘single band transmission’ cases perform better than the other cases considered in this section. This highlights the increasing importance of interference avoidance as we move from low interference (low SNR) to high interference (high SNR) regimes. ‘Two user - equal power distribution’ avoids (or reduces) interference by turning off the users, whereas, the ‘single band transmission’ case avoids interference completely by assigning a single band to each user. It is interesting to note that the ‘two user - equal power distribution’ case was a clear winner in the intermediate SNR regime in the four-user  $4 \times 4$  MIMO IC studied earlier. This difference

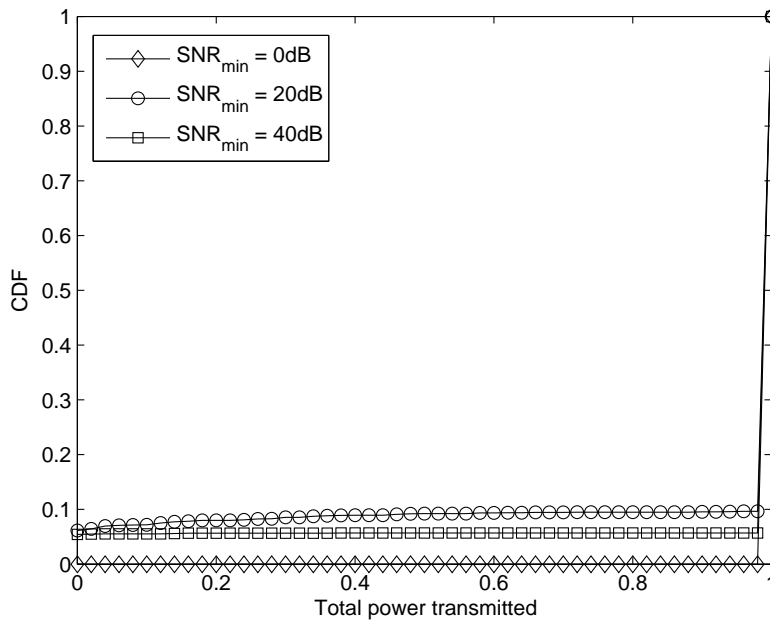


Figure 5.10: Distribution of the total power transmitted by each user in the four-user SISO IC with four frequency channels ( $n_t = n_r = 1$ ,  $N = 4$ ,  $N_b = 4$ ,  $\rho = 0$ ,  $MUI = 1$ ,  $\sigma = 0$ , Rayleigh fading assumed).

in the two cases has two main implications. Firstly, we expect less number of users to be turned off on an average in the present case. Secondly, it reiterates the fact that interference avoidance by confining the power to a fewer channels is even more important in the case of frequency channels than the spatial channels. As noted earlier, this is due to the fact that the frequency channels are common to all the users, whereas the spatial channels are not.

In the high SNR regime, we note that the single-band transmission case nearly achieves optimal sum-rate. In other words, it is optimal to avoid interference completely by confining the transmit power of each user in a single frequency band. This is in consonance with our observations in the previous cases where the max power beamforming case was optimal. It should be noted that the single band transmission case also performs much better than the cases where users are turned off. This again reiterates the optimality of avoiding interference by turning off the bands than by turning off the users in the high SNR regime.

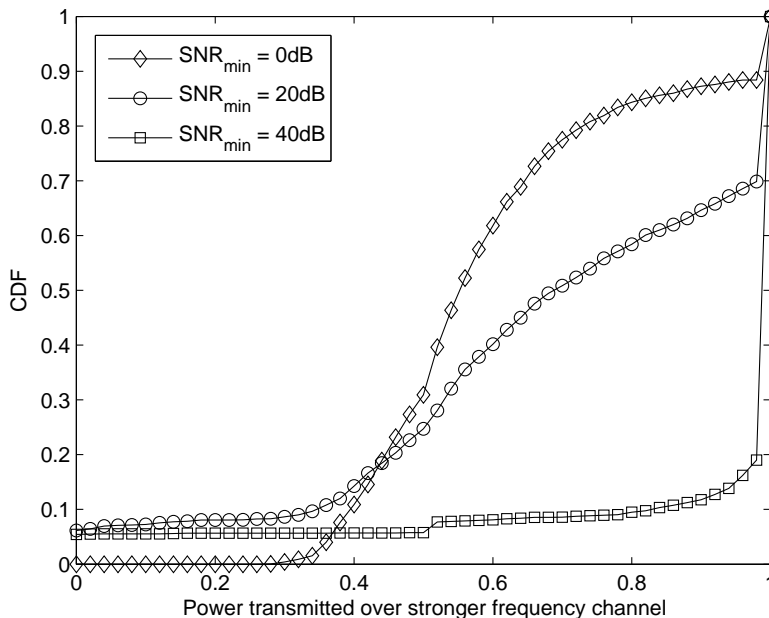


Figure 5.11: Distribution of the power transmitted by each user over stronger frequency channel in the four-user SISO IC with four frequency channels ( $n_t = n_r = 1$ ,  $N = 4$ ,  $N_b = 4$ ,  $\rho = 0$ ,  $MUI = 1$ ,  $\sigma = 0$ , Rayleigh fading assumed).

With this insight into the optimal sum-rate, we now look at the optimal power allocation more closely. In Fig. 5.10, we plot the distribution of the total power transmitted by each user in the three SNR regimes: low ( $SNR_{min} = 0$  dB), intermediate ( $SNR_{min} = 20$  dB) and high ( $SNR_{min} = 40$  dB). We first note that it is optimal to let all four users transmit in the low SNR regime. This result is in consonance with all the cases studied so far and highlights the importance of ‘allowing’ interference in this regime. In the intermediate SNR regime, we note that each user is turned off for  $\approx 8\%$  of the time. From the simulation results we noted that it is almost always optimal to let all four users transmit. In a small fraction of the cases, we note that it is optimal to let only three of the four users transmit. The exact power allocation over various bands will be studied later in this section. From this observation, we can at least say that one of the four users is turned off in  $\approx 4 \times 8\% = 32\%$  of the cases. This is significantly less than what we observed in the four-user  $4 \times 4$  MIMO IC where it

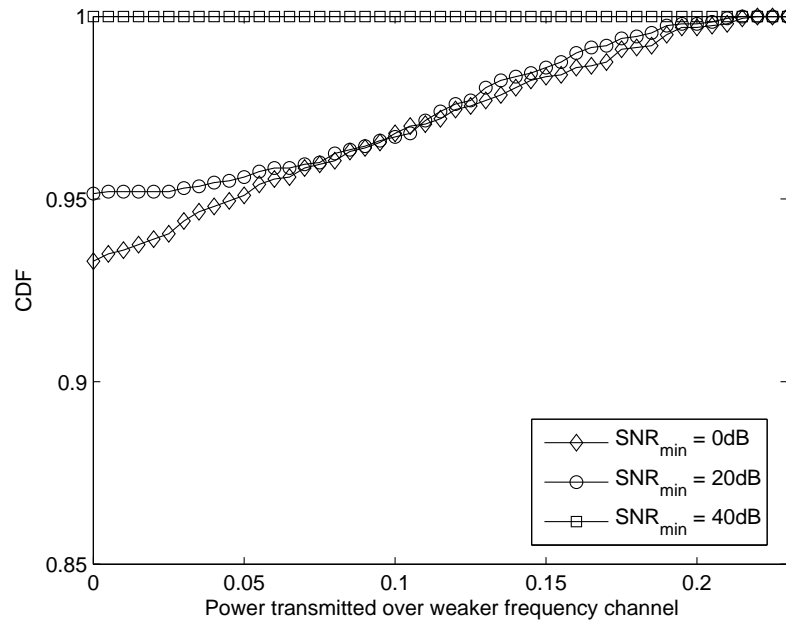


Figure 5.12: Distribution of the power transmitted by each user over weaker frequency channel in the four-user SISO IC with four frequency channels ( $n_t = n_r = 1$ ,  $N = 4$ ,  $N_b = 4$ ,  $\rho = 0$ ,  $MUI = 1$ ,  $\sigma = 0$ , Rayleigh fading assumed).

was optimal to turn one user off in almost all the cases. As we will see later in detail, the reason for this is again the optimality of turning off weaker channels in favor of turning off the users in this case. Readers must recall that it was optimal to turn off users over turning off spatial channels in this SNR regime in the four-user  $4 \times 4$  MIMO IC. As a side note, it is also observed that binary power control is sub-optimal in this regime. We now move over to the high SNR regime and note that it is optimal to turn off each user for  $\approx 5\%$  of the time. As noted in the four-user  $4 \times 4$  MIMO IC case earlier, this is an interesting result since it states that it is optimal to turn off fewer users in the high SNR regime as compared to the intermediate SNR regime. The exact number is however less than the MIMO IC case. This again highlights the fact that interference can be more neatly managed in this case of non-overlapping frequency bands than in the case of spatial channels (that are not aligned for each user).

We now present the distribution of the power transmitted over the strongest frequency channel in Fig. 5.11. Please recall that we define the strongest frequency channel as the one over which the highest fraction of power is transmitted. It may not necessarily coincide with the frequency channel having the highest channel gain. A perfunctory look at the plot indicates that it is optimal, in general, to transmit higher fraction of power over the strongest channel as compared to the corresponding four-user  $4 \times 4$  MIMO IC case studied earlier. In the low SNR regime, it is optimal to transmit around 40% – 70% of the transmit power over the strongest channel. It is even optimal for each user to confine all the power only in the strongest channel for  $\approx 12\%$  of the time. This is precisely the reason why neither ‘equal power distribution’ nor ‘single band transmission’ yields optimal sum-rate in this regime. In the intermediate SNR regime, we note that it is optimal for each user to transmit all the power in the strongest channel for  $\approx 30\%$  of the time. This actually means that it is optimal for at least one of the four users to transmit all its power in a single band. In small number of cases, two users perform single band transmission as a part of the optimal power allocation strategy. This is indicated by the probability of single band transmission that is greater than 25%. Moving on to the high SNR regime, we note that it is optimal for each user to confine its transmit power in a single ‘optimal’ band in  $\approx 80\%$  of the cases. In some cases, one of the users is turned off and the other three distribute their powers over the four channels, with the major chunk being transmitted over the strongest channel. This case corresponds to the values that lie between 0.8 – 1 in the CDF plot. In an extremely small number of cases, it is optimal for one of the four users transmit over just two bands by distributing the over equally over them. This is indicated by a small step at 0.5, which corresponds to  $P_{max}/2$ .

We now present the distribution of power transmitted over the weakest frequency channel in Fig. 5.12. We first observe that a very little power is transmitted over this channel in all the SNR regimes. It is kept off in almost all the cases. This explains why ‘equal power distribution’ is sub-optimal in the low SNR regime. Comparing these results with the results found for the four-user  $4 \times 4$  MIMO IC, we note that the power transmitted over the weakest channel in this case is lower than the MIMO IC case. This again reiterates the optimality



of transmitting higher fraction of power in the stronger channels in the multi-band IC than the corresponding MIMO IC.

### 5.6.2 Summary of the Main Results

- It is optimal to let all the users transmit in the low SNR regime by distributing power over the frequency channels. However, equal power distribution is not optimal. In fact, it is optimal in most of the cases to turn off the weakest frequency channel. This result indicates the optimality of ‘allowing’ interference in the low SNR regimes.
- It is optimal to let all the users transmit in the high SNR regime too. The optimal power allocation strategy involves transmission of each user over a single ‘optimal’ frequency band such that the sum-rate is maximized. Thus complete interference avoidance is optimal in the high SNR (high interference) regime. In a few cases, it is optimal to turn off one user and let the other three distribute power over the four frequency channels, with the major chunks transmitted over the stronger channels.
- Binary power allocation is observed to be optimal in the low and high SNR regimes. However, it is optimal to let a user transmit at reduced power in the intermediate SNR regime.
- As was the case in the corresponding four-user  $4 \times 4$  MIMO IC, it is optimal to turn off more users in the intermediate SNR regime than in the high SNR regime. In the high SNR regime, interference is efficiently avoided by turning off the weaker channels, as opposed to turning off the users.
- Comparison of the current case with the corresponding four-user  $4 \times 4$  MIMO IC reveals that it is, in general, optimal to transmit comparatively higher power in the stronger channels in the present case than the corresponding MIMO IC case. On the other hand, it is optimal to turn off weaker channels more often in the present case. This result, along with the fact that comparatively lesser users are turned off, indicates

the optimality of interference avoidance by turning off weaker channels as opposed to turning off users in the present case.

## 5.7 Two-User $2 \times 2$ MIMO IC with Two Frequency Channels

In this section, we study the optimal power allocation strategies that maximize the sum-rate of a two-user  $2 \times 2$  MIMO IC with two frequency channels. So far, we had considered the cases in which the IC had either all the spatial channels (single-band MIMO IC) or all the frequency channels (multi-band SISO IC). This is the first case where we are considering a mix of the two different types of orthogonal channels. It should be noted that each user in this IC has a total of four orthogonal channels for transmission (two spatial channels in each frequency channel). Thus, it would be interesting to compare the results of this case with the earlier cases where the two-user IC had either four spatial or four frequency channels. It would be interesting to know if the similarity of bands and antennas from the sum-rate perspective extends to these types of general multi-band MIMO IC cases too.

In this section, we consider the following power allocation strategies to get insight into the optimal power allocation:

- **Optimal Sum-Rate:** In this case, we find the optimal power allocation strategy that maximizes the sum-rate of the multi-band MIMO IC. The optimal strategy is found by solving the sum-rate maximization problem formulated earlier in this chapter. This case acts as a benchmark for evaluating the performance of the sub-optimal power allocation strategies in various SNR regimes.
- **Max Power Beamforming:** In this case, each user transmits on one of the two Eigen-channels in one of the two bands, such that the sum-rate is maximized. This is analogous to the beamforming case in the two-user  $4 \times 4$  MIMO IC and the single-band

transmission case in the two-user four-band SISO IC case. The choice of the optimal transmission mode is not trivial. We perform exhaustive search to find the optimal channel for each of the two users. Exhaustive search is feasible since there are only  $\binom{4}{1}^2 = 16$  choices to check.

- **Equal Power Distribution:** In this case, each user transmits at the maximum power by distributing it equally over the two frequency bands. The power is further divided equally over the two spatial channels in each frequency band. This case does not require any optimization and is analogous to the equal power distribution cases of two-user  $4 \times 4$  MIMO and two-user four-band SISO ICs.
- **Single User - Equal Power Distribution:** In this case, only one of the two users is allowed to transmit. The allowed user transmits at the maximum power and distributes it equally over the frequency bands and then over the spatial channels in each band. The user with the higher capacity is selected for transmission.
- **Single Band - Equal Power Distribution:** In this case, we assume that each user transmits over one of the bands by transmitting equal power over the two spatial channels. The optimal band for transmission is selected such that the sum-rate is maximized. The selection of the optimal band is not trivial and is done by performing exhaustive search in the present case. This case is particularly interesting in understanding the optimal power allocation strategy in the high SNR regime.
- **Transmission over two Optimal Channels:** We extend the previous case to a more general case where each user selects two spatial channels for transmission but the spatial channels may lie in different frequency bands. Thus, the users are not confined to transmit over a single frequency channels. The selection of the optimal channels is not trivial and is done by performing exhaustive search. The combination that yields maximum sum-rate is selected. Since there are only  $\binom{4}{2}^2 = 36$  choices, exhaustive search is quite feasible.

### 5.7.1 Numerical Results

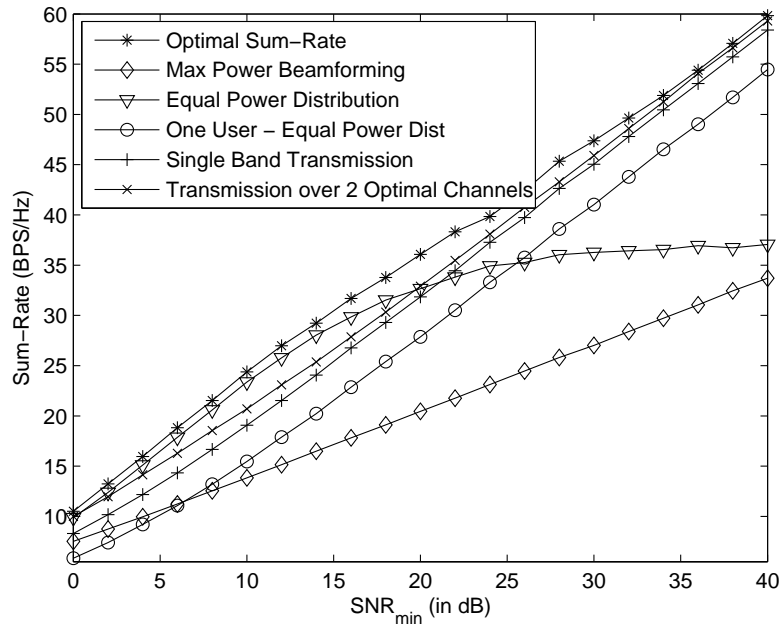


Figure 5.13: Numerical results of the sum-rate achievable in all the cases in the two-user two-band  $2 \times 2$  MIMO IC ( $n_t = n_r = 2$ ,  $N = 2$ ,  $N_b = 2$ ,  $\rho = 0$ ,  $MUI = 1$ ,  $\sigma = 0$ , Rayleigh fading assumed).

The sum-rate results for all the power allocation strategies considered in this section are presented in Fig. 5.13. We first note that it is optimal for both the users to transmit simultaneously in all the SNR regimes. This is expected since the degrees of freedom available with each user are much more than the bare minimum required to avoid interference as a part of the optimal strategies. We will look more into this when we study the distribution of the total power transmitted by each user later in this section. In the low SNR regime, we note that the equal power distribution case performs closest to the optimal case amongst the cases considered in this section. This suggests that distribution of power over the available channels is optimal in this regime. However, there is a noticeable difference between the two cases even in the low SNR regime. This signifies that even though power distribution seems optimal, it is not optimal to distribute power exactly equally over the channels. We will study the

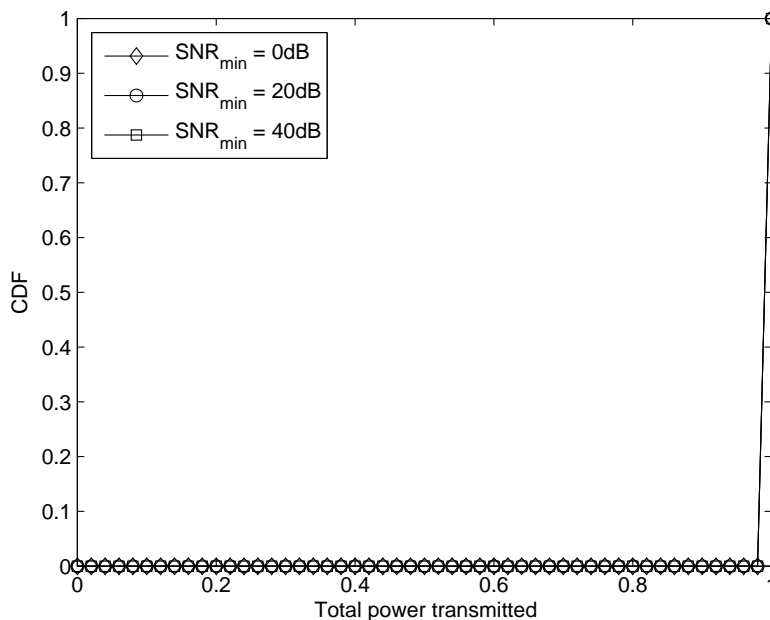


Figure 5.14: Distribution of the total power transmitted by each user in the two-user two-band  $2 \times 2$  MIMO IC ( $n_t = n_r = 1$ ,  $N = 2$ ,  $N_b = 2$ ,  $\rho = 0$ ,  $MUI = 1$ ,  $\sigma = 0$ , Rayleigh fading assumed).

exact power allocation strategy over various channels later in this section. Moving forward to the intermediate SNR regime, we note that the equal power distribution case becomes highly sub-optimal. This highlights the increasing importance of interference avoidance as we move from the low to high SNR regimes. We further look at the  $SNR_{min}$  cross-over point at which the equal power distribution starts performing worse than the ‘transmission over 2 optimal channels’ case and note that it lies in between the corresponding cross-over points for the two-user  $4 \times 4$  MIMO IC and two-user four-band SISO IC. This further highlights that interference avoidance is relatively more important in the case of frequency channels than the spatial channels (for equal number of total orthogonal channels). Moving further towards the high SNR regime, we note that it is nearly optimal to let each user choose two optimal channels and distribute equal power over them. It is quite interesting to note that single band transmission is not optimal in this regime. Thus, there are some cases in which

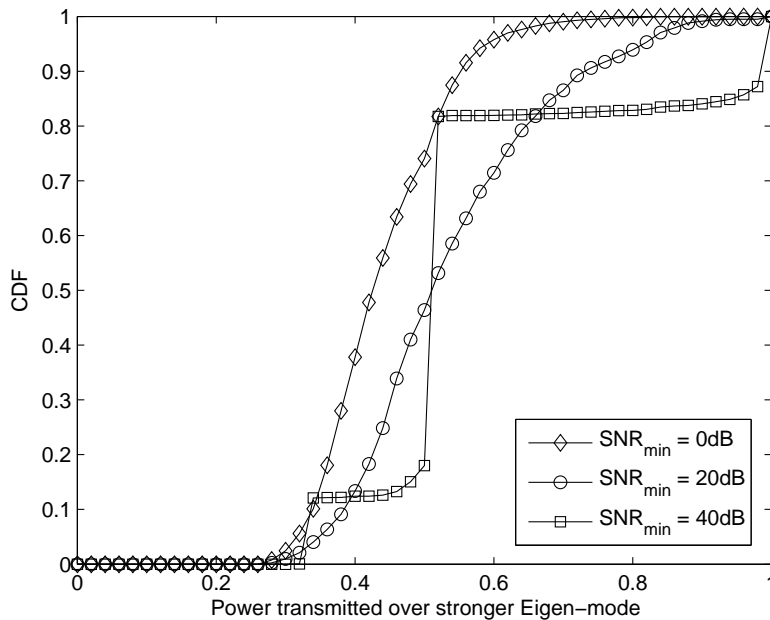


Figure 5.15: Distribution of the power transmitted by each user over stronger Eigen-mode in the two-user two-band  $2 \times 2$  MIMO IC ( $n_t = n_r = 1$ ,  $N = 2$ ,  $N_b = 2$ ,  $\rho = 0$ ,  $MUI = 1$ ,  $\sigma = 0$ , Rayleigh fading assumed).

it is optimal to transmit over spatial channels which may lie in different frequency bands.

With this insight into the optimal power allocation, we now look at the distribution of the total power transmitted by each user in Fig. 5.14. We consider three SNR regimes for our study: low ( $SNR_{min} = 0$  dB), intermediate ( $SNR_{min} = 20$  dB) and high ( $SNR_{min} = 40$  dB). In all SNR regimes, we note that it is optimal to let both the users simultaneously transmit in all the optimal power allocation strategies. This is consistent with the results obtained in the similar cases because the degrees of freedom available with each user are much more than the bare minimum required to avoid interference completely.

We now plot the distribution of the power transmitted by each user over the strongest and the weakest Eigen-modes in Fig. 5.15 and Fig. 5.16, respectively. It should be recalled that the strongest and weakest modes are defined as the ones over which maximum and minimum

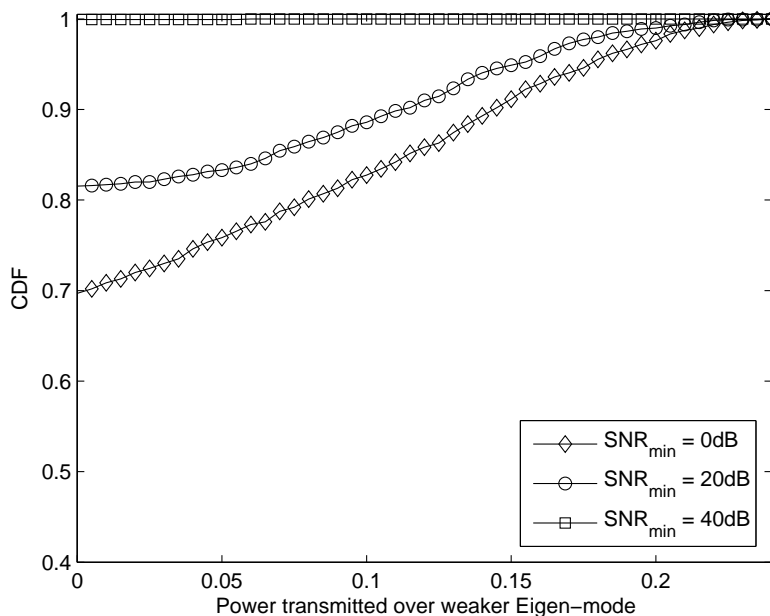


Figure 5.16: Distribution of the power transmitted by each user over weaker Eigen-mode in the two-user two-band  $2 \times 2$  MIMO IC ( $n_t = n_r = 1$ ,  $N = 2$ ,  $N_b = 2$ ,  $\rho = 0$ ,  $MUI = 1$ ,  $\sigma = 0$ , Rayleigh fading assumed).

fractions of power are transmitted, respectively (amongst spatial or spectral channels). They may not necessarily correspond to the strongest and weakest Eigen-modes of the interference-free channel. It should be further borne in mind that there is only one strongest (and likewise one weakest) Eigen-mode defined per user (and not per frequency band). We first note that it is optimal to distribute power over the available orthogonal channels in the low SNR regime. However, it is sub-optimal to distribute power equally over all the orthogonal channels. This can be easily inferred from the distribution of the power transmitted over the strongest mode in the low SNR regime. We observe that it is optimal to transmit  $\approx 35\% - 55\%$  of the total power over the stronger mode in almost all the cases. We further note that it is optimal to turn off the weakest mode of each user for  $\approx 70\%$  of the time.

In the intermediate SNR regime we note that it is optimal to transmit even higher power in the strongest channel than in the low SNR regime. In most of the cases, it is optimal to

transmit  $\approx 40\%$  to  $70\%$  of the total power in the strongest mode. On the other hand, the weakest mode of each user is turned off for  $\approx 80\%$  of the time. This highlights the increasing importance of interference avoidance as we move from lower to higher SNR regimes.

As was the case in all the previously discussed ICs, the high SNR regime is most well behaved. Firstly, we observe that the weakest mode of each user is turned off. This is rather expected since at least one degree of freedom is required for interference avoidance. We further note that there are two main optimal power allocation strategies in this SNR regime. In the first strategy, each user selects two optimal orthogonal channels and transmits equal power over them. This case corresponds to the step at 0.5 in the CDF of the power transmitted over the strongest mode. The height of the step shows that it is optimal power allocation scheme in  $\approx 70\%$  of the cases. The second optimal strategy is the one where one user transmits over one optimal channel and the other user distributes its power equally over three channels (using one for interference avoidance). This corresponds to the steps at  $1/3$  and  $1$ . The same height of the two steps further shows that both are a result of the same event. The reasonably frequent occurrence of the second strategy explains why equal power distribution over two optimal channels do not achieve maximum sum-rate.

### 5.7.2 Summary of Main Results

- It is optimal for both the users to transmit simultaneously in all the SNR regimes. This is expected because of the presence of much more degrees of freedom than the number of users.
- It is further optimal for both the users to distribute the power over spatial channels in all the SNR regimes. This is due to the fact that more degrees of freedom are available than the bare minimum required for interference avoidance as a part of the optimal strategies. The additional degrees of freedom let both the users simultaneously transmit over more than one orthogonal channel while avoiding interference from each other.



- The sum-rate achievable by equal power allocation is quite close to the optimal sum-rate in the low SNR regime. However, this strategy is shown to be sub-optimal when we studied the distribution of power transmitted over strongest and weakest Eigen-modes.
- There are two optimal states in the high SNR regime. First is the one in which one of the users perform beamforming and the other distributes its power equally over three modes (using one for interference avoidance). The second, and the more probable, case is the one in which each user selects two ‘optimal’ Eigen-modes and distributes power equally over them. It is interesting to note that these optimal Eigen-modes may lie in different bands, thus rendering single band transmission sub-optimal.
- Comparison of the results obtained in this case with the corresponding single-band MIMO and multi-band SISO cases reiterates the fact that interference avoidance is relatively more important in the case of frequency-channels than the spatial channels (for the same number of orthogonal channels). Thus, the results in the present case lie in between the results found in the two base cases.

## 5.8 Four-User $2 \times 2$ MIMO IC with Two Frequency Bands

In this section, we study the optimal power allocation strategies in the four-user  $2 \times 2$  MIMO IC with two frequency channels. The objective of studying this case is to understand the effect of having orthogonal channels both due to the presence of non-overlapping frequency bands and uncorrelated antennas in the case when the total number of orthogonal channels is equal to the number of users. In this case, there are a total of four orthogonal channels (two in each frequency channel). This particular configuration is chosen so that we can compare the results with already studied cases of four-user four-band SISO IC and four-user  $4 \times 4$  MIMO IC (both having four orthogonal channels). Due to the same reason the node

topology and all the simulation parameters are kept same as the ones in the base cases.

To gain insight into the optimal sum-rate, we consider the following power allocation strategies:

- **Optimal Sum-Rate:** In this case, we find the optimal power allocation strategy that maximizes the sum-rate by solving the sum-rate maximization problem. The sum-rate thus achieved acts as a benchmark to evaluate the performance of other power allocation strategies considered.
- **Max Power Beamforming:** In this case, each user transmits at the maximum power  $P_{max}$  over an optimally chosen spatial channel. The choice of the spatial channel is made such that the sum-rate is maximized. Please note that there are two frequency channels, each containing two spatial channels. Thus the optimal choice involves choosing the frequency channel and then choosing the optimal spatial channel therein. This problem can be formulated as a mixed-integer optimization problem. However, if the optimization parameters are not very high (as in the present case), it can be effectively solved by employing exhaustive search. The number of parameters in this case is  $\binom{4}{1}^4 = 256$ .
- **Equal Power Distribution:** In this case, each user transmits at the maximum power by distributing it equally over the Eigen-channels in each frequency band. This is a fixed transmission strategy and does not involve any optimization.
- **Three User - Equal Power Distribution:** In this case, three of the four users are allowed to transmit. The allowed users transmit at the maximum power  $P_{max}$  by distributing it equally over the Eigen-channels in each frequency channel such that the sum-rate is maximized. We perform exhaustive search to identify the optimal set of users that should be allowed to transmit. The exhaustive search is feasible since there are only  $\binom{4}{1} = 4$  cases to check.

- **Two User - Equal Power Distribution:** In this case, only two of the four users are allowed to transmit such that the sum-rate is maximized. The allowed users transmit at maximum power  $P_{max}$  by distributing it equally over all the spatial channels in each frequency band. The choice of the optimal set of users is not trivial and can be achieved by formulating a mixed-integer optimization problem. However, the exhaustive search can be quite handy if the number of optimization parameters is not very high. In the present case, we have only  $\binom{4}{2} = 6$  choices and hence exhaustive search is quite feasible.
- **One User - Equal Power Distribution:** In this case, only one of the four users is allowed to transmit. The user that achieves highest capacity by distributing its power equally over the spatial channels in each frequency band is allowed to transmit. We again perform exhaustive search to identify the optimal user (there are only  $\binom{4}{1} = 4$  choices).

### 5.8.1 Numerical Results

The sum-rate results for all the power allocation strategies considered in this section are presented in Fig. 5.17. In the low SNR regime, we note that the equal power allocation strategy performs marginally better than the other strategies but is still a long way from achieving the optimal sum-rate. Comparing this to the four-user four-band SISO IC and four-user  $4 \times 4$  MIMO IC, we note that the relative difference between the sum-rates achievable by equal power allocation and the respective optimal cases increases as we move from the MIMO IC to the multi-band IC case. This interesting observation highlights the fact that the equal power distribution is not profitable in the multi-band ICs because it leads to a large interference due to the perfect alignment of the channels at all the users. By perfect alignment we mean that the signal transmitted by one user over a particular band acts as interference for all the users transmitting in that band. This is however not the case in the MIMO ICs, where the spatial channels of one user are not perfectly aligned with the spatial channels of the other users. Thus the interference power depends upon the mutual

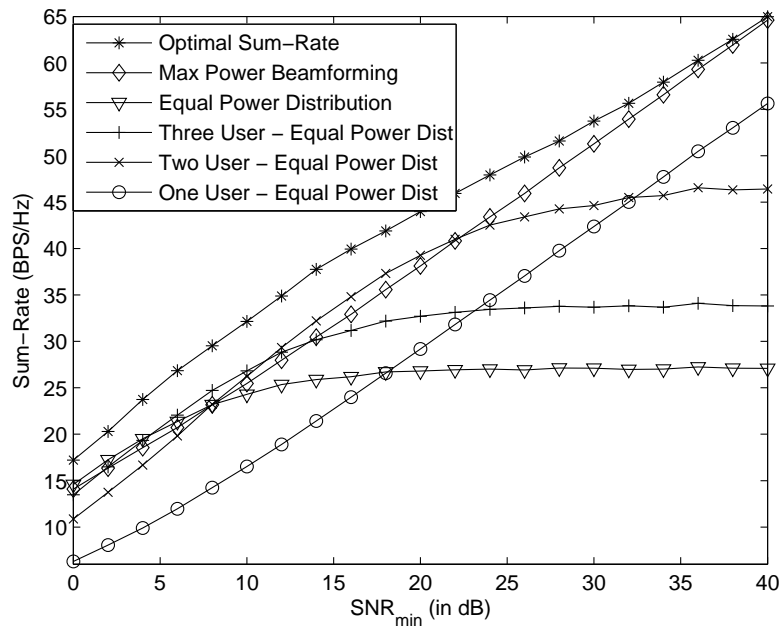


Figure 5.17: Numerical results of the sum-rate achievable in the four-user  $2 \times 2$  MIMO IC with two frequency channels ( $n_t = n_r = 2$ ,  $N = 4$ ,  $N_b = 2$ ,  $\rho = 0$ ,  $MUI = 1$ ,  $\sigma = 0$ , Rayleigh fading assumed).

interaction of the spatial channels of the users, thereby giving some inherent interference avoidance capability. Moving forward, we note that the sum-rates achievable by turning off two or three users are highly sub-optimal in this regime. Sum-rate achievable by turning off even one user is lower than the sum-rate achievable in equal power distribution case, thereby suggesting that the simultaneous transmission of all the users is optimal in this regime. We will validate this observation and study the exact power allocation over various frequency channels later in this section.

In the intermediate SNR regime, we again note that none of the power allocation techniques achieve optimal sum-rate. We further note that the ‘two user - equal power distribution’ case performs marginally better than the max power beamforming case and much better than the rest. This trend was also observed in the four-user four-band SISO IC and the four-user  $4 \times 4$  MIMO IC cases. This observation highlights the importance of avoiding interference by

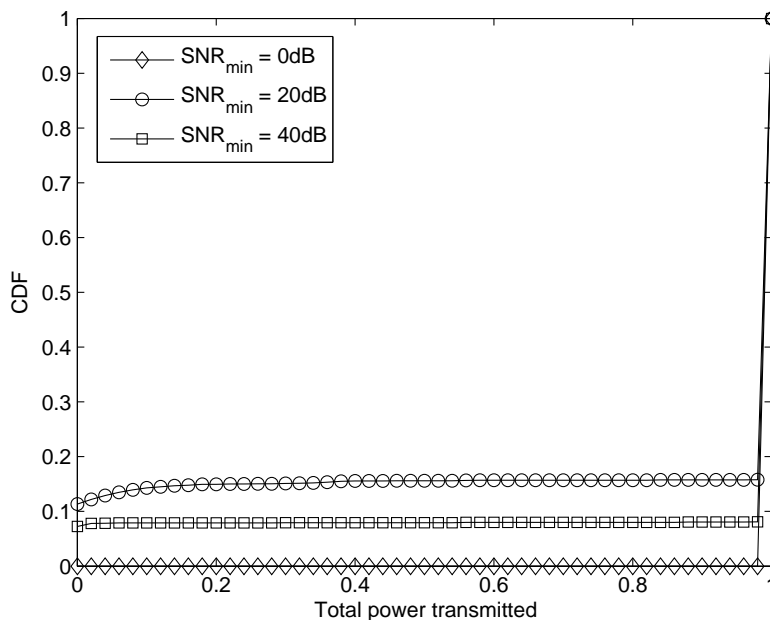


Figure 5.18: Distribution of the total power transmitted by each user in the four-user  $2 \times 2$  MIMO IC with two frequency channels ( $n_t = n_r = 2$ ,  $N = 4$ ,  $N_b = 2$ ,  $\rho = 0$ ,  $MUI = 1$ ,  $\sigma = 0$ , Rayleigh fading assumed).

turning off users in this regime. To compare this case with the already studied four-user ICs, we look at the exact cross-over  $SNR_{min}$  at which the ‘two user - equal power distribution’ case starts performing worse than the max power beamforming case. In the present case it is 22 dB, as opposed to 19 dB in four-user four-band SISO IC and 26 dB in four-user  $4 \times 4$  MIMO IC. Thus the cross-over  $SNR_{min}$  reduces as we move from the single band MIMO IC to the multi-band SISO IC. In other words, it is optimal to avoid interference by turning off the users in case of MIMO ICs and by confining power in a few channels in case of multi-band ICs. The performance of the present case lies in between these two extreme cases. We will look at this in detail when we study the distribution of the total power transmitted by each user later in this section.

In the high SNR regime, we note that the max power beamforming case nearly achieves the optimal sum-rate. This is consistent with the results obtained in all the ICs studied so far.

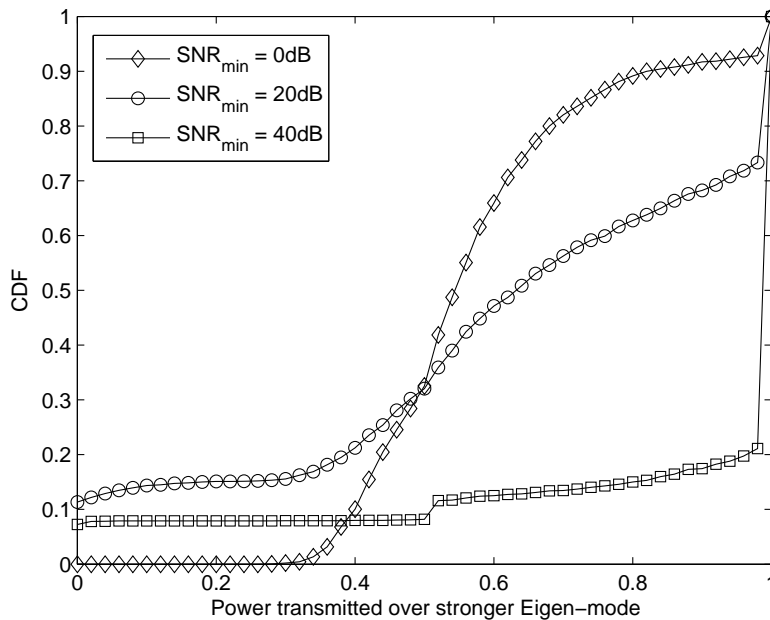


Figure 5.19: Distribution of the power transmitted by each user over stronger frequency channel in the four-user  $2 \times 2$  MIMO IC with two frequency channels ( $n_t = n_r = 2$ ,  $N = 4$ ,  $N_b = 2$ ,  $\rho = 0$ ,  $MUI = 1$ ,  $\sigma = 0$ , Rayleigh fading assumed).

It is further observed that on an average the sum-rates achievable by turning off the users are highly sub-optimal in this regime. This indicates the optimality of letting all the users transmit simultaneously. The interference is avoided by letting each user transmit only in its designated frequency channel, which is chosen such that the sum-rate is maximized. In a very small fraction of cases, it is optimal to turn off one user and let the others distribute power over the frequency channels. We will return to this result when we study the distribution of the power transmitted by each user over the strongest channel later in this section.

With this insight into the optimal power allocation strategies, we now look at the distribution of the total power transmitted by each user in Fig. 5.18. We consider three main SNR regimes: low ( $SNR_{min} = 0$  dB), intermediate ( $SNR_{min} = 20$  dB) and high ( $SNR_{min} = 40$  dB). As expected, it is optimal to let all the four users transmit simultaneously in the low SNR regime. This highlights the importance of ‘allowing’ interference in this regime. This

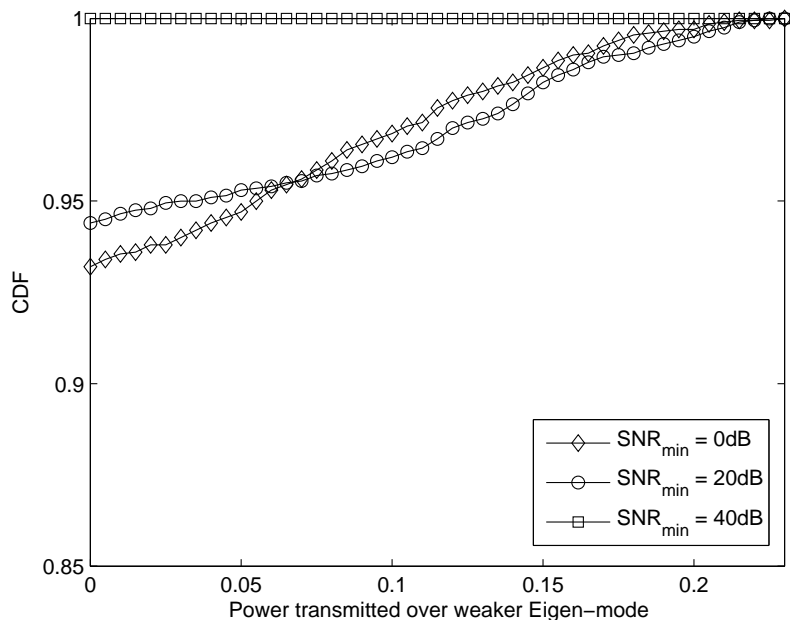


Figure 5.20: Distribution of the power transmitted by each user over weaker frequency channel in the four-user  $2 \times 2$  MIMO IC with two frequency channels ( $n_t = n_r = 2$ ,  $N = 4$ ,  $N_b = 2$ ,  $\rho = 0$ ,  $MUI = 1$ ,  $\sigma = 0$ , Rayleigh fading assumed).

result is consistent with the results obtained for the other four-user ICs studied earlier. In the intermediate SNR regime, we note that it is optimal to turn off each user for  $\approx 12\%$  of the time. This seemingly ordinary result provides some useful insights when compared to the results obtained in the previously studied four-user ICs. We earlier noted that it is optimal to turn off each user for  $\approx 8\%$  and  $\approx 22\%$  of the times in the four-user four-band and four-user  $4 \times 4$  MIMO ICs, respectively. Thus the trend suggests that it is optimal to turn off more users in the MIMO ICs as compared to the analogous multi-band SISO ICs. This is due to the fact that interference can be elegantly avoided in case of frequency channels, which are common to all the users. However, this is not the case in MIMO ICs, where the spatial channels are specific to each user and the optimal strategy depends upon their mutual interactions. It is thus relatively easier to find an optimal strategy that avoids enough interference without turning off the users in the multi-band ICs as compared to the

multi-antenna ICs. As a side note, we also observe that the binary power control is not optimal in the intermediate SNR regime. This is consistent with the results found in all the three and four-user ICs studied earlier. In the high SNR regime, we note that it is optimal to turn off each user for  $\approx 8\%$  of the time. This is an interesting result since it states that it is optimal to turn off less users in the high SNR regime as compared to the intermediate SNR regime. This also highlights the importance of avoiding interference by confining the power to a fewer channels in the high SNR regime, as opposed to avoiding interference by turning off the users in the intermediate SNR regime. We will shortly return to this result when we study the distribution of power transmitted by each user over the strongest channel. As a side note, we also observe that binary power control is optimal in this regime.

Moving forward, we now study the distribution of the power transmitted by each user over the strongest channel presented in Fig. 5.19. Please note that the strongest channel in this case is defined as the orthogonal channel (spatial channel in either of the frequency band) over which the maximum fraction of power is transmitted as a part of the optimal power allocation. Due to the mutual interference, this may not necessarily coincide with the orthogonal channel having maximum strength. In this case too, we look at three main SNR regimes: low ( $SNR_{min} = 0$  dB), intermediate ( $SNR_{min} = 20$  dB) and high ( $SNR_{min} = 40$  dB). In the low SNR regime, we note that it is optimal to transmit  $\approx 35\% - 65\%$  of the total power over the strongest channel. It is even optimal for each user to perform beamforming for  $\approx 8\%$  of the time. This result has two main implications. Firstly, it provides the reason for non-optimality of equal power allocation strategy in this regime. Secondly, it again highlights the importance of transmitting relatively more power over the stronger channels in the multi-band SISO ICs as compared to the single-band MIMO ICs. The reason for this behavior has already been explained in terms of the perfect alignment of the frequency channels at each user. In the intermediate SNR regime, we note that the likelihood of beamforming increases to  $\approx 27\%$  for each user. This means that on an average one of the four users perform beamforming in all the optimal strategies. In an extremely small number of cases it is optimal to let two users simultaneously perform beamforming. Moving further



to the high SNR regime, we note that the most likely optimal strategy is to let all the users simultaneously perform beamforming. In particular, it is optimal to let each user perform beamforming for  $\approx 80\%$  of the time. In some optimal strategies, it is optimal to turn off one user and let another distribute its power equally over two channels, while the rest two perform beamforming. This event corresponds to the small step at 0.5. In some of the cases, one user is turned off and the other three distribute power over the four channels with the major chunk being transmitted over the stronger channels. This event corresponds to the values that lie between 0.6 – 1.0. The occurrence of such events in which power is distributed over the channels is higher in this case than the analogous MIMO IC case and lesser than the analogous multi-band case.

The distribution of power transmitted by each user over the weakest channel is presented in Fig. 5.20. The results reiterate most of the observations already discussed in this section. In the high SNR regime, it is optimal to keep the weakest channel turned off. In the low and intermediate SNR regimes too, it is optimal for each user to turn off its weakest channel for  $\approx 95\%$  of the time. This explains the sub-optimality of equal power distribution in the low SNR regime.

### 5.8.2 Summary of the Main Results

- It is optimal to let all users transmit in the low SNR regime. However, equal power distribution is not optimal. It is optimal to turn off the weakest Eigen-mode of each user in this regime.
- It is optimal to let all the users transmit in the high SNR regime too. The users avoid interference by confining the transmit power over a single Eigen-channel (in a single band). Whenever it is not feasible to avoid enough interference by beamforming, it is optimal to turn off one user, while the rest of the users distribute power over the Eigen-channels in both the bands.

- Binary power allocation is optimal in the low and high SNR regimes. However, it is optimal to let a user transmit at reduced power in the intermediate SNR regime.
- As noted in all the four-user ICs, it is optimal to turn off more users in the intermediate SNR regime than in the high SNR regime. In the high SNR regime, interference is efficiently avoided by turning off the weaker Eigen-modes, as opposed to turning off the users.
- The sum-rate results for the present case are quite similar to the ones obtained for the four-user  $4 \times 4$  MIMO IC and the four-user four-band SISO ICs studied earlier. This again highlights the prime importance of the number of orthogonal channels in an IC and not their source (antennas, bands, etc.).

## 5.9 Conclusions

In this chapter, we have studied the problem of maximizing the sum-rate of the multi-band ICs by treating interference as Gaussian noise. We have considered both the single antenna and multiple antenna cases in our study. Some of the main contributions and conclusions are as follows:

- We have provided a mathematical framework to determine the maximum ergodic sum-rate of a multi-band multi-antenna IC treating interference as Gaussian noise. The problem is reduced to finding the optimal fraction of power to be transmitted over each spatial channel in each frequency channel. The underlying optimization problem is shown to be quite similar to the one studied in the previous chapter for the single band MIMO ICs. This enables us to extend the solution methods studied for the single band MIMO ICs easily to the current problem. To the best of our knowledge, we are the first ones to study this multi-band multi-antenna IC problem in detail.
- We have further extended the BB/RLT algorithm to find the optimal power allocation

for the current problem. It should be noted that the reformulation and linearization of the current problem is relatively more involved than its single-band counterpart due to the higher number of optimization parameters.

- We have further established similarity between the presence of spatial and frequency channels in an IC. Our results have shown that the optimal power allocation strategies for an single-band  $n_t \times n_t$  MIMO IC are nearly same as those of  $N_b$  band SISO IC whenever  $n_t = N_b$ . In other words, the results indicate that the fundamental factor affecting the sum-rate in an IC is the number of orthogonal channels and not their source (such as frequency channels, Eigen-channels, etc.).
- We have generalized the above result further by showing that the optimal power allocation strategies for an  $N_b$ -band  $n_t \times n_t$  MIMO IC are similar to those of single-band  $n \times n$  MIMO IC and  $n$ -band SISO IC whenever  $n_t N_b = n$ . This generalization is based on the fact that an  $N_b$ -band  $n_t \times n_r$  MIMO IC has  $\min\{n_t, n_r\} N_b$  degrees of freedom.
- Due to the above mentioned similarity, all the results found in the previous chapter for the single-band MIMO ICs hold for the multi-band ICs too. We discuss all these results in terms of the number of orthogonal channels  $n = \min\{n_t, n_r\} N_b$  (assuming uncorrelated antennas) below:
  - In the very low SNR regime, system is essentially noise limited and it is optimal for all the users to transmit at the full power  $P_{max}$  over a single orthogonal channel.
  - It is optimal to distribute power over the orthogonal channels in the low SNR regime. Equal power distribution, however, is not optimal in general. This is due to the fact that in most of the optimal power allocation strategies, the weaker channels are turned off for interference avoidance.
  - It is optimal to transmit most of the power in the strongest channels in the intermediate SNR regime. In some cases, it is even optimal to confine all the power in the strongest channel.

- In the high SNR regime, it is optimal in most of the cases to let  $n$  users transmit at the maximum power  $P_{max}$  by confining it to their respective strongest channels. Thus, it is optimal to avoid interference completely in this regime. However, in some cases the spatial channels are so aligned that complete interference avoidance is not possible. In such cases, ‘bad’ users are turned off and the rest of the users ( $< n$ ) are allowed to distribute power over the orthogonal channels.
- Even though the frequency channels and spatial channels have nearly the same effect on the optimal power allocation strategies, there is a minor difference due to the dissimilarity in the way the spatial and frequency channels affect the perceived interference. On one hand, the frequency channels are common to all the users and are perfectly isolated from each other at all the users. On the other hand, this demarkation is not so neat in the case of spatial channels because they are defined for a particular user and are not same for the whole IC. Thus, the net interference perceived by each user depends upon the alignment of its Eigen-channels with the Eigen-channels of the transmitting users. Due to this fundamental difference, interference avoidance is more important in the case of frequency-channels than in the case of spatial channels.
- A lower bound on the sum-rate achievable by power control can be found by letting  $n = \min\{n_t, n_r\}N_b$  users transmit simultaneously at the maximum power  $P_{max}$  by confining it in their respective strongest channels. This bound will be reasonably tight in the interference-limited high SNR regime.

## Chapter 6

# Optimal Sum-Rate vs. Beamforming and Interference Alignment

In the previous chapters we have studied the problem of maximizing the sum-rate of the multi-band multi-antenna IC treating interference as noise. In this chapter, we compare the optimal sum-rate found in the previous chapters to the two main strategies: Optimal Beamforming and Interference Alignment (IA).

In the optimal beamforming strategy, each user transmits at an ‘optimal’ power over a single ‘optimal’ spatial channel such that the sum-rate is maximized. This case is different from the ones studied in the previous chapters because it also includes power control. Thus the main objective of considering this case is to study the value of power control in beamforming.

We also compare the optimal power control results with the ones achievable by Interference Alignment (IA). IA has recently been shown to achieve  $N/2$  degrees of freedom per orthogonal spatial, spectral or temporal slot in an  $N$ -user IC. This means that IA achieves at least half the sum-rate of its no-interference counter-part [28]. This is an interesting result since it indicates that the capacity of an IC is not fundamentally limited by interference, as was initially believed. It further indicates that the capacity of an IC should increase linearly

with an increase in the number of users. However, it is difficult to find analytical solutions to the IA problems in general and even the feasibility of IA over a finite number of signalling dimensions is an open problem. Since the achievability of IA is not the main focus of this work, we do not consider its effects in this study. Instead, we assume that all the  $N$ -user ICs considered in this chapter are capable of achieving  $N/2$  degrees of freedom. The resulting sum-rate is referred henceforth as the IA bound. Denoting the capacity of an isolated MIMO link by  $C_M$ , the IA bound can be evaluated as  $\frac{N}{2}C_M$ . In this case, an IC achieves half the sum-rate of that of its no-interference counterpart. The comparison of IA bound with the optimal power control results shows that the optimal power control performs better than the IA bound in the low-SNR regime for reasonably high number of users. As expected, the performance of IA bound gets better as compared to power control with the increase in SNR.

We begin our study by formulating the sum-rate maximization problem when each user employs optimal beamforming strategy.

## 6.1 Optimal Beamforming

In this section, we compare the sum-rates achievable by optimal power control with the ones achievable by ‘optimal’ beamforming. Two main beamforming strategies are considered in this section: one in which each user is allowed to perform beamforming in all the frequency bands and the other in which each user is allowed to perform beamforming in only a single band. The objective in both the cases is to maximize the sum-rate. We begin our study by formulating the sum-rate maximization problem when each user performs beamforming in each frequency band.

We start by defining the new variables required. Let  $\mathbf{b}_{T_i}^l \in C^{1 \times n_t}$  and  $\mathbf{b}_{R_i}^l \in C^{1 \times n_r}$  be the complex beamforming weights of the Tx and Rx, respectively, of the  $i^{th}$  SU in the  $l^{th}$  frequency band. Let  $f_i^l$ , for  $i \in \{1, 2, \dots, N\}$  and  $l \in \{1, 2, \dots, N_b\}$ , be the power transmitted

by the  $i^{\text{th}}$  user in the  $l^{\text{th}}$  frequency band. The total power transmitted over all the Tx antennas by the  $i^{\text{th}}$  SU is then  $\sum_{l=1}^{N_b} f_i^l \leq P_{max}$ . We now examine the transmit symbol covariance matrix of  $i^{\text{th}}$  SU in the  $l^{\text{th}}$  frequency band, which is given by:

$$\mathbf{Q}_i^l = f_i^l \begin{bmatrix} b_{T_{i1}} b'_{T_{i1}} & b_{T_{i1}} b'_{T_{i2}} & \dots & b_{T_{i1}} b'_{T_{i n_t}} \\ b_{T_{i2}} b'_{T_{i1}} & b_{T_{i2}} b'_{T_{i2}} & \dots & b_{T_{i2}} b'_{T_{i n_t}} \\ \vdots & & \ddots & \vdots \\ b_{T_{i n_t}} b'_{T_{i1}} & b_{T_{i n_t}} b'_{T_{i2}} & \dots & b_{T_{i n_t}} b'_{T_{i n_t}} \end{bmatrix}. \quad (6.1)$$

It is evident from (6.1) that all the columns of  $\mathbf{Q}_i^l$  are linearly dependent and hence it has a single non-zero eigenvalue and the rest lie in the null space. Since  $\mathbf{Q}_i^l \succ \mathbf{0}$ , it can be expressed as  $\mathbf{Q}_i^l = \mathbf{U}_i^l \Lambda_i^l \mathbf{U}_i^{l \dagger}$ , where  $\Lambda_i^l$  is a diagonal matrix of the eigenvalues of  $\mathbf{Q}_i^l$  with only one of them being non-zero. Assuming that the norm of beamforming vector is one, it can be easily shown that the only nonzero eigenvalue of  $\Lambda_i^l$  is  $f_i^l$ . Physically, it establishes that each SU uses only one channel mode in each frequency band for transmission. To incorporate this fact in the general multi-band MIMO capacity optimization problem (5.9), let us define a diagonal matrix  $\Gamma_i^l$  with all the diagonal elements equal to zero except one, which is unity. By incorporating  $\Gamma_i^l$ , the mathematical formulation of the optimal beamforming capacity problem can be written as:

$$\begin{aligned} \max \quad & \sum_{i=1}^N C_i \\ \text{s.t.} \quad & C_i = \sum_{l=1}^{N_b} \log_2 \det(\mathbf{I} + \rho_{ii}^l \mathbf{R}_i^{l-1} \widehat{\mathbf{H}}_{ii}^l \Gamma_i^l \Lambda_i^l \widehat{\mathbf{H}}_{ii}^{l \dagger}) \\ & \mathbf{R}_i^l = \sum_{\substack{j=1 \\ j \neq i}}^N \rho_{ji} \widehat{\mathbf{H}}_{ji}^l \Gamma_j^l \Lambda_j^l \widehat{\mathbf{H}}_{ji}^{l \dagger} + \mathbf{I} \\ & Tr\{\Gamma_i^l\} \leq 1, \text{diag}\{\Gamma_i^l\} \in \{0, 1\}, \forall i, l \\ & \sum_{l=1}^{N_b} Tr\{\Lambda_i^l\} \leq P_{max}, \text{diag}\{\Lambda_i^l\} \succeq \mathbf{0} \\ & 1 \leq i \leq N, 1 \leq l \leq N_b. \end{aligned} \quad (6.2)$$

Please note that this is a mixed-integer non-linear non-convex optimization problem. In this formulation, each user is allowed to perform ‘optimal’ beamforming in each frequency band. However, from our findings in the previous chapters we know that the case where each user is allowed to perform beamforming in only a single band is more relevant to our present

study. Therefore, we slightly modify the above formulation to restrict the transmission of each user to a single band. In that case, only of the  $\Gamma_i^l$  will be non-zero and rest all will be zero. The resulting formulation can be expressed as:

$$\begin{aligned}
 \max \quad & \sum_{i=1}^N C_i \\
 \text{s.t.} \quad & C_i = \sum_{l=1}^{N_b} \log_2 \det(\mathbf{I} + \rho_{ii}^l \mathbf{R}_i^{l-1} \widehat{\mathbf{H}}_{ii}^l \Gamma_i^l \Lambda_i^l \widehat{\mathbf{H}}_{ii}^{l\dagger}) \\
 & \mathbf{R}_i^l = \sum_{\substack{j=1 \\ j \neq i}}^N \rho_{ji} \widehat{\mathbf{H}}_{ji}^l \Gamma_j^l \Lambda_j^l \widehat{\mathbf{H}}_{ji}^{l\dagger} + \mathbf{I} \\
 & \sum_{l=1}^{N_b} \text{Tr}\{\Gamma_i^l\} \leq 1, \text{diag}\{\Gamma_i^l\} \in \{0, 1\} \\
 & \sum_{l=1}^{N_b} \text{Tr}\{\Lambda_i^l\} \leq P_{max}, \text{diag}\{\Lambda_i^l\} \succeq \mathbf{0} \\
 & 1 \leq i \leq N, 1 \leq l \leq N_b.
 \end{aligned} \tag{6.3}$$

The objective in the above formulation is to identify the optimal spatial channel in the optimal frequency band and optimal transmit power for each user such that the sum-rate is maximized. This is different from the beamforming cases studied in the previous chapters since it also includes power control. Thus the main objective of considering this case is to study the value of power control in beamforming. We consider following cases as the part of this study.

### 6.1.1 Two-User Single-Band $2 \times 2$ MIMO IC

We first study the value of power control in beamforming in the two-user  $2 \times 2$  MIMO IC. This IC was studied in Chapter 4 from sum-rate maximization perspective. For consistency, we consider the same fixed IC with the same simulation parameters. To gain insight, we consider the following power allocation strategies:

- **Optimal Power Control:** In this case, each user is allowed to perform optimal power control such the net sum-rate is maximized. This case provides optimal sum-rate as discussed in the previous chapters.
- **Optimal Single-Band Beamforming:** In this case, each user is allowed to transmit at an optimal power over a single optimal spatial channel such that the sum-rate is



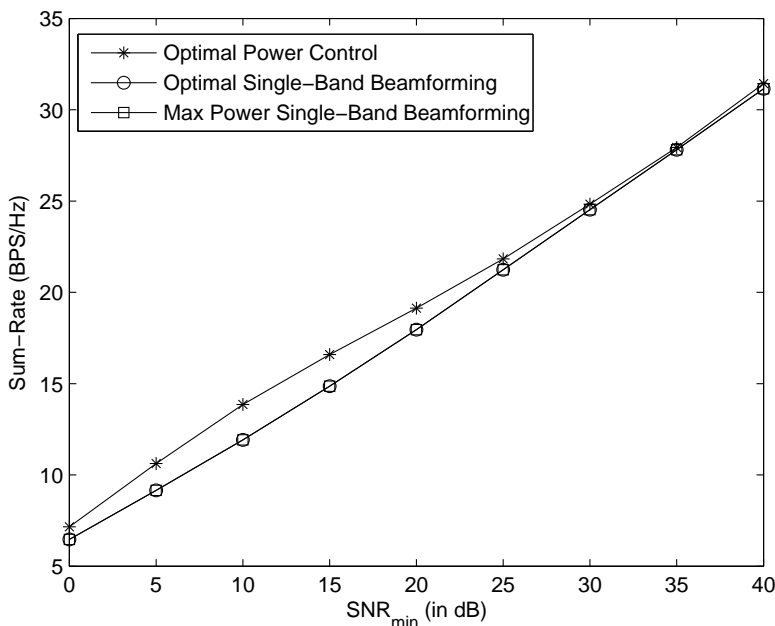


Figure 6.1: Comparison of the sum-rates achievable by beamforming with the optimal case in the two-user  $2 \times 2$  MIMO IC. ( $n_t = n_r = 2$ ,  $N = 2$ ,  $MUI = 1$ ,  $\sigma = 0$ ,  $\rho = 0$ ).

maximized. The corresponding ergodic sum-rate is evaluated by using the framework presented in (6.3).

- Max Power Single-Band Beamforming:** In this case, each user transmits at maximum power  $P_{max}$  over an optimal spatial-channel such that the sum-rate is maximized. The choice of optimal spatial channel for each user is not trivial. Exhaustive search is applied in the present case to find the optimal set of frequency channels. Exhaustive search is feasible because there are only  $\binom{2}{1}^2 = 4$  choices to check.

The sum-rate results presented in Fig. 6.1 clearly indicate that power control is not important in the current IC. In other words, the sum-rates achievable in the optimal beamforming and max power beamforming cases are exactly the same. This is expected in the present case because the number of orthogonal channels is equal to the number of users. Therefore, the optimal beamforming strategy for each user is to select an optimal channel and transmit at

the maximum power  $P_{max}$ .

We now consider a case where the number of orthogonal channels is less than the number of users.

### 6.1.2 Three-User Single-Band $2 \times 2$ MIMO IC

We now study the value of power control in beamforming in the three-user  $2 \times 2$  MIMO IC. This IC was also studied in Chapter 4 from sum-rate maximization perspective. For consistency, we consider the same IC model with the same simulation parameters.

To gain insight, we consider following power allocation strategies:

- **Optimal Power Control:** In this case, each user performs optimal power control such that the sum-rate is maximized. This corresponds to the optimal sum-rate case studied in Chapter 4.
- **Optimal Single-Band Beamforming:** In this case, each user is allowed to transmit at an optimal power over a single optimal channel such that the sum-rate is maximized. The corresponding ergodic sum-rate is evaluated by using the framework presented in (6.3).
- **Max Power Single-Band Beamforming:** In this case, each user transmits at maximum power  $P_{max}$  over an optimal spatial channel such that the sum-rate is maximized. The choice of optimal channel is not trivial and can be achieved in the present case by exhaustive search. Exhaustive search is feasible because the number of choices is only  $\binom{2}{1}^3 = (8)$ .
- **Two-User Max Power Single-Band Beamforming:** This special case is included to understand to optimality of turning one of the users off (especially in the high interference scenarios). In this case, two of the three users are selected to transmit

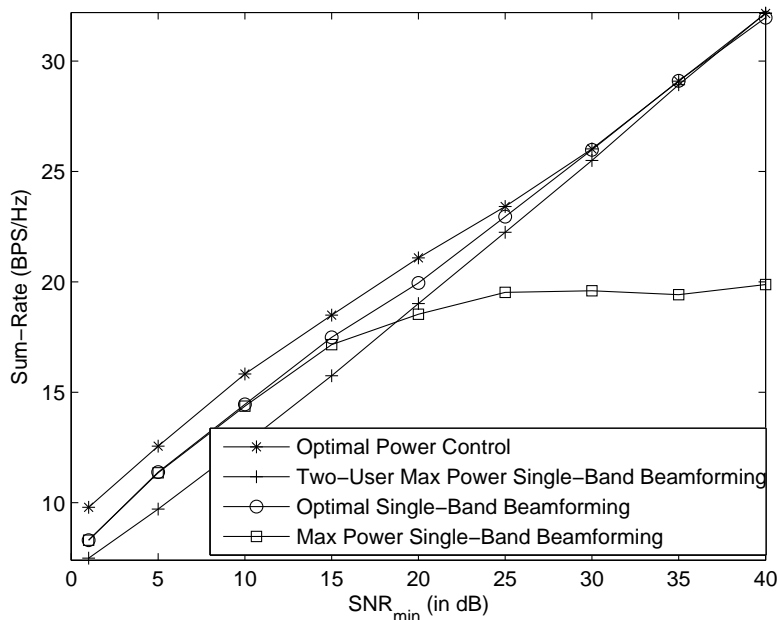


Figure 6.2: Comparison of the sum-rates achievable by beamforming with the optimal case in the three-user  $2 \times 2$  MIMO IC. ( $n_t = n_r = 2$ ,  $N = 3$ ,  $MUI = 1$ ,  $\sigma = 0$ ,  $\rho = 0$ ).

simultaneously. Each selected user then selects an optimal spatial channel for transmission. The selection of the users and spatial channel is done to maximize the sum-rate under the said constraints. This problem of user and Eigen-channel selection can be formulated as a non-linear mixed-integer optimization problem (similar to (6.3)). For this example, we perform an exhaustive search through all the feasible options. The exhaustive search in this case is quite feasible since there are only  $\binom{3}{2} \binom{2}{1} \binom{2}{1} (= 12)$  cases to check.

The sum-rate results for the present case are presented in Fig. 6.2. This is an interesting case since the number of orthogonal channels is less than the number of users. In the low SNR regime, we note that there is no value of power control in beamforming because it is optimal to let all the users transmit at the maximum power. However, as we move from the low to high SNR regime, the value of power control increases. In the limiting case of high SNR regime, it is optimal to completely turn off one user and let the other two perform

beamforming by transmitting at the maximum power  $P_{max}$ . In the intermediate SNR regime, it is optimal to let one of the users transmit at a reduced power.

Therefore, we note that power control is important in beamforming when the number of users is higher than the number of available orthogonal channels.

## 6.2 Comparison with Interference Alignment

The optimal sum-rate of multi-band MIMO IC is compared to two special cases, viz., no-interference (NI) and the IA bound, for different system parameters. The NI case is a hypothetical case and assumes that each SU is isolated from the other SUs in the network. This provides an upper bound to the optimal results. As discussed earlier in this chapter, the IA bound represents the sum-rate achievable by performing IA. It is basically half the sum-rate of the NI case. It should be noted that the IA bound is included just for the purpose of comparison and the feasibility of interference alignment over a limited number of signalling dimensions is an open problem. Please note that the ergodic sum-rates presented in this section are also averaged over *random geometries*.

The channel model is assumed to be a combination of large scale and small scale fading components. On the large scale, we assume that channel suffers from an exponential path loss with a path loss exponent of 3 and from log-normal shadowing with a standard deviation of 1 dB. Small scale fading effects are modeled as Rayleigh distributed. Antennas at both the Tx and Rx of all the users are assumed to be independent in terms of small-scale fading but perfectly correlated in terms of log-normal shadowing. The interference power is controlled by varying the *MUI* factor (high *MUI* means high interference power).

In Fig. 6.3, we present the sum-rates achievable by the proposed optimal power allocation in low ( $MUI = 1$ ) and high ( $MUI = 5$ ) interference scenarios. As expected, the sum-rate achievable in low interference scenario is higher than that achievable in the high interference scenario for both the single band and the multi-band MIMO IC. Another interesting

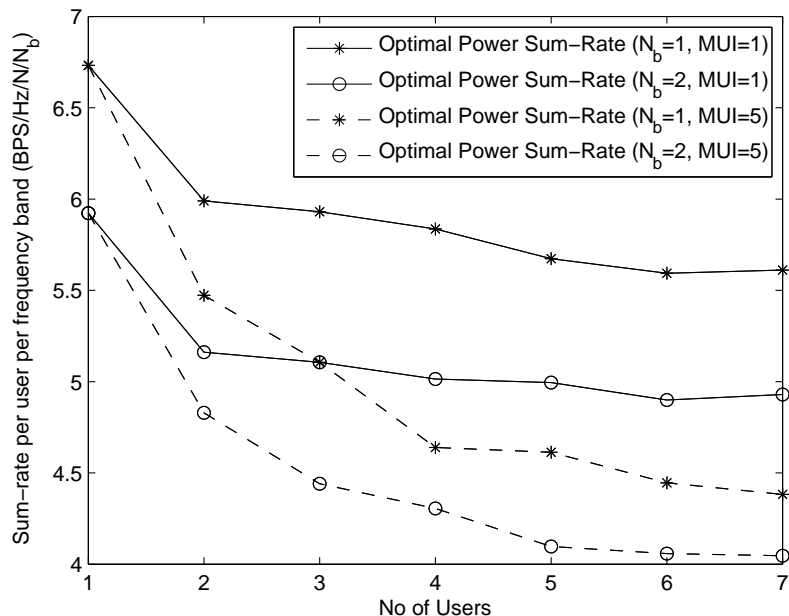


Figure 6.3: Comparison of sum-rates of the single band and multiple band systems in low ( $MUI = 1$ ) and high ( $MUI = 5$ ) interference scenarios ( $n_t = n_r = 2$ ).

observation is that the sum-rate scales better with the increase in frequency bands in the high interference scenario as compared to the low interference scenario. This means that the percentage increase in the sum-rate achieved by increasing the number of bands from one to two is higher in the high interference scenario as compared to the low interference scenario. This essentially means that the ICs get more benefit by doing power control (interference avoidance) in the high interference scenario. We also note that the rate of decrease of sum-rate reduces considerably for  $N > MUI$ . This is because the number of dominant interferers (lying inside the circle of radius  $d_{max}$ ) is constant for  $N > MUI$ , whereas, the less dominant interferers (lying outside the circle) continues to grow with  $N$ . It should also be noted that IA is most useful in the cases when all the users interfere strongly with each other. Therefore, we consider  $MUI = N$  in all our subsequent cases to facilitate a fair comparison between the optimal power sum-rate and the IA bound.

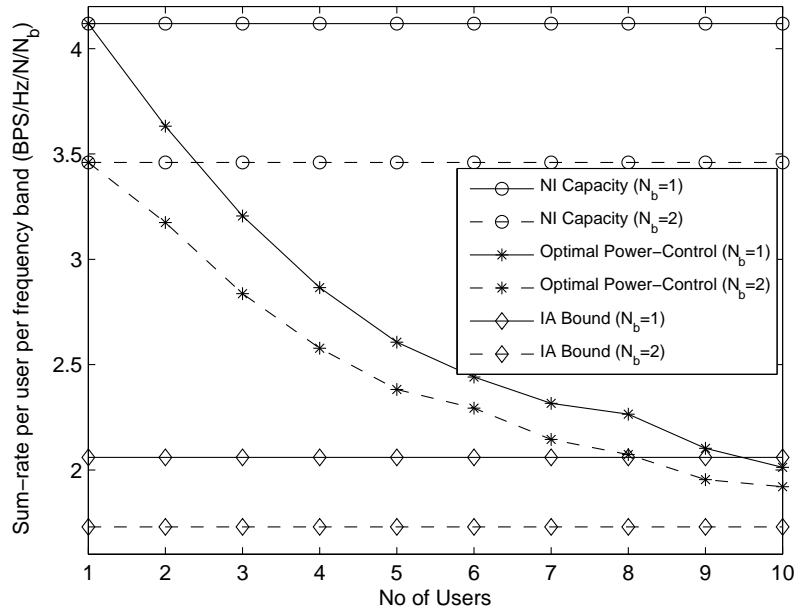


Figure 6.4: Comparison of the sum-rates of single and multiple band systems for the case when  $MUI = N$  ( $n_t = n_r = 1$ ).

### 6.2.1 Effect of the Number of Bands and Antennas

In Fig. 6.4, we consider a SISO IC and compare the optimal sum-rate to the NI capacity and the IA bound. The first observation is that the NI capacity per frequency band reduces when we increase  $N_b$  from 1 to 2. This is due to the fact that doubling the number of bands does not allow a doubling of capacity (due to the fact that the power is limited), thus the capacity per frequency band goes down. The optimal sum-rate per user per frequency band is observed to be higher than the IA bound for a small to moderate number of SUs. The per user sum-rate decreases with the increase in interference power in the optimal power control case but remains constant in the IA case. Due to this, the optimal method performs worse after a certain cross-over point (referred henceforth as  $N_{CO}$ ). This highlights the effectiveness of IA in high interference scenarios. Another interesting observation is that the cross-over point  $N_{CO}$  is higher when there are a higher number of orthogonal frequency

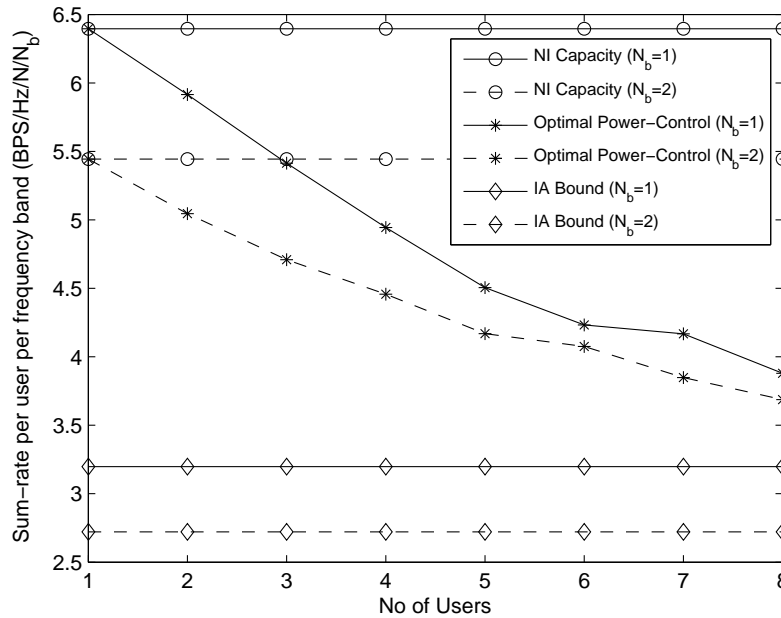


Figure 6.5: Comparison of the sum-rates of single and multiple band systems for the case when  $MUI = N$  ( $n_t = n_r = 2$ ).

bands available for transmission. This means that the performance of the proposed technique improves significantly with the increase in the number of orthogonal frequency bands. This is an important result from the cognitive radio perspective, where we expect to have several orthogonal frequency bands for the use of SUs. A similar comparison is carried out for a  $2 \times 2$  multi-band MIMO IC in Fig. 6.5. In addition to the already mentioned results, we observe that the performance of the optimal power control technique is better in this case than the SISO IC case due to the presence of additional spatial channels. In particular, the cross-over points  $N_{CO}$  are higher in this case than their counterparts in the SISO IC case. Thus, the presence of additional spatial and/or spectral channels improves the interference avoidance capability of the power control technique. We also note that the sum-rate scales better with the increase in the number of orthogonal frequency bands in the high interference case.

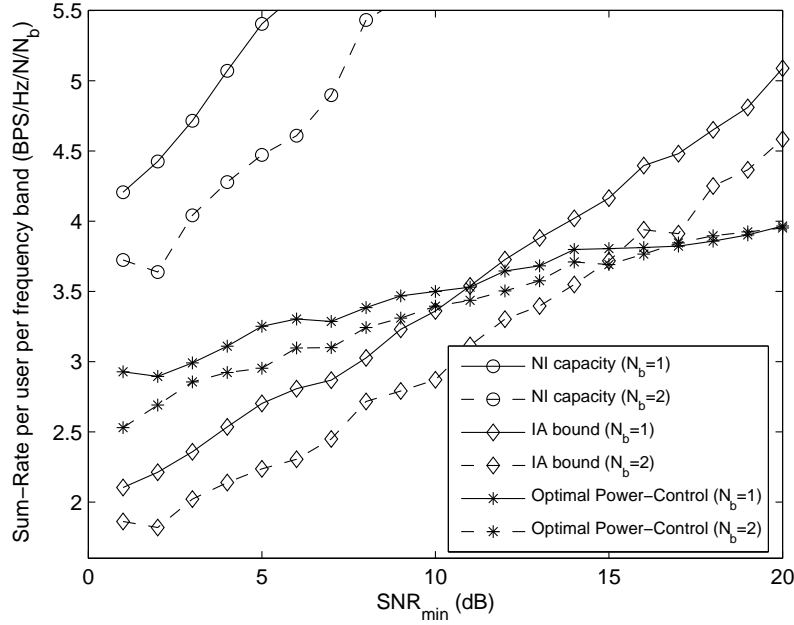


Figure 6.6: Comparison of the sum-rates of single and multiple band systems at various values of  $SNR_{min}$  ( $MUI = N = 4$ ,  $n_t = n_r = 1$ ).

### 6.2.2 Effect of $SNR_{min}$

In Fig. 6.6, we study the effect of  $SNR_{min}$  on the performance of our proposed technique and its comparison to the IA bound. We consider a four-user SISO IC and compare the optimal results with the NI capacity and the IA bound. We observe that the proposed power control technique performs better than the IA bound in the low  $SNR$  regime. This is due to the fact that the sum-rates achievable in IA are highly sub-optimal in the low  $SNR$  regime. As we increase  $SNR_{min}$ , IA starts performing better than the proposed technique after a certain  $SNR_{min}$  value (referred henceforth as  $SNR_{CO}$ ). We also observe that the  $SNR_{CO}$  is higher when there are multiple bands for transmission. This reiterates the fact that the performance of the optimal power control technique improves as compared to the IA bound when there are more orthogonal frequency bands available for transmission. Repeating the same comparison for the  $2 \times 2$  multi-band MIMO IC in Fig. 6.7, we observe that the cross-over



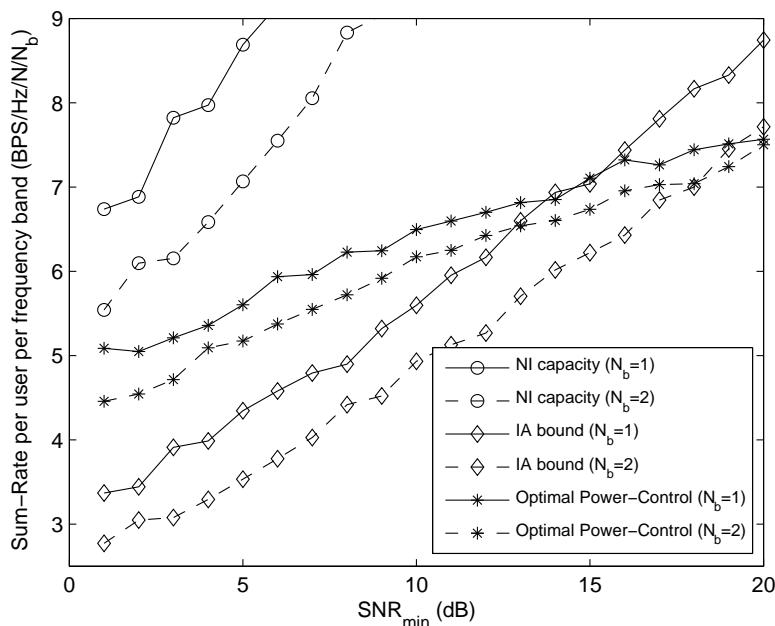


Figure 6.7: Comparison of the sum-rates of single and multiple band systems at various values of  $SNR_{min}$  ( $MUI = N = 4$ ,  $n_t = n_r = 2$ ).

points,  $SNR_{CO}$ , are higher in this case as compared to the SISO case. Another interesting observation from Fig. 6.6 and 6.7 is that the sum-rate scales better with the increase in the number of orthogonal frequency bands for the optimal power control case in the high  $SNR$  regime.

### 6.3 Conclusion

In this chapter, we have shown that the sum-rate achievable by optimal power control while treating interference as noise in a multi-band multi-antenna IC is much higher than the one achievable by IA in low and intermediate SNR regimes. The performance of the power control technique improves further relative to IA when we increase the number of frequency-channels and/or antennas. This result is especially promising from the cognitive radio perspective, where SUs typically operate in a relatively low SNR regime and are generally expected to

have multiple frequency bands available for transmission. In the high SNR (high interference) regime, however, IA performs better than the power control technique.

We have also studied the value of power control in beamforming by comparing the optimal power control results with the ones achievable by letting each user perform ‘optimal’ beamforming. We have shown that it is important to perform power control when the number of orthogonal channels is less than the number of users. Moreover, the value of power control in this case increases as we move from low to high interference scenarios.

# Chapter 7

## Conclusions

In this thesis, we have studied the problem of characterizing the capacity of multi-band multi-antenna interference channels by treating interference as noise. It should be noted that the single-band SISO, single-band MIMO and multi-band SISO ICs are special cases of our work. While the single band SISO and multi-band SISO ICs are relatively well understood, the same is not true for single-band MIMO ICs. All the results found in this thesis for the general case of multi-band MIMO IC also apply to this relatively less-understood case of single-band MIMO IC.

The main contributions and conclusions made in this thesis are as follows:

- **Sum-Rate Maximization Problem Formulation:** We have provided a mathematical framework to determine the maximum ergodic sum-rate of a multi-band multi-antenna IC treating interference as Gaussian noise. The problem is reduced to finding the optimal fraction of power to be transmitted over each Eigen-channel in each frequency band. The underlying optimization problem is shown to be quite similar to the one already known for the single-band MIMO IC. This enables us to extend the solution methods studied for the single band MIMO ICs easily to the current problem [61].
- **BB/RLT Global Optimization Algorithm:** The sum-rate maximization problem

of multi-band multi-antenna IC is hard to solve both analytically and numerically due to its non-linear and non-convex nature. We have extended the BB/RLT global optimization algorithm to solve this problem, which was first proposed to find the maximum sum-rate of a MIMO IC under the assumption that each user's transmit power is equally distributed over all the spatial channels. This assumption eases the mathematical formulation of the problem significantly, but unfortunately, the simplified results do not provide the maximum achievable sum-rate, in general. Thus our contributions include the global optimal solution to the sum-rate maximization problems of single-band MIMO [60] and multi-band MIMO [62] ICs.

- **Similarity Between the Spatial and Frequency channels:** We have shown that the spatial and frequency channels are surprisingly similar from the sum-rate perspective in an IC. The optimal power allocation strategies for a single-band  $n_t \times n_r$  MIMO IC (with  $n_t = n_r$ ) are nearly the same as those of  $N_b$ -band SISO IC whenever  $n_t = N_b$ . In other words, the fundamental factor affecting the sum-rate in an IC is the number of orthogonal channels and not their type (such as frequency channels, Eigen-channels, etc.). We generalize this result further by showing that the optimal power allocation strategies for an  $N_b$ -band  $n_t \times n_t$  MIMO IC are similar to those of single-band  $n \times n$  MIMO IC and an  $n$ -band SISO IC whenever  $n_t N_b = n$ . This generalization is based on the fact that an  $N_b$ -band  $n_t \times n_r$  MIMO IC has  $\min\{n_t, n_r\} N_b$  degrees of freedom. This result is especially important because of the dissimilarity in the way the spatial and frequency channels affect the perceived interference. On one hand, the frequency channels are common to all the users and are perfectly isolated from each other at each user. On the other hand, this demarkation is not so neat in the case of spatial channels because they are defined for a particular user and are not same for the whole IC. Thus the spatial channel of different users are not orthogonal to each other.
- **Rules-of-Thumb for Optimal Power Allocation Strategies:** From our study of some special cases of the multi-band multi-antenna ICs, we put forth some rules-

of-thumb for understanding the optimal power allocation strategies. These rules are discussed below in terms of the number of orthogonal channels  $n = \min\{n_t, n_r\}N_b$  (assuming uncorrelated antennas). Please note that these channels can be spatial, spectral or mix of both due to the above mentioned equivalence.

- *Very Low SNR Regime:* In this regime, the system is essentially noise limited and it is optimal for all the users to transmit at the full power  $P_{max}$  over a single orthogonal channel.
  - *Low SNR Regime:* It is optimal to distribute power over all orthogonal channels for all users in the low SNR regime. Equal power distribution, however, is not optimal in general. This is due to the fact that in most of the optimal power allocation strategies, the weaker channels are turned off for interference avoidance.
  - *Intermediate SNR Regime:* It is optimal to transmit most of the power in the strongest channels in the intermediate SNR regime. In some cases, it is even optimal to confine all the power in the strongest channel. This is due to the increasing importance of interference avoidance as we move from low to high SNR regimes.
  - *High SNR Regime:* In the high SNR regime, it is optimal in most of the cases to let  $n$  users transmit at the maximum power  $P_{max}$  by confining it in their respective strongest channels. Thus, it is optimal to avoid interference completely in this regime. However, in some cases the spatial channels are so aligned that complete interference avoidance is not possible. In such cases, ‘bad’ users are turned off and the rest of the users ( $< n$ ) are allowed to distribute power over the orthogonal channels.
- **Lower Bound on the Optimal Sum-Rate:** A lower bound on the sum-rate achievable by power control is found by letting  $n$  users transmit simultaneously at the maximum power  $P_{max}$  by confining it in their respective strongest channels. This bound will be reasonably tight in the interference-limited high SNR regime due to the above

mentioned rules-of-thumb.

- **Comparison of Power Control with Interference Alignment:** We have shown that the sum-rate achievable by optimal power control while treating interference as noise in a multi-band multi-antenna IC is much higher than the one achievable by IA in low and intermediate SNR regimes. The performance of the power control technique improves further relative to IA when we increase the number of frequency-channels and/or antennas. This result is especially promising from the cognitive radio perspective, where users typically operate in a relatively low SNR regime and are generally expected to have multiple frequency bands available for transmission. In the high SNR (high interference) regime, however, IA performs better than the power control technique.
- **Value of Power Control in Beamforming:** We have also studied the value of power control in beamforming by comparing the optimal power control results with the ones achievable by letting each user perform ‘optimal’ beamforming. We have shown that it is important to perform power control in beamforming when the number of orthogonal channels is less than the number of users. Moreover, the value of power control in this case increases as we move from low to high interference scenarios.

# Bibliography

- [1] C. E. Shannon, “A mathematical theory of communication”, *Bell System Technical Journal*, vol. 27, pp. 379-423 and 623-656, 1948.
- [2] T. M. Cover and J. A. Thomas, *Elements of Information Theory*. New York: Wiley, 1991.
- [3] R. Togneri and C. J. S. deSilva, *Fundamentals of Information Theory and Coding Design*. Chapman & Hall/ CRC, Boca Raton, 2002.
- [4] R. J. McEliece, *The Theory of Information and Coding*. Reading, MA: Addison-Wesley, 1977.
- [5] C. E. Shannon, “Two-Way Communication Channels”, in Proc. 4<sup>th</sup> *Berkeley Symposium on Mathematical Statistics and Probability*, Berkeley, CA, 1961, pp. 611-644.
- [6] A. B. Carleial, “A Case where Interference does not Reduce Capacity”, *IEEE Transactions on Information Theory*, vol. IT-21, pp. 569-570, Sept. 1975.
- [7] R. Ahlswede, “The Capacity Region of a Channel with Two Senders and Two Receivers”, *Annals Probability*, vol. 2, no. 5, pp. 805-814, 1974.
- [8] A. B. Carleial, “Interference Channels”, *IEEE Transactions on Information Theory*, vol. IT-24, pp. 60-70, Jan. 1978.

- [9] H. Sato, "Two-User Communication Channels", *IEEE Transactions on Information Theory*, vol. IT-23, pp. 295-304, May 1977.
- [10] T. S. Han and K. Kobayashi, "A New Achievable Rate Region for the Interference Channel", *IEEE Transactions on Information Theory*, vol. 27, no. 1, pp. 49-60, Jan. 1981.
- [11] R. Etkin, "Spectrum sharing: Fundamental Limits, Scaling Laws, and Self Enforcing Protocols", Ph.D. dissertation, Univ. of California, Berkeley, Dec. 2006.
- [12] R. Etkin, D. Tse and H. Wang, "Gaussian Interference Channel Capacity to Within One Bit", *IEEE Transactions on Information Theory*, vol. 54, no. 12, pp. 5534-5562, 2008.
- [13] R. Etkin, D. Tse and H. Wang, "Gaussian Interference Channel Capacity to Within One Bit: the Symmetric Case", in Proc. *IEEE Information Theory Workshop*, Punta Del Este, 2006, pp. 601-605.
- [14] I. Sason, "On Achievable Rate Regions for the Gaussian Interference Channel", *IEEE Transactions on Information Theory*, vol. 50, no. 6, pp. 1345-1356, June 2004.
- [15] X. Shang, G. Kramer, and B. Chen, "A New Outer Bound and the Noisy-Interference Sum-Rate Capacity for Gaussian Interference Channels", *IEEE Transactions on Information Theory*, vol. 55, no. 2, pp. 689-699, 2009.
- [16] V. S. Annapureddy and V. Veeravalli, "Gaussian Interference Networks: Sum Capacity in the Low Interference Regime and New Outer Bounds on the Capacity Region", *IEEE Transactions on Information Theory*, vol. 55, no. 7, pp. 3032-3050, 2009.
- [17] A. S. Motahari and A. K. Khandani, "Capacity Bounds for the Gaussian Interference Channel", *IEEE Transactions on Information Theory*, vol. 55, no. 2, pp. 620-643, 2009.



- [18] G. Bresler and D. N. C. Tse “3 User Interference Channel: Degrees of Freedom as a Function of Channel Diversity”, in Proc. *47<sup>th</sup> Annual Allerton conference on Communication, control, and computing*, Monticello, IL, 2009, pp. 265-271.
- [19] S. Sridharan, A. Jafarian, S. Vishwanath, S. A. Jafar and S. Shamai, “A Layered Lattice Coding Scheme for a Class of Three User Gaussian Interference Channels”, in Proc. *46<sup>th</sup> Annual Allerton conference on Communication, control, and computing*, Urbana-Champaign, IL, 2008, pp. 531-538.
- [20] D. N. C. Tse and P. Viswanath, *Fundamentals of Wireless Communication*. Cambridge, U.K.: Cambridge Univ. Press, 2005.
- [21] G. J. Foschini and M. J. Gans, “On Limits of Wireless Communications in a Fading Environment when using Multiple Antennas”, *Wireless Personal Communications*, vol. 6, no. 3, pp. 311-335, March 1998.
- [22] E. Telatar, “Capacity of Multi-Antenna Gaussian Channels”, *European Transactions on Telecommunications*, vol. 10, pp. 585-596, Nov. 1999.
- [23] D. Tse, P. Viswanath, and L. Zheng, “Diversity-Multiplexing Tradeoff in Multiple-Access Channels”, *IEEE Transactions on Information Theory*, vol. 50, no. 9, pp. 1859-1874, Sept. 2004.
- [24] P. Viswanath and D. Tse, “Sum Capacity of the Vector Gaussian Broadcast Channel and Uplink-Downlink Duality”, *IEEE Transactions on Information Theory*, vol. 49, no. 8, pp. 1912-1921, Aug. 2003.
- [25] W. Yu and J. Cioffi, “Sum Capacity of Gaussian Vector Broadcast Channels”, *IEEE Transactions on Information Theory*, vol. 50, no. 9, pp. 1875-1892, Sept. 2004.
- [26] S. Vishwanath, N. Jindal, and A. Goldsmith, “Duality, Achievable Rates, and Sum-Rate Capacity of MIMO Broadcast Channels”, vol. 49, no. 10, *IEEE Transactions on Information Theory*, vol. 49, no. , pp. 2895-2909, Oct. 2003.

- [27] M. Maddah-Ali, A. Motahari and A. Khandani, "Signaling over MIMO Multi-Base systems- Combination of Multi-Access and Broadcast Schemes", in *Proc. IEEE International Symposium on Information Theory*, Seattle, WA, 2006.
- [28] V. R. Cadambe and S. A. Jafar, "Interference Alignment and the Degrees of freedom for the  $K$  user interference channel", *IEEE Transactions on Information Theory*, vol. IT-54, no. 8, pp. 3425-3441, Aug. 2008.
- [29] M. Shen, A. Høst-Madsen and J. Vidal, "An Improved Interference Alignment Scheme for Frequency Selective Channels", in *Proc. IEEE International Symposium on Information Theory*, July 2008, pp. 559-563.
- [30] S. W. Choi, S. A. Jafar and S.-Y. Chung, "On the Beamforming Design for Efficient Interference Alignment", *IEEE Communications Letters*, vol. 13, no. 11, pp. 847-849, 2009.
- [31] T. Gou and S. A. Jafar, "Degrees of Freedom of the  $K$  User MIMO Interference Channel", in *Proc. Asilomar Conference on Signals, Systems and Computers*, Pacific Grove, CA, 2008, pp. 126-130.
- [32] R. Tresch, M. Guillaud and E. Riegler, "On the Achievability of Interference Alignment in the  $K$ -user Constant MIMO Interference Channel", in *Proc. IEEE Workshop on Statistical Signal Processing*, Cardiff, U.K., Sept. 2009, pp. 277-280.
- [33] K. Gomadam, V. Cadambe and S. Jafar, "Approaching the Capacity of Wireless Networks through Distributed Interference Alignment", in *Proc. IEEE Global Telecommunications Conference*, New Orleans, LA, 2008.
- [34] Justin M. Kelly, "On the Benefit of Cooperation of Secondary Users in Dynamic Spectrum Access", M.S.E.E. Thesis, Virginia Polytechnic Institute and State University, 2009.

- [35] J. Zander, "Performance of Optimum Transmitter Power Control in Cellular Radio Systems", *IEEE Transactions on Vehicular Technology*, vol. 41, pp. 57-62, Feb. 1992.
- [36] G. J. Foschini and Z. Miljanic, "A Simple Distributed Autonomous Power Control Algorithm and its Convergence", *IEEE Transactions on Vehicular Technology*, vol. 42, no. 4, pp. 641-646, Nov. 1993.
- [37] Y.-H. Lin and R. L. Cruz, "Power Control and Scheduling for Interfering Links", in *Proc. IEEE Information Theory Workshop*, San Antonio, TX, Oct. 2004, pp. 288-291.
- [38] A. Gjendemsjø, G. E. Øien, and H. Holm, "Optimal Power Control for Discrete-Rate Link Adaptation Schemes with Capacity-Approaching Coding", in *Proc. IEEE Global Telecommunications Conference*, St. Louis, MO, Nov.-Dec. 2005, pp. 3498-3502.
- [39] A. Gjendemsjø, G. E. Øien, and P. Orten, "Optimal Discrete-Level Power Control for Adaptive Coded Modulation Schemes with Capacity Approaching Component Codes, in *Proc. IEEE International Conference on Communications*, Istanbul, Turkey, 2006.
- [40] R. Knopp and P. Humblet, "Information Capacity and Power Control in Single-Cell Multiuser Communications", in *Proc. IEEE International Conference on Communications*, Seattle, WA, June 1995, pp. 331-335.
- [41] A. Gjendemsjø, D. Gesbert, G. E. Øien, and S. G. Kiani, "Optimal Power Allocation and Scheduling for Two-Cell Capacity Maximization", in *Proc. 4<sup>th</sup> International Symposium on Modeling and Optimization in Mobile, Ad Hoc and Wireless Networks*, Boston, USA, Apr. 2006, pp. 1-6.
- [42] M. Ebrahimi, M. A. Maddah-Ali, and A. K. Khandani, "Power Allocation and Asymptotic Achievable Sum-Rates in Single-Hop Wireless Networks", in *Proc. 40<sup>th</sup> Annual Conference on Information Sciences and Systems*, Princeton, NJ, Mar. 2006, pp. 498-503.

- [43] M. Charafeddine and A. Paulraj, "Maximum Sum Rates via Analysis of 2-user Interference Channel Achievable Rates Region", in Proc. 43<sup>rd</sup> *Annual Conference on Information Sciences and Systems (CISS)*, Baltimore, MD, 2009, pp. 170-174.
- [44] N. Badruddin, S. R. Bhaskaran, J. Evans and S. Hanly, "Maximizing the Sum Rate in Symmetric Networks of Interfering Links under Flat Power Constraints", in Proc. *Annual Allerton Conference*, Illinois, USA, Sept. 2008, pp. 46-53.
- [45] A.Gjendemsjø, D. Gesbert, G. E. Øien, and S. G. Kiani, "Binary Power Control for Sum Rate Maximization over Multiple Interfering Links", *IEEE Transactions on Wireless Communications*, vol. 7, no. 8, pp. 3164-3173, 2008.
- [46] M. Chiang, C. W. Tan, D. P. Palomar, D. O'Neill, and D. Julian, "Power Control by Geometric Programming", *IEEE Transactions on Wireless Communications*, vol. 6, no. 7, pp. 2640-2651, July 2007.
- [47] L. Qian, Y. J. Zhang, and J. Huang, "MAPEL: Achieving Global Optimality for a Non-Convex Wireless Power Control Problem", *IEEE Transactions on Wireless Communications*, vol. 8, no. 3, pp. 1553-1563, Mar. 2009.
- [48] V. S. Annapureddy, V. V. Veeravalli and S. Vishwanath, "On the Sum Capacity of MIMO Interference Channel in the Low Interference Regime", in Proc. 42<sup>nd</sup> *Asilomar Conference on Signals, Systems and Computers*, Pacific Grove, CA, 2008, pp. 80-84.
- [49] P. A. Parker and D.W. Bliss, "Outer Bounds for the MIMO Interference Channel", in Proc. 42<sup>nd</sup> *Asilomar Conference on Signals, Systems and Computers*, Pacific Grove, CA, 2008, pp. 1108-1112.
- [50] E. Akuiyibo, O. Leveque and C. Vignat, "High SNR Analysis of the MIMO Interference Channel", in Proc. *IEEE International Symposium on Information Theory*, Toronto, ON, 2008, pp. 905-909.

- [51] Yong Peng and D. Rajan, “Capacity Bounds for a Cognitive MIMO Gaussian Z-Interference Channel” *IEEE Transactions on Vehicular Technology*, vol. 59, no. 4, pp. 1865-1876, 2010.
- [52] F. Negro, S. P. Shenoy, I. Ghauri and D. T. M. Slock, “On the MIMO Interference Channel”, in Proc. *Information Theory and Applications Workshop*, San Diego, CA, 2010.
- [53] An Liu, Youjian Liu, Haige Xiang and Wu Luo, “On the Rate Duality of MIMO Interference Channel and Its Application to Sum Rate Maximization”, in Proc. *IEEE Global Telecommunications Conference*, Honolulu, HI, 2009.
- [54] B. S. Blum, “MIMO Capacity with Interference”, *IEEE Journal on Selected Areas in Communications*, vol. 21, pp. 793-801, June 2003.
- [55] S. Ye and R. S. Blum, “Optimized Signaling for MIMO Interference Systems with Feedback”, *IEEE Trans. Signal Process.*, vol. 51, no. 11, pp. 2839-2848, Nov. 2003.
- [56] W. Yu, W. Rhee, S. Boyd, and J. M. Cioffi, “Iterative Water-Filling for Gaussian Vector Multiple-Access Channels”, *IEEE Trans. Inform. Theory*, vol. 50, no. 1, pp. 145–152, Jan. 2004.
- [57] J. Liu, Y. T. Hou, Y. Shi and H. Sherali, “On the Capacity of Multiuser MIMO Networks with Interference”, *IEEE Transactions on Wireless Communications*, vol. 7, no. 2, pp. 488-494, Feb. 2008.
- [58] H. D. Sherali and C. H. Tuncbilek, “A Global Optimization Algorithm for Polynomial Programming Problems using a Reformulation-Linearization Technique”, *Journal of Global Optimization*, vol. 2, no. 1, pp. 101-112, 1992.
- [59] H. D. Sherali and W. P. Adams, *A Reformulation-Linearization-Technique for Solving Discrete and Continuous Nonconvex Problems*. Boston, MA: Kluwer Academic Publishing, 1999.

- [60] H. S. Dhillon and R. M. Buehrer, "On the Sum-Rate of MIMO Interference Channel", accepted for publication in *IEEE Global Telecommunications Conference*, Miami, FL, 2010.
- [61] H. S. Dhillon and R. M. Buehrer, "Cognitive MIMO Radio: Incorporating Dynamic Spectrum Access in Multiuser MIMO Network", in *Proc. IEEE Global Telecommunications Conference*, Honolulu, HI, 2009.
- [62] H. S. Dhillon and R. M. Buehrer, "On the Maximum Sum-Rate of Cognitive MIMO Interference Channels", accepted for publication in *IEEE Military Communications Conference*, San Jose, CA, 2010.
- [63] FCC Spectrum Policy Task Force, "FCC Report of the Spectrum Efficiency Working Group", Nov. 2002.
- [64] Q. Zhao and B. Sadler, "A Survey of Dynamic Spectrum Access", *IEEE Sig. Process. Mag.*, vol. 24, no. 3, pp. 79-89, May 2007.
- [65] I. F. Akyildiz, W. -Y. Lee, M. C. Vuran and S. Mohanty, "NeXt Generation/Dynamic Spectrum Access/Cognitive Radio Wireless Networks: A Survey", *Comput. Networks*, vol. 50, no. 13, pp. 2127-2159, 2006.
- [66] S. Haykin, "Cognitive Radio: Brain-Empowered Wireless Communications", *IEEE J. Select. Areas Commun.*, vol. 23, no. 2, pp. 201-220, Feb. 2005.
- [67] J. Mitola, "Cognitive Radio for Flexible Mobile Multimedia Communication," in *Proc. IEEE Int. Workshop Mobile Multimedia Commun. (MoMuC)*, San Diego, CA, Nov. 1999, pp. 3-10.
- [68] S. Shankar, C. Cordeiro and K. Challapali, "Spectrum Agile Radios: Utilization and Sensing Architectures", in *Proc. IEEE Int. Symp. New Frontiers Dynamic Spectr. Access Networks (DySPAN)*, Baltimore, MD, Nov. 2005, pp. 160-169.

- [69] G. Ganesan and Y. Li, "Cooperative Spectrum Sensing in Cognitive Radio Networks", in *Proc. IEEE DySPAN 2005*, Baltimore, MD, Nov. 2005, pp. 137-143.
- [70] H. Zheng and C. Peng, "Collaboration and Fairness in Opportunistic Spectrum Access", in *Proc. IEEE Int. Conf. Commun. (ICC)*, Seoul, vol. 5, May 2005, pp. 3132-3136.
- [71] C. Peng, H. Zheng and B. Y. Zhao, "Utilization and Fairness in Spectrum Assignment for Opportunistic Spectrum Access", *ACM Mobile Networks and Applications Journal (MONET)*, vol. 11, pp. 555-576, May 2006.
- [72] S. Hayashi and Z.-Q. Luo, "Spectrum Management for Interference-Limited Multiuser Communication Systems", *IEEE Trans. Inform. Theory*, vol. 55, no. 3, pp. 1153-1175, Mar. 2009.
- [73] L. Cao and H. Zheng, "Distributed Spectrum Allocation via Local Bargaining", in *Proc. IEEE Sensor and Ad Hoc Commun. and Networks (SECON)*, Santa Clara, CA, Sept. 2005, pp. 475-486.
- [74] R. Etkin, A. Parekha and D. Tse, "Spectrum Sharing for Unlicensed Bands", in *Proc. IEEE DySPAN*, Baltimore, MD, Nov. 2005, pp. 251-258.
- [75] L. Cao and H. Zheng, "On the Efficiency and Complexity of Distributed Spectrum Allocation", in *Proc. Second Int. Conf. on Cognitive Radio Oriented Wireless Networks and Commun. (CROWNCOM)*, Orlando, FL, Aug. 2007, pp. 357-366.
- [76] J. P. Kermoal, L. Schumacher, K. Pedersen, P. E. Mogensen, and F. Frederiksen, "A Stochastic MIMO Radio Channel Model with Experimental Validation", *IEEE Journal on Selected Areas in Communications*, vol. 20, pp. 1211-1226, 2002.
- [77] E. Biglieri, R. Calderbank, A. Constantinides, A. Goldsmith, A. Paulraj, and H. V. Poor. *MIMO Wireless Communications*. Cambridge University Press, 2007.

- [78] A. J. Goldsmith and P. P. Varaiya, "Capacity of Fading Channels with Channel Side Information" *IEEE Transactions on Information Theory*, vol. 43, no. 6, pp. 1986-1992, 1997.
- [79] O. Oyman, R. U. Nabar, H. Bolcskei and A. J. Paulraj, "Tight Lower Bounds on the Ergodic Capacity of Rayleigh Fading MIMO Channels", in Proc. *IEEE Global Telecommunications Conference*, Taipei, Taiwan, Nov. 2002, pp. 1172-1176.